Development of cyclophilin inhibitors for the treatment of pancreatitis

Thesis submitted in accordance with the requirements of University of Liverpool for the degree of Doctor of Philosophy

By

Xiaoying Zhang

September 2018

Statement of originality

I declare that the work in this thesis was carried out in accordance with the Regulations of the University of Liverpool. The work is original except where indicated by specific reference in the text and no part of the dissertation has been submitted for any other degree.

The author in conjunction with her primary supervisor, Professor Robert Sutton, has conducted all aspects of experimental design and plan for this study. The second and third supervisor Dr David Criddle and Dr Qibo Zhang have provided thoughtful provision and supports for the whole study. The author performed all experiments included in this thesis entirely independently. The thesis has not been presented to any other University for examination either in the United Kingdom or overseas.

This is dedicated to my beloved parents

Abstract

Introduction: Emerging evidence suggests the pivotal role of the mitochondria permeability transition pore (MPTP) in the development of acute pancreatitis (AP). Genetic ablation of cyclophilin D (CypD), the key regulator of MPTP opening, exerts marked protective effects in AP, but pharmacologic inhibition of MPTP has had inconsistent results possibly due to nonspecific inhibition on other cyclophilins such as the endoplasmic reticulum-based protein folding chaperone cyclophilin B (CypB). This study sought to comprehensively define the effects of cyclophilin inhibitor in murine isolated pancreatic acinar cells (PACs) and multiple experimental AP models. This work has also evaluated the effects of MPTP inhibition via cyclophilin D in experimental chronic pancreatitis (CP).

Methods: Responses of freshly isolated murine PACs to taurolithocholic acid 3-sulphate (TLCS), palmitoleic acid (POA) or caerulein were examined following preloading with cyclosporin A (CsA, 100 nM to 50 μM) to assess the protective effects of CsA on kinetic cell death activation and cellular reactive oxygen species (ROS) generation. Response was examined using fluorescent dyes recorded by plate reader, together with western blotting to measure protein folding chaperones glucose regulated protein 78 (GRP-78) and CypB expression. Pharmacological MPTP inhibitory strategies with multiple independent cyclophilin inhibitors were administered to assess the severity of murine experimental AP induced by retrograde common duct infusion of 50 μL 3 mM TLCS (TLCS-AP), 2 hourly fatty acid ethyl ester (FAEE-AP: mixture of 1.35 g/kg ethanol and 150 mg/kg POA) intraperitoneal injection (ipi) or 7 hourly ipi of 50 μg/kg caerulein (CER-AP). Genetic and pharmacological MPTP inhibition was targeted to investigate the role of CypD in the development and recovery of repetitive caerulein-induced murine CP models.

Results: Pancreatic toxins exposure of isolated control PACs induced marked propidium iodine uptake and caspase 3/7 intensity accompanied by abundant ROS generation, as well as early GRP-78 and CypB overexpression. Pharmacologic MPTP inhibition with CsA protected PACs against cell death and ROS production at lower concentrations (1-5 μM; $p<0.05$). CsA at low to medium doses (1-5 mg/kg) dramatically alleviated ($p<0.05$) severity markers of TLCS-AP, FAEE-AP and CER-AP while higher doses were associated with elevated IL-6 and myeloperoxidase levels. CC-1233, a novel cyclophilin inhibitor with higher affinity to CypD than CsA, reduced the severity of TLCS-AP at all doses tested, but exacerbated all biochemical and immunological parameters except for trypsin activity in FAEE-AP and CER-AP. Genetic ablation of CypD or pharmacologic inhibition of cyclophilins with SCY-635/CC-4635 preserved PAC structure and enzymatic function while reducing collagen deposition in experimental CP.

Conclusion: Inhibition of the MPTP opening with cyclophilin inhibitors reduces pancreatic injury and alleviates the experimental AP and CP in murine models but requires careful optimisation of the treatment regimen. Protection of PAC injury appears a feasible approach to reduce the long-term injury in CP. Inappropriate application of cyclophilin inhibitors at too high a dosage may exacerbate inflammation and disease course due to off-target effects.

Acknowledgements

First and foremost, I would like to thank Prof Robert Sutton who provided me with the research chance for his supreme inspiration, profound strategies and constructive guidance throughout my entire study, with enjoyable exhilarating, scientific and splendid PhD training. I would also like to thank my co-supervisor, Dr David Criddle and Dr Qibo Zhang, who are dramatically supportive to provide suggestions and considerations on both research and daily life.

Great appreciation for Chinese Scholarship Council (CSC) and University of Liverpool who funded my tuition fees and stripes during my PhD, many thanks again to Prof Sutton for the financial support on research and conferences. Thanks to Prof Qing Xia, who initiated my curiosity in pancreatology during my medical training period in West China Hospital, Sichuan University, and constantly provide supporting throughout the last 4 years.

Many thanks to Dr Li Wen, Dr Wei Huang, Dr Tingting Liu and Dr Yulin Ouyang, for the instructions with the initial experimental setting, Ms Diane Latawiec, for the assistance in blinded histopathological scoring as one of the two independent investigators. All the staff from Biomedical Service Unit, especially technicians responsible for the mice colony breeding, animal care and personal competencies training. Thanks to Prof Alexey Tepikin and all members from his group, especially Dr Michael Chvanov for the kindly supporting and advice on my project for the *in vitro* work. Mr Michael Neil from Department of Pathology for helping with preparing the wax embedded blocks and H&E staining. Ms Jean Devine, Mr William Taylor and Mrs Suzana Philip from the Department of Clinical Biochemistry for helping with amylase analyses. Dr Kalirai Helen, Mrs Patricia Gerard, for providing IHC induction training and facilities. Mr Van veen Theun, Mrs Rhiannon Clarke from Liverpool Innovate Biobank for providing slides scanning service. Our industrial collaborator Cypralis for providing compounds and research support. Finally, many thanks to Mr Rajarshi Mukherjee, Mr Quentin Nunes, Mrs Becky Taylor and all other members from Liverpool Pancreatitis Research Group.

Table of Contents

List of Tables

List of Figures

List of Abbreviations

AP	Acute pancreatitis
ACh	Acetyl Choline
AP-1	Activator protein 1
ADP	Adenosine diphosphate
ALI	Acute lung injury
ANT	Adenine nucleotide translocase
α-SMA	alpha-smooth muscle actin
ATP	Adenosine triphosphate
ATF- 6	Activating transcription factor 6
BK	Bradykinin
Ca^{2+}	General Ca^{2+}
$[Ca^{2+}]_c$	Cytosolic Ca^{2+} concentration
$[Ca^{2+}]_e$	Extracellular Ca^{2+} concentration
$[Ca^{2+}]_m$	Mitochondria Ca^{2+} concentration
CCh	Carbachol
CCK	Cholecystokinin
CER	Caerulein
CM-H2DCFDA	Chloromethyl 2', 7'- dichlorodihydrofluorescein diacetate
CsA	Cyclosporin A
CypA	Cyclophilin A
CypB	Cyclophilin B
CypC	Cyclophilin C
CypD	Cyclophilin D
CYP2E1	Cytochrome p450 2E1
CP	Chronic pancreatitis
CRAC	Calcium release-activated channels
DAB	3, 3'- Diaminobenzidine
DEB025	D-MeAla3-EtVal4-cyclosporin (Alisoporivir)
DMSO	Dimethyl sulphoxide
ΔΨm	Mitochondria membrane potential
EAP	Experimental acute pancreatitis
ECL	Enhanced chemiluminescence
ECM	Extracellular matrix
ECP	Experimental chronic pancreatitis
eIF2	Eukaryotic Initiation Factor 2
ELISA	Enzyme-linked immunosorbent assay
EMMPRIN	Extracellular matrix metalloproteinase inducer
ER	Endoplasmic reticulum
ERK	Extracellular signal-regulated kinases
ETC	Electron transport chain
EtOH	Ethanol
EAP	Experimental acute pancreatitis
FA	Fatty acid
FAEE	Fatty acid ethyl ester
Gpbar	G protein-coupled bile acid receptor
HEPES	4-(2-hydroxyethyl)-1-piperazineethaqnesulphonic acid

HRP	Horseradish peroxidase
HSC	Hepatic stellate cell
H_2O_2	Hydrogen peroxide
HSPGs	Heparin sulphate proteoglycans
IL-1β	Interleukin-1 beta
IL-6	Interleukin-6
IL-8	Interleukin-8
IMM	Inner mitochondrial membrane
IMPDH2	Inosine-5'-monophosphate dehydrogenase 2
IRE1	Inositol requiring protein 1
JNK	c-Jun N-terminal Kinases
KO	Knockout
MAP	Mild acute pancreatitis
MAPK	Mitogen-activated protein kinases
MMP	Matrix metallopeptidase
MPO	Myeloperoxidase
MPTP	Mitochondria permeability transition pore
NAADP	Nicotinic acid adenine dinucleotide phosphate
NADH/NAD^+	Nicotinamide adenine dinucleotide
NAC	N-acetylcysteine
NADPH	Nicotinamide adenine dinucleotide phosphate
NFAT	Nuclear factor of activated T-cells
NK-1	Neurokinin-1
NTCP	Na^+-Taurocholate co-transporting polypeptide
OATP	Organic anion transporting polypeptide
OMM	Outer mitochondrial membrane
OSCP	Oligomycin sensitivity-conferring protein
PAC	Pancreatic acinar cell
PEG	Polyethylene glycol
PEI	Pancreatic exocrine insufficiency
PERK	Protein kinase like ER resident kinase
PI	Propidium iodide
POA	Palmitoleic acid
POAEE	Palmitoleic acid ethyl ester
PPIF(*Ppif*$^{-/-}$)	Peptidylprolyl isomerase F/cyclophilin D knock out
PPIase	Peptidylprolyl *cis-trans* isomerase
PSC	Pancreatic stellate cell
RAP	Recurrent acute pancreatitis
RCT	Randomised clinical trial
ROS	Reactive oxygen species
RyR	Ryanodine receptor
SAP	Severe acute pancreatitis
SERCA	Sarcoplasmic/endoplasmic reticulum Ca^{2+}- ATPase
SOCE	Store-operated Ca^{2+} entry
STIM 1	Stromal interaction molecular 1
TGF-β1	Transforming growth factor - beta 1
TLCS	Taurolithocholic acid 3-sulphate
TNF- α	Tumour necrosis factor- α
UPR	Unfolded protein response
WT	Wild type

CHAPTER 1

INTRODUCTION

1.1 Pancreatitis

Pancreatitis, manifest with acute, recurrent and chronic three inflammation types of pancreas. Although epidemiology of pancreatitis is well known, there is still a lack of definitive and specific medical treatment for necrosis, inflammation and fibrosis due to less elucidated understanding with cellular mechanisms of disease initiation and progression.

1.1.1 Acute Pancreatitis

Acute pancreatitis (AP) is a necro-inflammatory disease with initial inappropriate zymogen activation, which is an important health concern across the world with the incidence of first attack in different population studies ranges from 15 to 45 among 100,000 per year [1-10]. The mild acute pancreatitis (MAP) is self-limited with complete resolution in 2 weeks, however, it can also progress to severe life-threatening form with serious complications including both local necrotic collection and persistent organ failure with up to 30% mortality rate[11-14].

The most common aetiologies of AP involve alcohol, gallstones, hyperlipidaemia, trauma, and few idiopathic cases, which initiate pathological activity of pancreatic enzymes, leading to both local and systemic injury, and organ failure in some severe cases[15, 16].

1.1.2 Recurrent Acute Pancreatitis

Recurrent Acute Pancreatitis (RAP) refers to more than two AP episodes on set[17]. As a clinical entity with recurrence, RAP generally occurs in a setting of normal

morpho-functional gland[18]. In some AP cases, formation of tissue scarring and stricture may lead to flow obstruction in pancreas and RAP[19].

Alcohol and gallstone aetiologies are combined frequency of more than 70%, which is further confirmed in a study including data from 5 European countries[20-22] for recurrent acute pancreatitis. Hypertriglyceridemia is a well-established cause of RAP. Other most frequent causes for RAP include heavy alcohol consumption, sludge, bile crystals and stones in the duct, or dysfunction of oddi sphincter, ductal anatomical variation, obstruction and genetic factos[18, 23, 24].

1.1.3 Chronic Pancreatitis

Chronic pancreatitis (CP) defines as a pathologic fibro-inflammatory syndrome of the pancreas in individuals with genetic, environmental and/or other risk factors who develop persistent pathologic responses to parenchymal injury or stress[25-29]. Scarring of the parenchyma may be focal, patchy or diffuse. The deposition and remodelling of fibrotic tissue is protective following injury, however it could impede normal pancreatic function with persistent accumulation. Progressive fibrotic reorganisation and acinar cell atrophy may lead to exocrine pancreatic insufficiency (EPI) followed by endocrine dysfunction with key features of malabsorption, malnutrition, diabetes, and pancreatic calcification[30, 31]. The incidence of CP in European countries ranges from 5 to 10 for every 100,000 inhabitants with a 20 years median survival.[32] The calculated prevalence is around 120 per 100,000 population [33, 34].

Chronic pancreatitis associated with heavy alcohol intake and cigarette smoking in about 60-80% of cases[35], other aetiology of CP has been characterized as hereditary, idiopathic, obstructive and hyperlipidaemia[36]. While Yadav reported CP develops from predominately non-gallstones related pancreatitis in US[8], studies from China revealed an association with alcohol in 35% and gallstones in about 34% of CP patients[37], suggesting a regional discrimination.

1.1.4 Disease progression and continuum

Over the last two decades, emerging clinical data of human studies suggests that AP and CP represent a disease continuum. Comfort has first proposed the concept that recurrent AP attacks lead to CP through healing of the necrotic arears with fibrotic tissue[38]. Later, Klöppel and Maillet described the sentinel acute pancreatitis event (SAPE) hypothesis that based on the necro-fibrosis theory and suggested AP as a sentinel event in the pathogenesis of CP, which aberration and continuous exposure with various risk factors during repair process leads to CP[39] and later confirmation was made from clinicopathological studies with CP patients. Although most MAP cases resolve without complications, a subset continues to have recurrent attacks of pancreatitis. As an intermediary stage in the pathogenesis of CP development and progression, partial RAP patients progress to CP during their natural course [40, 41]. Overall, the risk of recurrence after the first AP attack was noted to be 20%, and the risk of progression to CP was 36% with patients who suffered at least one recurrence [42-45]. In a national wide survey from Japan, the transition from AP to CP was noted to be 14.8%, which was 26% with alcohol and only 1.7% in patients related to gallstone[46, 47].

There are some common pathways connecting the progression with various elements. The progression relies on complicated interactions between impaired immune response with low extent inflammation and multiple factors from clinic like local complications and from environment such as heavy alcohol consumption, smoking, genetic factors or ongoing risk factors. These mutual interactions result in decreased progression threshold and finally lead to CP. Although the exact diseases progression pathophysiology from acute to chronic is remaining unclear, CP development has been generally characterized with three stages. Starting with pre-pancreatitis phase, the first stage is related to risk factors like genetic mutations, alcohol and smoking. Followed by the second stage with AP on set and inflammation. A severe attack could lead to the PSCs activation which is dependent on macrophage and finally lead to fibrosis formation and accumulation, especially with continuous stimuli that caused interplay between pro- and anti-inflammatory pathways. With modulation of immune response, finally progresses to last stage of CP [48, 49]. Not all AP, however, proceeds to recurrent, and not all RAP progresses to CP. The progression is determined by a comprehensive network involves multiple risk factors[50], which has been mentioned above.

1.2 Current clinical management and trials in pancreatitis

1.2.1 Clinical management for pancreatitis

For years, treatments for acute pancreatitis are still mainly supportive like fluid and nutritional therapy with low to moderate evidence according to the latest American Gastroenterology Associate (AGA) clinical guidelines (**Table 1.1**)[51]. Although the consensus recommended management for AP has been greatly improved in the last

few decades, specific and effective therapies are still lacking due to the poorly understood pathobiology of the disease. Laparoscopic cholecystectomy or endoscopic biliary sphincterotomy are the main therapeutic approach procedures for RAP of biliary aetiology. The management of CP is challenging and requires a personalized approach focused on the individual patient's main symptoms, goals and quality of life[52]. Apart from endoscopic and surgical management, pancreatic enzyme replacement therapy (PERT), is evidence-based recommendation as routinely used medical therapy in CP patients with exocrine pancreatic insufficiency (EPI) according to the United European Gastroenterology (UEG) evidence based guidelines (**Table 1.2**)[31]. The management for CP also includes education and counselling on abstinence of alcohol and tobacco in patients.

Table 1.1 Summary of Recommendations of AGA Clinical Guidelines for the Initial Management of Acute Pancreatitis

Recommendation	Strength	Evidence quality
1A. In patients with AP, the AGA suggests using goal-directed therapy for fluid management. Comment: The AGA makes no recommendation whether normal saline or Ringer's lactate is used. Conditional Very low. 1B. In patients with AP, the AGA suggests against the use of HES fluids.	Conditional	Very low
2. In patients with predicted severe AP and necrotizing AP, the AGA suggests against the use of prophylactic antibiotics.	Conditional	Low
3. In patients with acute biliary pancreatitis and no cholangitis, the AGA suggests against the routine use of urgent ERCP.	Conditional	Low
4. In patients with AP, the AGA recommends early (within 24 h) oral feeding as tolerated, rather than keeping the patient nil per os.	Strong	Moderate
5. In patients with AP and inability to feed orally, the AGA recommends enteral rather than parenteral nutrition.	Strong	Moderate
6. In patients with predicted severe or necrotizing pancreatitis requiring enteral tube feeding, the AGA suggest either NG or NJ route.	Conditional	Low
7. In patients with acute biliary pancreatitis, the AGA recommends cholecystectomy during the initial admission rather than after discharge.	Strong	Moderate
8. In patients with acute alcoholic pancreatitis, the AGA recommends brief alcohol intervention during admission.	Strong	Moderate

ERCP: Endoscopic Retrograde Cholangio-Pancreatograpy
NG: nosogastric
NJ: nosojejunal

Table 1.2 UEG Evidence Based Guidelines for Chronic Pancreatitis

Medical therapy for exocrine pancreatic insufficiency	Evidence Grade
Enzyme replacement therapy (PERT): PERT is indicated for patients with CP and PEI in the presence of clinical symptoms or laboratory signs of malabsorption. In case of unsatisfactory clinical response, the enzyme dose should be increased (doubled or tripled) or a proton pump inhibitor (PPI) should be used.	1A strong agreement 2B strong agreement

1.2.2 Clinical trials in AP

Since 1974, either single or multiple centres based short or long period clinical trials have been conducted all over the world on acute pancreatitis to evaluate the beneficial of various pharmacological agents (**Table 1.3**), including somatostatin or its analogue that reduces pancreatic secretion; protease inhibitors like aprotinin, nafamostat, gabexate mesilate and ulinastatin; antioxidants like vitamin C, E and selenium; agents which modulate inflammation as platelet activating factors lexipafant, steroids and tumour necrosis factor- alpha (TNF-α) antibody; antibiotics and probiotics[53-55].

Considering that several randomized controlled trials (RCT) with anti-pancreatic secretion therapy using somatostatin in AP have showed inconsistent clinical benefit [56-58], while both studies conducted on patients with severe type[59] and meta-analysis suggested an overall mortality advantage with somatostatin applied in severe acute pancreatitis[60], the pancreatic secretion inhibition was thought to be protective in severe class. Similar clinical dilemma was observed in the administration of its analogue, octreotide [61-63] , however, study suggested that a high dose administration may efficiently reduce the risk of SAP developing [64] and alleviating inflammation. Nevertheless, with respect to the administration time, dosage and suitable patients' category, both somatostatin and octreotide need further investigation [65],

Regarding of the anti-protease therapy in treating AP, there is no solid evidence supporting its clinical use[66]. While single protease inhibitor application like gabexate mesilate, has shown contradictory clinical benefit [67-69], continuous regional arterial infusion with combined nafamostat (a synthetic serine protease inhibitor)

and antibiotics provide further possibility[70, 71].

The anti-inflammatory drug lexipafant, antagonist of platelet activating factor receptor, failed to show reduction on multiple organ dysfunction syndrome (MODS) and mortality with severe AP (SAP) patients in a double-blinded randomised clinical trial (RCT) [72-74].

The prophylactic use of antibiotics also showed no significance to reduce mortality, or the requirement for surgical intervention[75-77]. Other pharmacological treatments such as antioxidant therapy has long been controversial with no convincing evidence for its application in clinical[78]. The experimental studies had shown that oxygen radical scavengers could reduce the severity[79], indeed several trials did report significantly shorter hospital stay[80, 81] and reduction in complications and organ dysfunction[82] following antioxidant therapy. However, with most attempts to establish the antioxidants therapy in clinical practice barely successes[83, 84], inconsistent results showed no significant difference in organ dysfunction but a trend towards more multiple organ dysfunction (MOD) in patients on active antioxidants, which suggested severity augmentation in predicted severe acute pancreatitis[85].

In a large multicentre RCT conducted by Dutch AP study group, bacterial translocation was reduced by combined probiotic prophylaxis and probiotic strains treatment, but not in patients with organ failure who developed increased bacterial translocation and enterocyte damage [86]. The later following on study further stated that probiotic prophylaxis in combination with probiotic strains did not reduce the risk of infectious complications but was associated with increased mortality risk,

which clearly indicated that probiotic prophylaxis should not be administered in the predicted severe cases[87].

Despite an increased understanding in pathophysiology of acute pancreatitis during last two decades, the current treatment for AP remains supportive[88], there is still a large clinical need for specific therapy. With the panoramic view on all the listed agents implemented to ameliorate AP in human clinical trials, the contradictory results also alert us the difficulties in translate bench findings to human therapy in terms of all concrete situations.

Table 1.3 Brief summary of medical treatments used in clinical trials for acute pancreatitis

Study	Year	Country	Centre	Study period	Treatment
Abraham[89]	2013	India	multiple (15)	12-month	Ulinastatin
Balldin[90]	1983	Sweden	single	5-year	Aprotinin
Bansal[84]	2011	India	single	1 year	Antioxidants (VitA, C, E)
Barreda[91]	2009	Peru	single	/	Antibiotics imipenem
Berling[92]	1994	Sweden Norway Finland	multiple (4)	/	Aprotinin
Besselink[86]	2008	Netherlands	multiple (15)	3 years	Probiotics (ecologic 641)
Bredkjaer[93]	1988	Denmmark	single	/	Indomethacin
Buchler[68]	1993	Germany Austria	multiple (29)	1988-1990	Gabexate mesilate
Chen[69]	2000	Taiwan	single	/	Gabexate mesilate
Chen[94]	2002	China	multiple	2000.4-2000.7	Ulinastatin

Choi[95]	1989	Hongkong	single	1.5 years	Somatostatin
Debas[96]	1980	Canada	single	/	Glucagon
Delcenserie[97]	1996	France	single	1988.7-1993.10	Antibiotics: Ceftazidime Amikacin Metronidazole
Delcenserie[98]	2001	France	multiple	/	Antibiotics: Ciprofloxacin
Dellinger[75]	2007	North America and Europe	multiple (32)	2003.2-2004.12	Antibiotics: Meropenem
Dürr[99]	1978	Germany	single	/	Glucagon
Finch[100]	1976	USA	single	1971.1-1973.12	Antibiotics: Ampicillin
Garcia-Barrasa[77]	2009	Spain	single	1999.5-2003.12	Antibiotics: Ciprofloxacin
Imrie[101]	1978	UK	single	34 months	Aprotinin
Isenmann[102]	2004	Germany	multiple (19)	1999.1-2002.6	Antibiotics: Metronidazole Ciprofloxacin
Johnson[74]	2001	UK	multiple	1994.11-1996.8	Lexipafant
Kingsnorth[72]	1995	UK	multiple (5)	/	Lexipafant
Kronborg[103]	1980	Denmark	/	/	Glucagon
Luengo[58]	1994	Spain	/	/	Somatostatin
Luiten[104]	1995	Netherlands	multiple (16 hospitals)	1990.4.22- 1993.4.19	Antibiotics: Colistin Amphotericin Norfloxacin with short course of Cefotaxime
Martinez[105]	1984	Spain	single	During 1982	Calcitonin
McKay [63]	1997a	UK	multiple (8)	1991.11-1993.4	Octreotide
McKay[73]	1997b	UK	multiple (11)	14 months	Lexipafant
MRC [106]	1977	UK	multiple	/	Aprotinin Glucagon
Nordback[107]	2001	Finland	single	1995.9-1999.5	Antibiotics: Imipenem

Olah[108]	2007	Hungary	single	3 years	Probiotics: Synbiotic
Paran[109]	1995	Israel	/	/	Octreotide
Pederzoli[110]	1993a	Italy	/	/	Antibiotics: Imipenem
Pederzoli[111]	1993b	Italy	multiple (19)	1989.1-1990.12	Gabexate mesilate
Pettilä [112]	2010	Finland	single	2003.6-2007.8	Activated protein C
Rokke[113]	2007	Norway	multiple (7)	1997-2002	Antibiotics: Imipenem
Sainio[114]	1995	Finland	single	4.5 years	Antibiotics: Cefuroxime
Sateesh[80]	2009	India	single	2 years	Antioxidants: Vitamin C N-acteyl cysteine Antoxyl Forte
Sharma[115]	2011	India	single	2007.3-2008.5	Probiotics: Fructooligosaccharide
Sillero[116]	1981	Spain	single	1 year	Cimetidine
Siriwardena[85]	2007	UK	multiple (3)	3.5 years	Antioxidants: Selenium Vitamin C N-acetyl cysteine
Trapnell[117]	1974	UK	multiple	5 years	Aprotinin
Uhl[61]	1999	Germany	multiple (32)	2.5 years	Octreotide
Valderrama[67]	1992	Spain	/	/	Gabexate mesilate
Vege[118]	2015	USA	single	3 years	Antioxidant: Pentoxifylline
Wang [119]	2011	China	single	4 months	Thymosin alpha
Wang[120]	2013	China	/	/	Somatostatin Ulinastatin
Wang[64]	2013	China	single	1 year	Octreotide
Wang[59]	2016	China	/		Somatostatin Ulinastatin Gabexate
Xue[121]	2009	China	single	1 year	Antibiotics: Imipenem Cilastatin
Yang[122]	2012	China	multiple	15 months	Octreotide

1.2.3 Clinical trials in CP

Apart from surgical and endoscopic interventions, the pharmacological treatments for CP mainly focused on antioxidants and PERT. PERT as a routinely used evidence based recommendation for CP patients with exocrine pancreatic insufficiency, although the concrete application might vary, its therapeutic role is without any doubt. Unlike PERT, however, due to lack of robust evidence, the antioxidant therapy is still not fully incorporated into clinical practice.

Morris-Stiff[123] found evidence for antioxidants deficiency in CP, and supplementation in these cases decreases analgesics demanding and hospital admission frequency. Nevertheless, the early notion that free oxygen radicals is crucial in the pathogenesis of CP facilitates the implementation of a series clinical trials in practice for CP using antioxidants (**Table 1.4**).

Antioxidant treatment was reported to improve life quality and function in cognition and emotion, significant hospital stay, pain, and to decrease inflammatory markers in patients with CP[124-127]. However, like studies conducted in AP, there is also conflict results suggested that antioxidants administration in patients with alcohol related painful CP does not improve neither pain nor life quality, despite increased antioxidants levels detected in blood[128].

Table 1.4 Antioxidant therapy in clinical trials for chronic pancreatitis

Author	Year	Study design	Study period	Enrolled patients	Antioxidants intervention
Banks[129]	1997	Crossover	/	26	Allopurinol
Bhardwaj[125]	2009	RCT	6 months	147	Selenium, β-carotene, α-tocopherol acetate, VC, Methionine
Bilton[130]	1994	RCT	20 weeks	30	SaMe
Castaño[131]	2000	Observational	52 weeks	19	Se, beta-carotene, VC, VE, SaMe
Dhingra[127]	2013	RCT	3 months	61	Selenium, β-carotene, VC, VE, Methionine
Díte P[132]	2003	Observational	54 weeks	70	VC and VE
Durgaprasad[133]	2005	RCT	6 weeks	20	Curcumin
Jarosz[134]	2010	RCT	6 months	91	VC and VE
Kirk[126]	2006	RCT	20 weeks	36	Se, β-carotene, VC, VE, SaMe
Salim [135]	1991	RCT	5 days	78	Allopurinol, DMSO
Siriwardena[128]	2012	RCT	6 months	92	Selenium, α-tocopherol acetate, Ascorbic acid, Methionine
Uomo[136]	2001	observational	108 weeks	3	Se, VA, VC, Mg, VE, SaMe

1.3 Need for treatment in pancreatitis

To date, the medical treatment for AP is limited to supportive and similarly, the current available therapy for CP aims at symptoms control and complications management, with no specific and radical medical products to interrupt disease progression for both acute[137] and chronic[138] pancreatitis. The failure or mixed results of extensive human RCTs including employment of protease inhibitors, anti-secretory, anti-inflammatory and anti-oxidants agents, which originally proved to be beneficial in experimental models demonstrate the variable and complexity of the disease. Despite the unsatisfied clinical results, there is still an unmet clinical demand which drives the motivation to better understand the physiological and pathological mechanism in pancreatitis. Experience acquired also provide a solid foundation for future exploration in pancreatitis.

1.4 Physiology of pancreas

The pancreas is a retroperitoneal glandular organ that consists of endocrine and exocrine dual secretory compartments. The only 1-2% endocrine component of pancreas contains five types of scattered Langerhans islets cells, which secrets insulin, glucagon, and somatostatins to regulate glucose homeostasis, the rest almost 98% exocrine pancreas is highly specialized for daily food digestion. Digestive enzymes (Proteases, pancreatic lipase and amylase, ribonuclease, deoxy-ribonuclease, gelatinase and elastase, etc.) and bicarbonate (1500–2000 mL of isosmotic alkaline fluid daily) are two critical secretory products for proper food digestion. The exocrine acinar cell are responsible for synthesis and secretion of digestive enzymes, whereas the epithelial cells lining small pancreatic ducts are the

main source of bicarbonate[139] (**Table 1.5**).

Table 1.5 The exocrine and endocrine function of pancreas

Normal Pancreatic Function		
Exocrine Function		Endocrine Function
Pancreatic acinar cell	Pancreatic duct cell	Islet of Langerhans, α, β, δ and F cells, etc
Secretion of enzymes, amylase, carboxylesterase, sterol esterase, lipase, Dnase, Rnase, etc. 1 Proteolytic enzymes (Trypsin, Chymotrypsin, Carboxypeptidase) 2 Lipid digesting enzymes (Pancreatic lipase, Phospholipase, Cholesterol esterase) 3 Pancreatic Amylase 4 Ribonucleases & deoxyribonucleases	Provide electrolytes 1 CL^- : secreted by acinar cells with small volume of water 2 $HCO3^-$: secreted by ductal cells with lager volume of water	Manufactures glucagon, insulin, somatostatin and pancreatic polypeptide for absorption into the bloodstream
Aid in digestion of proteins, fat and carbohydrates		Release hormone

1.4.1 Pancreatic acinar cells (PACs)

Pancreatic acinar cells (PACs) synthesize, store and secret copious quantities of the major active (lipase and amylase) and inactive (zymogen and trypsinogen) digestive enzymes, into an extensive system of ducts that channel secreted proteins into the duodenum, poised to respond to episodic feeding event. The PACs in exocrine pancreas have the highest rate of protein synthesis to fit the dietary need among all human tissues in adults which certainly requires large quantity of protein synthesis which need mitochondria to supply the energy[140].

Adapted from the physical activity needs, PACs have been demonstrated to have high basal-to-apical polarity. The basolateral part is composed almost entirely of rough endoplasmic reticulum, which forms a dense tubular network around the nucleus in the region and is copiously productive[141]. In contrast to the basal pole, the apical region is dominated by a zymogen granule rich and endo-lysosomal rich secretory pole, with mitochondria surrounding the apical pole and nucleus, also lying beneath the basolateral plasma membrane, providing energy source for these regions[142].

1.4.2 Pancreatic stellate cells (PSCs)

Pancreatic stellate cells (PSCs) are small quiescent cells located between acinar cells and around small ducts or vessels in the exocrine regions of normal pancreas, which only makes up 4-7% of the pancreatic mass[143]. Similar with hepatic stellate cells (HSCs), mediated by paracrine and autocrine stimuli, the PSCs will transform into myofibroblast-like activate state to proliferate and secrete excessive amounts of extracellular matrix (ECM) molecules to form pancreatic fibrosis[144].

1.5 Ca^{2+} signal and pancreatic cellular process

In eukaryotic cells, resting cytosolic calcium concentration ($[Ca^{2+}]c$) is around 100nM, whereas extracellular calcium concentration ($[Ca^{2+}]e$) is as high as 1mM[145]. The calcium homeostasis is well regulated through coordination of multiple proteins including membrane channels, calcium pumps and exchangers[146]. The cellular Ca^{2+} signal drives numerous process[147], such as gene expression[148, 149], secretion[150], contraction[151], cell proliferation[152], cell division[153] and cell death[154].

1.5.1 Physiologic Ca^{2+} signalling in the pancreas

The endoplasmic reticulum (ER) acts as the main intracellular calcium store and regulate calcium fluxes. Pancreatic secretion is maintained and modulated by delicate interaction between neural, hormonal and mucosal factors upon feeding stimulation[155] and Ca^{2+} plays the central controller of these physiologic activities within acinar cell[156].

1.5.1.1 Calcium signalling in PACs

The ER Ca^{2+} homeostasis is maintained by both pumps and channels, including the sarco-/ ER calcium – ATPase (SERCA) on the ER membrane that pumps Ca^{2+} to the ER lumen from cytoplasm, and the calcium channels located on the plasma membrane to regulate movement of Ca^{2+} from the extracellular space[157].

Cholecystokinin (CCK) and acetylcholine (ACh) are two physiological activators for the secretion of acinar cell enzyme and fluid, to evoke $[Ca^{2+}]c$ elevation in PACs. In brief, adenosine diphosphate (ADP) ribose cyclase and phospholipase C (PLC) were activated, respectively, upon CCK or Ach binds to their relative receptor on plasma membrane to form the second messenger nicotinic acid adenine dinucleotide phosphate (NAADP), cyclic ADP ribose (cADPR) and inositol trisphosphate (IP3)[158]. These second messengers further bind to receptors on the intracellular Ca^{2+}-releasing channels, including the IP3 receptors (IP3Rs) that locate in apical region and the ryanodine receptors (RyRs) that mostly distribute in the basolateral region, to elicit Ca^{2+} release from ER Ca^{2+} store. Ca^{2+} elicits further Ca^{2+} release through these receptors, which becomes inhibitory at higher concentrations.

The elevated Ca^{2+} levels are then cleared through plasma membrane Ca^{2+} ATPase pumps (PMCA) out of the cell to restore the normal basal Ca^{2+} level[147, 159].

The reduction of ER calcium due to Ca^{2+} release from ER store triggers aggregation and relocation of stromal interaction molecule 1 (STIM1) proteins to subplasmalemmal puncta where they interact with and activate Orai1, the structural component of the calcium release-activated channels (CRAC)[160]. Depletion of ER Ca^{2+} concentrations stimulate opening of store-operated calcium channels (SOC) on the plasma membrane, allowing Ca^{2+} flux into the cell. The elevated cytosolic Ca^{2+} levels were then prompt uptaken by the SERCA pumps to refill ER Ca^{2+} store[161, 162].

Three distinct groups of mitochondria located in separate sub-cellular domains, including peri-apical, peri-nuclear and sub-plasmalemmal supplying ATP for SERCA, PMCA and the ATP-dependent activities to complete signal process within PACs[147, 163-166].

1.5.1.2 Calcium signalling in PSCs

CCK binds to two receptors (CCK1R and CCK2R, with comparable affinity) that are expressed in many tissues, including the exocrine pancreas[167]. Stimulation with CCK regulates a wide range of physiological and pathophysiological processes.

It was demonstrated that both CCK1 and CCK2 receptors are expressed on rat PSC[168], however, PSCs do not display Ca^{2+} signals when stimulated with CCK, ACh, or carbachol (CCh) while all of them elicit a major Ca^{2+} signal response in the

neighbouring PACs[144]. On the contrary, bradykinin (BK) consistently evoked Ca^{2+} signals in PSCs, but had no effect on Ca^{2+} in closely neighbouring PACs[169-171].

1.5.2 Pathologic Ca^{2+} signalling in the pancreas

1.5.2.1 Abnormal Ca^{2+} signalling in PACs

Early in 1995, the hypothesis was proposed that abnormal, prolonged elevation of intracellular calcium concentration is the key trigger of PAC injury and the onset of AP[172]. IP3Rs, RyRs and Ca^{2+} ATPase pumps are the main sites that pancreatic toxins act to induce excessive Ca^{2+} release through resulting in the depletion of internal Ca^{2+} stores including within the ER[162, 173-176].

Upon supramaximal concentration of CCK and ACh exposure of PACs, leading to Ca^{2+} release into cytosol from the ER through IP3Rs and RyRs. Depletion of ER Ca^{2+} store activates redistribution of STIM1 to form the puncta ER- plasma membrane junctions with Ca^{2+} release-activated Ca^{2+} entry channels. Ca^{2+} in the apical region of PACs are overloaded and spread to basolateral region, causing global Ca^{2+} rise. Less ATP production by impaired mitochondria leads to failure of SERCA and PMCA pumps, resulting further accumulation of Ca^{2+} in PACs is activated through SOCE channel as compensatory mechanism for Ca^{2+} loss from internal cellular stores[177], allowing further release from the ER and so sustaining cytosolic Ca^{2+} overload.

1.5.2.2 Abnormal Ca^{2+} signalling in PSCs

Although the attained inflammatory mediator BK levels could induce Ca^{2+} signals in normal PSCs, there are insufficient data clarify it is BK elicited Ca^{2+} signals that

initiate PSCs activation. Nevertheless, a possible events sequence is suggested by Ole Peterson's group that released activated protease, such as kallikrein and trypsin, into the interstitial to act as kininogens and release BK, which in turn induce Ca^{2+} signals in PSCs, followed by activation, proliferation and ECM secretion of PSCs[169]. Trypsin and thrombin, which generated Ca^{2+} signalling in the nuclear that possibly resulting in proliferation of "primed" activated PSC to contribute to pancreatic injury[171]. They've also found that PSC seems to play a key role in a vicious circle to promote necrotic cell death in PACs, which the released trypsin from a few dying PACs generate Ca^{2+} signals in the PSCs and cause further damage in PACs and lead to more trypsin liberation[169].

Despite BK is the principal agent that evoking Ca^{2+} signals in the PSCs *in vitro*, in experimental alcoholic AP, PSCs showed less responsive to BK and then acquired sensitivity to trypsin[169, 170, 178].

Although no Ca^{2+} signals present in PSCs when stimulated with CCK, ACh, or muscarinic receptor activator carbachol (CCh), the activation of pro-fibrogenic pathways induced by CCK is comparable with transforming growth factor – beta (TGF- β) stimulated PSCs and these PSCs were found co-localized with alpha-smooth muscle actin (α-SMA), which depicts that CCK receptors may directly affect PSC activation.

1.6 Pancreatic toxins and calcium overload in AP

Bile acids, non-oxidative alcohol metabolites fatty acid ethyl ester (FAEE) and supramaximal CCK are three mostly studied AP-associated toxins. The PAC injury is initiated by excessive Ca^{2+} release from intracellular ER stores, studies with bile acids[173, 175], FAs and FAEEs[174, 179] confirmed the critical role of Ca^{2+} overload during the pathological process of PAC injury. Notably, despite all the pancreatic toxins mentioned above induce profound Ca^{2+} release from ER, the underlying mechanism and approaches of which are different.

1.6.1 Bile acid and AP

Bile acid, the water-soluble end products of cholesterol metabolism[180], are formed in the liver but absorbed actively from the small intestine. Ever since the first AP model was described[181] by retrograde infusion of bile and olive oil into a canine pancreas through the ampulla of Vater, bile salts including sodium taurocholate (Na-TC), and bile acid taurolithocholic acid 3-sulphate (TLCS) have been reported to induce AP in rodents. Until recent decades, the underlying mechanism of bile acids induced pancreatitis started to emerge, especially with the identification of the presence of G protein-coupled bile acid receptor (Gpbar) on the apical pole of PACs[182]. Data suggested that bile acids entry via Na^+-Taurocholate co-transporting polypeptide (NTCP) from the luminal surface or via Na+- independent but HCO_3^- dependent exchangers such as organic anion transporting polypeptide (OATP) from the basolateral membrane of PACs, with TLCS stimulates OATP receptor 1 at the luminal surface[183], induce Ca^{2+} release through both IP3Rs and RyRs opening, leading to elevations of pathological cytosolic and mitochondria calcium overload

on PACs, intra-pancreatic trypsinogen activation and acinar cell death. Additionally, TLCS is also able to inhibit Ca^{2+}-ATPase pumps by mitochondrial ATP production inhibition, and may occur via a direct action on SERCA pumps[184].

1.6.2 Fatty acid/Fatty acid ethyl ester and AP

Alcohol abuse, one of the most frequent aetiology in AP, however is not the greater proportion in heavy drinkers who develop pancreatitis compare to those who do not[185], suggesting the importance of additional cofactors.

Pancreas is found to degrade alcohol via both oxidative and non-oxidative ethanol metabolism. Ethanol can be metabolized by esterification with fatty acids (FA) to form fatty acid ethyl esters (FAEE) through non-oxidative pathway. Thus, pancreas has the highest rates of organ FAEE syntheses[186-190].

In vitro studies on isolated PACs support for the pivotal role of FAEE in the pathogenesis of alcoholic AP, whereas high concentration on ethanol and its oxidative metabolite acetaldehyde have little effects on the functional performance of PACs, relatively low concentrations of various FAEEs, is the key event for the initiation of pancreatitis. In the mitochondria, FAEEs are hydrolysed by FAEE hydrolase into fatty acids, such as hydrolysed product of POAEE, induced a concentration dependent, slowly rising, and sustained increase in calcium[179].

Ethanol alone only cause minimal pancreatic damage but sensitizes pancreatic acini to injury due to other stressors[191-193]. Whereas Ca^{2+} release induced by FAEEs via

IP3Rs, leading to the impairment of mitochondrial function and subsequent PAC necrosis. FAs, on the contrary, fail to induce significant Ca^{2+} release at levels reached *in vivo*.

Based on the study which depicts that the pancreatic injury is dependent on the formation of FAEEs[194, 195], a novel alcoholic AP model using combination of ethanol and FA was developed[196], with clinical relevant aetiology, pathobiology, clinical course, histopathology and outcome, mirroring alcoholic AP in humans.

1.6.3 CCK/ Caerulein and AP

Caerulein is a ten amino acid oligopeptide similar in action and composition to CCK, a hormone synthesized from the duodenal mucosa endocrine I-cells in response to nutrients, particularly proteins and 12-carbon chain or longer FAs in the small intestine into the bloodstream to stimulate smooth muscle and increase secretion of digestive enzymes.

Over a century ago, hormone secretin was found to stimulate pancreatic secretion. Since 1977, Lampel and Kern[197] described a nonlethal, acute oedematous pancreatitis model induced by intravenous infusion of caerulein (5 μg/kg/h) in rats for 24 h. Thereafter, experimental AP is successfully induced with caerulein in various species including mice[198, 199] , dogs[200] and rabbits[201]. Due to the strong reproducibility, simplicity, and the ease with which processes of intracellular protease activation can be studied, this model is highly favored[202].

The mechanism for CCK/caerulein induced AP model has been intensively studied over the past years. CCK stimulates acinar cells both directly[203] and indirectly via vagal nerve responses to activate muscarinic ACh receptors on PACs, causing pancreatic enzymes release into the small intestine, which can be altered by elements that can ultimately lead to AP. It has been shown that the supramaximal concentrations of CCK/caerulein triggers a series of signalling cascade pathways within the PAC, including co-localisation of lysosomal hydrolase and trypsinogen[204]. Precisely, the supramaximal concentration of secretagogue binds to its receptor initiate formation of NAADP, cADPR and IP3. These second messengers then bind to their receptors RyR and IP3R on the ER membrane, respectively, which elicits abnormal Ca^{2+} signalling causing Ca^{2+} overload, results in pancreatic injury. The process is mediated by CCK1 receptor expressed on PACs.

The mode of CCK action is biphasic with low concentration ranges are associated with physiological responses and activate high affinity receptors, while low affinity receptors are activated by high concentrations of CCK associated with hyperstimulation and Ca^{2+} overload[205]. Thus, this model is most similar to the AP caused by scorpion venom and cholinergic toxins that are regarded to represent supraphysiologic neurohumoral stimulation[202].

Despite similar action and composition with CCK, due to longer half-life *in vivo* compare to CCK and improved stability against biological degradation, caerulein is predominately preferred in experimental models[206].

1.7 Pancreatic toxins and collagen production in CP

Caerulein and ethanol are two most studied toxins to induce pancreatic injury in CP. Rat PSCs are activated on exposure to ethanol and acetaldehyde[207]. Both stimulus at clinical relevant concentrations induced type I collagen expression, activator-protein (AP-1) and extracellular signal-regulated kinase 1/2 (ERK1/2), c-Jun NH (2)-terminal kinase/stress-activated protein kinase (JNK/SAPK), and p38 mitogen activated protein kinases (MAPK) activation in a time dependent manner in rat PSCs[208].

As mentioned before, ethanol itself, does not cause Ca^{2+} oscillations in PACs, while FAEE elicits Ca^{2+} rise even at low concentrations, leading to impairment of mitochondrial function and subsequent necrosis of PACs. In human PSCs, however, ethanol itself upregulates DNA synthesis and procollagen type I-c peptide production while another type of FAEE, the palmitic acid ethyl ester (PAEE) has no impact on proliferation and collagen production; interestingly, both ethanol and PAEE could increase AP-1, activate ERK, JNK and p38 MAPK pathway and induce interleukin-8 (IL-8) production[209].

Despite substantial efforts on clarifying the pathogenesis and natural course of CP, a satisfactory clinical relevant animal model has not yet been established[210]. The notion that recurrent AP episodes cause chronic pancreatic injury in human has led to the development of using repeated bouts of caerulein-induced AP (CER-AP) during several weeks to induce chronic pancreatic injury with collagen deposition and inflammatory infiltration to mimic human CP pathogenesis.

Furthermore, CCK could direct activate PSCs to induce collagen synthesis through activation of pro-fibrogenic pathways such as Akt, ERK, and Src, which are mainly mediated by CCK2 receptor on PSCs[168].

1.8 Mitochondria dysfunction in pancreatitis

Mitochondria dysfunction is an early event which plays a central role in different pancreatitis models, and tissues from patients of pancreatitis also had marker of mitochondria damage and impaired autophagy[211]. A principle effect of mitochondria defect is cell death, resulted from either mitochondrial outer membrane permeabilization (MOMP) that directly promoted intrinsic apoptosis or mainly through mitochondria permeability transition-driven necrosis[154, 212-215]. Perturbations of Ca^{2+} signalling has been linked to both types in the PACs. When oscillatory global rises of $[Ca^{2+}]c$ may induce apoptosis, whereas sustained $[Ca^{2+}]c$ elevation promote necrosis, the differences may relate to mitochondria function. Ca^{2+} overload can drastically reduce ATP production, with partial mitochondria depolarisation which does not adversely influence ATP production leads to apoptosis, while full membrane potential collapse and ATP deletion promotes necrosis[154].

1.8.1 Intrinsic apoptosis and pancreatitis

Intrinsic apoptosis is a form of regulated cell death initiated by a variety of extracellular or intracellular microenvironment perturbations including ER stress, oxidative stress, demarcated by MOMP, and precipitated by executioner caspases, mainly caspase 3[216]. The irreversible and widespread MOMP directly promotes release of apoptotic factors, which normally reside in the mitochondrial

intermembrane space release (cytochrome c, *etc*,) to cytosol. The process is controlled by pro-apoptotic or anti-apoptotic members of BCL-2 family, which are activated as specific organelles or cellular compartments experience homeostasis perturbations, operating as cellular transducers of stress signalling[216].

Despite human pancreatitis mostly manifested as necrosis, *in vivo*, cell death pattern is less distinctive between each other. While apoptosis allows for the rapid clearance by macrophages or other cells with phagocytic activity[217], necrosis triggers acute exudative inflammation of surrounding tissues, for which it has been generally believed that the apoptosis in AP is protective and may shift the severity of disease, thereafter, it is more favourable. Indeed, studies suggest that promotion of apoptosis is beneficial, whereas inhibition is harmful[218, 219].

In CP, apoptosis, however, appears to promote the severity of disease, which was shown to play key role both in the initial stages and during the progression of CP. Increased mitochondria membrane potential ($\Delta\Psi m$), loss of ATP, and significantly increased activation of caspases, p53, Bax expression and cytochrome c release with differential grade levels according to disease classification were found in pancreatic tissues from CP patients, suggest the involvement of mitochondria intrinsic pathways[220]. As pro-apoptotic protein, p53 has also been shown overexpressed in 50% CP patients in a separate study[221].

1.8.2 MPTP-driven necrosis and pancreatitis

MPTP-driven necrosis is a form of regulated cell death triggered by perturbations of the intracellular microenvironment and relying on Cyclophilin D (CypD)[216]

MPT pore (MPTP) is a 40 nm, Ca^{2+} - sensitive channel with multi- compartments on the inner mitochondrial membrane (IMM), in response to toxins stimulation, calcium overload and oxidative stress, which enables a sudden increase of the permeability for the IMM to become non-selectively permeable to molecules smaller than 1500 Da, causing mitochondrial membrane potential (Δψm) collapse, proton gradient dissipation, ATP loss and finally cell death[222-224].

During early studies, several proposed components of MPTP include adenine nucleotide translocator (ANT), voltage-dependent anion channel (VDAC) and phosphate carrier (PiC) haven later been revealed to be not indispensable for MPTP in genetic manipulation studies[225-227]. Findings on *Ppif*$^{-/-}$ mice (ablation of mitochondria matrix protein CyPD) have demonstrated that CypD is an important modulator which sensitizes the MPTP to Ca^{2+}, but not an essential pore component[228, 229]. Recent discoveries have identified F-ATP synthetase as its central component and the interaction between CypD possibly implicate novel structure of MPTP, as reports suggested the dimers of F0F1-ATP synthase form the MPTP and the regulator CypD) binds to the F0F1-ATP synthase in the oligomycin sensitivity-conferring protein (OSCP) subunit[224, 230, 231], suggesting the mitochondria matrix protein CypD to be a viable target for MPTP inhibition.

Indeed, with emerging data shown MPTP to be the central mediator of universal necrotic pathway activation, studies on pancreatic acinar cell reported that sustained cytosolic Ca^{2+} overload induced by diverse AP precipitants such as bile acids or FA/FAEEs lead to Ca^{2+} dependent MPTP opening, mitochondrial membrane

potential depletion, uncoupling of oxidative phosphorylation, impaired ATP production and finally acinar cell necrosis[173, 232-235], which depicts the central role of MPTP opening in pancreatic injury. The non-oxidative alcohol metabolites FAEEs are also shown to bind and accumulate within the inner mitochondrial membrane, where hydrolases act to release high concentrations of FAs locally[174]. FAs, relevant to hypertriglyceridemic AP, have direct effects on the electron transport chain without depolarization of the inner mitochondria membrane[159].

CypD-deficient mice has shown to develop less severe AP in response to the combined administration of ethanol and CCK[236]. And Mukherjee has demonstrated the mechanism and consequences of MPTP opening to be fundamental of multiple forms of AP via toxin-induced IP3R and RyRs calcium channel release, resulted in diminished ATP production, leading to impaired calcium clearance, defective autophagy, zymogen activation, cytokine production, and necrosis, with genetic and pharmacological inhibition of CypD protect against pancreatic injury in mouse and human PACs and in four diverse experimental models of AP[237].

1.8.3 Mitochondria homeostasis and pancreatitis

Mitochondria architecture involves in multiple functions crucial for cell viability, proliferation, senescence, and signalling. In particularly through the balance between fusion and fission events, mitochondrial dynamics represent the central mechanism for bioenergetics adaptation to metabolic needs of the cell and constantly undergo fission and fusion to regulate the expansion and morphology of the mitochondrial network. Through growing, splitting, fusing and moving within the cell and the

dynamics of mitochondria are therefore essential for regulating their number, size, location and also repairing damaged components by segregating exchanging material. The fusogenic mitofusion have recently been linked to mitochondria biogenesis and respiratory functions, impacting on cell fate and organism homeostasis[238-240].

The cellular organelles, such as mitochondria, endolysosomes, ER as a highly dynamic network of interacting compartments, which exchange signals and materials to maintain and balance cellular homeostasis. Disordering of theses organelles, in particular those leading to autophagic/ lysosomal and mitochondria dysfunctions, is increasingly implicated in the pathogenic mechanism of both acute and chronic pancreatitis[241].

1.9 Endoplasmic reticulum stress

The PACs have abundant ER due to its prominent role in digestive enzyme synthesis and the secretory pathway. ER contributes to synthesis and correct folding for one-third of proteins, and is inextricably linked to the maintenance of cellular homeostasis as well as the balances between health and disease[242]. Being the main cellular compartment for Ca^{2+} storage, ER plays a pivotal role in the regulation of Ca^{2+} levels and reciprocally many ER functions are controlled in a Ca^{2+} -dependent way, thereby regulating the calcium homeostasis of the whole cell[243, 244].

1.9.1 Physiology of ER

ER provides post-translational modification, proper folding, attainment of native state and finally their transportation for protein maturation with a system consists of multiple chaperones that simultaneously promote folding and perform quality control[245]. Once proteins enter the ER lumen, the chaperone-assisted folding process, start with their native conformation and undergo multiple post-translational modifications, incorrectly folded proteins are retained in the ER, bound to the chaperone, until the folding process is complete[246-248].

The primary peptide-binding chaperone is glucose regulated protein or glucose related peptide-78 (GRP-78, also known as BiP), which belongs to the heat shock protein (HSP) 70 family. Upon exposure to stress, GRP-78 is released from ER stress sensors which are described below for binding with unfolded proteins.

1.9.2 Unfolded Protein Response

The protein folding capacity in ER is limited by chaperone resources and can be exceeded with high demanding during growth and differentiation, or perturbations such as protein overexpression or expression of mutated protein, insufficient energy provision, oxidative stress and calcium depletion[248]. When large quantities of unfolded proteins flux into ER, which exceeds the capacity for protein load, leads to accumulation and aggregation of misfolded or unfolded proteins in the ER lumen. To restore ER homeostasis, a specific stress response called the unfolded protein response (UPR) as well as the ER associated protein degradation (ERAD) to couple

the ER protein load with the folding capacity and subsequent degradation of unfolded proteins are activated[249].

Three signalling components expressed in the ER membrane are activated in response to stress: the double-stranded RNA-activated protein kinase-like ER resident kinase (PERK), also called pancreatic eukaryotic initiation factor-2α kinase, activating transcription factor (ATF) 6 and the inositol requiring protein 1 (IRE1)[250]. Under homeostasis state, the three sensors are kept inactive through association with the abundant ER resident GRP-78/BiP. While excessive unfolded proteins accumulate in the ER, GRP-78 shifts away from three sensors and preferentially associates and help with unfolded proteins. Owing to BiP dissociation, three ER stress sensors are able to transmit an organelle-specific stress signal into a global cellular signal upon activation to facilitate their downstream signalling partners[248]. PERK activation leads to subsequent phosphorylation of eIF-2 and results in a general decrease translation initiation. Activation of ATF6 and IRE1 regulate expression of ER-based chaperones and other protective molecules[248, 251-253].

Thus, the UPR clears misfolded proteins and alleviate stress through shutting down translation or upregulating molecules that help folding, however, prolonged unresolved ER stress, and increased UPR activation may lead to cell death mediated largely by increased expression of the transcription factor CCAAT/enhancer binding protein (C/EBP) homologous protein (CHOP)[254-256]. Therefore, the UPR can either be adaptive to restore ER homeostasis, or to activate cell death.

1.9.3 ER stress and AP

Kubisch investigated the presence and activation of major ER stress sensors in PACs and demonstrated the activation of ER stress occurs early in the arginine model of pancreatitis[257]. Studies shown that CCK8 at supramaximal concentrations was able to activate all of the major pathways of UPR, including PERK within 5-20 minutes and to induce CHOP expression as well[258]. The pancreatic precipitant FA has also been shown to induce ER stress in pancreas with different effects due to various FA type[259].

While study suggested activation of the UPR pathway is protective[260] and chaperone GRP-78 plays an anti-apoptotic role in regulating the cell death response during AP[261], Suyama's group demonstrated that ER stress-CHOP pathway accelerate pancreatitis through inflammation associated with caspases and IL-1beta[262].

1.9.4 ER stress and CP

Not only a close association has been suggested between AP and ER stress[263], emerging data also indicates that ER stress is chronically activated and induced early in CP pancreatic injury through pathologic calcium signalling independent of trypsinogen activation[264]. Lugea's group also found that in long term ethanol feeding mice, defective UPR results in ER dysfunction and acinar cell pathology[265].

Notably, the PACs seem to be particularly susceptible to ER homeostasis perturbations, and mechanisms that relieve this stress have been shown to be necessary for normal pancreatic development; for instance, PACs death and atrophy

were the predominant outcome of ablating PERK in the exocrine pancreas, a subset of severely affected animals harboured some acini that had apparently differentiated into duct-like structures[266].

1.10 Reactive oxygen species (ROS)

Reactive oxygen species (ROS) refers to oxygen that containing both free radicals and other reactive molecules, including superoxide anion ($O2^{\bullet -}$), hydroxyl radical $OH^{\bullet}$ and hydrogen peroxide (H_2O_2). Functionally, ROS is important in innate immunity, protein folding and cell signalling transduction.

1.10.1 Sources of ROS

Physiologically, cellular ROS derives from different sources[267].

Oxidative phosphorylation in the mitochondria which generates majority of all primary cellular ROS, especially $O2^{\bullet -}$ as a result of electron transport chain (ETC) activity in the mitochondria[268].

In addition to Mitochondria, ROS is also generated as natural by-products during normal metabolism of oxygen in the ER. ROS levels dramatically increase under stress, the persistent elevated ROS in the context of a compromised ER stress response may initiate a vicious cycle for significant damage to cells, leading to ER collapse and cell death. It has also been observed that ROS accumulated from UPR oxidize thiol groups in RyRs to activate these receptors in muscle and neurons, which resulting in calcium efflux from the ER[248]. ROS generated by ER peroxidases are reported to possibly involved in the ER overload response mediated induction of NF-κB activity[247, 269].

1.10.2 ROS and AP

Similar with ER stress, oxidative stress is known to occur early in pancreatitis[270]. Study suggests that the mitochondria dysfunction induced ROS modulates ATP generation, which when inhibited could result in acinar necrosis. Neutrophil generated ROS and mitochondrial ROS result in the activation of inflammatory pathways in acute pancreatitis. It has also been shown that ROS accumulation from UPR under prolonged ER stress contributes to cell death[271, 272].

The generation of ROS may constitute a protective mechanism that disposes of stressed PACs, since bile acid induced ROS production increased apoptosis with a concomitant reduction of necrosis[213, 273], however, the protective role of ROS in experimental AP barely show any beneficial from RCTs for antioxidant therapy as mentioned in previous section.

1.10.3 ROS and CP

Oxidative stress occurs early in cells exposed to alcohol or its metabolite acetaldehyde. Both acetaldehyde and intracellular oxidative stress can activate stellate cells. Early studies stated activation of PSC originates tissue damage which due to cell death and tissue ischemia derived from free O_2 Radicals caused lipid peroxidation and chemoattractant. Braganza also demonstrated strong association of oxidative stress and chronic pancreatitis. Later reports clarified that antioxidants treatment attenuated high glucose induced PSC activation[274] and ROS might be candidates for the development of anti- fibrosis therapy targeting PSCs[275]. Similar with antioxidant therapy applied in AP trials, however, the results from RCTs also showed inconsistent effects in CP.

1.11 Cyclophilins

1.11.1 Peptidyl-prolyl cis-trans isomerase and cyclophilin family

Peptidyl-prolyl-cis/trans isomerases (PPIases) are ubiquitously expressed foldases function in protein folding by catalysing the conversion between cis and trans isomers of proline imidic peptide bonds in oligopeptides[276] (see **Figure 1.1**).

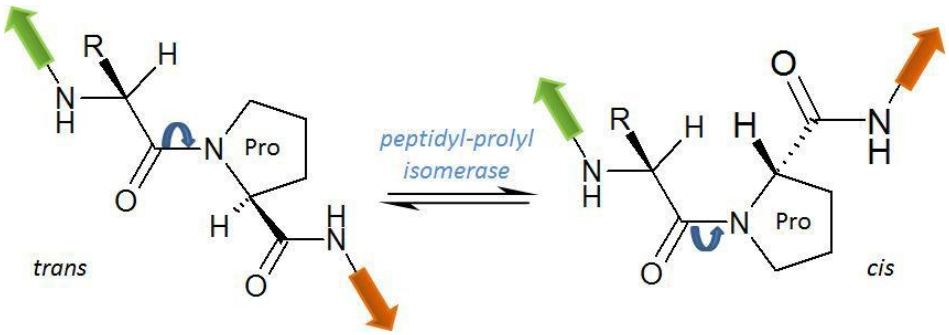

Figure 1.1 Schematic illustration of the cis - trans isomers action

The interconvention between the two forms is catalysed by peptidyl-prolyl isomerases (cyclophilins, FKBPS or parvulins)

The PPIases are highly abundant in both prokaryotes and eukaryotes, including cyclophilins[276], FK-506-binding proteins (FKBPs)[277] and parvulins[278] three families, which have been implicated in a wide range of biological functions such as protein folding, post-translational modifications and protein transportation, assembly of essential cellular protein complexes, and cell signalling *etc*. Each of the PPIases class has their specific natural inhibitors, the cyclophilins are inhibited by cyclosporins, peptolide (SDZ 214-103 and its analogues) and sangliferhrins, the FKBPs bind to and are inhibited by FK506, ascomycin (analogue of FK506, also called FK520) and rapamycin (also known as tacrolimus), the third class parvulins can be inhibited by naphtoquinone julone. Inhibition of PPIase is proven to be

beneficial in immunosuppression, inflammation, cell death, cancer, protozoan and viral infection.

As the first discovered family of the PPIases in 1980s by Fischer's group[279], cyclophilins regulate a diverse array of protein functions, including molecular chaperones, protein folding, intracellular trafficking, and maintenance of multiprotein complex stability[280], most of them are characterized by high-affinity binding to the inhibitor, immunosuppressant cyclosporin A (CsA).

Since the discovery of the first cyclophilin, at least 20 different human cyclophilin isoenzymes have been identified and found broadly distributed among all organs and cellular compartments in organisms ranging from bacteria to humans[281, 282]. In human, cyclophilins are found to be present in large amounts in brain cortex, parotid, thymus, spleen, pancreas, lymph node, kidney, intestines, heart, fatty tissue, liver, lung, and skin, in a range of 0.8-2.8 μg/mg protein of tissue[283]

Four best studied isoforms of cyclophilins CypA, CypB, CypC and CypD (encoded by gene PPIA, PPIB, PPIC and PPIF, respectively) are classified predominantly on the basis of distinctive cellular locations in the cytoplasm, ER and mitochondria, providing unique functions, which will be further described in the next few sections.

Other cyclophilins, for instance, a number of nuclear cyclophilins, including CypE, CypG, Cyp H, Cyp J and Cyp60 remain within the nucleus where they are engaged in spliceosome formation and function[284], whereas the largest member RanBP2 (360

kDa) functions in the nuclear membrane and acts as a nucleoporin[285]. While 4 main cyclophilins are involved in viruses replication and cancer, similarly, Cyp40, CypE, CypG, and CypH are also involved in replication of diverse viruses [286], and both Cyp40 and CypJ are engaged in malignant transformations[287], CyP60 also plays an important chaperone role in the translocation of extracellular cyclophilin receptor CD147 to the cell surface[288].

1.11.2 Cyclophilin A

The 18-kDa cytosolic CypA is the most abundant cyclophilin, accounting for 0.1–0.4% of total cellular protein[289], involved in protein folding, cellular signalling transduction, immunosuppression and apoptosis. CypA is a modulator of $CD4^+$ T cell signal transduction[290], T helper type 2 (Th_2) cytokine production, and a secreted growth factor that augments the proliferation of human embryonic brain cells and vascular smooth muscle cells. It is also known to regulate HIV infectivity and to modulate hepatitis C viral replication[286].

CypA also acts as one of the inflammatory mediators involved in the pathogenesis of Rheumatoid Arthritis (RA)[291], and CypA treatment has been reported to induce macrophage chemoattractant protein-1 (MCP-1), TNF-α , IL-8 and IL-1 expression in a dose- dependent manner.

1.11.3 Cyclophilin B

The 22kDa Cyclophilin B (CypB) is unique with ER targeting sequence, despite the fact that it is also been found in the nucleus and detectable in blood, milk,

extracellular space and released from cartilage chondrocytes in response to activated matrix metalloproteinases (MMPs).

CypB promotes protein conformation alteration and facilitates the nuclear retrotransport. As one of the ER protein folding chaperones, CypB is reported to be a component of enzymes forming ER-localized large multiprotein complex consists of roughly 10 molecular chaperones including GRP-78, GRP-94, GRP-172, CypB, *etc*., which aids and monitors newly synthesized protein folding during ER quality control[292-294]. The physically association with GRP-78 in this complex, suggesting CypB plays a role during ER stress. Later on, siRNA-based CypB knockdown studies consistently indicate it is crucially required for cell survival in response to ER stress and characterized by suppression of Ca^{2+} leakage from ER, ROS production, Bax translocation to the mitochondrial, mitochondria membrane depolarization, and also by reduction of caspase activation. Ca^{2+} leakage from the ER accelerate electron transport and stimulate ROS production[295], and blockage of Ca^{2+} leakage from ER, as a result of CypB overexpression in the ER, inhibited both mitochondria damage and ROS production.

Similar with CypA, CypB has also been demonstrated to participate in multiple functions such as signal transduction including hepatitis virus replication[296], immunosuppression[297], chemotaxis[298], malignant progression and regulation of genes implicated in multiple cancers[299]. Other studies also identified CypB as the key regulator of several signals that fuel oncogenesis in glioblastoma, including mutant p53, c-Myc (MYC) and Chk1[300]. CypB has shown to facilitate the nuclear

retrotransport and to regulate Jak2 expression post-transcriptionally[301]. Interacting with a number of proteins, CypB not only to regulate Ca^{2+} homeostasis, but also to promote protein synthesis, proliferation and folding, such as the interaction with IgG to promote its biosynthesis, to regulate Stat3-dependent cell proliferation[302]. Moreover, CypB is associated with type I collagen formation with the finding that post translational prolyl-3-hydroxylation of type I collagen by P3H1 was essentially absent in CypB-deficient cells and tissues from CypB-knockout mice[303].

1.11.4 Cyclophilin C

CypC contains similar ER-targeted sequence as CypB, but differs from both CypA and CypB due to restrict distribution mostly in kidney. Friedman's group has compared the expression pattern of cyclophilin A, B and C in mouse tissues using in situ hybridization, revealing that CypA and B are widely expressed, whereas the CypC is tissue specific expressed in a restricted arears including kidney, bone marrow, mouse ovary, and testis but not detectable in liver, spleen, small intestine, *etc*. Within the kidney, CypA and B are expressed diffusely relatively homogenously throughout the kidney parenchyma, whereas expression of CypC is highest in the outer medulla, revealing a spiked appearance.

Using monoclonal antibodies reactive against CypC, Friedman's group also found that CypC expression correspond to the proximal tubular cells including the S3 segment of the nephron, which occurs in the medullary rays, and concentrated at their luminal aspect[304]. CypC has been reported to involve with the class I molecule

HLA-A2, and depletion or overexpression of CypC impaired the degradation of class I molecules[305].

CypC-associated protein (CyCAP) or Mac-2 binding protein has been identified as the binding protein for CypC in mice[306] and for Mac-2 (galectin-3) in human, both of which are localized in ER area, where is close to the nuclear membrane [307]. CyCAP has regarded as protective in the response to endotoxins by down-modulating the pro-inflammatory response *in vivo*[308] and proved to be a mediator for fibronectin fragment-induced MMP-13 expression[309]. Moreover, CyCAP appears to manipulate macrophage functions by activating nuclear factor of activate T cells (NFAT) and the resultant IL-2 production[310].

1.11.5 Cyclophilin D

The 22kDa mitochondria matrix located CypD expresses in all human cell types with a lower level than CypA, respect to its mitochondrial targeting[311], CypD plays a pivotal role in modulating mitochondria permeability transition pore (MPTP) opening and mitochondria Ca^{2+} homeostasis control, ensuring optimal metabolic function and appropriate cell death activation[228, 312, 313]. CypD is reported to interact with varieties of proteins at mitochondria, including ANT-VDAC complex, PiC, ATP synthase, p53, C1QBP, GSK3- β/ERK2, SIRT3, STAT3, IP3R1-GRP75-VDAC1 complex, amyloid-beta protein, Bcl2, HSP60, HSP90-TRAP1, MST1, DnaJC15, etc[314], and CypD ablation mice were used in muscular dystrophy[315], Parkinson's disease[316], multiple sclerosis[317, 318], Alzheimer's disease and aging[319-321] to study the MPTP, suggesting its indispensable role in MPTP opening.

Recently, CypD ablation has been reported to trigger a metabolic shift in *Ppif*$^{-/-}$ mouse kidneys towards glycolysis and Krebs cycle activity, interestingly activation of pro-surviving ERK1/2 kinase and inhibited expression of pro-apoptotic and pro-fibrotic JNK and TGF-β1 proteins in *Ppif*$^{-/-}$ females was observed[322], suggesting a gender differentiate protection effect in response to stimuli.

1.11.6 Extracellular cyclophilins

Up to now, CypD, CypE, CypH and Cyp40 have been found to occur only intracellularly[323], while both CypA and CypB were detected in patients' serum in severe inflammatory diseases such as sepsis. CypC and CypL1 have also been found in extracellular spaces despite their intracellular location at ER and nucleus or cytoplasm, respectively. CypC was found to be secreted from different cultured cells whereas CypL1 has been detected in the exosome-enriched fraction from normal human urine[323].

1.11.6.1 Extracellular cyclophilins and chemotactic activities

Studies have demonstrated the chemotactic activity of extracellular CypA and CypB for monocytes, neutrophils, eosinophils and T lymphocytes[324]. Indeed, extracellular cyclophilins exhibit cytokine-like properties and mediate numerous intracellular events. In patients with ongoing RA, CypA within synovial fluid was identified directly correlate with neutrophil numbers present in the same fluid. Furthermore, CypA is able to induce a rapid local inflammatory response characterized by neutrophil influx, when injected in vivo into mouse footpads. Later on, studies

suggest that CypA to be secreted and released by various live or dead cells and activated platelets in response to inflammatory stimuli and oxidative stress into extracellular tissue spaces[324]. The secretion of CypA was shown to proceed via a vesicular pathway, with secreted CypA protein detectable within 30 minutes of stimulation ROS stimulation[325].

1.11.6.2 Interactions between extracellular cyclophilins and the receptor CD147

The chemotactic capacity of extracellular cyclophilins depend on their interaction with the cell surface signalling receptor CD147 in a manner that is proline-dependent and mediated through the active site of the isomerase, which has been identified and characterized by nuclear magnetic resonance (NMR) techniques. The cyclophilins catalyse the cis and trans isomerase conversion of proline imidic peptide bonds but at different sites of CD147 domain. CypA catalyses the PPIase of proline 211 in the extracellular domain of CD147, similarly, CypB also enzymatically catalyse residue of proline but at proline 180[326].

Known as extracellular matrix metalloproteinase inducer (EMMPRIN), CD147 is a 269-amino-acid-long type I transmembrane glycoprotein expressed by a wide array of cell types, including all human peripheral blood leukocytes, haematopoietic, epithelial, endothelial cells and fibroblasts[327]. CD147 has been shown to be the principal signalling receptor for extracellular cyclophilins to mediate their chemotactic activity towards a variety of immune cells.

CD147 involves in a wide range of both physiological and pathological activities and correlates well with MMP-1 levels that stimulate collagenase production by

fibroblasts through MAPK pathway[328]. High CD147 expression on monocytes or macrophages significantly up-regulated MMP-2 and MMP-9 production in RA. CD147 mediated signalling orchestrated by other proteins interactions including integrins, syndecan-1 and CD147 enzyme ligands, the cyclophilin class of peptidyl-prolyl isomerases[291, 329].

1.11.6.3 Cyp/CD147 & Inflammation

The binding of CypA towards CD147 is required for CypA-mediated MMP-9 production, in turn to transduce NF- κB signalling. While inhibition of ERK1/2 or JNK MAPK pathway suppressed CypA-induced MMP-9 production by inhibiting the activity of NF- κB[330], macrophages may be stimulated via MMP-9 expression and promote inflammation via pro-inflammatory cytokine secretion[331].

The Cyp/CD147 interaction lead to chemotactic response, which contributes to the leukocytes recruitment from the periphery into tissues during inflammation. Blocking these binary interactions using agents targeting either CD147 or cyclophilin activity demonstrated significant anti-inflammatory effects to suppress neutrophil influx into inflamed tissues and decrease migration of immune cells to the site of inflammation. For instance, in lipopolysaccharide (LPS) induced lung injury, asthma-mediated responses and arthritis model, treatment with anti-CD147 mAb blocked Cyp-CD147 interaction, reduced up to 50% tissue neutrophilia and brought >50% reduction in lung eosinophilia and airway hyper-responsiveness, which finally inhibited joint inflammation by more than 75% reduction,

respectively. Vice versa, Cyp-CD147 interactions can be blocked with CsA non-immunosuppressive analogue NIM811 via cyclophilin inhibition[332] as well.

Notably, both the signalling and chemotactic activities of CypA and CypB are also depend on heparin sulphate proteoglycans (HSPGs) on the membrane, as HSPGs removal from neutrophils cell surface eliminated signalling responses and abolished cyclophilin-dependent chemotaxis and adhesion of neutrophils and T cells[329, 333, 334].

1.11.6.4 Cyp/CD147 & Ca^{2+} mobilization

The mobilization of $[Ca^{2+}]c$ relates to the ability of cell-cell and cell-ECM adhesion. CD147 enhanced calcium mobilization via binding with CypA on neutrophils, anti-CD147 antibody blocked CypA-induced $[Ca^{2+}]c$ and small interfering (Si)-CD147 or anti-CD147 mAb dramatically reduced calcium mobilization in neutrophils[291].

1.11.6.5 Cyp/CD147 & Fibrosis

CD147 is able to stimulate MMPs secretion, which is responsible for the reconstruction of ECM. Extracellular CypA affected transcription of several genes, including CD147 in smooth muscle cell and pancreatic cancer cells, however, study failed to show that CypA-induced smooth muscle cell proliferation is blocked by anti-CD147 antibody[329], while Allain and colleagues demonstrated a strong inhibitory effect of anti-CD147 antibody on CypB mediated adhesion of lymphocytes to fibronectin, a process dependent on CypB induced signalling[333].

Furthermore, cyclophilin inhibition was shown to reduce liver fibrosis in non-alcoholic steatohepatitis, possibly augment activity of chemotherapy against hepatocellular carcinoma and decrease the metastatic spread[335].

1.12 Natural cyclophilin inhibitors

1.12.1 Discovery of CsA

Following a programme for antibiotics screening from Sandoz Ltd of Basel (now known as Novartis), Switzerland, a specific fungus was discovered to synthesize neutral and lipophilic metabolites, which were later termed as cyclosporin.

Cyclosporin A, as the first isolated and characterized cyclosporin is the main cyclosporin produced by the fungus *Tolypocladium inflamtum Gams* (*Beauveria nivea*) after several reclassify. Since the discovery of the cyclic undecapeptide drug cyclosporin A in 1973, the structures of cyclosporins were then determined and published in 1976 showing that the cyclosporins were indeed cyclopeptides[336]. Each cyclopeptide was made up of 11 amino acids, with one new amino acid[337].

Later, the cyclosporins were found to mediate immunosuppression through inhibiting T lymphocyte proliferation. Borel then have summarized the properties of cyclosporin A which outlined orally to a Cambridge transplantation group, which then started the first animal test outside Sandoz and proved to be satisfactory, the following clinical trials also begun in Cambridge[338]. CsA was further developed as an immunosuppressive agent and approved by the US Food and Drug Administration for clinical use in 1982 in solid organ transplantation.

1.12.2 Structure, metabolism, distribution and bioavailability of CsA

The atomic structure and the alignment of 11 amino acid, first elucidated in 1976, suggest CsA is a lipophilic cyclic undecapeptide (**Figure 1.2**), with a molecular weight 1202kDa containing 7 *N*-methylated peptide bonds and 3 non-proteinogenic amino acids, with the carbon chain of the unique amino acid (N-methylated 4-butenyl-4-methyl-threonine; Mebmt) at the position 1 is essential for its biologic activity[339].

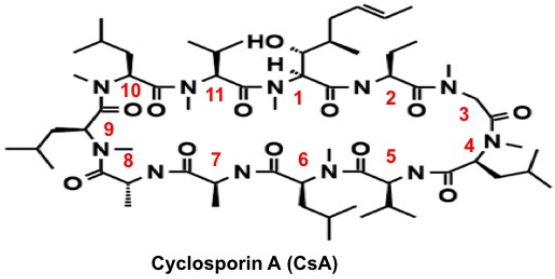

Figure 1.2 Atomic structure and amino acid alignment of CsA

Oral CsA is available with two dosing forms: either the oil-based formulation (Sandimmune) or the newer microemulsion formulation (Sandimmune Neoral). The intravenous formulation of CsA consists in the form of CsA, polyoxyethylated castor oil (Cremophor EL) and ethanol.

CsA is converted through isoenzymes of the hepatic cytochrome P-450 superfamily into metabolites with higher polarity but retain the cyclic structure. Precisely, primarily metabolised via bio trans formation by liver cytochrome P 450IIIA (LM-3c) in rabbits, IIIA (PCN) in rats and IIIA (HLp/NF) in humans[340, 341 342, 343], resulting in qualitatively similar metabolite profiles in blood, bile and urine. In human, CsA is extensively metabolised by the liver into N-demethylated,

hydroxylated, dihydroxylated, hydroxydemethylated cyclized metabolites, rather than degradation of the compound[344], which are excreted mainly into the bile and faeces[345].

There are more than 30 CsA metabolites have been observed and been excreted as relatively inactive and unconjugated. However, traces of sulphate conjugated CsA-metabolites have been detected in human plasma and bile[346, 347], and a glucuronide of metabolite M18 has also been detected in human bile collected from liver- grafted patients[348-350].

About 60% of circulating CsA in the blood cells are bound to the erythrocytes, 10% to the leukocytes, and the remainder bound to plasma lipoproteins[351], showing 34% associated with LDL, another 34% with HDL, 10% with VLDL and the remaining 22% is bound with non-lipoproteins[352]. While tissue drug concentrations appear to correlate with tissue levels of cyclophilin and lipids, animal studies have showed CsA is extensively distributed throughout the body with highest concentrations present in liver, kidneys, endocrine glands and adipose tissue. Skin and adipose tissue were the main storage site for unchanged CsA[353]. In human, CsA and its primary metabolites were found in the renal tissue of patients on CsA therapy until the time of nephrectomy. Most of CsA and its metabolites are excreted into the bile and faeces, and only 1% of total biliary CsA is the parent compound[345, 354].

CsA exhibits linear elimination with a half- life up to 19 hours but vary in different recipients, which is age-dependent. Patients with hepatic impairment or reduced LDL levels in serum, and possibly also in the elderly has a decreased drug clearance.

Oral absorption of CsA is slow and incomplete with maximum plasma concentration occurs after 3-4 hours and bioavailability is approximately 30%. Absorption of CsA can be reduced by low bile flow and intestinal abnormalities or diarrhoea[355, 356], or enhanced following a meal due to bile secretion.

1.12.3 CsA action: calcineurin dependent immunosuppression

CsA is a widely used anti-rejection drug in transplantation and auto-immune diseases due to its ability to reduce T cells through the inhibition of calcineurin pathway.

Within the cell, CsA has a high binding affinity at nanomolar for most cyclophilins at varied affinities to inhibit the cis-trans isomerase activity. It is well established that CsA through formation of a complex with cyclophilin first, such binding of binary complex between cyclophilins and CsA formed in the cytoplasm will further bind with calcium-calmodulin-dependent protein of calcineurin sequentially to form a ternary complex. Only CsA residues 9-11 and 1-3 are in contact with cyclophilins. The other amino acid residues 4-8 protrude out from the cyclophilin surface and are implicated in specific protein interactions with calcineurin[357], which regulates subsequent activation of nuclear factor of activated T cells (NFAT) translocation factors. The final binding inhibits the serine-threonine protein phosphatase activity

of NFAT through dephosphorylation, which, in turn, inhibit the translocation of NFAT, leading to reduction of numerous transcriptional activation of early cytokine genes including interleukin 2 (IL-2), IL-4, IL-3, CD40L, tumour necrosis factor-α (TNF-α), granulocyte-macrophage colony-stimulating factor and interferon gamma[358].

Calcineurin is a Ca^{2+}/Calmondulin- activated serine/threonine protein phosphatase involved in a number of process[359], both pro- and anti-apoptotic roles have been reported for its activation[360], which is likely due to high specialized role plays in different tissue.

1.12.4 CsA action: anti-tumour effects (apoptosis and cell growth arrest)

CypA, B, C, D and Cyp40 overexpression were found in multiple human cancer, especially CypA overexpression were reported in more than 10 types of cancer including lung, pancreas, hepatocytes and other carcinoma[299]. The PPIase activity of cyclophilins can be inhibited by CsA, which also reported to induce apoptosis in various cancer cell lines, which may partially via cyclophilin inhibition.

Two major mechanisms responsible for induction of apoptotic cell death in rat glioma cell by CsA were identified as described by Kaminska[361]: 1) apoptotic cell death induced by CsA was associated with a persistent activation of MAPK, in particular JNK and p38 MAPK, leading to accumulation of phosphorylated c-Jun and ATF-2 and formation of the AP-1 transcription factor followed by transcriptional activation of Fas ligand expression[362], it was also demonstrated that

CsA down-regulates Akt signalling, resulting in transcriptional activation of Fas ligand expression[363], the up regulated Fas ligand then binds receptor Fas and induces extrinsic apoptotic cell death. 2) It was reported that CsA treatment results in up-regulation of p53 and Bax proteins contributed intrinsic mitochondria apoptotic cell death, which was associated with a persistent activation of mitogen activated kinase kinase 3 (MKK3)-p38 MAPK signalling pathway[364].

In human cancer cells, substance P (SP, belongs to the tachykinin family) induces cell proliferation and neurokinin-1 (NK-1) receptor antagonists could inhibit this effect. NK-1 receptor antagonists exert a broad-spectrum anti-tumour action against multiple cancer cells. As a tachykinin receptor antagonist, CsA exerts selectivity for both NK-1 and NK-2 receptors, to inhibit the ligand SP [365] induced inflammation (IL-6), pain and the active migration of various tumour cells that is a crucial requirement for invasion and development of metastasis[366, 367].

CsA blocks SP-induced mitogen stimulation and inhibit cell proliferation. While CsA at 30μM upregulated the level of p21WAF1/Cip1 protein, which is a universal inhibitor of cyclin kinases to inhibit cell proliferation, increased the number of cells in the G1 phase of cell cycle and significantly reduced the number of proliferating cells in the S phase, CsA at 60 μM high concentration of anti-tumour action is radical and irreversible in 7 human cancer cell lines[367], whereas 10 μM CsA was reported to only have partial and reversible antitumor action against the AGS gastric and HT29 colon carcinoma cell lines, and CsA administration intraperitoneally at 2

or 10 mg/kg every second days significantly decreased tumour volumes (by 70%) with similar efficacy[368].

1.12.5 CsA action: MPTP inhibition

Early in 1980s, it was reported that treatment with CsA inhibited mitochondria respiration in renal tubular cells. Later in 1987, CsA was observed not only inhibited mitochondria respiration, but also blocked the mitochondria efflux of Ca^{2+}, which was observed in reversible opening of the MPTP[369, 370], Crompton and co-workers first discovered that MPTP opening could be pharmacologically inhibited by CsA[371]. The inhibitory effect of CsA (150 *p*mol CsA /mg of mitochondria protein) was later confirmed by another research group on isolated liver mitochondria[372].

Following earlier study that there existed a mitochondria CypD, in 1990 Halestrap and Davidson[373], who reported that Ki of CsA for CypD and MPTP inhibition were similar at 5nM and the number of CsA-binding sites involved in MPTP inhibition in liver and heart mitochondria (about 125 *p*mol/mg or protein) were very close to the amount of CypD presents in mitochondria matrix, which revealed the mechanism that CsA through binding to CypD to inhibit MPTP opening. Later in 1996, it was confirmed that pharmacological target of CsA to be the 21kDa human mitochondria CypD protein[374], and studies with mice deficient in CypD have further confirmed CypD as the target for CsA to inhibit MPTP[228, 229, 375].

Since then, many studies employed CsA or its derivates targeting CypD in a variety of models to explore MPTP opening in liver, heart, brain, and skeletal muscle mitochondria.

1.12.6 CsA toxicity

Early in 1980s reports demonstrated that giant mitochondria containing disoriented cristae and paracrystalline presented in human renal biopsies, suggesting a nephrotoxic effect of CsA on mitochondrial function[376], other reports also showed neurotoxicity, hepatotoxicity[377] of CsA and some side effects, which are dose- and time-dependent, as also shown with tacrolimus (FK506). These adverse effects resolve after reducing dosage or discontinuing administration in patients, suggesting a possible calcineurin related dose dependent toxicity[378].

With most attributed the toxicity of immunosuppressant like CsA and FK506 to calcineurin dependent, about a decade ago, Pallet's study showed CsA induced interstitial fibrosis nephrotoxicity shown as epithelial phenotypic changes leading to the generation of protomyofibroblasts has been attributed to CypA mediated CsA induced ER stress, which can be protected by ER stress inhibitor salubrinal, an inhibitor of eIF2α dephosphorylation[379], later the same group have found that the CsA induced renal morphology changes involved JNK signalling and with JNK inhibitor reduces the occurrence[380]. Multi-omics study showed that in cultured human renal epithelial cells, CsA induced UPR pathways when treated with 15 μM, but no stress induction was detected with 5 μM[381]. Studies also reported that CsA induced persistent ER stress via CypB inhibition leading to a non- apoptotic cell

death, paraptosis, in several cervical cancer cells, showing completely disrupted ER structure, with dilation and extensive vacuolation presented positive for ER-Tracker and non-involvement of either lysosome or mitochondria architecture, and another study suggests CypB interact with CHOP, the pro-apoptotic protein in ER stress pathway[382, 383]. Studies also showed knock down both ER CypB and CypC induced ER- hyperoxidation phenotype which can be replicated by CsA due to depletion of CypB and CypC by inducing their secretion to the medium[384].

1.12.7 CsA therapeutic index

Long term CsA administration adversely affect the course of CER-AP[385], similar scenario was observed by Oie and co-workers[386] , who investigated the effect of 2-week CsA application with high dose (50 mg/kg/day) worsened ischemic disease model. However, single intravenous injection of CsA (10mg/kg) has shown reduced serum cytokine levels including TNF-α, IL-1β, and IL-10 in rats with acute necrotic pancreatitis induced by 5% sodium taurocholate[387], suggesting a time- and dose-dependent toxicity in rodents.

The first report on CsA preventing the heart from acute ischemia reperfusion/injury (IRI), showed CsA when administered only at 200nM-400nM, was protective against necrotic cell death[388]. Griffiths and Halestrap reported that CsA Pre-treatment at 200nM but not at 1μM to be beneficial following acute IRI[389].

While Administration CsA at 2mg/kg/day was without significant effect and a worsening pathology even reported on the use of much higher dose (30mg/kg

intraperitoneal injection, i.p) for two weeks in dystrophic mice[390, 391], studies from skeletal muscle disease suggested an effective dosage of CsA at 3-15 mg/kg[392, 393]. A pharmacokinetics study of CsA involved 48 healthy male volunteers shows that CsA oral administration produces linear pharmacokinetics in the dose-range of 200 to 800 mg (If calculated with the average weight for the volunteers as 70 kg, the optimal doses of CsA should be between the range of 3–10 mg/kg)[394].

The reason for the narrow therapeutic index was unclear but may attributed to the numerous adverse effect of CsA and its non-specific inhibitory effects on other cyclophilins or immunosuppression effect.

Implicated by the narrow therapeutic dose range of CsA in MPTP involved disease, numerous preclinical studies with CsA dosages range from 1-15mg/kg[395, 396] and several phase II [397-401] and phase III[402] clinical trials employed CsA at 2.5mg/kg single intravenous bolus injection have been conducted in ischemic heart disease since 2001, Di Lisa[403] and colleagues first implicated MPTP inhibition by CsA in the cardio-protective action of CsA through demonstrating reduced myocardial necrosis and preserved mitochondrial NAD^+ levels, and further study conducted by Hausenloy[404] confirmed that CsA administration limit myocardial infarct size due to MPTP inhibition but not calcineurin. Despite inconsistent results, regarding of the treatment time with CsA, there is a trend that suggests earlier treatment with CsA appeared to provide more favourable results.

1.12.8 Other natural cyclophilin inhibitors

Peptolide SDZ 214-103 (**Figure1.4 left**) is produced by fungus Cylindrotrichum oligospermum (Corda) Bonorden and was first discovered by Sandoz, now known as Novartis. As SDZ 214 contains a specific amino acid in position 8, resulting in an ester linkage, it is classified as a peptolides (a cyclic depsipeptide) rather than a peptide as CsA but share similar biological activity with CsA on cyclophilin and calcineurin inhibition[405]. Peptolide SDZ 214 synthetase appears to have higher substrate specificity than CsA synthesis and has been chemically modified in position 1 to 7 to reduce its immunosuppressive activity[405].

Sanglifehrin A (SFA) (**Figure 1.3 right**), was discovered in cultures of *Streptomyces flaveolus* DSM9954. The sanglifehrins are 22-membered macrolides conjugated to a spirolactam ring by a linear carbon chain[406]. Notably, although both peptolides and Sanglifehrins share the common biological activities as cyclophilin binding proteins to inhibit PPIases, SFA-cyclophilin complex binding with inosine-5'-monophosphate dehydrogenase 2 (IMPDH2) but not calcineurin to act on T cell activation and proliferation[407].

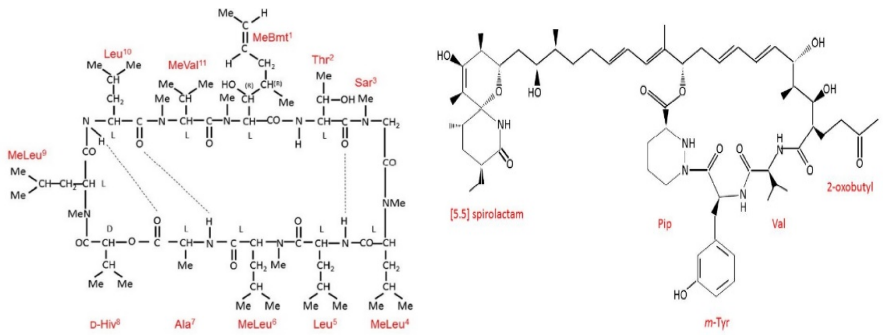

Figure 1.3 Structure of Peptolide (L) and Sanglifehrin (R)

1.13 Application of cyclophilin inhibitors

1.13.1 Development of cyclophilin inhibitors

With the discovery of CypD being the important facilitator of MPTP, a variety diseases involved MPTP have targeted CypD inhibition as novel approach for treatment. The currently available natural cyclophilin inhibitor CsA has potential drawbacks including calcineurin inhibition and several drug interactions, thus, lots of efforts have been made to generate potent, drug-like molecules through chemical design, synthesis and engineering based on the structure of natural cyclophilin inhibitors CsA, Peptolides[408], and Sanglifehrins[409, 410].

The advent of CsA-based non-immunosuppressive inhibitors such as Alisporivir (DEB025)[411], NIM811[412] and SCY-635[413], which have previously demonstrated clinical efficacy for Hepatitis C (HCV), also greatly facilitated the treatment for MPTP inhibition. These compounds have been modified to interfere their binding sites with calcineurin from the parent molecule at the 3-sarcosine or 4-N-methyl leucine positions to abolish or attenuate the immunosuppression (**Figure 1.4**), while retain the undecapeptide core structure of CsA to interact with cyclophilins.

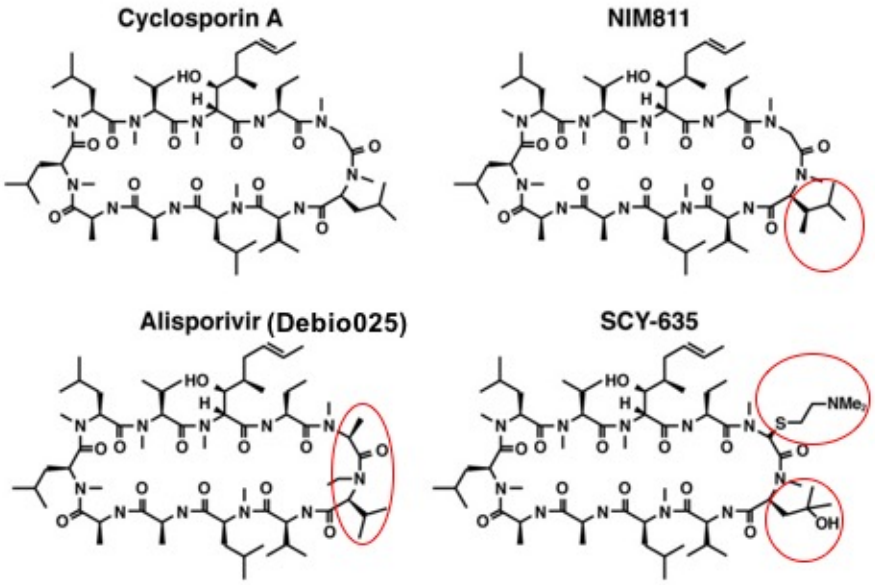

Figure 1.4 Structure of CsA and its non-immunosuppressive derivatives NIM811, DEB025 and SCY-635(Modified from Sam Hopkins et al. 2012[414])

DEB025 differs from CsA at position 3, with sarcosine having been replaced by MeAlanine, at position 4 with leucine having been replaced by valine and with the nitrogen being N-ethylated instead of N-methylated.

NIM811 differs from CsA by having methyl-isoleucine instead of methyl-leucine at position 4.

SCY-635 differs from CsA at position 3 and 4 with a dimethylamino-ethylthio substituent at the 3-sarcosine alpha carbon atom and a hydroxyl substituent at the gamma carbon of the 4-N-methyl leucine residue.

1.13.2 Cyclophilin inhibitors and MPTP-driven necrosis

CypD facilitates the MPTP opening and Ca^{2+} exchange between mitochondrial and the cytosol, which plays a key role in cell death[228, 415, 416], thus, CypD inhibition might be beneficial in preventing a cascade of events, triggered by MPTP opening dependent cell death. The discovery that MPTP can be pharmacologically inhibited through the binding with CypD by CsA, also facilitates studies associated with MPTP to develop novel therapy based on CsA or other cyclophilin inhibitors without immunosuppression.

As one of the non-immunosuppressive analogues derives from CsA, NIM811 was proved to prevent in situ mitochondrial inner membrane permeabilization and depolarization in hepatocytes to block calcium and inorganic phosphate induced MPTP induction, protects cell death equipotent with CsA at 0.5-2 μM, while CsA lost efficacy at 5-10 μM but NIM811 did not[417].

The beneficial of MPTP inhibition was also observed in muscular dystrophy. Treatment with DEB025 (in a cremophor based vehicle, administered at 50mg/kg/d, twice daily by subcutaneous injections for 6 weeks) reduced mitochondrial swelling and necrotic manifestations in mdx mice of Duchenne Muscular Dystrophy (DMD)[315]. It was also shown that low concentration of DEB025 prevents against cell death and with 10mg/kg orally dosage in vivo DEB025 also protects the muscles from necrosis and with faster relax in DMD models[418]. Notably, the study also suggests that DEB025 appeared to work better at 10mg/kg rather than 100mg/kg with uncertain mechanism.

With elucidation that genetic CypD ablation both *in vitro* and *in vivo*, protected pancreatic acinar cell from MPTP dependent necrosis, similar beneficial with low concentration of DEB025 at 100nM, CsA at 5μM also shown protection of PACs from necrosis and DEB025 at 10mg/kg intraperitoneal injection also proved effectively inhibit MPTP opening in 2 AP models, reducing all histopathological, biochemical, and immunological responses[237]. Whereas unpublished data (Mukherjee) suggested that high dose of DEB025 at 40mg/kg or 100mg/kg also showing great beneficial in acute biliary pancreatitis across all the biomarkers apart from IL-6, which suggested DEB025 start to lose efficacy at 40mg/kg while CsA at 20mg/kg only showed decreased IL-6 level in TLCS model.

1.13.3 Cyclophilin inhibitors and fibrosis

While CsA has been connected to interstitial fibrosis in kidney and synergistically act profibrotic effects with caerulein and ethanol in pancreas, based on which, long term CsA application was used to develop experimental chronic pancreatitis model in combination with ethanol feeding and caerulein insult[193], paradoxically, CsA itself at a low dose or its non-immunosuppressive analogues have exerted great potential in reducing fibrosis and inflammatory infiltration in muscular disease and liver fibrosis.

Early in 1991, researchers reported that in carbon tetrachloride (CCl_4) induced rat liver cirrhosis model, orally cyclosporin administration with 1 mg/kg body weight every second day for 6-week excellently reduced fibrosis and cirrhotic alteration, while 1mg/kg daily dose is less effective and 10 mg/kg CsA causes severe

hepatotoxicity[419]. Similarly, in HSCs, Ikeda[420] found at 5μM, CsA inhibited DNA synthesis of HSC and suppressed collagen synthesis, however, tacrolimus at 5μM only inhibited DNA synthesis of HSC. Mechanistically, Nakamuta[421] found CsA at 2μM suppressed HSC proliferation and collagen expression with predominantly suppressed activation of JNK and p38.

The beneficial of non-immunosuppressive analogue NIM811was also demonstrated in HSCs, showing suppressed transcriptional and synthetic of collagen and stimulated MMP-1 production with enhanced collagenase activity, inhibited proliferation of HSCs. In MAPK and TGF-β pathways, NIM811 upregulated phosphorylation of JNK and p38, but suppressed Smad2 and Smad3 phosphorylation, accompanied by increased Smad7 and decreased TGF-β receptor transcription[422].

Whilst NIM811 showed beneficial in reducing fibrosis state in HSC, the in vivo studies had inconsistent results. It was reported that in CCl_4 induced rat liver fibrosis model, NIM811 significantly suppressed mRNA expression of collagen type III, tissue inhibitor of metalloproteinase-1 and TGF-β, and protein expression of α-SMA in liver tissue after 6 weeks daily oral administration of 10mg/kg and 20mg/kg, with no stronger effect observed on all expression in 20mg/kg compared with 10mg/kg. In vitro studies revealed that cyclophilin B and/or D knockout were associated with collagen inhibition[423]. Whereas study from Rehman's[424] group reported mice gavaged with 20mg/kg NIM811 (8.3% polyethoxylated castor oil and 8.3% ethanol vehicle) 2h before bile duct ligation, and 10mg/kg daily afterwards for 2 weeks. Bile

duct ligation induced both necrosis and apoptosis with earlier occurrence of necrosis. NIM811 decreased both necrotic and apoptotic cell death, liver function (serum ALT), hepatocytes mitochondria depolarisation and permeabalization 6h after ligation shown by confocal microscopy, however, NIM811 did not prevent TNFα, TGF- β1 and procollagen α1(I) mRNA expression and had no impact on Sirius red stained fibrosis and α-SMA expression after ligation at 3 days and 2 weeks despite protection against cell death. As bile duct ligation is a severe and irreversible procedure, this difference between two studies may partially due to distinctive pathogenesis of the two liver fibrosis models, additionally, the solvent in the ligation model containing 8.3% ethanol, which may induce synergetic effects with chronic intake to exacerbate fibrosis.

The results from a prospective, randomized clinical trial comparing fibrosis development with CsA and tacrolimus treatment in liver transplant recipients for hepatitis C provide implication that cyclophilin inhibition may have an anti-fibrotic effect among steroid-free patients, who had less significantly less frequent liver fibrosis progression with CsA, compared with tacrolimus at one year post-transplantation[425].

Both CsA and its non-immunosuppressive derivate DEB025 have been studied in muscular diseases. Annamaria's group[392] found that CsA treatment (10mg/kg/d orally with drug-enriched chow) significantly reduced fibrosis with decreased TGF-β1 transcripts and expression levels in dystrophic mouse model. While study from Wissling's group[426] implicates orally gavage of DEB025 significantly decrease

extent of muscular fibrosis and markedly reduce the infiltration of activated macrophages and neutrophils over 6-week treatment period in mdx mice model of DMD, and in Millary's[315] study despite shown reduced mitochondrial swelling and necrotic manifestations in mdx mice with DEB025, the regimen only partially normalized the fibre area distribution and showed a minor (around 5%) reduction on fibrosis, which is possibly due to the high does employed at 50mg/kg/d, twice daily by subcutaneous injections for 6 weeks.

1.14 Necrosis-fibrosis theory in pancreatitis

While apoptotic cells are usually removed by phagocytes immediately, it is rare to find apoptotic cell ingesting phagocytes in clinical pancreatitis, necrosis is the main cell death form seen in human pancreatitis. The necro- inflammation- fibrosis can be viewed as a continuum of events within the framework of tissue defence, repair and regeneration.

During episodes of AP, Ca^{2+} overload initiates CypD mediated MPTP opening, results in pancreatic acinar cell necrosis, triggers host acute inflammatory response, acinar cells produce majority pro-inflammatory cytokines including IL-1β, TNF-α , IL-6, IL-18 and anti-inflammatory cytokine IL-10[427] which ensuing inflammatory cells recruitment and leading to further necrosis and injury. Necrosis and inflammation from recurrent episodes of AP results in scarring and marked fibrosis with ductal obstruction. Timely inflammation in adequate intensity is essential to eliminate harmful stimuli, however an insufficient inflammatory response can lead to sustained insult. Active resolution of inflammation is critical for tissue healing,

while propagation of acute inflammatory response could induce chronic inflammation if there is not enough appropriate resolution. PSCs not only produce collagen and other ECM proteins that lead to fibrosis, but also secrete cytokines that further promote inflammatory process to extended tissue destruction and replacement with fibrotic and adipose tissue[428, 429].

1.15 Hypotheses and study aims

Since CypD has been proposed to be the central regulator of MPTP, the CypD-deficient (*Ppif*$^{-/-}$) mice were found to prevent against MPTP opening[228, 229, 430]. With MPTP inhibition successfully applied in cardiovascular, muscular, neurological and hepatic diseases model that involved cell death, inflammation and fibrosis, which all these features also greatly fit into the key manifestation of both acute and chronic pancreatitis, it is rational to search the possibility for targeting MPTP by CypD inhibition as specific treatment for pancreatitis.

MPTP inhibition as a therapeutic pancreatic protection strategy, considering the plenty adverse effect of CsA and its non-specific CypD inhibition, for a novel pancreatic protective strategy to be successfully translated into the clinical setting, it is necessary to comprehensively investigate the cyclophilin inhibition effects on different experimental pancreatitis. Further study for the possibility of either non-specific or specific cyclophilin inhibitors application for MPTP opening as well as a scientific regimen also need to be identified and developed.

It is hypothesized that there may exist a bell shape dose response for CsA due to its narrow therapeutic index results from non- specific inhibition of various cyclophilins and other off-target effects. The minimal dose may have some beneficial for inflammation due to either immunosuppressive effect that calcineurin inhibition or extracellular Cyclophilin inhibition leading to the reduction of cytokines. However, the highest does may adversely affect the severity due to either ER stress induced necroptosis via depletion of ER based cyclophilins or the antitumor cytotoxicity of CsA, which exacerbate the inflammation and severity of pancreatitis. Only low to median dose with optimal drug intervention time and appropriate formulation has the best effect to reduce the MPT-driven necrosis of AP. This improvement may protect the morphology and function of pancreatic acinar cell, reduce inflammation and further benefit to ease the development and accelerate the recovery of chronic pancreatitis.

Hypothesis 1: CsA induces reactive oxygen species production mediating apoptotic cell death and ER stress in PACs.

Study aims: to examine the effects of CsA on apoptotic cell death pathway activation, ROS production and ER based chaperone expression in isolated murine pancreatic acinar cells.

Hypothesis 2: CsA has a narrow therapeutic index in AP resulting in a bell-shaped curve with loss of effect at higher doses.

Study aims: to examine the dose response of CsA in three models of experimental acute pancreatitis.

Hypothesis 3: Prevention of MPTP opening in AP by inhibition of cyclophilins has translational potential as a treatment for human AP.

Study aims: to examine the effects of different novel cyclophilin inhibitors in an acute biliary pancreatitis model.

Hypothesis 4: Early intervention is necessary for effective AP treatment by targeting early onset of pancreatic injury.

Study aims: to compare the effects of early versus late administration of cyclophilin inhibitors on disease severity in an acute biliary AP model.

Hypothesis 5: The MPTP has a role in the pathogenesis of CP induced by recurrent AP episodes through repeated necrosis-fibrosis.

Study aims: to determine the effects of genetic ablation of CypD on the progression and recovery of chronic pancreatitis including pancreatic exocrine function and pancreatic fibrosis.

Hypothesis 6: Prevention of MPTP opening in CP by inhibition of cyclophilins has translational potential as a treatment for human CP.

Study aims: to evaluate the effects of a non-immunosuppressive cyclophilin inhibitor on disease severity in a model using 2 weeks of repetitive AP episodes, assessing pancreatic exocrine function and pancreatic fibrosis.

CHAPTER 2

MATERIALS AND METHODS

2.1 Reagents and chemicals

Fluorescent dyes for necrotic cell death measurement propidium iodide (cat: P3566), apoptotic cell death measurement cell event™ caspase 3/7 Green ReadyProbes™ Reagent (cat: R37111) and general oxidative stress indicator measurement CM-H2DCFDA (cat: C6827), cell viability assessment 0.4% trypan blue stain (cat: T10282) for use with automated cell counter were obtained from Invitrogen (Paisley, UK).

Halt™ Protease Inhibitor Cocktail (100X) (cat: 78430), Halt™ Phosphatase Inhibitor Cocktail (cat: 78420) and Pierce™ bicinchoninic acid (BCA) assay kit (cat: 23225) used for intact protein extraction and quantification in western blotting were obtained from Thermo Scientific (Runcorn, UK). 78kDa glucose-regulated protein (GRP-78) rabbit antibody and cyclophilin B rabbit antibody were acquired from Abcam (Cambridge, UK). β-actin (13E5) rabbit antibody and anti-rabbit IgG, horseradish peroxidase (HRP)-linked secondary antibody (7074) were purchased from cell signalling (Hitchin, UK). ECL blotting substrates (cat:1705060) and all the other mentioned reagents used for western blotting were obtained from Bio-Rad (Deeside, UK).

Substrate Boc-Gln-Ala-Arg-MCA for trypsin measurement was purchased from Peptide Institute (Osaka, Japan); cOmplete™ Mini Protease Inhibitor Cocktail Tablets were obtained from Roche GmbH (Mannheim, Germany). IL-6 and TGF-Beta1 Quantikine ELISA Kit from R&D Systems (M6000B and MB100B, Abington, UK). Picro Sirius Red stain kit (ab150681) and Trichrome stain kit

(ab150686) for collagen deposition, rabbit specific HRP/DAB detection kit (ab64261) for IHC staining and colorimetric lipase activity assay kit (ab102524) for enzymatic quantification were purchased from Abcam (Cambridge, UK). Synthetic SEL/CC compounds of novel cyclophilin inhibitors and solvent formulation were supplied by Cypralis (Essex, UK).

Reagents used for staining including, pH 9 antigen retrieval buffer (cat. K8004) was obtained from Dako (Cambridge, UK), antibody diluent (ab64211), anti α-smooth muscle actin (ab5694) antibody were acquired from Abcam (Cambridge, UK). Counterstaining reagents including Gill III haematoxylin (cat. 3801540), erosin (cat. 3801600), Scott's Tap Water Substitute (cat. 3802900) and 1% acid alcohol (cat. 3803650) were obtained from Leica Microsystems (Milton, UK).

Reagents such as collagenase (C9407), cyclosporin A (30024), taurolithocholic acid 3-sulphate (T0512), palmitoleic acid (P9417), caerulein (C9026), trypsin from bovine pancreas (T1426), myeloperoxidase from human Leukocyte (M6908), dimethyl sulfoxide (DMSO, D2650) as well as all other reagents and chemicals mentioned in the method part but not listed above were purchased from Sigma-Aldrich (Dorset, UK).

2.2 Consumable materials

The 70 μm nylon mesh cell strainer, 15 and 50 mL falcon tubes, *etc* were obtained from Fisher Scientific (Loughborough, UK). Disposable Countess™ cell counting chamber slides were purchased from Invitrogen (Paisley, UK). The microscope

slides and 22*50 mm cover slips were purchased from VWR (Leighton Buzzard, UK). The 4%–12% Mini-PROTEAN ® TGX™ Precast Gels system and Immuno-Blot PVDF membrane were obtained from Bio-Rad (Deeside, UK).

2.3 Solution preparation

2.3.1 Preparation of NaHEPES

Chemicals used to prepare for NaHEPES media were all obtained from Sigma-Aldrich (Dorset, UK). The recipe of NaHEPES solution containing: 140 mM sodium chloride, 10 mM HEPES, 4.7 mM potassium chloride, 1.13 mM magnesium chloride, 10 mM D-glucose. The media pH was adjusted to 7.35 with NaOH. For pancreatic acinar cell isolation and experiments with the presence of extracellular calcium NaHEPES solution was supplemented with 1 mM calcium chloride.

2.3.2 Preparation of collagenase

NaHEPES (Ca^{2+} free) was added to collagenase powder resulting in 2mg/mL collagenase stock solution. The stock solution was aliquoted and stored at -20℃. Before each cell isolation, the aliquoted stock collagenase was further diluted with fresh prepared NaHEPES (supplemented with 1mM Ca^{2+}) to 0.2-0.4mg/mL final concentration and pre-warm in waterbath before injected into the main duct of pancreata.

2.3.3 Preparation of buffer for western blotting

The buffer used for western blotting were self-prepared with the detailed composition listed as below in **Table 2.1**.

Table 2.1 Buffer composition for western blotting

Buffer	Composition	pH
Whole cell lysis	150 mM NaCI, 0.1% Triton X-100, 50 mM Tris-HCI	8.0
Loading	4% SDS, 10% 2-mercaptoethanol, 20% glycerol, 0.004% bromophenol blue, 0.125 M Tris-HCI	/
Running	25mM Tris base, 190mM glycine, 0.1% SDS	8.3
Transfer	48mM Tris base, 39mM glycine, 20% methanol, 0.04% SDS	/
Wash	(TBS-T: Tris buffered saline- tween 20) 20mM Tris base, 150mM NaCl, 0.1% Tween 20	7.6

2.3.4 Other solution preparation

Trypsin homogenize buffer pH 6.5, containing (in mM): 3-(N-morpholino) propanesulfonic acid (MOPS) 5, sucrose 250 and magnesium sulphate 1.

Trypsin assay buffer was made from 50 mM Tris, 150 mM NaCl, 1 mM $CaCl_2$ and 1% (w/v) bovine serum albumin, pH 8.0.

2.4 Equipment

Equipment used for cell counting, tissue homogenization, fluoresce intensity and optical density recording, *etc* were listed below in **Table 2.2**.

Table 2.2 Main equipment

Equipment	Usage	Brand
Aperio Scanners	Slides scanning	Leica
Automated cell counter	Quick automatic cell counting and viability screening	Invitrogen
Centrifuge	Centrifugation	Thermo
Micro Plate Reader	Fluorescent, colorimetric and ELISA assay	BMG
Mini – PROTEAN Trtra Electrophoresis system	Western blot	Bio-Rad
Micro infusion pump	Common duct bile acid infusion	Harvard
PT Link system	For antigen retrieval	Dako
Syngene system	Imaging for western blot	Syngene
Tissue tearor	Homogenize pancreatic and pulmonary tissue	Biospec products

2.5 Animals

All animal studies were performed in accordance with protocols defined by the Scientific (Animal) Procedures Act 1986, following the Replacement, Reduction and Refinement (3Rs principle) and in compliance with the UK Home Office regulation under project licence (70/8109) approved by the Ethical Committee at University of Liverpool.

The CsA concentration/dose responsive experiments were performed using CD1 mice (Charles River, UK), synthesized cyclophilin inhibitors were tested in C57BL/6J mice and chronic pancreatitis in vivo experiments were conducted on C57BL/6J mice (as age and sex matched controls for knockout experiments; Charles

River, UK). Cyclophilin D-deficient mice (C57BL/6J) colony generated by targeted disruption of the ppif gene encoding for mitochondrial cyclophilin D was breed and maintained in facility of animal unit, Biomedical Service, University of Liverpool, which originally provided to the Liverpool pancreatitis group by Dr. David Yellon (University College, London) and Jeff Molkentin (Children's Hospital Medical Centre, Cincinatti) as a gift. Mice were housed under standardized condition at 23 ± 2°C, humidity 40%-60% with a 12-hour light/dark cycle and *ad libitum* access to laboratory chow and water.

2.6 Isolation of murine PACs

PACs were isolated using collagenase digestion and filtration procedure. Briefly, male 6-8-week-old CD1 mice were humanely sacrificed by cervical dislocation. The abdominal cavity was subsequently exposed by a transverse subcostal incision to excise and dissect the normal pancreata part straight from the spleen with further rinsing in NaHEPES buffer. Then, pancreata was injected via the ductal system or directly into the tissue with pre- warmed collagenase at 0.2 mg/mL followed by 16-minute incubation in NaHEPES solution at 37°C. After which, the preparation together with collagenase contained buffer was transferred into 15 ml falcon tube subjected to repeated mechanical disassociation in NaHEPES buffer using open cut 1 ml pipette tip, the obtained cloudy solute was then passed through a 100 μm nylon mesh cell strainer to remove large clumps of cell debrides and chunks of connective tissue. After a further twice wash in NaHEPES and centrifugation at 200 g for 2 minutes, the supernatant was discarded and the cell pellet was re-suspended in NaHEPES buffer.

All isolated PACs suspensions with cell viability > 75%, determined by automated cell counter exclusion with 0.4% trypan blue dye staining were used within 2 h for *in vitro* experiments. Trypan blue is a vital stain recommended for use in estimating the number of live and dead cells in the cell suspension. The activity of this dye is based on the fact that the chromophore is negatively charged and dose not react with the internal region of the cell unless the membrane is damaged. The dye enters into only dead cells and stains them blue, while live cells have intact cell membranes and remain bright and unstained. Precisely, to determine PACs viability and density, mix 1 part 0.4% trypan blue dye and 1 part PACs suspension in a micro test tube (10 µL of each) with gently pipet up and down. Immediately (within 5 mins of mixing), 10µL of the mixture was loaded into the outer opening of either chamber of a disposable polygon plastic counting slides prior to insertion into automated cell counter. The isolated PACs suspension was diluted with NaHEPES till the desired density level for further *in vitro* experiment.

2.7 Measurement of kinetic cell death pathway activation in PACs

The dynamic necrotic and apoptotic cell death were analysed using POLARstar Omega fluorescence microplate reader with Propidium iodide (PI) and caspase 3/7 probe double staining to detect real time membrane event by recording incorporation florescence intensity (FI) up to 14 hours in PACs clusters.

PI is membrane impermeant which does not enter viable cells with intact membranes. When PI does gain access to nucleic acids, it brightly only once it passes through the compromised plasma membrane and binds to DNA with

intercalates its fluorescence increases dramatically, therefore has been used to label cells undergoing necrosis.

Caspase3/7 Green Reagent is a fluorogenic, no wash, early indicator of apoptosis for live cell applications. This peptide DEVD conjugated to a nucleic acid-binding dye that is non-fluorescent when not bound to DNA and an intrinsically non-fluorescent, as the DEVD peptide inhibits binding of the dye to DNA. Upon activation of caspase 3 or caspase 7, the DEVD peptide is cleaved and the free dye can bind DNA, generating a bright green fluorescence. Thus, to detect the apoptotic cell death that follows caspase activation.

In general, freshly isolated acinar cells (2×10^6 cells per mL, viability >75%) were co-incubated with PI (1.5 μM; λexcitation/ λemission= 540/620 nm) / caspase 3/7 (1 μM; λexcitation/ λemission= 420/540 nm) and various concentrations of CsA at 100 nM, 1 μM, 5 μM, 10 μM, 25 μM or 50 μM for 30 minutes (aliquoted CsA stock solution of 10 mM, 5 mM, 2 mM, 1 mM, 200 μM and 20 μM were prepared in DMSO and stored at -20°C for up to 1 month). Pre-treated PACs suspensions and PACs free NaHEPES were then seeded into a 96-well microplate in duplicates with 190 μL per well and placed into BMG plate reader pre-set at 37 °C with 10 cycles FI over baseline monitoring. The pre-treated PACs were further exposed to taurolithocholic acid 3-sulphate (TLCS, 500 μM), palmitoleic acid (POA, 100 μM) or caerulein (CER, 10 nM), 10 μL of each from stock solution for time course cell death detection. 10 μL Triton X-100 (0.25%) and NaHEPES were applied to CsA-free cells as positive control to determine the full cell death FI level and negative

control, separate 10 μL NaHEPES was also added to blank control wells (without cells and CsA but NaHEPES and dye alone) to record the background signal. The ratio of fluorescence increase over baseline at each minute was used to represent real time cell death level.

2.8 Measurement of reactive oxygen species production in PACs

Intracellular reactive oxygen species (ROS) generation was measured by POLARstar Omega Plate reader using general oxidative stress indicator chloromethyl 2', 7'- dichlorodihydrofluorescein diacetate (CM-H2DCFDA) fluorescense dye, which is a chloromethyl derivative from H2DCFDA, allowing for covalent binding to intracellular components, permitting longer retention within the cell. CM-H2DCFDA passively diffuses into cells, where its acetate groups are cleaved by intracellular esterase and its thiol-reactive chloromethyl group reacts with intracellular glutathione and other thiols. Subsequent oxidation yields a fluorescent adduct that is trapped inside the cell, thus facilitating long-term studies.

Briefly, freshly isolated PACs (2×10^6) were resuspended in NaHEPES buffer and loaded with 10 μM CM-H2DCFDA together with various concentrations of CsA for 30 minutes in a waterbath at 37°C protect from light. The pre-treated PACs were then washout and resuspended in NaHEPES after 5 minutes centrifugation at 600g. The washed PACs was loaded with various concentrations of CsA at 100 nM, 1 μM, 5 μM, 10 μM, or 25 μM and further seeded on a 96-well plate, 190 μL per well. Following 10 cycles baseline FI assessing at an excitation wavelength of 480nm and an emission wavelength of 525nm, finally, 10 μL of multiple toxins including TLCS (500 μM), POA (100 μM) and CER (10nM) were added into designate wells to

detect ROS fluorescence intensity. 10 μL high concentrations of H_2O_2 (1mM) and NaHEPES were used as positive control to evaluate the full capacity of ROS production and the basal production control, respectively. The ratio of fluorescence increase was used to represent the ROS production level.

2.9 Western blotting

Freshly isolated PACs aliquots were co-incubated with various concentrations of CsA and different toxins, including TLCS (500 μM) in 37°C waterbath for 2-6h. Treated PACs were spun at 100g for 2 min and the supernatants were removed and kept at -80°C for further cytokine analysis. PACs pellets were washed 3 times with ice-cold PBS and lysed with whole cell lysis buffer supplemented with protease inhibitor and phosphatase inhibitor cocktail by gently pipetting up and down. PACs lysates were then sonicated on ice for 10 seconds before stored in -80°C until assayed. Upon thawing lysates on ice, following 10-minute centrifugation at 16,000 g, 4 °C, PACs lysates supernatant was collected for protein concentration measurement using the Pierce™ bicinchoninic acid (BCA) assay according to the manufacturer's instructions.

Same amount of proteins (20 μg) were mixed with sample loading buffer (ddH2O to equalise the total volume between samples). After denatured by heating at 100°C for 10mins, proteins were separated by sodium-dodecyl-sulphate polyacrylamide gel electrophoresis (SDS-PAGE) using 4%–12% Mini-PROTEAN ® TGX™ Precast Gels system in running buffer at 270V for 40 minutes. Proteins were then transferred onto polyvinylidene fluoride (PVDF) membrane for 45 minutes at 150 V in transfer

buffer. Membranes were then washed once in tris-buffered saline mixed with tween 20 (TBST). 5% non-fat dry milk dissolved in TBST was prepared to block the remaining surface of the PVDF membranes for 1 hour at room temperature to prevent nonspecific binding of the detection antibody. Protein immunoblots were incubated with specific primary antibodies 78kDa glucose-regulated protein (GRP78) rabbit antibody and CypB rabbit antibody (diluted to 1:1000 in 5% milk/TBST buffer) overnight at 4 °C. Membranes were then washed 3 times with TBST every 10 minutes prior to a further probe with anti-rabbit horseradish peroxidase (HRP)-conjugated secondary antibody diluted 1:1000 in 5% milk/TBST for 1 hour at room temperature. This was followed by a half an hour of 10 minute-interval washes. To test for equal loading, membranes were washed in TBST and incubated with anti β-actin antibody diluted 1:1000 in 5% milk/PBST for 1 h at room temperature, before washing and probing with secondary antibody. Protein bands were visualized using a commercial enhanced chemiluminescence (ECL) detection kit (**Figure 2.1**). Membranes were scanned, recorded digitally, and quantified using GeneTools from SynGene.

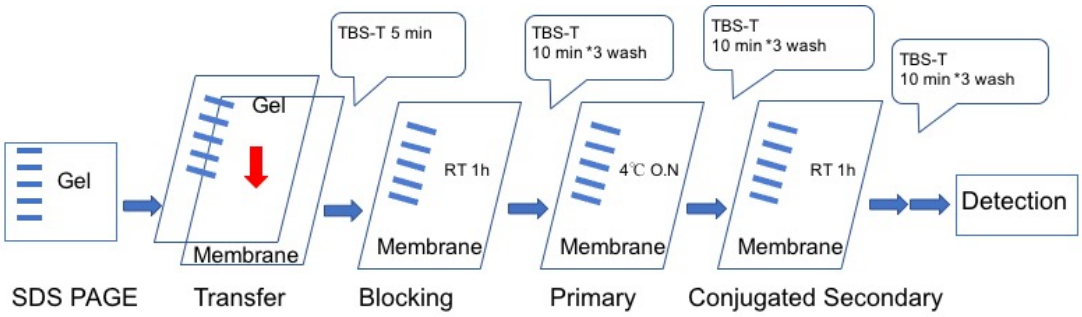

Figure 2.1 Western blotting brief work flow diagram

2.10 Experimental acute pancreatitis (EAP)

Experimental acute pancreatitis (EAP) was induced in mice through multiple approaches according to represent different clinical aetiologies. Acute biliary pancreatitis induced by bile acid retrograde duct perfusion (TLCS-AP) and acute alcoholic pancreatitis induced by fatty acid ethyl ester (FAEE-AP), metabolites of palmitoleic acid (POA) and ethanol through non-oxidative pathway in pancreas are two models that with most clinical relevant cause in human pancreatitis. A third AP model with hyperstimulation of cholecystokinin analogue caerulein (CER-AP) to induce gastric, biliary, and pancreatic secretion was also employed for its standardised protocol and uniform injury in pancreas.

2.10.1 Induction of experimental acute biliary pancreatitis (TLCS-AP)

Acute biliary pancreatitis (ABP) was induced by retrograde infusion of bile acid TLCS into the common bile duct of mice as previously described[431, 432] with slightly modifications. Briefly, the pancreatic head and the attached surrounding duodenum were exposed following a midline laparotomy with gentle reverse liver traction. Cannulation of the common duct was performed (as described in Figure 2.3) with a 30-gauge needle first punctured through the duodenal wall in parallel to the papilla, then further introduced 5 mm into the common duct. The other end of the needle was pre-placed into a polyethylene catheter connected to a micro-infusion pump. The common hepatic duct was identified at the liver hilum and clamped with a micro vessel clamp to prevent hepatic reflux. Overall, 50 μL of either normal saline or 3 mM TLCS (dissolved in normal saline with methylene blue 300 μM) was infused into the common bile duct at a rate of 5 μL/min over 10 minutes. Before

suturing the abdominal wall, the clamp was removed. Anaesthesia was achieved with isoflurane and buprenorphine (0.1mg/kg) was given by subcutaneous injection before laparotomy for pre-emptive analgesia and post-operatively at 12 h.

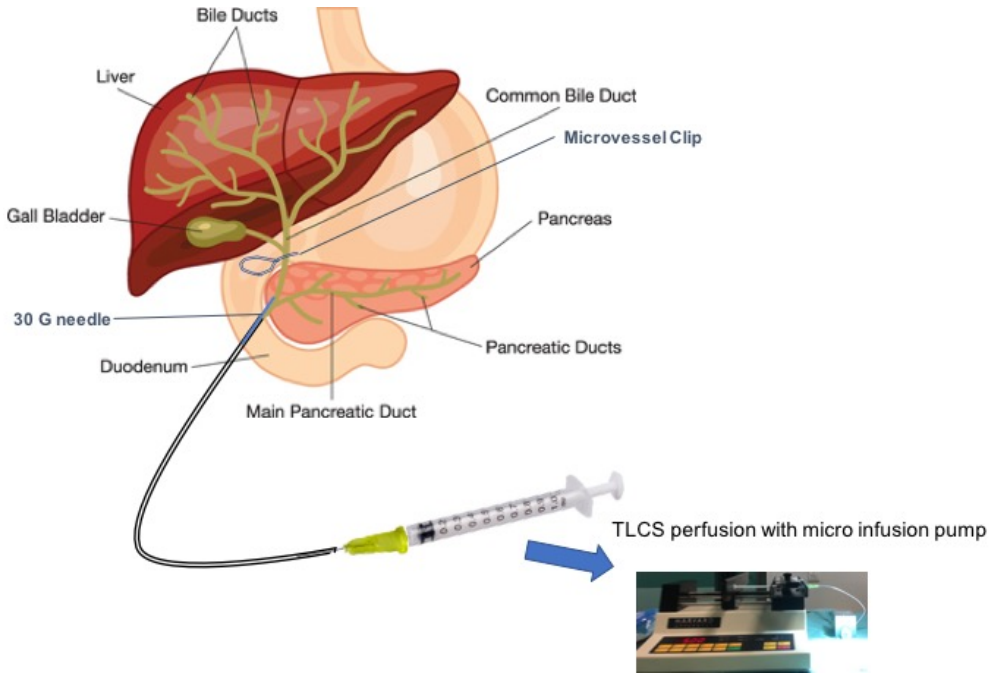

Figure 2.2 Simplified anatomy illustration for TLCS-AP induction

With the aid of a dissecting microscope, the ampulla of vater was identified and the bile duct was cannulised by a 30G tipped needle, which was inserted to a polyethylene tubing connected to a syringe placed on a micro infusion pump. A microvessel clip placed at the liver hilum across the bile duct. Mixture of bile acid (3mM TLCS) and methylene blue solution was infused at 5 μL/min over 10 minutes using an infusion pump. After closing the abdomen layers, the animals were allowed to awake. Control mice received same operation procedure without infusion of TLCS. Animals were sacrificed at 24 h after the perfusion.

2.10.2 Induction of experimental acute alcoholic pancreatitis (FAEE-AP)

Mice received two hourly i.p injection with pure ethanol (1.35g/kg) based POA (150 mg/kg)[196] or 40% ethanol (diluted with polyethylene glycol 400 and normal saline) based POA (300 mg/kg) solution. For the POA-pure ethanol protocol, 200 μL normal saline was immediately pre-injected at the injection site to avoid local damage (peritoneal organs) provoked by pure ethanol. Analgesia was achieved by subcutaneously injection of 0.1 mg/kg per body weight buprenorphine hydrochloride. The control mice received compatible volume of saline injection. Animals were sacrificed at 24 h after the first injection.

2.10.3 Induction of experimental acute hyperstimulation pancreatitis (CER-AP)

Hyperstimulation AP (CER-AP) was induced by seven hourly i.p injections of 50 μg/kg/h caerulein[433], with a humane sacrifice at 12 h after the first injection. 0.1 mg/kg buprenorphine was given by subcutaneous injection to reduce pain and discomfort due to multiple caerulein injections. The control mice received a compatible volume of saline injection.

2.11 EAP assessment

Serum amylase level and pancreatic histopathology score were used to evaluate the establishment of experimental acute pancreatitis. The severity of three EAP models was routinely assessed by local and distant injury characterized by inflammation (neutrophil infiltration and cytokine cascades), including pancreatic myeloperoxidase (MPO), pulmonary MPO and serum IL-6. For FAEE- and CER-AP, pancreatic trypsin activity was also detected to evaluate the local pancreatic injury.

To acquire sample for above assessments, mice were sacrificed by CO_2 asphyxia at designate time point after EAP induction. Following confirmation of death, blood was first taken by cardiac puncture or from superior vena cava. Allowing naturally clot for 2h at room temperature, collected blood was centrifuged at 1,500 g, 4°C for 10mins. Serum was separated and stored in -80°C until measurement of amylase and cytokine levels. Once blood has taken, upon chest cavity opening, the right pulmonary lobe was removed and rinsed in PBS followed by snap frozen in dry ice for pulmonary MPO measurement, while the left pulmonary lobe was injected with 0.5 mL 10% neutral formalin through porta pulmonis before taken and fixed in 10% neutral formalin for haematoxylin-eosin (H&E) staining. Thirdly, the pancreata was detached either from the duodenum in TLCS-AP or the from the spleen in FAEE- and CER-AP. For TLCS-AP, the pancreatic head were rapidly separated from duodenum and divided into 2 pieces, half of the pancreatic sample was fixed in 10% formalin, whereas the other half was snap frozen in dry ice for assessment of pancreatic MPO. For FAEE- and CER-AP, the pancreatic body part was removed from spleen and divided into 3 pieces, apart from H&E and MPO sample, the last one-third part was collected for pancreatic trypsin activity detection.

2.11.1 Measurement of serum amylase

Serum amylase was measured at Clinical Biochemistry Department in Royal Liverpool & Broadgreen University Hospital Trust, using kinetic enzymatically method. This method was based on cleavage of the ethylidene protected substrate, 4,6- ethylidene-(G7)-1,4-nitrophenyl-(G1)- α-D-maltoheptaoside by α-amylase and the subsequent hydrolysis of all the degradation products to *p*- nitro phenol with the aid of α-glucosidase (100% chromophore liberation)[434]. The colour absorbance of

the final product *p*-nitro phenol was measured photometrically to reflect the levels of α-amylase. The results were expressed as U/L.

2.11.2 Grading pancreatic histopathology scoring

For morphological examination, pancreata was fixed in 10% neutral buffered formalin overnight and then dehydrated and paraffin embedded. 6 μm sections were stained with haematoxylin and eosin (H&E).

In brief, whole sections were deparaffinised in xylene and rehydrated through serially decreasing ethanol/ddH_2O solutions from 100% to 95% to 70%, before rinsing in tap water. Slides were then incubated in haematoxylin for 10 minutes, rinsed in running tap water and agitated in 0.25% HCl/ddH_2O for 5 seconds. A further rinsing in tap water followed, before a 30 second agitated incubation in Scott's tap water. After another rinse, slides were agitated in 100% ethanol for 30 seconds then placed in eosin to incubate for 2 minutes. The slides were then agitated in 100% ethanol for 1 minute, followed by two 30-second washes in fresh ethanol and three 30 second agitations in xylene before mounting.

The histopathological change was further blindly evaluated on 10 random fields (×20 high power fields) of each slide under light microscopy by 2 independent examiners using a scoring system for the evaluation of oedema, infiltration and necrosis on a 0 (absent) to 3 (extensive) scale as previously described in detail[435] (**Table 2.3**) calculating summated mean ± SEM, for ≥6 mice/group. The agreement of these scores between two independent investigators was evaluated and confirmed before assessing the slides from experimental groups.

Table 2.3 Pancreatic histopathological grading criteria in AP

Parameter	Score	Indication
Oedema	0	Absent
	1	Focal increased between lobules
	2	Diffused increased
	3	Acini disrupted and separated
Infiltration	0	Absent
	1	In ducts (around ductal margins)
	2	In the parenchyma (<50% of the lobules)
	3	In the parenchyma (>50% of the lobules)
Necrosis	0	Absent
	1	Periductal necrosis (<5%)*
	2	Focal necrosis (5-20%)
	3	Diffused parenchymal necrosis (>20%)

*Approximate percentage of cells involved per field examined.

2.11.3 Measurement of pancreatic and pulmonary MPO activity

MPO activity was used as a marker of neutrophil infiltration and determined as previously described[436]. Briefly, frozen pancreatic and pulmonary tissue were homogenized with a tissue tearor in 1 mL 100 mM sodium phosphate buffer (pH 7.4) with protease inhibitor 10,000 unit/mL. The homogenates were repeatedly centrifuged at 16,000 g, 15 minutes, 4°C and resuspended in fresh homogenize buffer for 2 or 3 times followed by last resuspended in 100 mM sodium phosphate buffer (pH 5.4) containing 0.5% hexadecyltrimethylammonium bromide (HETAB), 10 mM EDTA and protease inhibitors, with further three freeze-thawed cycles and sonicated for 30 seconds, finally centrifuged for 15 min at 16,000 × g. After which, MPO activity was measured in the supernatants (**Figure 2.3**). The enzyme activity was determined spectrophotometrically as the MPO-catalysed change with 3,3,5,5-tetramethylbenzidine as the substrate (TMB) in the redox reaction with presence of H_2O_2. Absorbance was recorded at 655 nm.

A standard curve was generated using myeloperoxidase from human leukocytes. MPO activity was calculated as the difference between the values at 0 and 3 min based on protein amount.

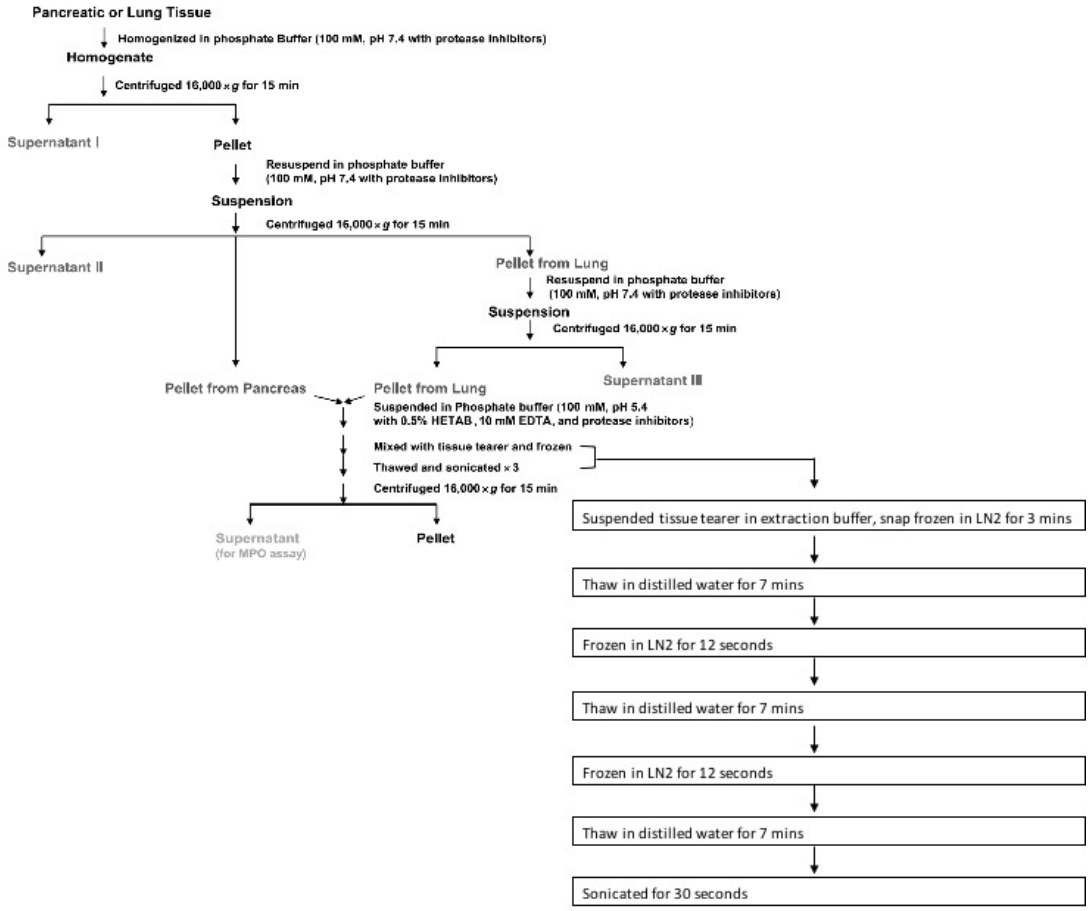

Figure 2.3 Flowchart for collection of supernatant for MPO assay

Preparing MPO assay from pancreas and lung required cycles of centrifugation and resuspension in buffer with protease inhibitors to remove MPO inhibitory activities of enzymes as shown above. Pulmonary samples needed one more centrifugation and resuspension cycle. The supernatants collected were used for testing MPO activity (Adapted from Dawra et al., 2008[436]).

2.11.4 Measurement of pancreatic trypsin activity

Trypsinogen is activated to trypsin when trypsin activation peptide is cleaved off and thus can be used as a marker of trypsinogen activation. It was determined by measuring enzymatic activity of trypsin fluorometrically with Boc-Glu-Ala-Arg-methylcoumarin amide (MCA) as substrate[437-439], using POLARstar Omega microplate reader.

Briefly, pancreata were homogenised with a tissue tearor on ice in homogenization buffer. The resulting homogenates were centrifuged at 1,500 g for 5 min at 4°C. The supernatant was loaded to a 96-well plate containing pre-warmed assay buffer and Boc-Gln-Ala-Arg-MCA substrate (λexcitation/ λemission = 380nm/ 440nm). A standard curve was generated using commercially purified trypsin from bovine pancreas. Pancreatic trypsin activity was calculated as the difference of fluorescence intensity between 0 min and 5 min and then was normalized to the protein amount determined with BCA assay.

2.11.5 Measurement of serum IL-6

IL-6 levels were determined in serum by using a double-antibody quantikine enzyme-linked immunosorbent assay kit. The assay was performed according to manufacturer's instructions, with all samples run in duplicates. Recombinant murine IL-6 supplied within the kit was used as a standard. Average readings for the duplicates were calculated based on determination of the optical density using BMG microplate reader set to 450nm with wavelength correction set to 540nm.

2.12 Experimental Chronic Pancreatitis (ECP)

Age and sex matched $CypD^{-/-}$ and wild type (WT) C57BL/6J mice received repetitive intraperitoneal caerulein injections (50 μg/kg, 6 hourly per day, thrice a week) as AP episodes for up to 4 weeks, control mice received comparable injections of normal saline. Mice were euthanized by CO_2 asphyxiation at 2, 4 and 6 weeks with various resolution period after last caerulein injection to mimic chronic pancreatic injury. Following confirmation of death, blood was first taken by cardiac puncture. The pancreata was detached from the spleen, weighed and divided into 3 pieces, for further assessing of morphology, biochemistry, fibrosis and immunohistochemistry study.

2.13 ECP Assessment

2.13.1 Morphology

Pancreatic morphology was used to evaluate the establishment of experimental chronic pancreatitis. Pancreata tissue samples fixed in 10% neutral formalin were embedded in paraffin. 6μm sections were prepared and stained with haematoxylin and eosin (H&E) for morphological examination. The chronic histopathological change was further blindly evaluated on 6 random fields (×20 high power fields) of each slide under light microscopy using a scoring grading system for the evaluation of inflammatory infiltration, interlobular fibrosis, necrotic sequellar foci, architecture (acinar atrophy, perilobular fibrosis, and intralobular fibrosis), and trichrome stained collagen deposition on a 0 (no alterations) to 3 (severe alterations) scale as previously described in detail[440] with minor modification (**Table 2.4**), calculating summated mean ± SEM, for ≥4 mice/group.

Table 2.4 Pancreatic histopathological grading criteria in CP

Parameter		Score	Indication
Inflammation		0	No alterations
		1	Few alterations
		2	Moderate alterations
		3	Severe alterations
Fibrosis Masson Trichrome		0	No alterations
		1	Few alterations (<5%)
		2	Moderate alterations (5-25%)
		3	Severe alterations (>25%)
Necrotic sequelae foci		0	No alterations
		1	Few alterations (<5%)
		2	Moderate alterations (5-25%)
		3	Severe alterations (>25%)
Architecture	Acinar atrophy	0-3	No alterations
	Perilobular fibrosis		Few alterations (<5%)
	Intralobular fibrosis		Moderate alterations (5-25%)
			Severe alterations (>25%)

2.13.2 Picro Sirius Red staining for collagen

As one of the best understood techniques to define collagen content, Picro Sirius Red was applied to characterise type I collagen deposition[441]. The method is used on paraffin sections of pancreas fixed 1 week in a neutral buffered formalin solution followed by manufacturer's instruction (**Figure 2.4**). In bright- field microscopy collagen is red on a pale-yellow background, with nuclei stained as grey or brown.

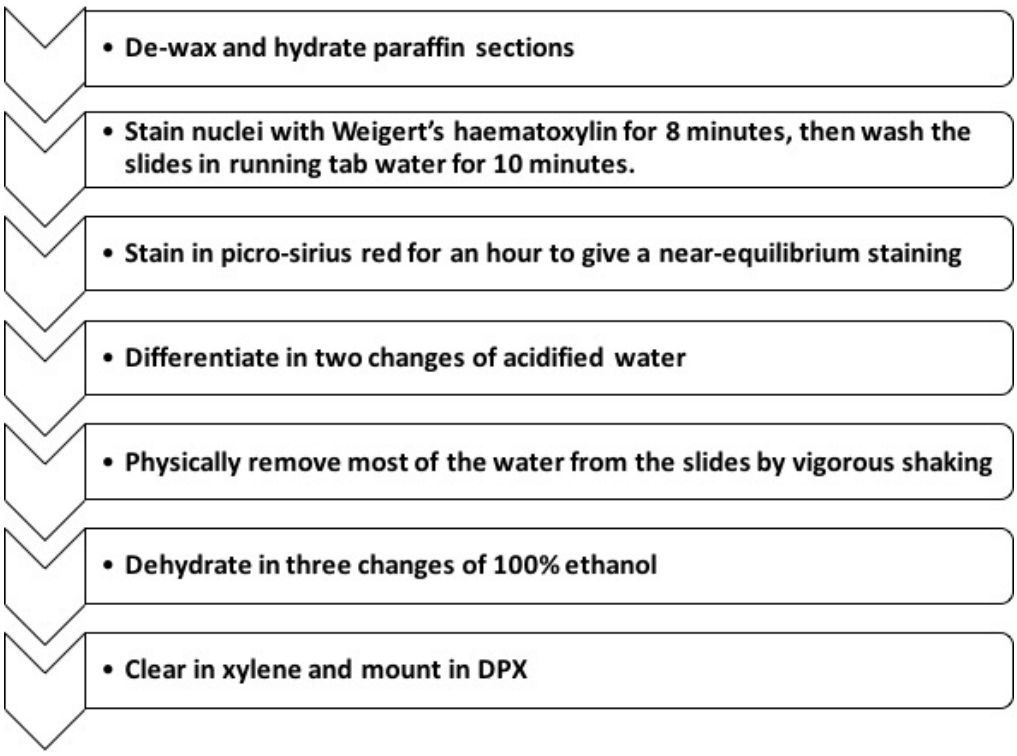

Figure 2.4 Flowchart for Picro Sirius Red staining

Collagen deposition was determined using ImageJ (version 1.5) software, calculated as the proportion of collagen stained in red as percentage of the total area measured. 10 fields were randomly selected from non-overlapping scanned images of each section for collagen quantification per section. Images were scaled to enable the measurement of each stained area in μm^2, converted to greyscale, using threshold algorithm. Optimal colour settings were kept consistent across all images.

2.13.3 Masson Trichrome staining for collagen

Masson's Trichrome is often used to differentiate between collagen and smooth muscle in tumours, and the increase of collagen in diseases. As the name implies, three dyes (see **Table 2.5**) are employed selectively staining muscle, collagen fibres, fibrin and erythrocytes. The general rule in trichrome staining is that the less porous tissues are coloured by the smallest dye molecule; whenever a dye of large molecular size is able to penetrate, it will always do so at the expense of the smaller molecule. The tissue section is stained first with the acid dye, Biebrich Scarlet, which binds with acidophilic tissue components. Then when treated with the phosphor acids, the less permeable components retain the red, while the red is pulled out of the collagen. At the same time causing a link with the collagen to bind with the aniline blue.

Table 2.5 Masson's Trichrome Reagents composition

Bouin's Fixative	Saturated picric acid 1500ml / Formaldehyde 500ml / Glacial acetic acid 100 ml
Biebrich Scarlet	Biebrich Scarlet 2.7gm /Acid fuchsin 0.3gm/Distilled water 300ml / Glacial acetic acid 3ml
Weigert's Hematoxylin Equal amounts with A&B	Solution A: Hamatoxylin 5.0 gm / 95% alcohol 500 ml Solution B: 29% ferric chloride 20ml / Distilled water 475ml / hydrochloric acid 5 ml
Phospho -Acid Solution	Phosphotungstic acid 25g / Phosphomolybdic acid 25g / Distill water 1L
Aniline Blue	Aniline Blue 2.5g / Distilled water 100ml / Glacial acetic acid 1ml
1% Acetic Acid	Glacial acetic acid 10 ml / Distilled water 1L

The Masson's Trichrome Procedure was performed according to manufacturer's instruction detailed in **Figure 2.5** below.

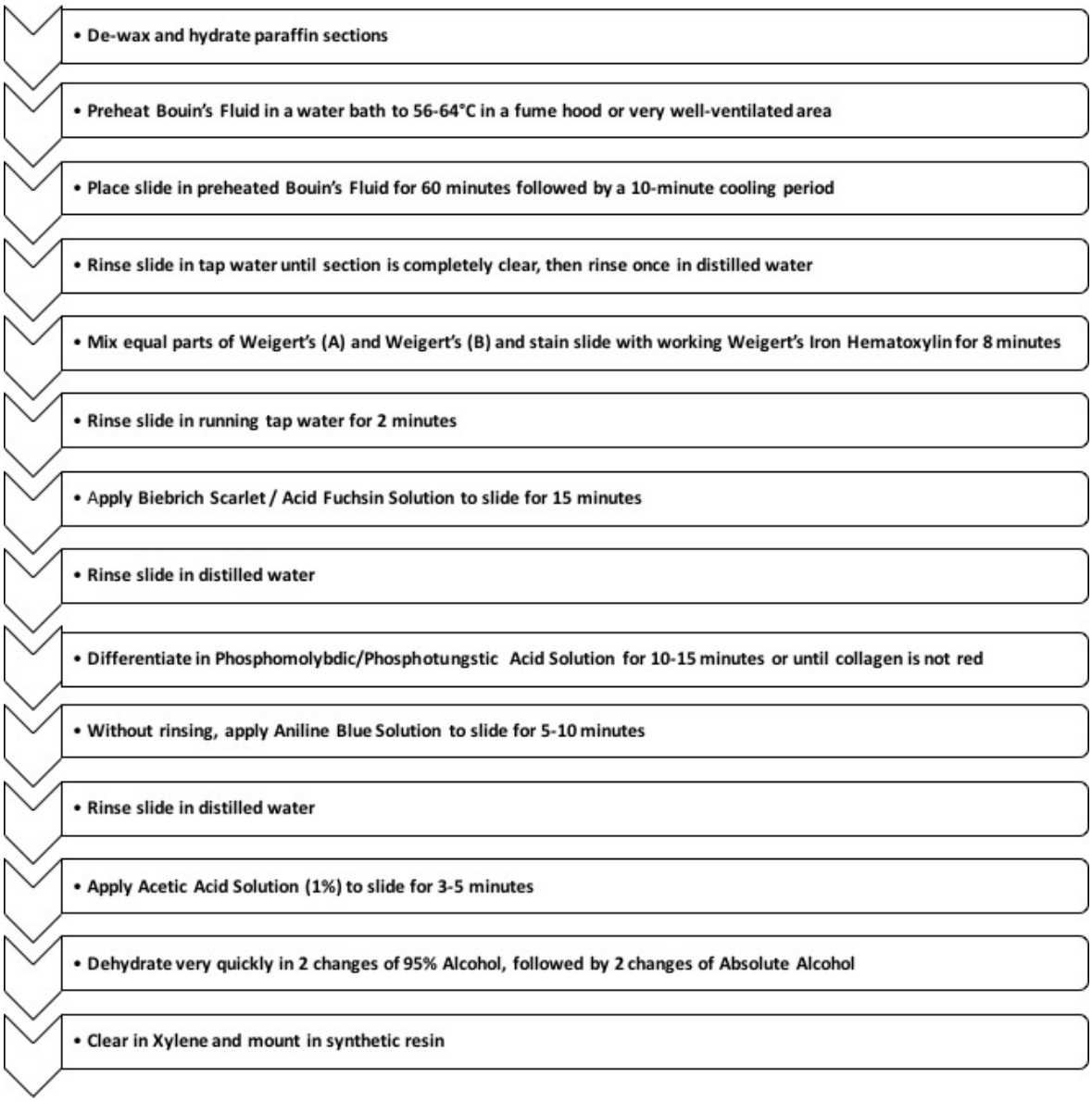

Figure 2.5 Flowchart for Trichrome staining

2.13.4 Immunohistochemistry staining (IHC)

The immunohistochemistry staining (IHC) procedure was performed following the protocol detailed as below.

Pancreata samples were fixed overnight in fresh 10% neutral formalin and embedded in paraffin. 6μm sections were prepared to be deparaffinised and antigen retrieval performed through boiling at 95°C in pH 9 antigen retrieval buffer using PT Link system. Tris buffered saline was prepared and used to make 0.1% TBS Tween 20 solution (TBST, same wash buffer also used in western). Following antigen retrieval and wash 3 times in TBST, the pancreatic section was treated with a series procedures using expose rabbit specific HRP/DAB detection IHC kit. First incubated for 30 min with 0.3% H_2O_2 to block endogenous peroxidase. Apply protein block (supplied in the kit) after 2 washes in TBST and incubate for 20 minutes at room temperature to block nonspecific background staining. Pancreatic sections were then washed with TBST and dried. The mouse alpha smooth muscle actin (α-SMA) expression were detected after sequential incubation, and finally visualized with chromogen 3, 3′-Diaminobenzidine (DAB). Precisely, following protein block wash, sections were covering with α-SMA antibody diluted 1:200 in antibody diluent and incubate overnight at 4 °C, antibody diluent alone is used as control. After another 4 washes with TBST, apply enough drops of goat anti-rabbit horseradish peroxidase (HRP)-conjugate (supplied in the kit) to cover pancreatic tissue and incubate for 20 minutes at room temperature. Rinse 3 times in wash buffer with additional DAB chromogen for 5-10 minutes at room temperature to visualise bound antibody. Rinse 4 times in buffer and after the final wash with TBST, pancreatic sections were left to rest in distilled water before placing the slides

in Mayer's haematoxylin to counterstain 30 seconds for nuclei staining. Slides were subsequently washed in running tab water until clear before dip in 1% acid alcohol for 5 seconds then placing in 2% ammonium hydroxide for a further 30 seconds. Slides were then agitated in 90% ethanol for 30 seconds, followed by 3 changes of 100% ethanol for a further 3*30 seconds, replacing the ethanol after the first minute. Finally, the slides were cleaned in two changes of xylene for 1 minute of each before mounting in a mixture of distyrene plasticizer xylene (DPX).

Stained slides were scanned with Aperio ScanScope^{TM} system at × 200 magnification and using semi-quantified grading system.

2.13.5 Measurement of enzymatic function

Serum amylase was detected as previously described in 2.11.1. For reserved pancreatic amylase level, 25 mg pancreatic tissue was homogenized in ice cold phosphate buffered saline buffer containing protease inhibitor cocktail (1 tablet per 10 mL). Homogenates were then centrifuged at 16000g, 4°C for 10 minutes. Supernatant was collected for amylase detection, and the final pancreatic amylase level was calculated based on arbitrary protein amounts according to BCA assay.

For reserved pancreatic lipase, 40 mg pancreatic tissue was homogenized in assay buffer supplied with the colorimetric lipase assay kit adding protease inhibitor cocktail (1 tablet per 10 mL). Homogenates were centrifuged at 16000g, 4°C for 10 minutes. Supernatant was collected for lipase detection according to manufacturer's instruction, standard curve was generated by glycerol. The final pancreatic lipase was evaluated based on kinetic glycerol production in certain periods and calculated with arbitrary protein amounts according to BCA assay.

2.13.6 Measurement of serum TGF-β1

Activated TGF-β1 level was determined in serum by using a double-antibody quantikine® ELISA kit. Serum was premixed with HCl and incubate at room temperature, and then neutralized by NaOH/HEPES solution. The assay was performed according to manufacturer's instructions, with all samples run in duplicates. Recombinant TGF-β1 supplied within the kit was used as a standard. Average readings for the duplicates were calculated based on determination of the optical density using BMG microplate reader set to 450nm with wavelength correction set to 540nm.

2.14 Drug preparation

Cyclosporin A, SEL-3639, SEL-3714, SEL-1233 and CC/SCY635 (compounds supplied in powder by Cypralis) were first dissolved in DMSO to make 50 mg/mL or 100 mg/mL stock and further diluted with 10% Cremophor in normal saline. The dilution procedure was freshly made before each dosing through drop by drop titration with a mini stirrer bar to get a clear ready to use formulation.

For part of SEL1233 intervention, compound was dissolved in polyethylene glycol 400 based formulation which was supplied directly by Cypralis.

2.15 Software

Microsoft Word 2010 served as a main tool for drafting and editing this thesis. Statistical analysis was conducted with SPSS 24. Table and charts were made in Microsoft Excel 2010 and graphs were exported with Origin 9. Slides images were obtained using Aperio ImageScope (version 12.3.3). Image J 1.5 was used to

quantify the collagen deposition and positive IHC staining. GeneSnap (version 7.12) and GeneTools (version 4.02) were used for western blot image capture and band analysis. Figure legends were prepared in Microsoft PowerPoint 2010. The reference list was generated using Endnote X8.

2.16 Statistics

Kolmogorov-Smirnov and Levene test were used to check the data distribution and homogeneity of variances, respectively. Normally distributed data with equal variance were presented as mean ± SEM and analysed by parametric Student's t-test and one-way ANOVA with post-hoc LSD test. Mann–Whitney or analysis of variance on non-parametric Kruskal-Wallis tests were performed on non-normally distributed data, which were presented as medians with range, using SPSS v22.0, with p values <0.05 considered significant**.**

CHAPTER 3

Effects of CsA on PACs exposed to pancreatitis toxins

3.1 Summary

This chapter has investigated and evaluated, *in vitro*, the protective capabilities of CsA against TLCS, POA or caerulein induced cell injury, including necrotic and apoptotic cell death activation, ROS production and ER based chaperone expression.

The findings of this chapter demonstrate that CsA significantly inhibited TLCS-, POA- or CER- induced necrotic cell death in mouse PACs with less efficacy at higher concentration.

CsA inhibited bile acid TLCS -induced necrotic cell death accompanying with reduced ROS production and CypB overexpression in TLCS treated PACs. CsA did not appear to protect acinar cell from toxin induced caspase 3/7 dependent apoptosis, on the contrary, the adverse effects of high concentration CsA exacerbated ROS production and promoted apoptosis of PACs, as seen in TLCS treated PACs that CsA upregulated ER chaperone expression and ROS production, promoting toxin-induced caspase 3/7 related apoptosis. Caerulein also exerted the ability to generate ROS production and promoting apoptosis, while POA, however, had no impact on ROS production, but showed decreasing trend.

The beneficial effects of CsA, consistently observed at low micromolar concentration, highlights the incomplete understanding the impotence of ROS and its balance in cellular function and cell fate which warrants further investigation.

3.2 Introduction

Emerging data suggests the interrelations of ROS, ER stress and cell death[442-444]. It is well known that pancreatic precipitants could disrupt calcium signalling, elicit sustained cytosolic Ca^{2+} overload, feature prominent in triggering PACs injury, cause MPTP opening, ATP depletion and consequent necrotic cell death[445].

Physiological low-level ROS function as redox messengers in intracellular signalling, while excess ROS induced oxidative stress may occur during AP development and modify Ca^{2+} signalling events in the acinar cell[446]. Sustained cytosolic calcium rises level resulted in maintained ROS elevation locally within the acinar cell which could affect cell death pattern to promote apoptosis but not necrosis with bile acid induced injury[213].

When various UPR- induced mechanisms fail to alleviate ER stress, both the intrinsic and extrinsic pathways for apoptosis can be activated[447]. In contrast to apoptosis, which thought to limit inflammation and shift disease severity in pancreatitis, necroptosis, a subtype of necrosis and regulated by MLKL and RIPK3 or partially RIPK1[216] could release massive amounts of damage-associated molecular patterns, which is generally considered to be a contribution to robust inflammation, as data suggested necroptosis is the predominate mode of acinar cell death in severe experimental mouse pancreatitis[448]. Despite both ROS and ER stress are generally regarded to promote apoptotic cell death, recent data suggest ROS are important contributors to neutrophil necroptosis induced by ligation of adhesion receptors, for which involves RIPK3-MLKL-p38 MAPK-PI3K axis with all molecular components are required to generate ROS via NADPH oxidase and

subsequent necrosis[449], what's more, it was verified that IR injury induced ER calcium release, leading to ROS overproduction, which was regulated by RIPK3 and contributed to MPTP opening that mediated cellular necroptosis[450], and ER stress has also been shown to induce necroptosis[451].

It was demonstrated that additional ER oxidative pathway is modulated by CypB and CypC, single knock down didn't produce any visible phenotype due to compensatory activities of CypB and CypC, while double genetic knockdown and pharmacological inhibition with CsA induced hyperoxidation phenotype of ER, which caused substantial oxidative stress[384]. Similarly, CypB-depleted glioblastoma cells showed higher ROS levels than control cells, and developed higher increase in ROS following H_2O_2 exposure, indicating reduced ability to handle oxidative stress[300].

Studies reported that ER stress activates the expression of the ER localized cyclophilin B gene. CypB interacted with the ER stress-related chaperones, GRP-78. Overexpression of wild type CypB blocks Ca^{2+} leakage from the ER to cytosol against the ER stress-inducing drug, the SERCA blocker thapsigargin, and ultimately prevents cell death in response to ER stress, whereas overexpression of an isomerase activity-defective mutant, CypB/R62A, not only increased Ca^{2+} leakage from the ER and ROS generation, but also decreased mitochondrial membrane potential, resulting in cell death following exposure to ER stress-inducing agents[295].

CsA has shown to induce persistent ER stress at higher concentration due to CypB inhibition[382] and to facilitate the expressions of ER chaperones such as GRP-78 and

GRP94[293, 294]. CsA is regarded to induce the removal of intracellular CypB, mobilized CypB from the ER to extracellular region, resulting ER multiprotein complex collapse by the absence of CypB, which affect ER chaperones for synthesis, folding and lead to ER stress[302].

To further characterize the PACs cell death pattern and the possible interlink between ROS production and ER chaperones following presence of pharmacological MPTP inhibition with CsA, the study was designed to examine the kinetic pancreatic cellular response to toxins with the presence of a wide range concentrations of CsA on cell death, ROS production and ER based chaperones.

3.3 Methods

Freshly isolated mice PACs (2*10^6/mL, viability>75%) either double stained with 1.5 μM PI and 1 μM caspase 3/7 or stained with CM-H2DCFDA probe, were co-incubated with CsA at different concentrations for 30 minutes, to detect cell death pathway activation and intracellular ROS production as previously described in chapter 2.8 and 2.9**.** Fluorescence intensity was counted in duplicates each experiment and repeated at least 6 experiments. The ratio of increase in fluorescence peak was used to represent the results.

For western blot, freshly isolated PACs suspension with various concentrations CsA and TLCS pre-treated for 2-6h were lysed for further detection as previously described in chapter 2.10.

3.4 Results

3.4.1 Kinetic necrotic cell death response to toxins

Isolated PACs were pre-treated with PI and CsA at different concentration ranges from 100nM to 50μM to detect kinetic necrotic cell death activation following 500 μM TLCS, 100 μM POA or 10 nM caerulein stimulation. PI intensity changes were shown as F/F_0 ratio. Kinetic necrotic cell death trace curve was presented in line plot throughout whole period (**Figure 3.1A - 3.5A**) and mean changes in PI fluorescence intensity over baseline are also shown (F/F0) in bar chart at every 6h interval during FI signal liner rising period (**Figure 3.1B -3.5B**).

All three toxins including 500μM TLCS, 100μM POA and 10nM CER induced necrotic cell death in PACs with various extent showing unique pattern (**Figure 3.1**). The PACs had a rapid PI intensity rises in response to 500μM TLCS exposure shown in blue, the signal trace demonstrated a continuous rise after initial steady period and reached the peak around 12h, which only caused 80% cell death when compare to the level that Triton shown in red induced highest FI intensity. However, 100μM POA shown in pink curve started to elicit a violent FI rise of necrotic cell death signal after 2h and reached the maximal cell death at 10-12h. Unlike TLCS and POA induced quick and progressive necrotic cell death, FI signal gradually rises with subtle increase in 10nM caerulein stimulated PACs shown in green, which takes 4-6 h to induce initial necrotic cell death activation.

Increasing concentrations of CsA lead to fierce cellular perturbation at initial period with rapid increase and fall, but then steadily increase cell necrosis, presenting a biphasic cellular response pattern, with lowest concentration and higher

concentration showing more necrotic cell death with time when applied to PACs itself (**Figure 3.2**).

When expose to TLCS, suppression of necrotic cell death towards the initial baseline approached >40% with long term application of CsA throughout whole liner response time period (**Figure 3.3**), showing reduced cell death with all concentrations of CsA.

There is no significant difference between all the groups during the initial period with POA. However, CsA at all concentrations started to show beneficial when POA induced modest to high level necrotic cell death with time (**Figure 3.4**).

Caerulein at 10nM alone doesn't induce significant necrotic cell death, but when co-expose to CsA, all groups induced significant necrotic cell death during early period before 6h, furthermore with low concentration CER started to activate necrotic cell death after 6h, only CsA at 5 μM shown in green depicts alleviated necrotic cell death activation (**Figure 3.5**).

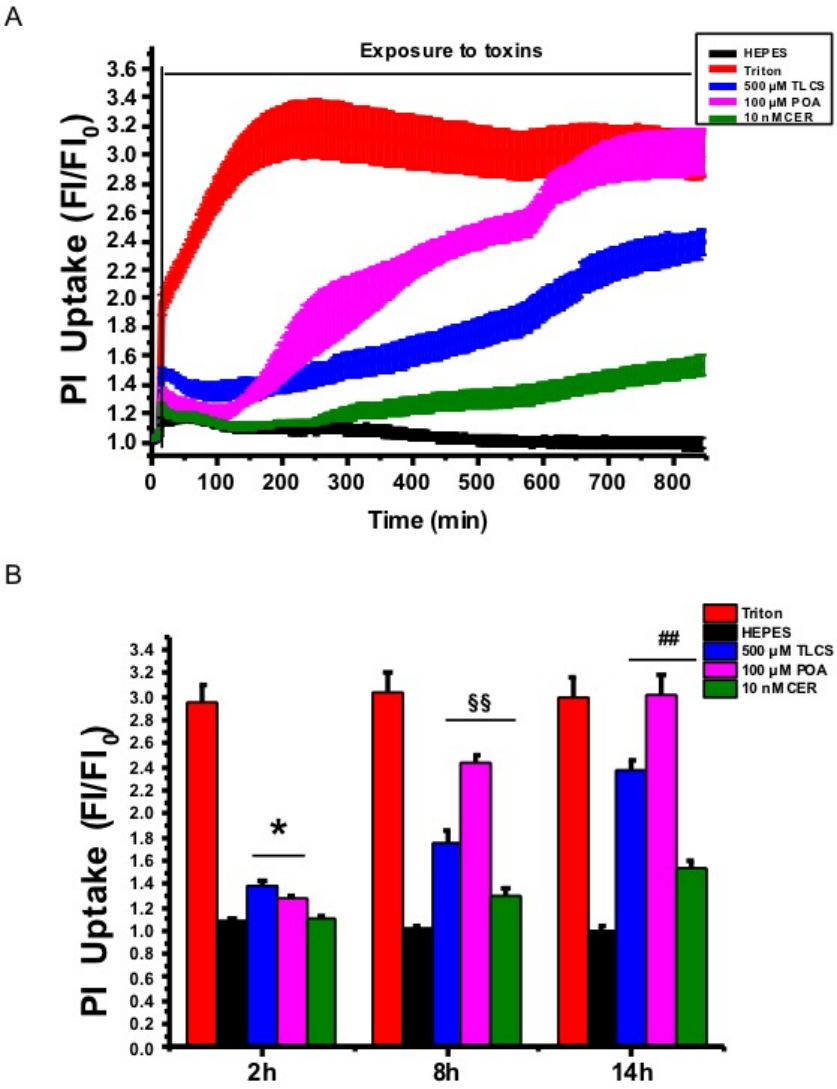

Figure 3.1 TLCS-, POA- or caerulein-induced necrotic cell death

PI loaded PACs were exposed to TLCS, POA or caerulein. Results are normalised to the basal fluorescence reading t=0 expressed as F/F_0. **(A)** Kinetic necrotic cell death activation trace curve and **(B)** Time course necrotic cell death activation induced by 500µM TLCS. 100µM POA and 10nM CER, indicate various kinetic necrotic cell death activation extent and action pattern. All data shown are mean ± SEM, with averages>6 experiments. $^{*}P<0.05$, $^{\S\S,\#\#}P<0.01$. Nuclei stained with Triton showed the total PI uptake intensity.

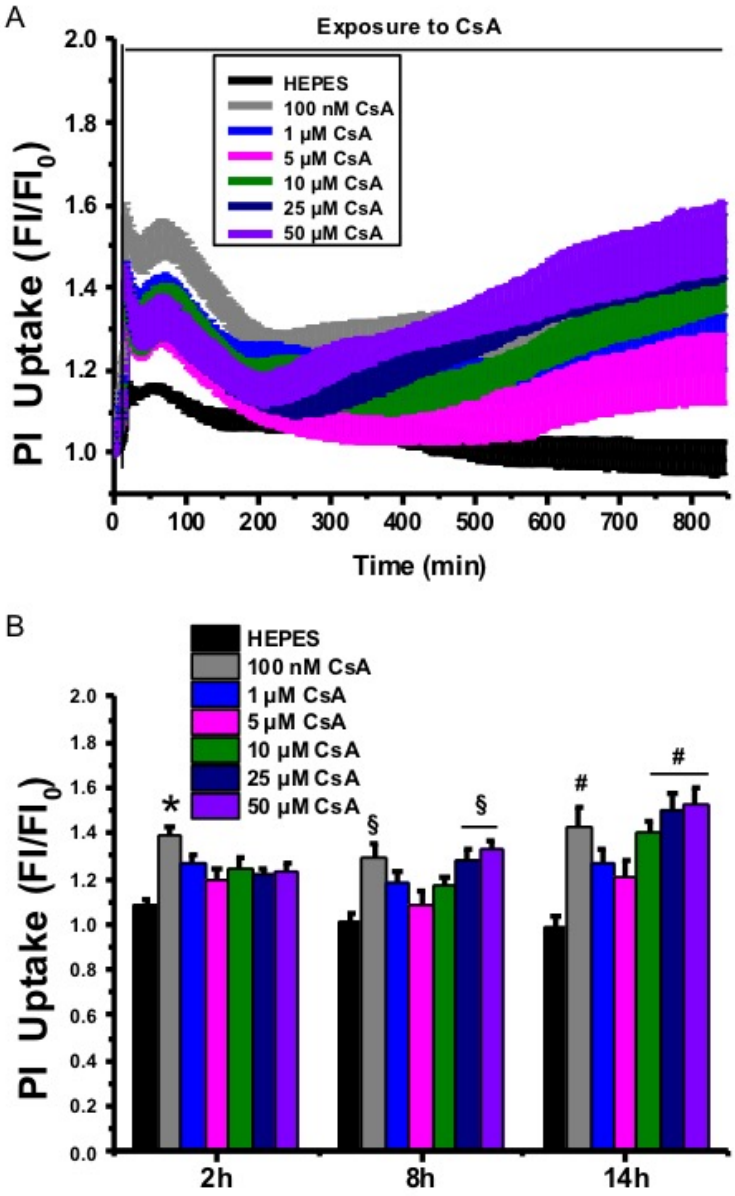

Figure 3.2 Necrotic cell death pathway activation of PACs in response to CsA

PI loaded PACs were treated with 100nM, 1µM, 5µM, 10µM, 25µM and 50µM CsA. Results are normalised to the basal fluorescence reading t=0 expressed as F/F_0. **(A)** Kinetic necrotic cell death activation trace curve, **(B)** Time course necrotic cell death activation in response to CsA.

All data shown are mean ± SEM, with averages of >6 experiments.

$^{*, \S, \#}P<0.05$, compare to NaHEPES control group.

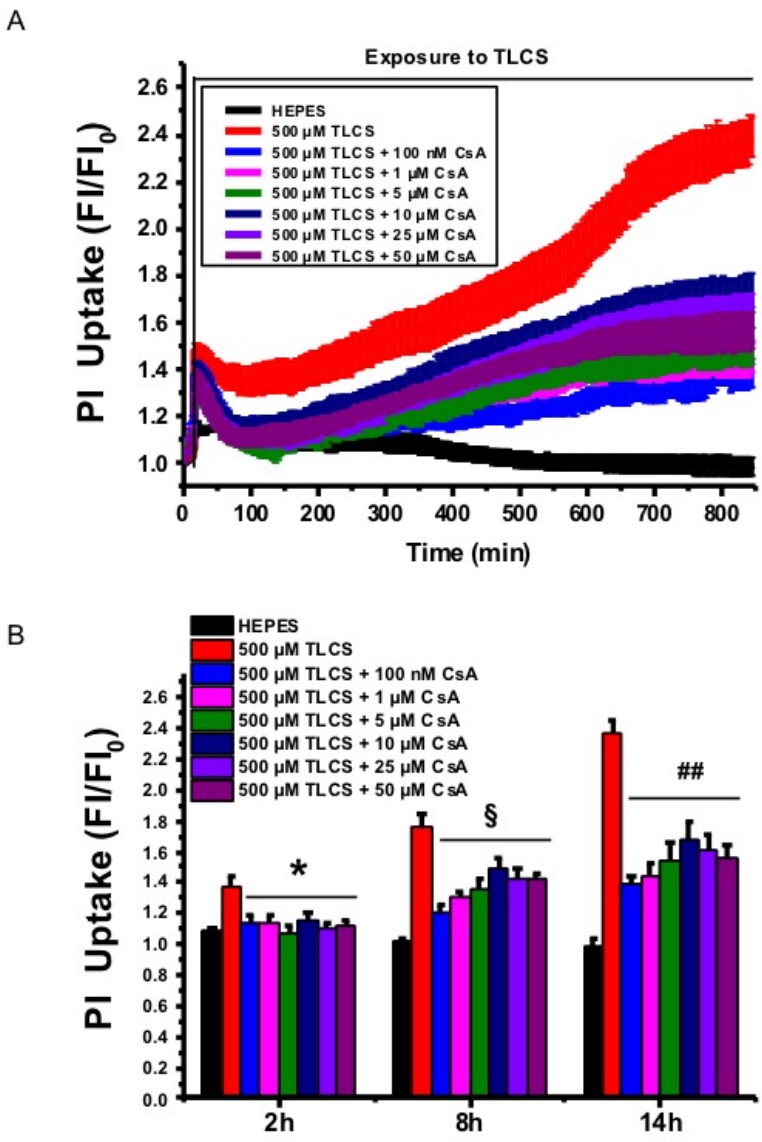

Figure 3.3 Effects of CsA in TLCS induced necrotic cell death

PI loaded PACs were expose to TLCS. Results are normalised to the basal fluorescence reading t=0 expressed as F/F_0. **(A)** Kinetic necrotic cell death activation trace curve and **(B)** Time course necrotic cell death activation following TLCS exposure in presence of CsA.

All data shown are mean ± SEM with averages >6 experiments. CsA at all concentrations significantly reduced TLCS induced necrotic cell death.

$^{\#\#}P<0.01$, $^{*,\,\S}P<0.05$, compared to TLCS group.

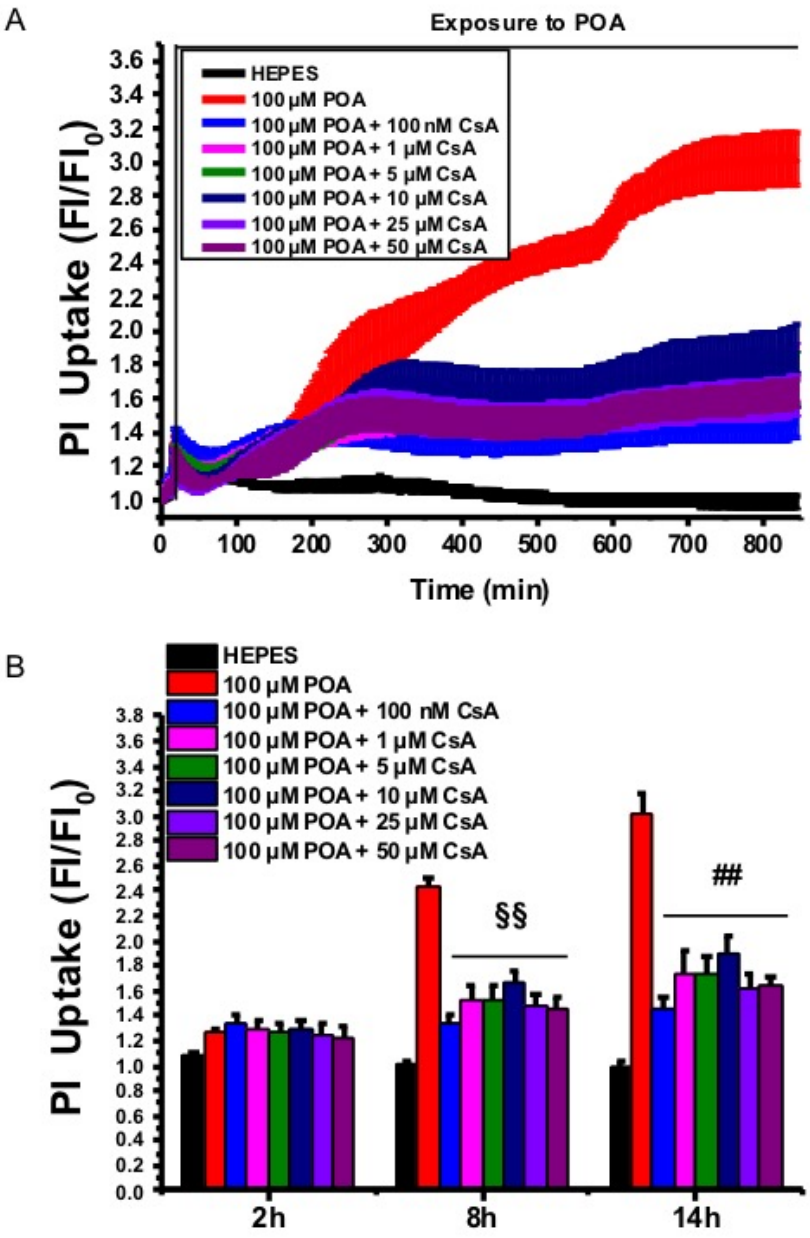

Figure 3.4 Effects of CsA in POA induced necrotic cell death

PI loaded PACs were expose to POA. Results are normalised to the basal fluorescence reading t=0 expressed as F/F_0. **(A)** Kinetic necrotic cell death activation trace curve and **(B)** Time course necrotic cell death activation following POA exposure in presence of CsA. All data shown are mean ± SEM, with averages of >6 experiments. $^{§§, ##}P<0.01$, compared to POA group.

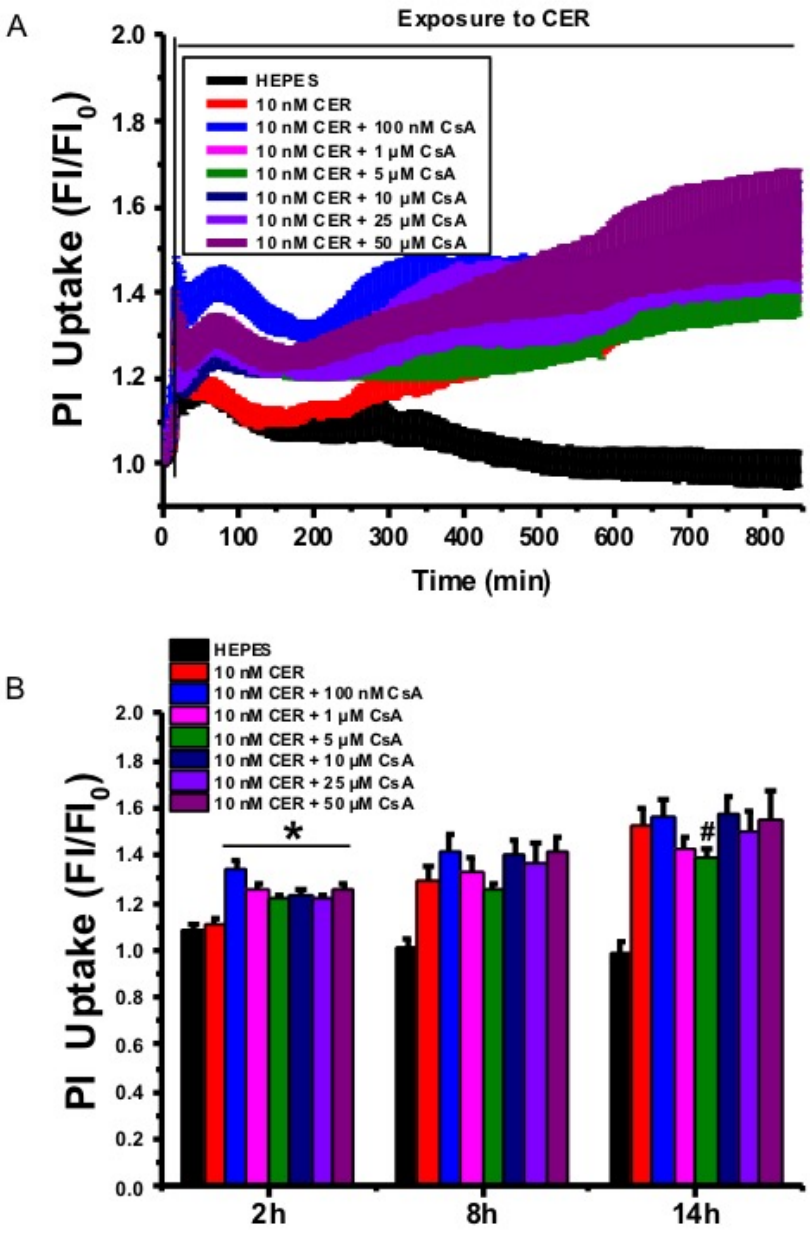

Figure 3.5 Effects of CsA in Caerulein induced necrotic cell death

PI loaded PACs were expose to POA. Results are normalised to the basal fluorescence reading t=0 expressed as F/F_0. **(A)** Kinetic necrotic cell death activation trace curve and **(B)** Time course necrotic cell death activation following POA exposure in presence of CsA. PI uptake showing mean ± SEM at 2h, 8h and 14h. All data shown are mean ± SEM, with averages of >6 experiments.

*, # $P<0.05$, compared to CER group.

3.4.2 Kinetic apoptotic cell death response to toxins

Isolated PAC suspension from mice were stained with Caspase 3/7 probes for 30 minutes and mixed with different concentration ranges from 100nM to 50μM of CsA to run the baseline. The pre-treated PACs were exposed to 500μM TLCS, 100μM POA or 10nM CER, respectively to investigate pathological acinar cell injury. Kinetic apoptotic cell death trace curve was presented in line plot throughout whole period (**Figure 3.6A -3.10A**), mean changes in caspase 3/7 fluorescence intensity over baseline were also shown as F/F_0 ratio in bar chart at every 6h interval at 2h, 8h and 14h (**Figure 3.6B -3.10B**).

500 μM TLCS and 100 μM POA induce steady modest caspase 3/7 activation rise while no significant activation has seen with 10nM CER exposure (**Figure 3.6**). The PACs had similar extent of caspase 3/7 activation intensity rises in response to 500 μM TLCS exposure shown in blue and 100 μM POA depicts in pink. CsA induced caspase 3/7 activation in a time and concentration-dependent manner (**Figure 3.7**) when applied to PACs itself. When expose to TLCS or CER, neither time- nor concentration-dependent significant suppression of apoptotic cell death towards the initial baseline with CsA application has been observed (**Figure 3.8** and **Figure 3.10**). However, when PACs was stimulated with POA, CsA at 5 μM shown in blue suggested alleviated apoptotic cell death activation (**Figure 3.9**). It appears that under toxin-and CsA-free situation, the PACs present a relative stable status shown as intensity even similar to the basal level in terms of necrotic cell death but on the contrary, the gradually increased apoptotic signal with time in caspase 3/7 stained PACs even with NaHEPES only.

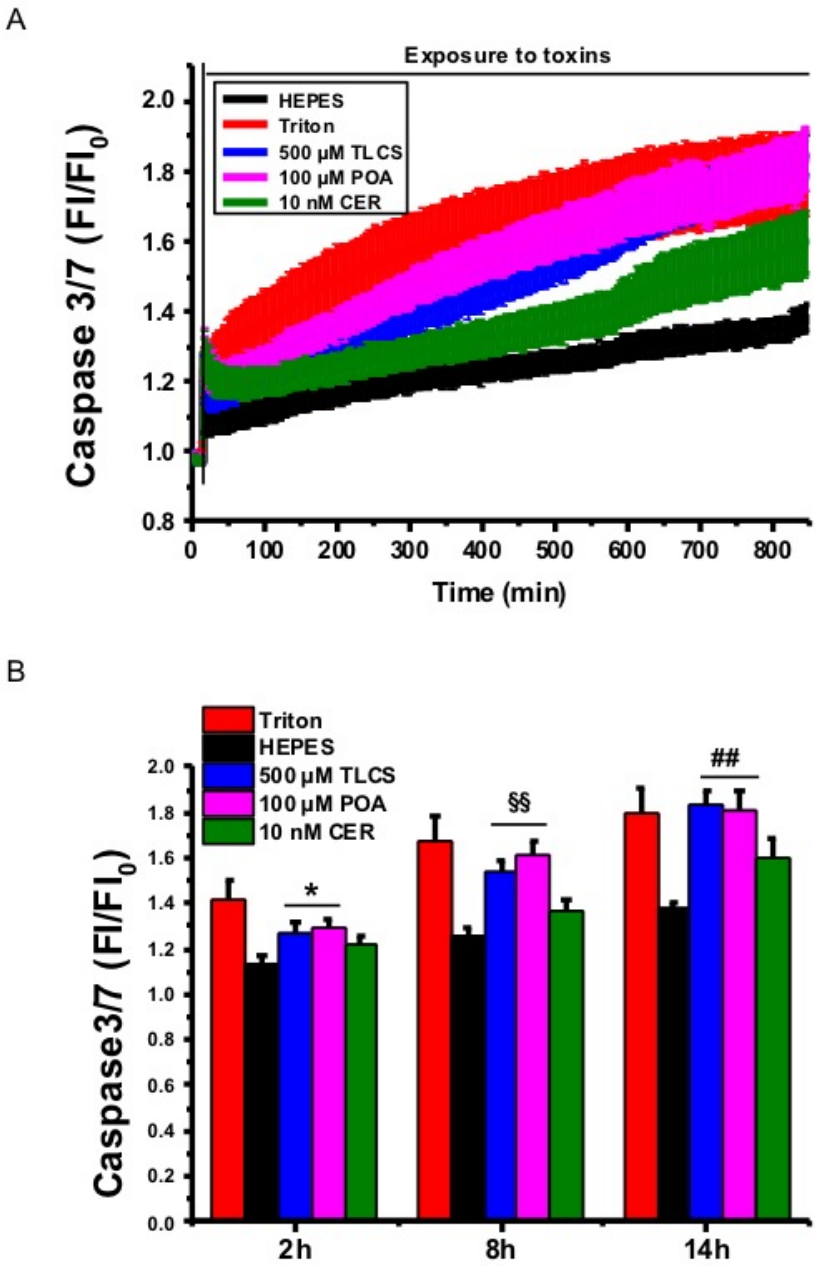

Figure 3.6 TLCS-, POA- or caerulein-induced apoptotic cell death

Cell event caspase 3/7 green reagent loaded PACs were loaded exposed to TLCS, POA or caerulein. Results are normalised to the basal fluorescence reading t=0 expressed as F/F_0. **(A)** Kinetic apoptotic cell death activation trace curve, **(B)** Time course apoptotic cell death activation induced by 500µM TLCS. 100µM POA and 10nM CER. Traces are. All data shown are mean ± SEM with averages of >6 experiments. $^{*}P<0.05$, $^{\S\S,\#\#}P<0.01$, compared to NaHEPES control group.

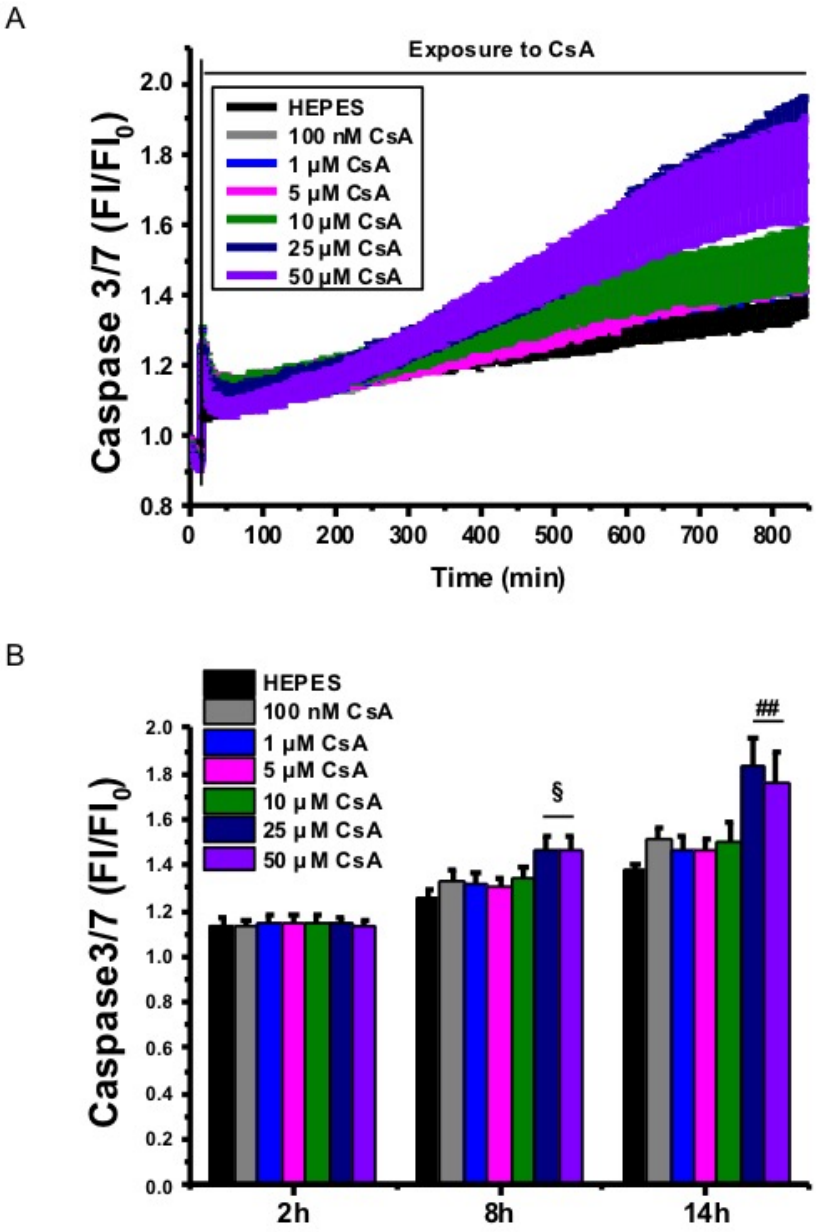

Figure 3.7 Apoptotic cell death pathway activation of PACs in response to CsA

CellEvent Caspase3/7 green reagent loaded cells were treated with 100nM, 1µM, 5µM, 10µM, 25µM and 50µM CsA. Results are normalised to the basal fluorescence reading t=0 expressed as F/F_0. **(A)** Kinetic apoptotic cell death activation trace curve, **(B)** Time course apoptotic cell death activation in response to CsA. All data shown are mean ± SEM, with averages of >6 experiments. $^{\S}P<0.05$, $^{\#\#}P<0.01$, compared to NaHEPES group.

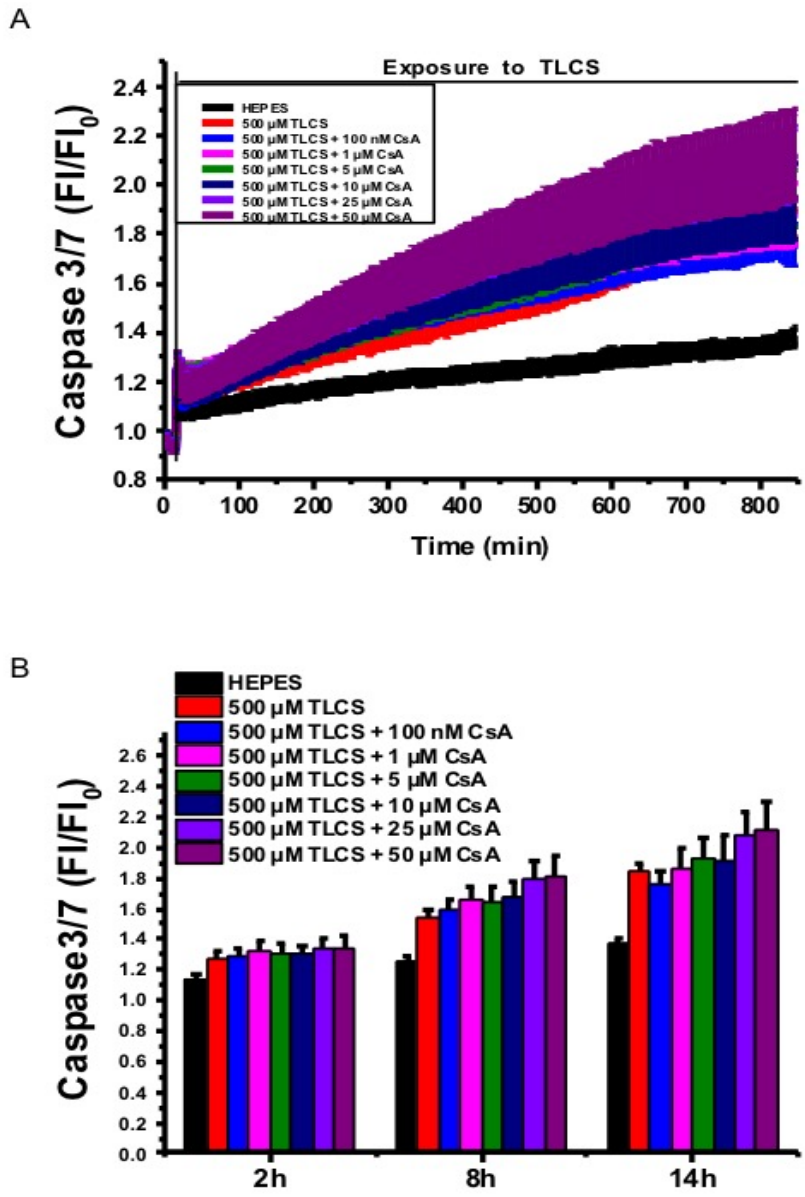

Figure 3.8 Effects of CsA in TLCS induced apoptotic cell death

CellEvent Caspase3/7 green reagent loaded cells treated with 100 nM, 1 µM, 5 µM, 10 µM, 25 µM or 50 µM CsA were exposed to 500 µM TLCS. Results are normalised to the basal fluorescence reading t=0 expressed as F/F_0. **(A)** Kinetic apoptotic cell death activation trace curve and **(B)** Time course apoptotic cell death activation following TLCS exposure in presence of CsA. Caspase 3/7 FI showing mean ± SEM at 2h, 8h and 14h. Traces are averages of >6 experiments. No significant difference in presence of CsA following TLCS treatment.

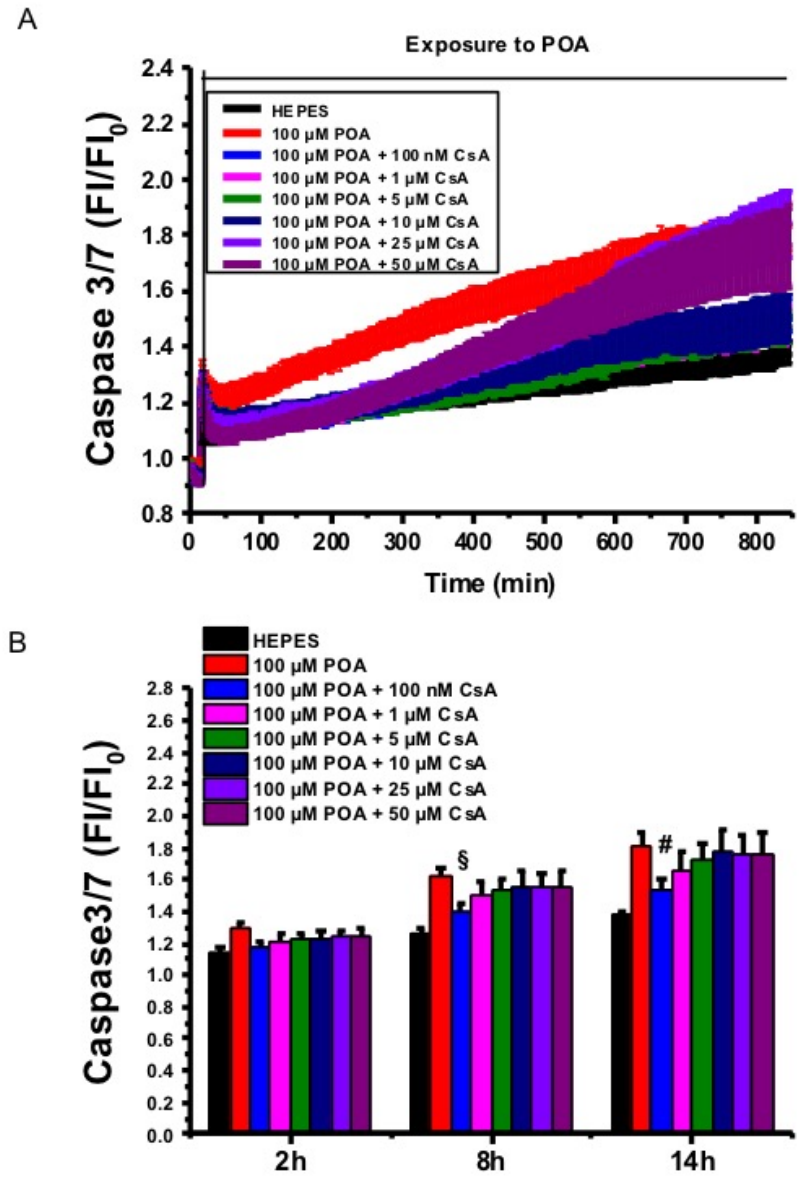

Figure 3.9 Effects of CsA in POA induced apoptotic cell death

CellEvent Caspase3/7 green reagent loaded cells treated with 100 nM, 1 µM, 5 µM, 10 µM, 25 µM or 50 µM CsA were exposed to 100 µM POA. Results are normalised to the basal fluorescence reading t=0 expressed as F/F_0. **(A)** Kinetic apoptotic cell death activation trace curve, **(B)** Time course apoptotic cell death activation in response to CsA. All data shown are mean ± SEM, with averages of >6 experiments. $^{\S,\#}P<0.05$, compared to POA group.

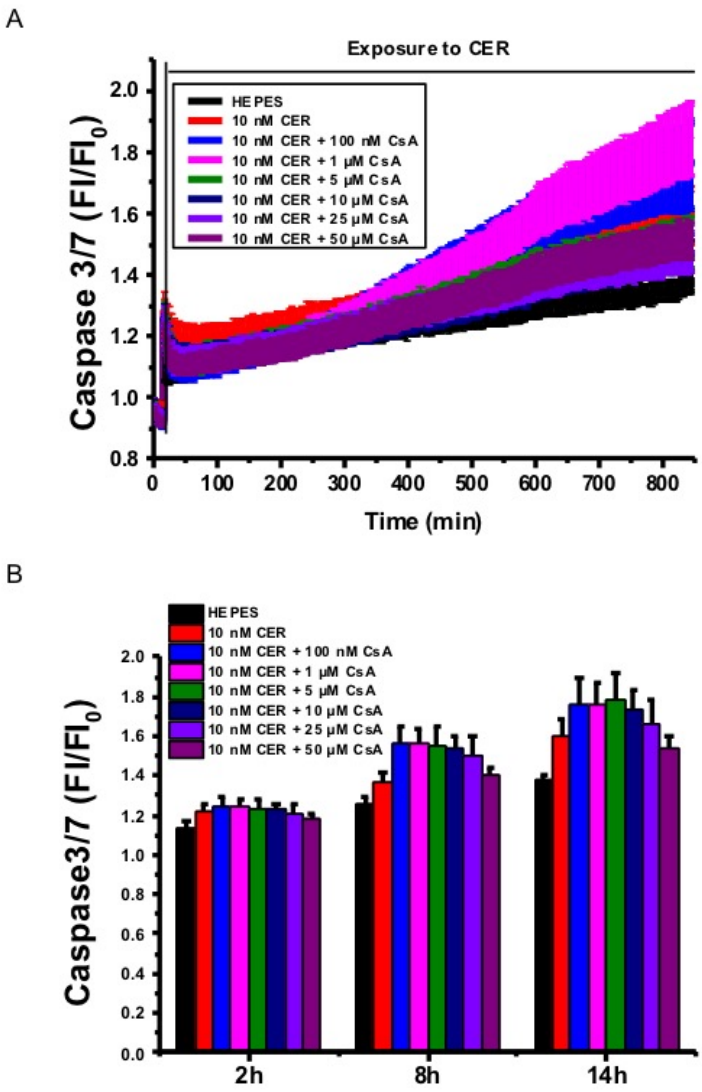

Figure 3.10 Effects of CsA in Caerulein induced apoptotic cell death

CellEvent Caspase3/7 green reagent loaded cells treated with 100 nM, 1 µM, 5 µM, 10 µM, 25 µM or 50 µM CsA were exposed to 10 nM CER. Results are normalised to the basal fluorescence reading t=0 expressed as F/F_0. **(A)** Kinetic apoptotic cell death activation trace curve, **(B)** Time course apoptotic cell death activation in response to CsA. All data shown are mean ± SEM, with averages of >6 experiments. No significant difference in presence of CsA following caerulein treatment.

3.4.3 Kinetic ROS generation in response to toxins

Isolated PAC suspension from mice were stained with fluoresce dye CM-H_2DCFDA for ROS production assay for 30 minutes and mixed with different concentration ranges from 100nM to 25μM of CsA were exposed to 500μM TLCS, 100μM POA or 10nM CER, respectively to investigate pathological ROS production. Kinetic intracellular ROS production trace curve was presented in line plot throughout whole period (**Figure 3.11A -3.15A**). Mean changes shown as CM-H_2DCFDA fluorescence intensity over baseline were also presented as F/F_0 ratio in bar chart at different time point (**Figure 3.11B -3.15 B**).

The high concentration of H_2O_2 treatment caused consistent rise of ROS generation as reflected by continuous increased intensity of CM-H_2DCFDA fluorescence intensity. Both 500μM TLCS and 10nM CER generate comparable extent of intracellular ROS production in PACs with similar pattern, while 100μM POA tend to decrease the cellular ROS generation (**Figure 3.11**). CsA itself generates ROS in a gradually time- and concentration- dependent manner, with CsA incubation at 1h earlier time point, comparable ROS production has shown in NaHEPES and all low CsA concentration incubated groups, only 25 μM CsA had higher but not yet significant ROS production compared to all other groups. After 2h incubation, however, all concentrations of CsA start to generate significant higher ROS levels compared to NaHEPES control group (**Figure 3.12**).

When exposed to TLCS and CER, both toxins started to induce early elevated ROS production at 1h, while CsA at lower concentrations showed suppression of toxins induced ROS generation, higher concentration of CsA at 25 μM does not suggest

any improvement. Following TLCS or CER exposure at later time point after 2h, PACs showed significantly reduced ROS production in presence of low CsA concentration. (**Figure 3.13, 3.15**). On the contrary, without increasing ROS production, POA alone or co-incubated with low concentration of CsA decreased ROS generation after 2h (**Figure 3.14**).

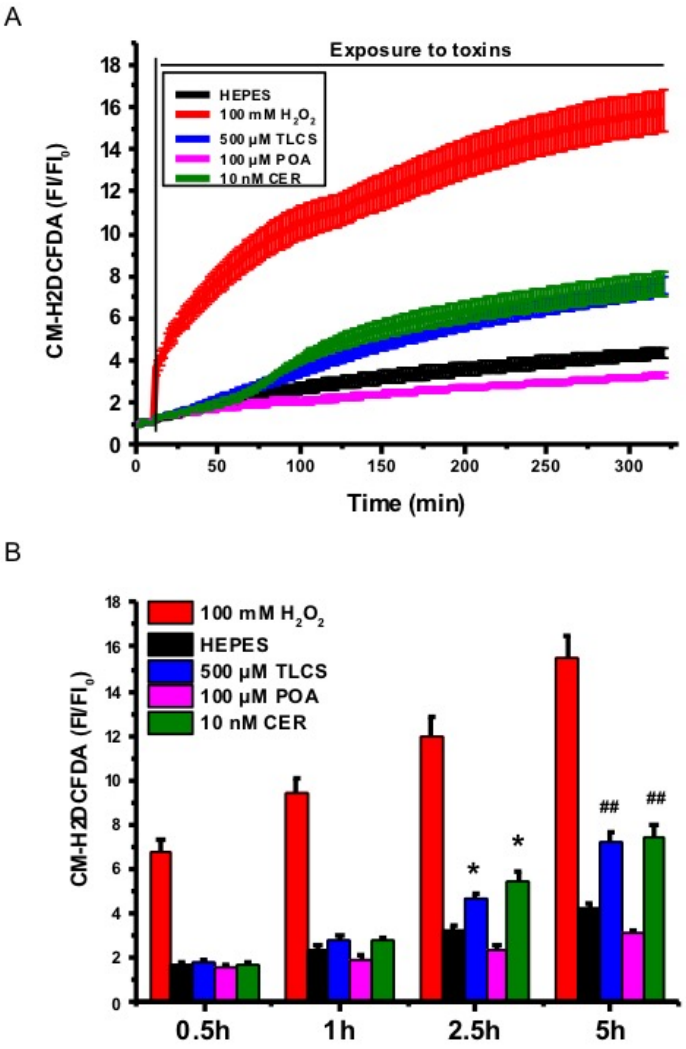

Figure 3.11 ROS generation of PACs following exposure to toxins

Basal ROS levels from CM-H_2DCFDA loaded cells were measured for 10 minutes prior to exposure to toxins. **(A)** Kinetic ROS generation trace curve and **(B)** Time course ROS generation when expose to toxins. No significant changes were observed within an hour. Data have been normalised to the initial fluorescence reading t=0 expressed as FI/FI_0. Traces are averages of >6 experiments. All data shown are mean ± SEM. $^{*,\#}P<0.05$, $^{\#\#}P<0.01$, compared to NaHEPES group.

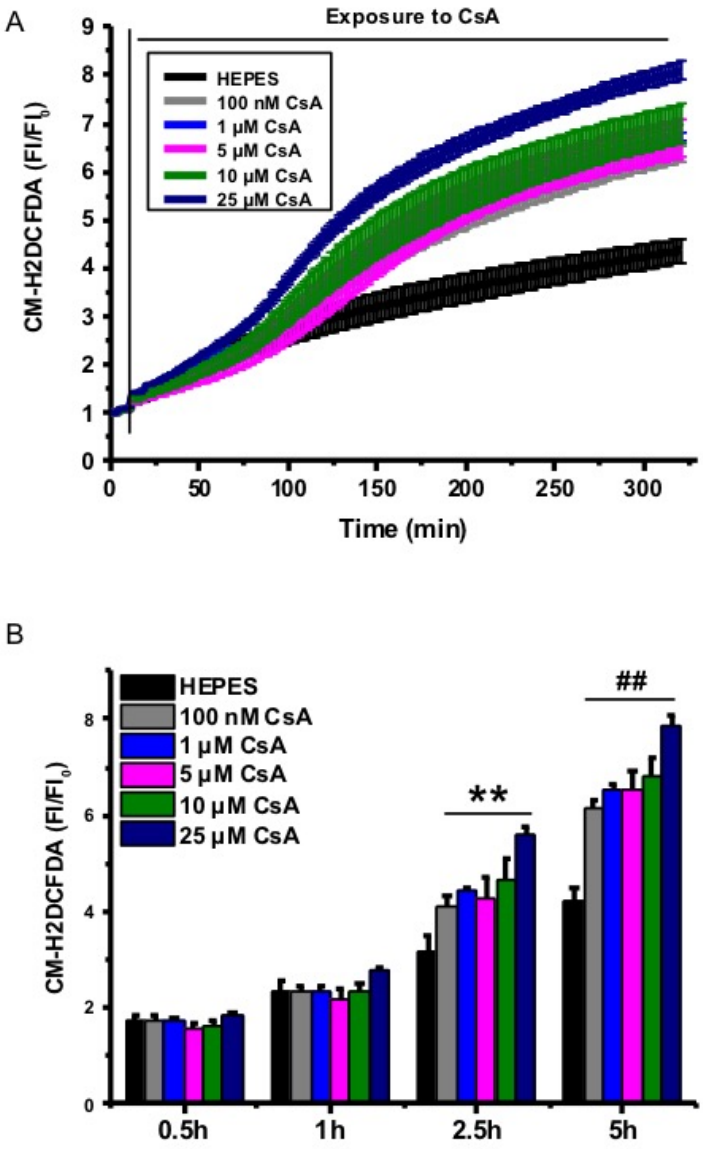

Figure 3.12 ROS generation of PACs in response to CsA.

FI of CM-H_2DCFDA loaded cells were measured for ROS generation, results are normalised to the basal fluorescence reading t=0 expressed as FI/FI_0. **(A)** Kinetic ROS generation trace curve and **(B)** Time course ROS generation in the presence of CsA from 100 nM, 1 µM, 5 µM, 10 µM and 25 µM. CsA induced time- and concentration-dependent ROS generation. Data have been normalised to the initial fluorescence reading t=0 expressed as FI/FI_0. Traces are averages of >6 experiments. All data shown are mean ± SEM. $^{**,\#\#}P<0.01$, compared to NaHEPES group.

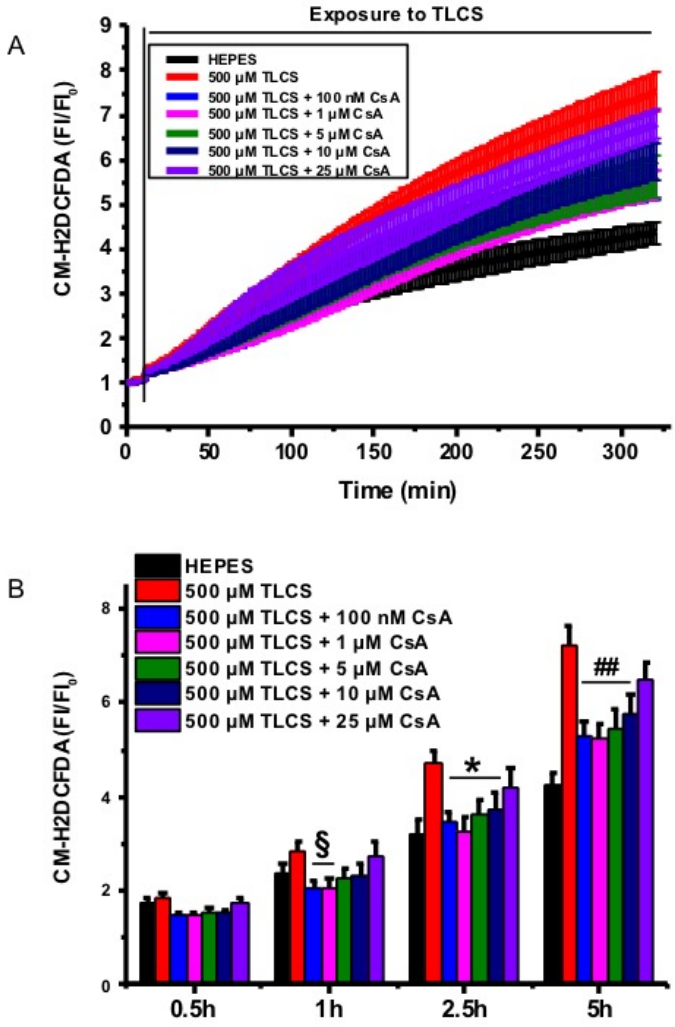

Figure 3.13 Effects of CsA in TLCS induced ROS generation

CM-H_2DCFDA loaded cells were measured for ROS generation, results are normalised to the basal fluorescence reading t=0 expressed as FI/FI_0. **(A)** Kinetic ROS generation trace curve and **(B)** Time course ROS generation following TLCS exposure in presence of CsA. FI/FI_0 showing mean ± SEM at 0.5h, 1h, 2.5h and 5h. Traces are averages of >6 experiments. All data shown are mean ± SEM. No significant difference in presence of highest concentration of CsA following TLCS treatment. $^{\S, *, \#}P<0.05$, compared to TLCS group.

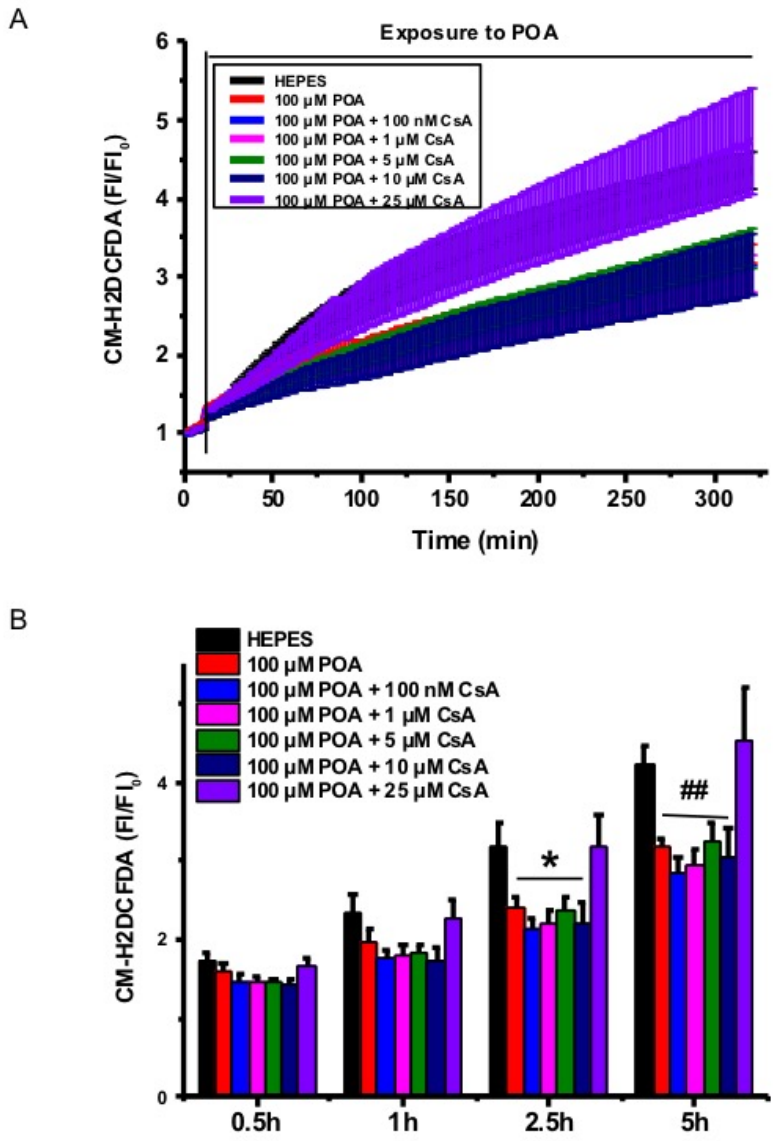

Figure 3.14 Effects of CsA on ROS production following POA exposure

CM-H_2DCFDA loaded cells were measured for ROS generation, results are normalised to the basal fluorescence reading t=0 expressed as FI/FI_0. **(A)** Kinetic ROS generation trace curve and **(B)** Time course ROS generation following POA exposure in presence of CsA. FI/FI_0 showing mean ± SEM at 0.5h, 1h, 2.5h and 5h. Traces are averages of >6 experiments. All data shown are mean ± SEM. POA alone or co-incubated with low concentration of CsA significantly decreased ROS generation at 2.5h. $^{*}P<0.05$, $^{\#\#}P<0.01$ compare to NaHEPES control group.

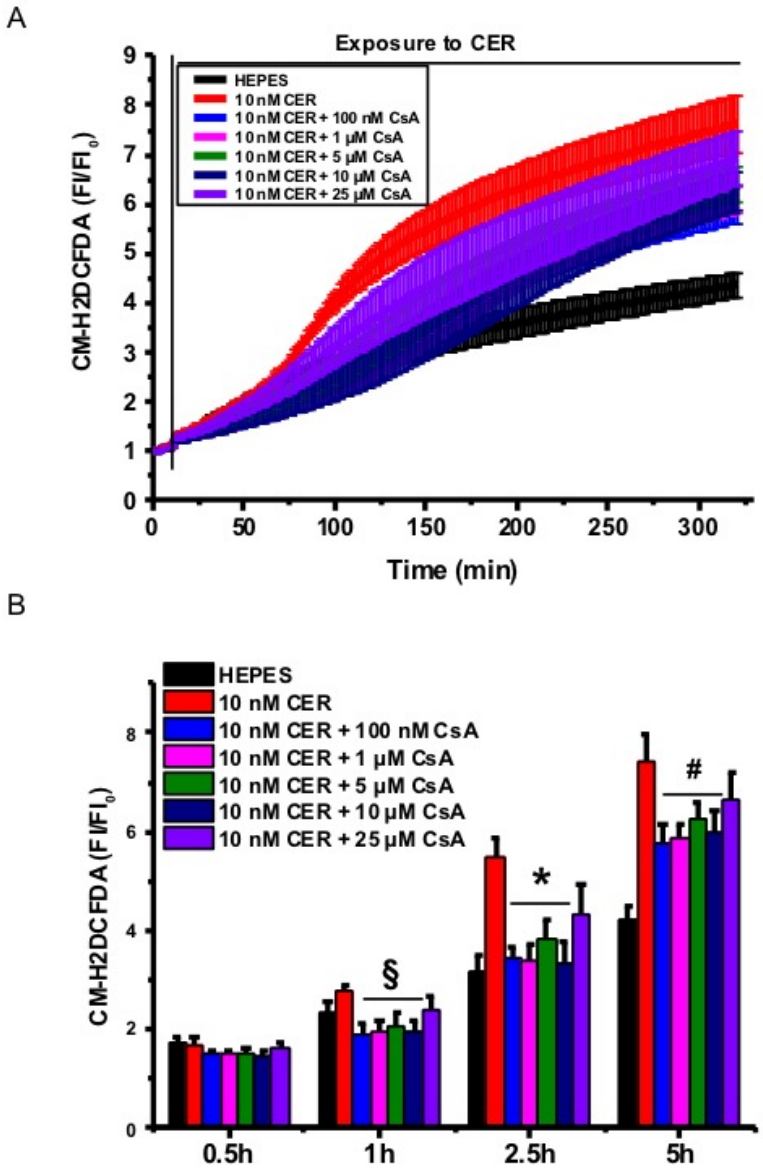

Figure 3.15 Effects of CsA in Caerulein induced ROS production

CM-H_2DCFDA loaded cells were measured for ROS generation, results are normalised to the basal fluorescence reading t=0 expressed as FI/FI_0. **(A)** Kinetic ROS generation trace curve and **(B)** Time course ROS generation following Caerulein exposure in presence of CsA. FI/FI_0 showing mean ± SEM at 0.5h, 1h, 2.5h and 5h. Traces are averages of >6 experiments. No significant difference in presence of highest concentration of CsA following caerulein treatment. $^{\S, *, \#}P<0.05$, compare to CER groups.

3.4.4 ER chaperone expression in response to toxins

Immunoblot analysis of the ER chaperones from PACs as early as 2 h and later time point at 6 h of treatment with CsA ranges from 100 nM to 50 µM demonstrated increased expression of both GRP-78 and CypB at 2h following TLCS exposure, however, sharply dropped till deprivation after 6h incubation. Short term treatment with CsA had very subtle effects on TLCS induced GRP-78 and CypB upregulation, while at 6h time point, CsA dramatically reversed the TLCS- induced GRP-78 deprive at all concentrations (**Figure 3.16 a, b**).

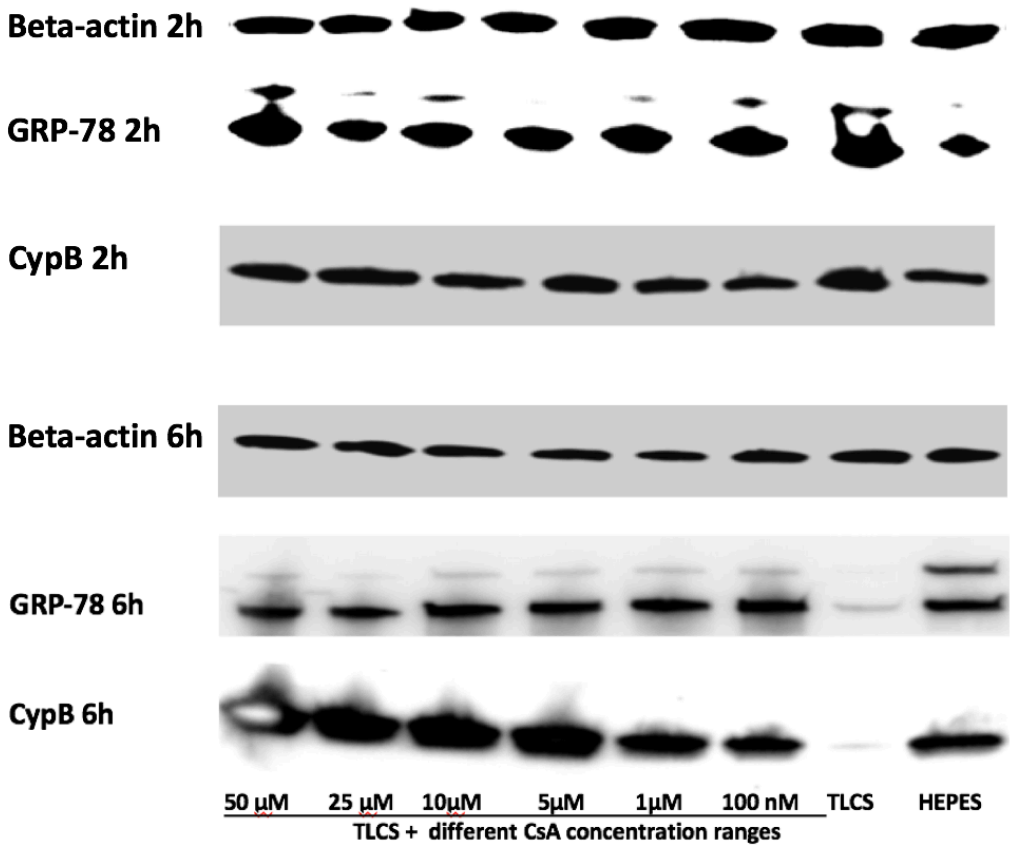

Figure 3.16 (a) Effects of CsA on ER-based chaperones following TLCS exposure

Freshly isolated PACs were co-incubated with 500µM TLCS and CsA ranges from 100nM to 50µM at 37℃, 95% O_2, 5% CO_2 incubator for 2h or 6h. ER chaperones GRP-78 and CypB expression were detected.

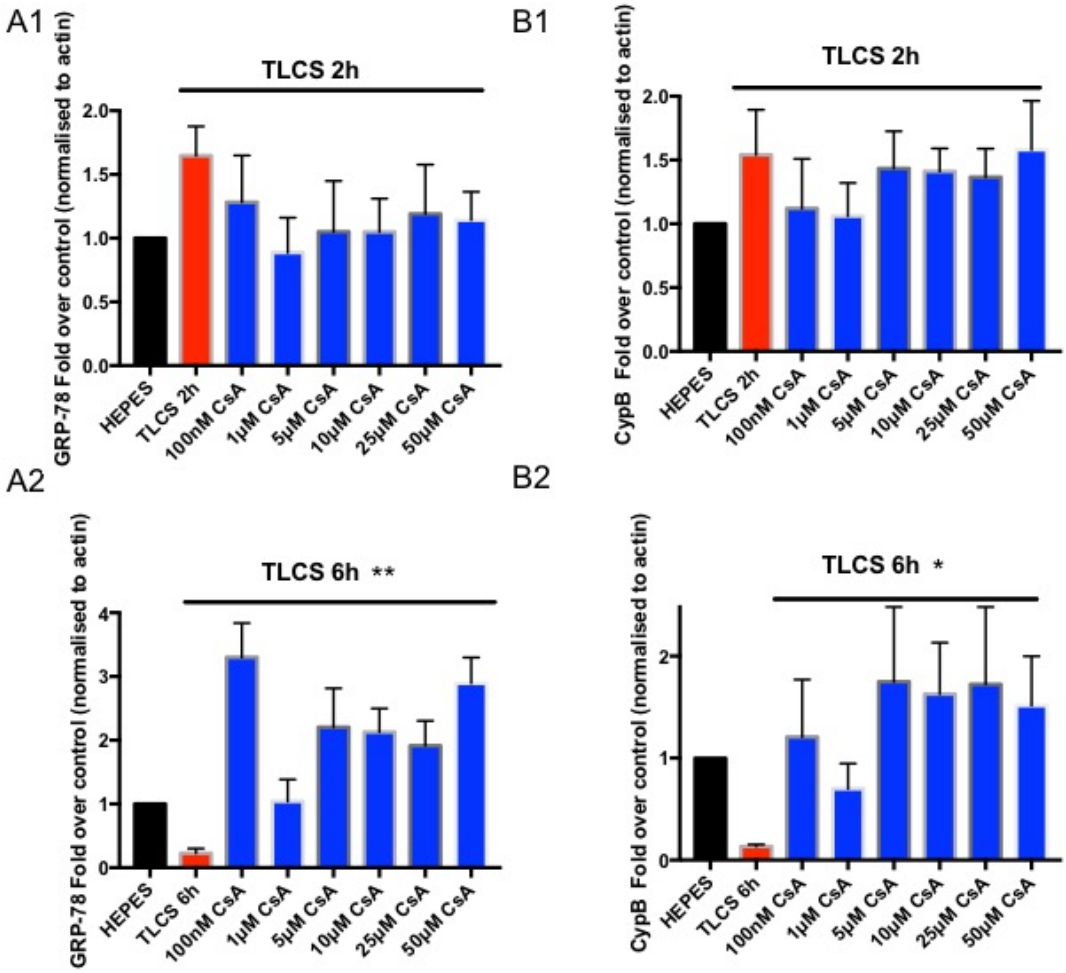

Figure 3.16 (b) Quantification of CsA effects on ER-based chaperones following exposure to TLCS

Freshly isolated PACs were co-incubated with 500μM TLCS and CsA ranges from 100nM to 50μM at 37℃, 95% O_2, 5% CO_2 incubator.

(A) GRP-78 and **(B)** CypB expression after **(1)** 2h and **(2)** 6h TLCS exposure were quantified in presence of CsA.

Data presented as fold over HEPES control based on normalised to actin level.

$^{**}P<0.01$, $^{*}P<0.05$ compared to TLCS group, values are mean ± SEM of 4 experiments of each.

3.5 Discussion

In general, fresh isolated kinetic cell findings obtained suggest that CsA induced pancreatic acinar cell death in a time- and biphasic dose- dependent manner, with 1-10 μM did not induce either necrotic or apoptotic cell death, which is in parallel with previously published studies on other cell types such as HEK293, epithelium cell or various cervical cancer cell lines including Hela cervical cancer cells and other mammalian cell types. In CsA treated SiHa cells, distorted ER with massive cytoplasmic vacuolation occurred with numbers and size increase with progression of time (48–72 h) both in the perinuclear region and the entire cytoplasm, which persisted even after removal of CsA and continued to increase in number as well as in size[382]. Those findings also support the findings obtained here that long term application induces cytotoxicity.

TLCS and POA induced PAC death exhibited similar profiles of action showing rapid aggressive increases in necrosis, while caerulein exerted a slow and mild injury pattern. At this concentration, however, caerulein was shown to elicit robust apoptosis.

The greatly increased necrosis by both TLCS and POA also confirmed previous published studies showing that both precipitants induced MPTP opening, membrane potential collapse and necrosis as mentioned in chapter 1.5. The aggressive response of POA on cell death, however adversely, distinctively inhibited ROS production. Previous reports on free fatty acid suggest a dual effect on ROS production depending on the mode of respiratory complex chain function. Free fatty acid increases the rate of ROS generation in the forward mode of electron transport by

slowing down the rate of electron flow through complexes I and III and between complexes III and IV due to release of cytochrome c from the inner membrane. On the contrary, due to their protonophoric action on the inner mitochondrial membrane, unsaturated fatty acids strongly inhibit ROS production, indicating an effect related to uncoupling action of fatty acids[452, 453]. The current study was conducted with POA, a monounsaturated fatty acid that induced aggressive maximal necrosis, but markedly inhibited ROS production, suggesting significant protonophoric uncoupling and that the injury originated in mitochondria.

PACs co-incubation with TLCS for 6h dramatically decreased GRP-78 expression, whereas early incubation increased the chaperones expression at 2h. A previous study suggested GRP-78 plays an anti-apoptotic role in regulating the cell death response during AP and knockdown of GRP-78 expression markedly promoted apoptosis and reduced necrosis in PACs[261]. It is likely that GRP-78 mediated UPR plays a self-defence role during initial injury with responsive up regulation to help with protein folding. With persistent TLCS exposure, this powerful aggressive toxin overcomes the self-defence mechanism, chaperones failed to relieve the stress and eventually leads to cell death.

These data confirm that varying numbers of PACs undergo both apoptosis or necrosis depending on the toxins and the exposure time to toxins, there is a difference in the magnitude of maximal fluorescence intensity increase in cell death as well as the time period needed to activate cell death pathway in terms of toxin type and concentrations.

Studies reported that CsA and its analogues at 10 μM were able to generate free radicals in smooth muscle cells independently of calcineurin[454], the over production of ROS may mediate the CsA toxicity[455]. PACs treated with CsA at all ranges concentrations showed consistently increased ROS production in a concentration- and time- dependent manner, the highest concentration CsA even overwhelmingly counterbalanced the inhibited ROS production by POA, suggesting a possible exacerbation may occur due to hyperoxidation state in the ER. Stocki reported that CsA induced CypB and CypC secretion out of the ER, depleting the ER of cyclophilins and inducing ER hyperoxidation state, causing ROS overburst[384].

Interestingly, when exposed to TLCS, the CsA treated PACs present roughly a 20% and 30% reduction of intracellular ROS levels at 2.5h and 5h compared to the CsA free PACs. Similarly, with all the results showing that CsA reduced the expression of CypB, however, following TLCS exposure for 6h, there is an increase of CypB expression shown in western blot. CypB[295] was previously shown to play a protective function against ROS-induced cell death under ER stress. CypB/WT overexpression significantly increased the resistance of the cells to ER stress induced apoptotic cell death in a PPIase - dependent manner via the suppression of Ca^{2+} depletion in the ER, and attenuating ROS generation and mitochondrial damage. Knockdown of CypB with a short interfering RNA targeting sequence in HeLa cells, which in turn was followed by increased expression of UPR markers, such as GRP78, indicating increased ER stress in the absence of CypB. Here, as TLCS induced massive Ca^{2+} release and cell death as previously reported by Criddle[173], CsA partially reversed the GRP-78 level from diminished TLCS induced

by CsA. It is possible that some protection afforded by CsA is due to upregulation of GRP-78 through the CsA induced ROS production.

Choi's study found elevated ROS, ER expansion, and abnormal unfolded protein responses in CypB-depleted glioblastoma cells and showed that genetic depletion or pharmacologic inhibition of CypB caused hyperactivation of the oncogenic RAS–MAPK pathway, induction of cellular senescence signals, and cell death[300]. These findings indicate that CypB alleviates oxidative and ER stresses and coordinates stress adaptation responses which is entirely consistent with the results obtained here.

CHAPTER 4

Effects of CsA on experimental acute pancreatitis

4.1 Summary

The data described in this chapter has demonstrated that cyclophilin inhibitor CsA is effective in protecting against experimental AP models with proper formulation and optimal dosing regimen in terms of lower dosage and adequate administration time.

Single i.p administration of CsA at low to medium dosage markedly reduced both local and systemic injury across all three AP models, however, CsA at high dosage tend to exacerbate the inflammation defined by pro-inflammatory cytokine IL-6 in FAEE- and CER-AP.

Although *in vivo* data are variable, 2 or 5 mg/kg CsA appear to be the optimal dosages. Administering higher dose of CsA lost protective effects and exacerbated systemic inflammation in both FAEE-AP and CER-AP, suggesting an off-target effect at high dose.

4.2 Introduction

Acute necrotizing pancreatitis diagnosed with more than 30% of the gland is affected by necrosis and accounts for 5% to 10% of pancreatitis cases. The revised Atlanta classification categorized different types of fluid collections following development of AP, these collections can be present within pancreatic parenchyma, adjacent to it, or both; which can be either sterile or infected[456]. Two thirds of necrotic pancreatic collections are sterile and will resolve with conservative management, while the remainder will become infected and require further intervention. Although it is generally accepted that infected pancreatic necrosis should be managed surgically, in all AP patients with complications of

necrosis, invasive intervention should be ideally delayed where possible until at least 4 weeks after initial presentation to allow the collection to become walled-off [52], which provided evidence for experiencing conservative management *i.e* medical treatment during the gap.

Previous findings showing that genetic knockout of CypD, the key regulator of MPTP opening, to reduce necrosis and severity of experimental AP[237], proving the potential logical translational thought with cyclophilin inhibitors application in acute pancreatitis. Indeed, *in vitro* study apply pharmacologic MPTP inhibitors CsA were shown to have beneficial effects in response to pancreatic precipitants in pancreatic acinar cell, these effects were reflected in significant improvement in pancreatic cellular necrosis as described in last chapter.

CsA has been shown to be beneficial in a large number of preclinical or clinical studies involves MPTP opening, however, the results were inconsistent and complicated to interpret and evaluate due to various drug formulation, administration modality differ in dosages and treatment time, side effects with long term application of CsA which greatly limited the MPTP inhibition power. DEB025 is a non-immunosuppressive analogue derived from CsA, demonstrating potent PPIase inhibition while binding to cyclophilins, which has now progressed to phase 3 clinical trials for hepatitis C treatment[457]. Preliminary study showed that DEB025 at 10mg/kg projects superb effects over 40mg/kg and 100mg/kg in reducing the severity of experimental acute pancreatitis, while pilot study using CsA at 20mg/kg *in vivo* has poor solubility with NaHEPES dilution and does not suggest fully beneficial effects compare to DEB025.

To fully investigate the action pattern for pharmacologic MPTP inhibition with cyclophilin inhibitors, to comprehensively define the effects spectrum of CsA and the possibility for drug development in pancreatitis, this chapter describes experiments designed to assess treatment with CsA at a broad range of dosages in three different experimental AP models, with an improved solvent formulation.

4.3 Methods

In vivo experiments were conducted on CD1 mice using three different EAP models induced by retrograde perfusion of TLCS, i.p injections of fatty acid-ethanol combination or supramaximal caerulein as previously described in chapter 2. Considering that there is a longer clearance time of CsA in rodents than in human and possible side effects, the administration modality was designed with a single i.p dose of CsA with wide ranges covered the previously proved either effective or ineffective dosage in other diseases models. To be precise, CsA at dose ranges from 0.5 mg/kg to 75 mg/kg were administered 1h after TLCS-AP and 2h after first injection of FAEE or CER. Adult male CD 1 mice were randomly divided into 8 groups in each model with: (1) negative control group with saline duct perfusion or i.p injection only, (2) positive AP group with toxin induction, (3) solvent control group with AP induction plus solvent injection (10% cremophor dissolved in saline with 1% DMSO), and (4-8) 5 treatment groups with various dosages of CsA (0.5, 2, 5, 20 and 75 mg/kg body weight) administration by single i.p injection. Sacrifice was performed 24h/12h after AP induction (**Figure 4.1**) to harvest blood and tissue sample for severity assessment including pancreatic histology, serum amylase,

pancreatic and pulmonary MPO and serum IL-6. These assays were performed as previously described in chapter 2.

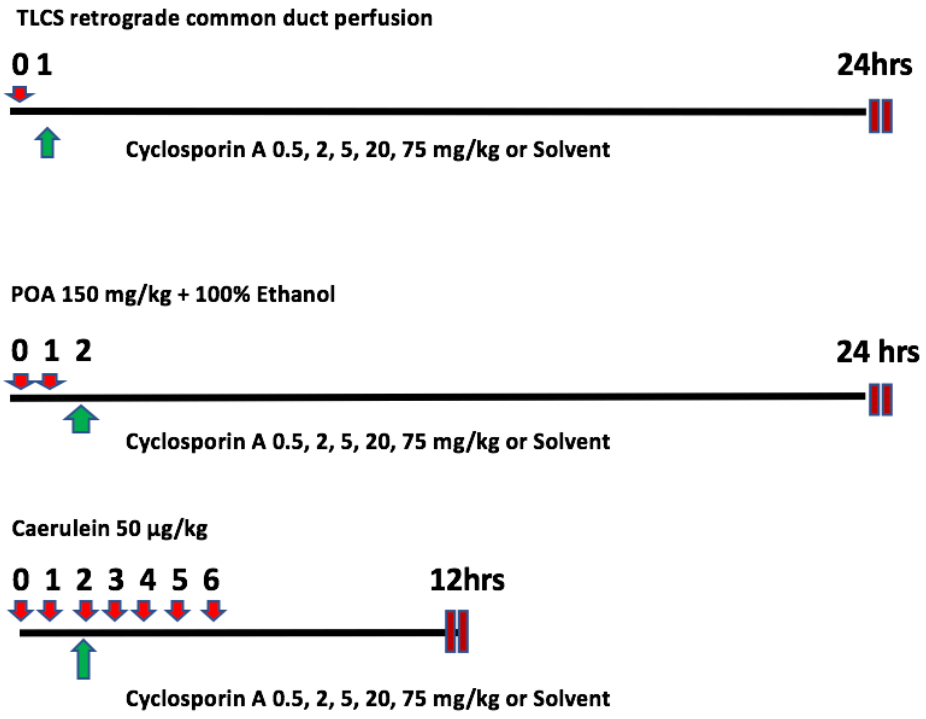

Figure 4.1 CsA dosing regimen in 3 experimental acute pancreatitis

CsA at 0.5 mg/kg, 2 mg/kg, 5 mg/kg, 20 mg/kg, 75mg/kg or same volume solvent (10% cremophor dissolved in saline with 1% DMSO) were administered after disease induction at designate time as described in the text.

4.4 Results

The effects of CsA (from 0.5mg/kg to 75 mg/kg) dose response on pancreatitis severity were assessed with biochemical, immunological, inflammatory markers, and histopathological scoring in TLCS-, FAEE- and CER-AP models.

Challenge with three toxins induced dramatic elevated serum amylase (**Figure 4.2**), indicating the successful induction of EAP, which were greatly decreased by the cyclophilin inhibitor CsA, with 5mg/kg medium dosage consistently reduced in all models ($P<0.05$).

Systemic inflammation shown as serum IL-6 levels in response to TLCS and FAEE challenge reflect prodigious rise, while only limited response observed in caerulein induced damage (**Figure 4.3**). All low to medium high dosages (0.5-20mg/kg) brought the increased IL-6 level back to parallel control level, whereas only 2 or 5mg/kg dosage significantly reduced IL-6 in TLCS- and FAEE-AP.

CsA at 2 or 5mg/kg also markedly reduced trypsinogen activation (**Figure 4.4)** and pancreatic MPO (**Figure 4.5 A2, A3)** in both FAEE- and CER-AP, respectively. CsA from minimal to maximal dosages, however all significantly reduced MPO levels in the inflamed pancreas by at least 50% in TLCS-AP (**Figure 4.5 A1)**, whereas only 2 and 5 mg/kg showed significance despite the reduction trend with all dosages in TLCS-AP induced lung MPO (**Figure 4.5 B1**). None of the broad dosages of CsA implicated any beneficial in FAEE induced lung MPO level (**Figure 4.5 B2**), while CsA at 5mg/kg had a significantly reduction, the high dose at 20 and 75mg/kg, however, showing extra exacerbation trend in lung MPO compare to CER-AP group (**Figure 4.5 B3**).

Treatment with the CsA solvent containing 10% cremophor and 1% DMSO did not show any difference across all the parameters in the severity of pancreatitis compared to AP group.

Typical histopathological changes of AP can be seen on haematoxylin & eosin stained representative sections in three models. TLCS, FAEE or caerulein produced the hall mark histopathological changes in the pancreas including severe destruction of the pancreatic tissue structure, characterized by extensive acinar cell oedema, massive infiltration of leukocytes and acinar cell necrosis. Treatment with CsA protected against toxin-induced destruction of the tissue architecture, significantly reduced toxins-induced acinar cell necrosis in the pancreas (**Figure 4.6a -4.8a**).

Mice with CsA treated at 5mg/kg dosage in TLCS- and CER-AP, 2mg/kg treated in FAEE-AP displayed marked morphological improvements in pancreatic overall scoring with dampened scores for oedema, infiltration and necrosis (**Figure 4.6b-4.8b**) compare to AP groups shown in blinded histology scoring of 10 randomly selected regions at × 200 magnifications per mouse.

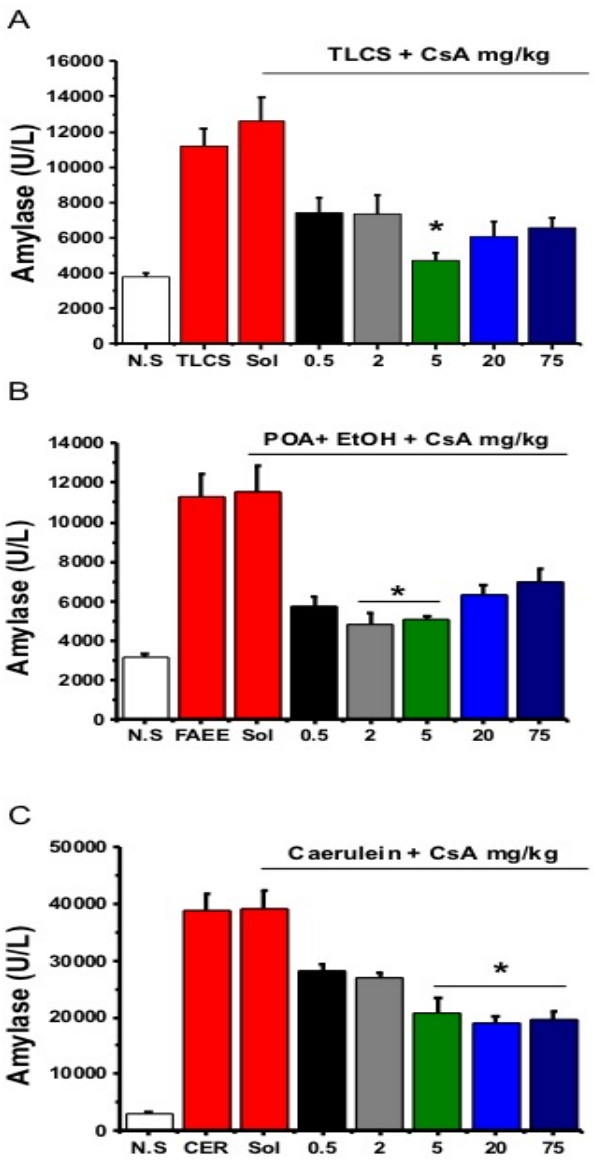

Figure 4.2 CsA dose response on serum amylase in 3 EAP models

Mice were subjected to saline (N.S) control groups, 3 toxins induced AP groups, AP plus solvent groups (Sol: 10% cremophor dissolved in saline with 1% DMSO), CsA treated AP groups with CsA at 0.5 mg/kg, 2mg/kg, 5mg/kg, 20 mg/kg and 75 mg/kg administered with single i.p injection in **(A)**TLCS-AP, **(B)** FAEE-AP, and **(C)** CER-AP. CsA at 5mg/kg consistently reduced amylase level in all AP models ($^{*}P < 0.05$, compared to each AP group, values are mean ± SEM of 6 mice per group).

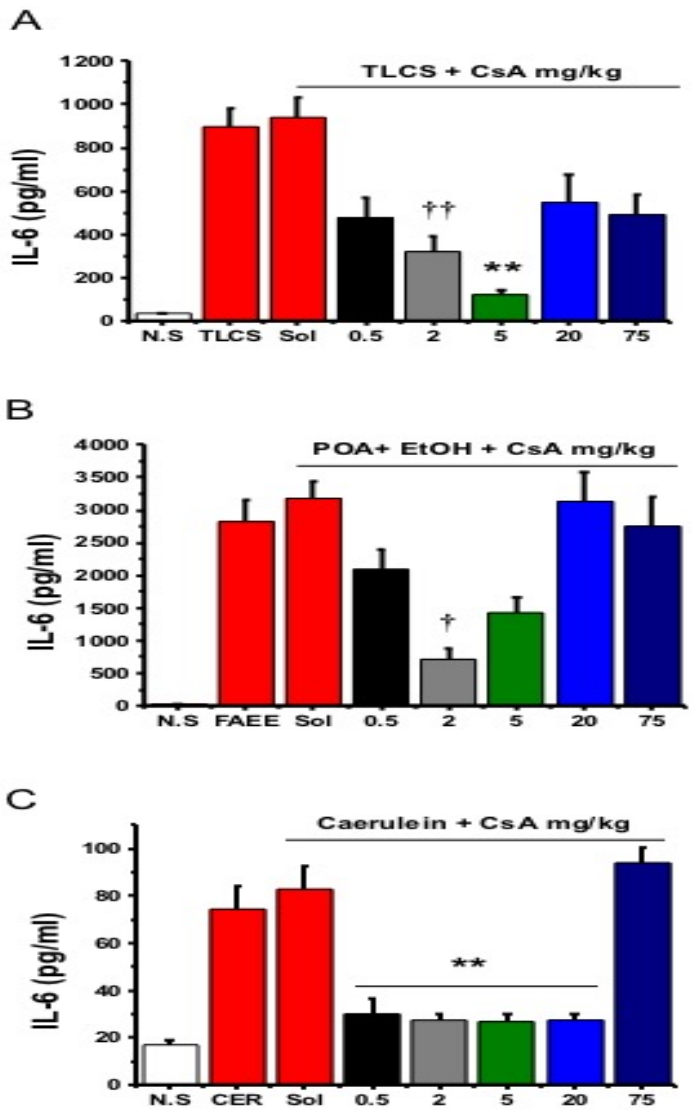

Figure 4.3 CsA dose response on serum IL-6 in 3 EAP models

(A) TLCS-AP, **(B)** FAEE-AP and **(C)** CER-AP.

CsA at 0.5 mg/kg, 2mg/kg, 5mg/kg, 20 mg/kg and 75 mg/kg were administered with single i.p injection.

$^{\dagger\dagger,**}P<0.01$, $^{\dagger}P < 0.05$ compared to TLCS-/FAEE-/CER-AP group.

Values are mean ± SEM of 6 mice per group.

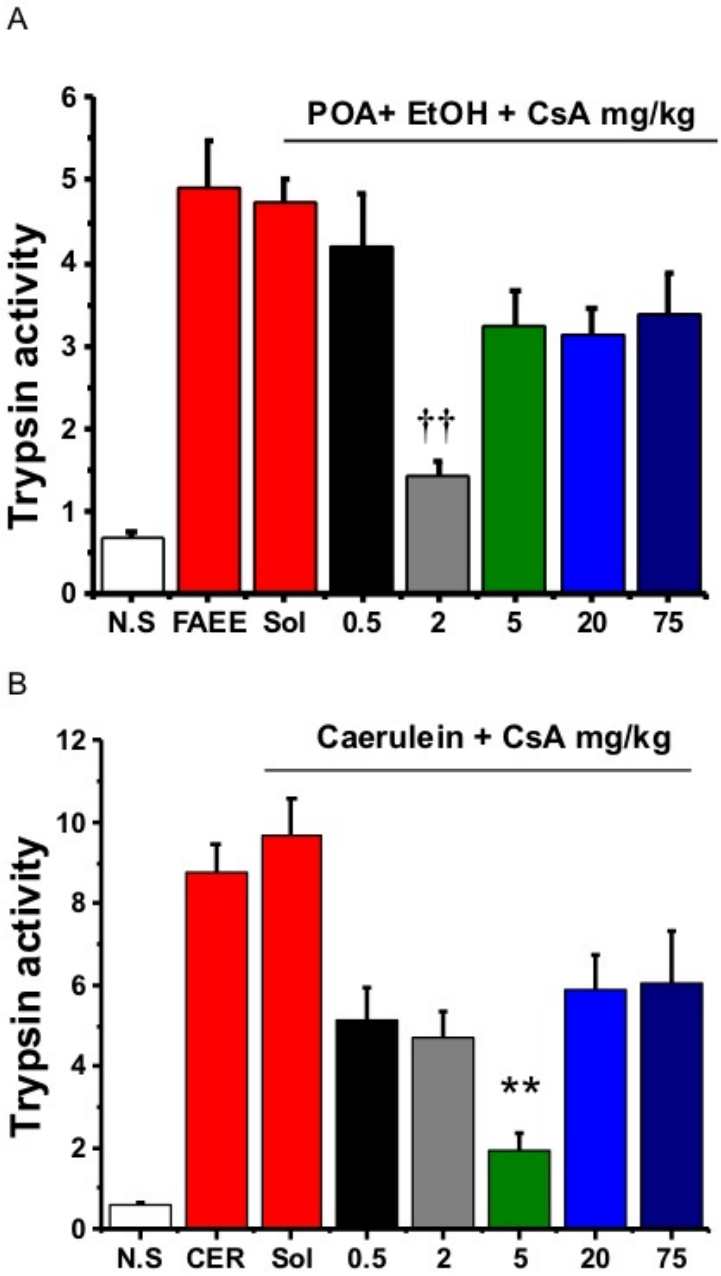

Figure 4.4 CsA dose response on pancreatic trypsin activity in 2 EAP models

CsA at 0.5 mg/kg, 2mg/kg, 5mg/kg, 20 mg/kg and 75 mg/kg were administered with single i.p injection in **(A)** FAEE-AP and **(B)** CER-AP.

$^{\dagger\dagger}P < 0.01$, compared to FAEE-AP group. $^{**}P < 0.01$, compared to CER-AP group. Values are mean ± SEM of 6 mice per group.

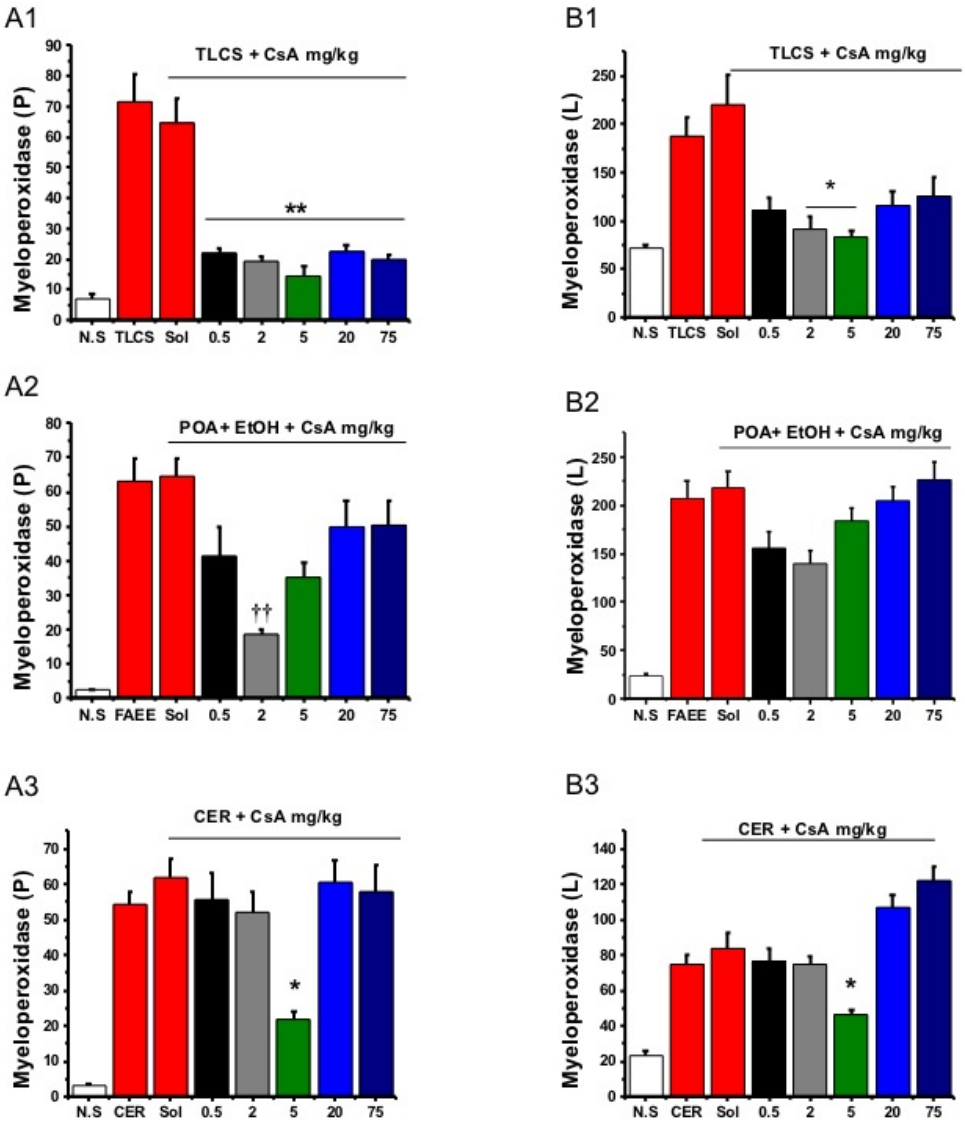

Figure 4.5 CsA dose response on myeloperoxidase in 3 EAP models

CsA at 0.5 mg/kg, 2mg/kg, 5mg/kg, 20 mg/kg and 75 mg/kg were administered with single i.p injection in **(1)** TLCS-AP, **(2)** FAEE-AP and **(3)** CER-AP.

Myeloperoxidase was normalised in pancreas **(A1-A3)** and Lung **(B1-B3)** with protein amounts.

$^{††,**}P<0.01$, $^{*}P < 0.05$ compared to TLCS-/FAEE-/CER-AP group.

Values are mean ± SEM of 6 mice per group.

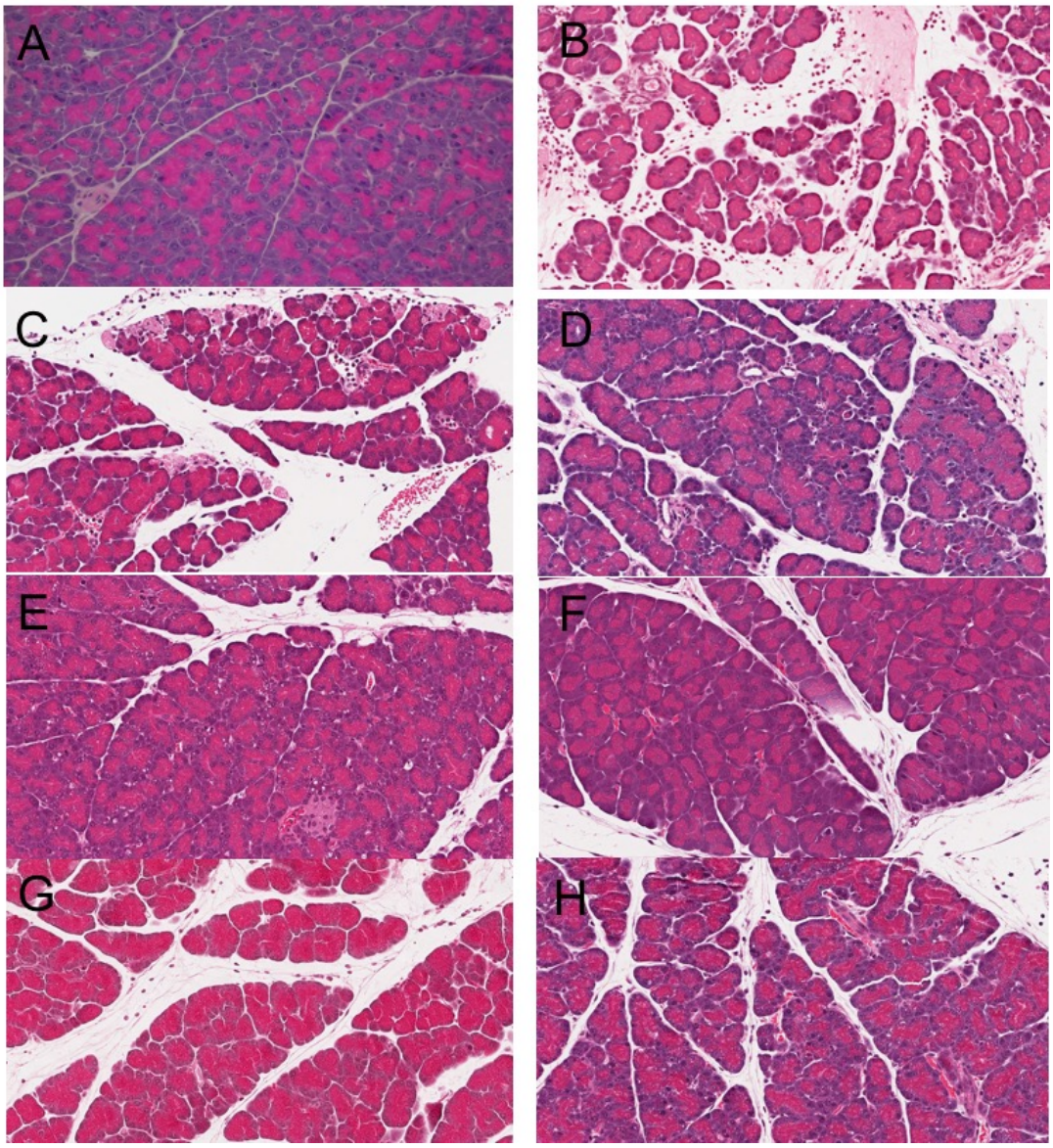

Figure 4.6 ***(a) Representative images on pancreatic morphology in TLCS -AP***

Mice received either retrograde infusion of 50 µL of 3 mM TLCS into the common duct or sham surgery. CsA was given 1 h after TLCS infusion and mice were sacrificed 24 h after the surgery. Morphological changes in the pancreas indicated the development of acute pancreatitis after TLCS infusion. Magnification × 200.

(A) Sham surgery, **(B)** TLCS-AP,

(C) TLCS + solvent, **(D)** TLCS + CsA 0.5 mg/kg,

(E) TLCS + CsA 2 mg/kg, **(F)** TLCS + CsA 5 mg/kg,

(G) TLCS + CsA 20 mg/kg, **(H)** TLCS + CsA 75 mg/kg.

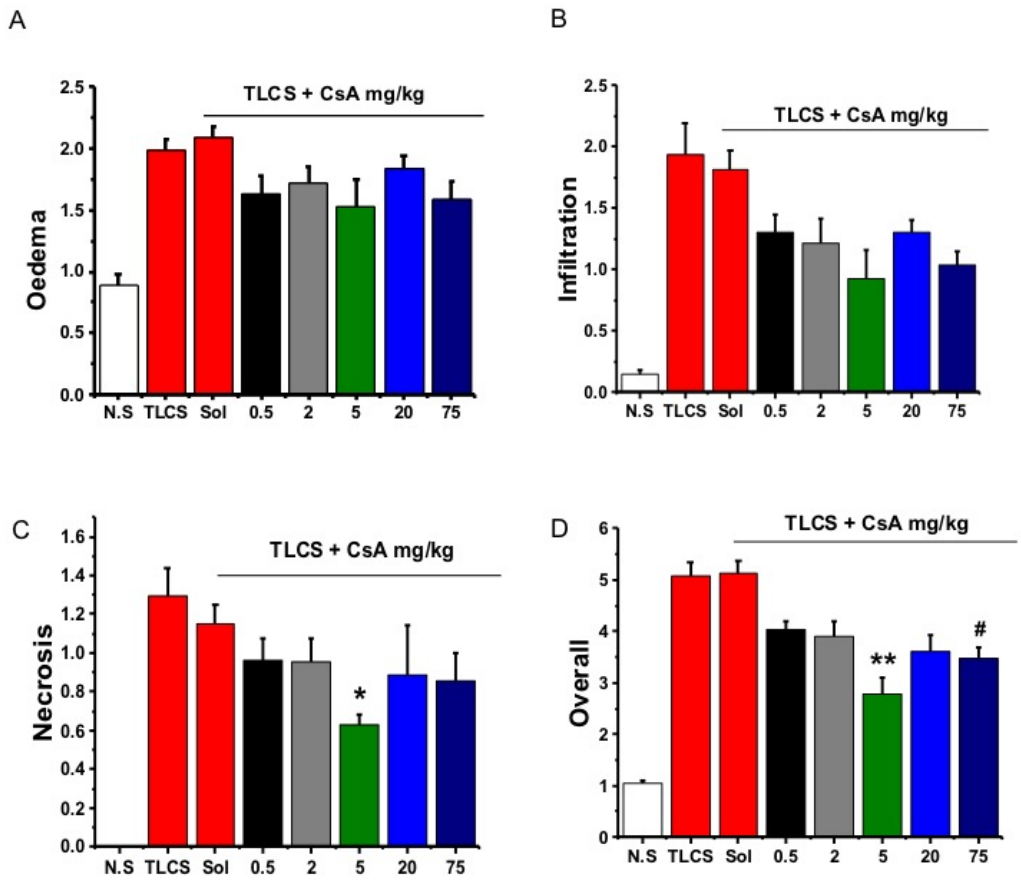

Figure 4.6 (b) CsA dose response on pancreatic histopathology in TLCS-AP

Mice received either retrograde infusion of 50 µL of 3 mM TLCS into the common duct or sham surgery. CsA was given 1 h after TLCS infusion and mice were sacrificed 24 h after the surgery.

(A) Oedema score, **(B)** Infiltration score, **(C)** Necrosis score, **(D)** Overall score.

*, $^{\#}P < 0.05$, **$P < 0.01$ compared to TLCS-AP group.

Values are mean ± SEM of 6 mice per group.

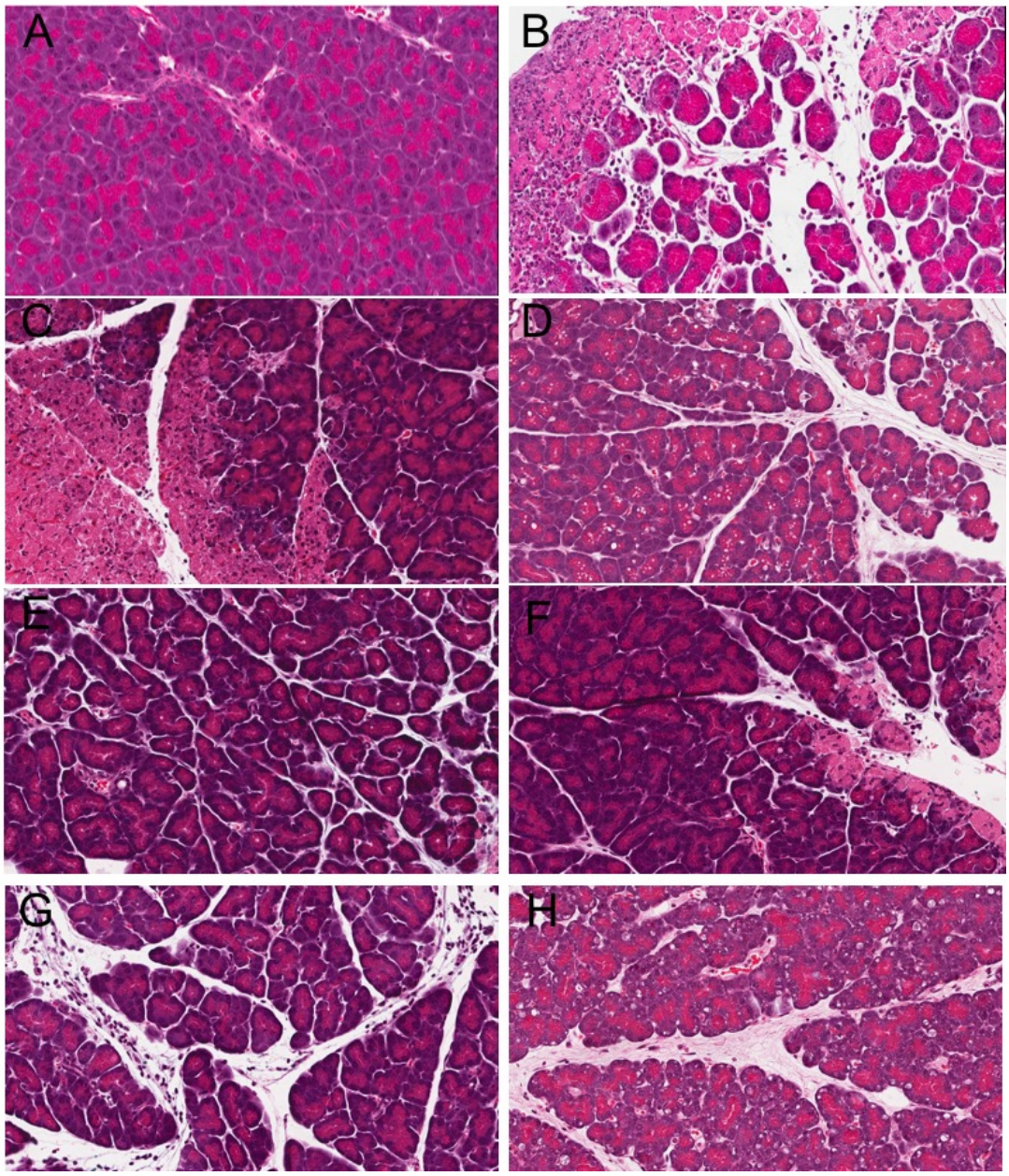

Figure 4.7 (a) Representative images on pancreatic morphology in FAEE -AP

Mice received two i.p injections of either 150 mg/kg POA & 1.35 g/kg ethanol mixture (FAEE) or saline, CsA was given at 2h after the first injection of FAEE and mice were sacrificed at 24 h. Magnification × 200.

(A) saline control, **(B)** POA + ethanol (FAEE-AP), **(C)** FAEE + solvent, **(D)** FAEE + CsA 0.5 mg/kg, **(E)** FAEE + CsA 2 mg/kg, **(F)** FAEE + CsA 5 mg/kg, **(G)** FAEE + CsA 20 mg/kg, **(H)** FAEE + CsA 75 mg/kg.

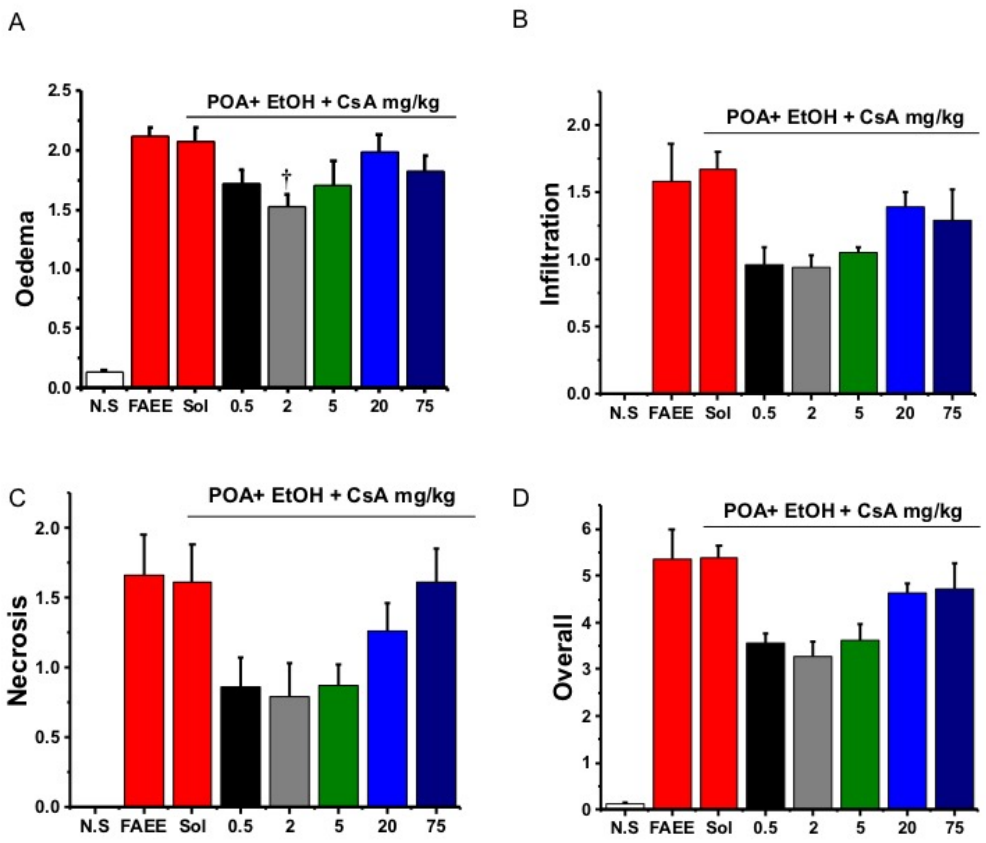

Figure 4.7 (b) CsA dose response on pancreatic histopathology in FAEE-AP

Mice received two i.p injections of either 150 mg/kg POA & 1.35 g/kg ethanol mixture (FAEE) or saline, CsA was given at 2h after the first injection of FAEE and mice were sacrificed at 24 h.

(A) Oedema score, **(B)** Infiltration score, **(C)** Necrosis score, **(D)** Overall score.

$^{\dagger}P < 0.05$ compared to FAEE-AP group.

Values are mean ± SEM of 6 mice per group.

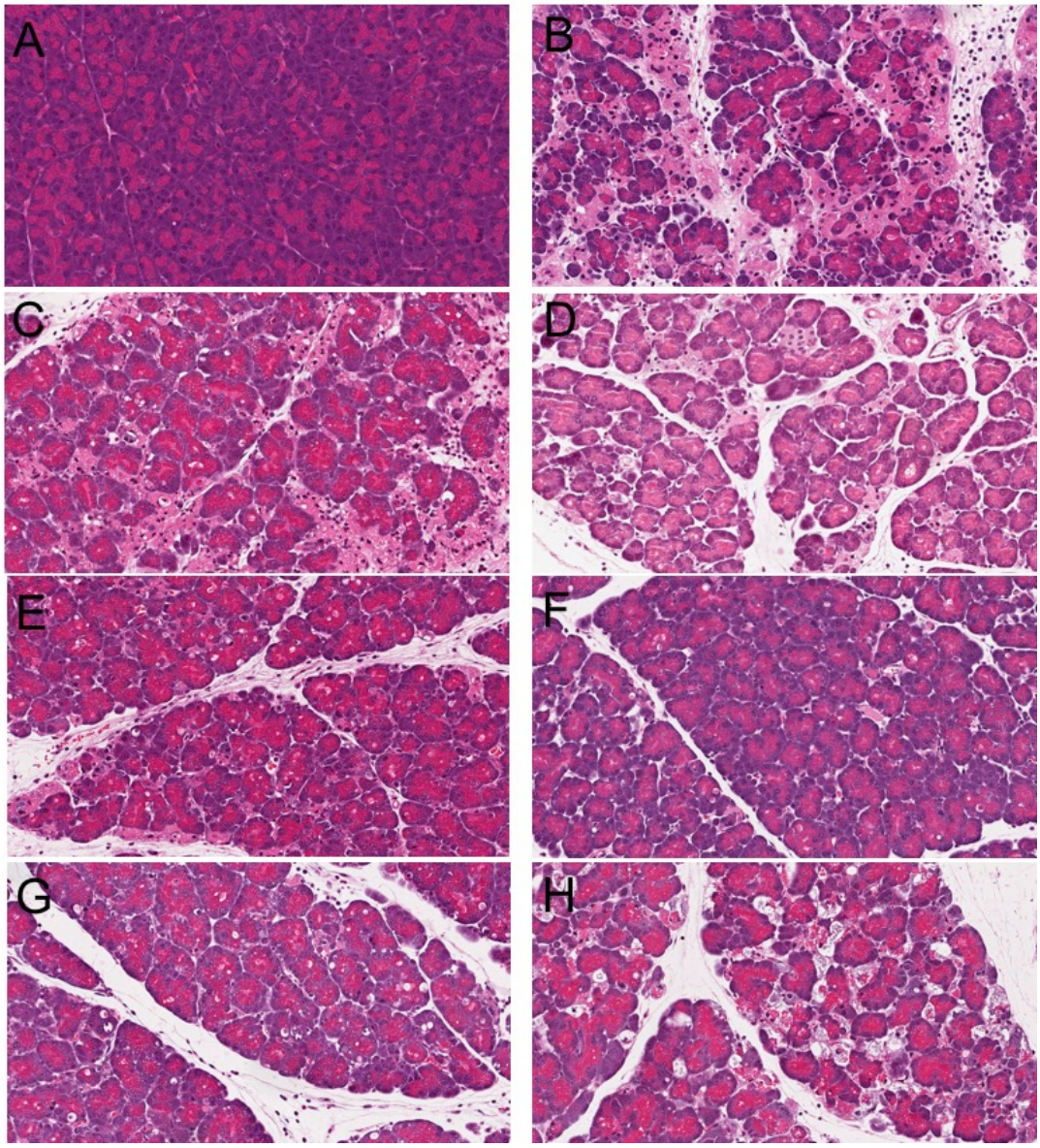

Figure 4.8 (a) Representative images on pancreatic morphology in CER -AP

Mice received 7 i.p. injections of either 50 μg/kg/h caerulein or saline. CsA was given 2h after first caerulein injection and mice were sacrificed at 12 h.

(A) Saline control, **(B)** Caerulein (CER-AP),

(C) CER + solvent, **(D)** CER + CsA 0.5 mg/kg,

(E) CER + CsA 2 mg/kg, **(F)** CER + CsA 5 mg/kg,

(G) CER + CsA 20 mg/kg, **(H)** CER + CsA 75 mg/kg.

Magnification × 200.

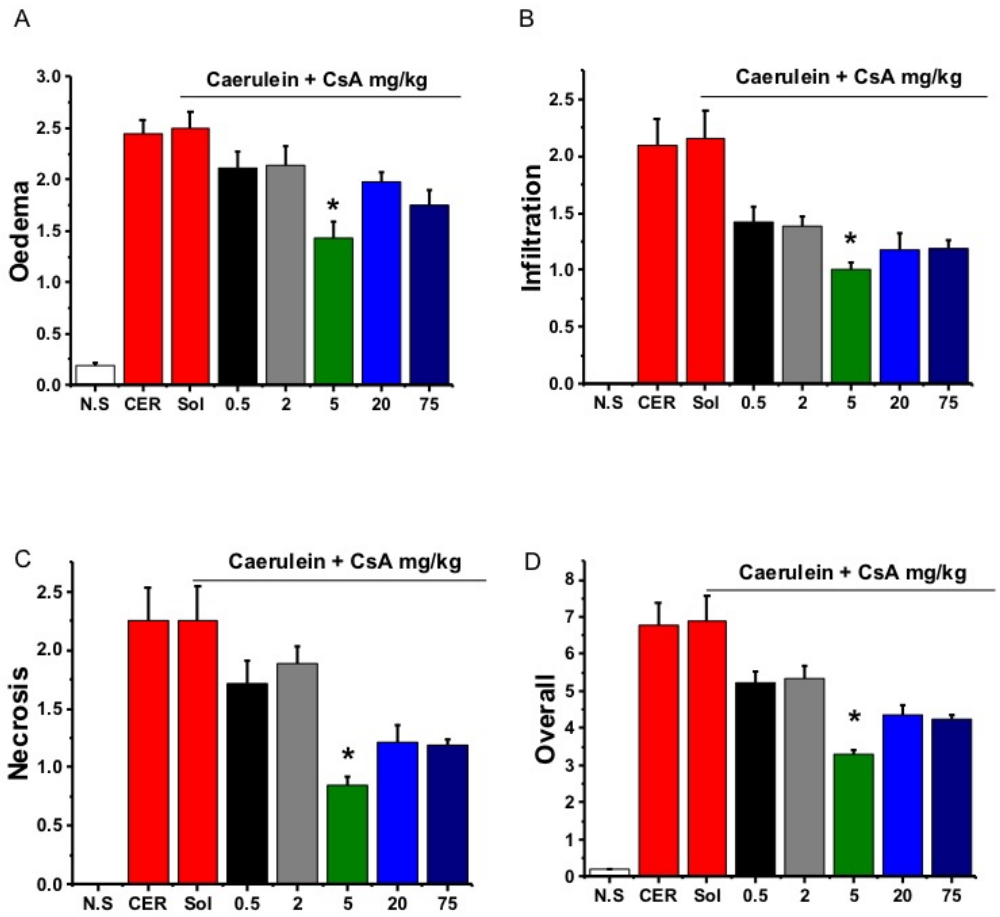

Figure 4.8 (b) CsA dose response on pancreatic histopathology score in CER-AP

Mice received 7 i.p. injections of either 50 μg/kg/h caerulein or saline. CsA was given at 2h after first caerulein injection and mice were sacrificed at 12 h.

(A) Oedema score, **(B)** Infiltration score, **(C)** Necrosis score, **(D)** Overall score.

$^{*}P < 0.05$ compared to CER-AP group.

Values are means ± SE of 6 mice per group.

4.5 Discussion

These findings show beneficial effects of the cyclophilin inhibitor CsA with a biphasic pattern, where both minimal dosage had very little effect and maximal dosage showed less efficacy, while remarkable alleviation has obtained from low to medium dosages of CsA treatment on the histology and severity of 3 experimental AP models, preventing acinar cell necrosis, reduce toxin induced both local and systemic inflammation. Consistent findings were obtained across all parameters with low to medium CsA administration with all the biochemical and immunological parameters. These observations corroborate our hypothesis that CsA with appropriate dosing regimen and solvent could possibly avoid or reduce detrimental non-specific inhibition induced toxicity either through any CypB/C inhibition induced ER stress or calcineurin induced immunosuppression.

The dosages of CsA (2-20 mg/kg) used in this chapter were estimated to provide concentrations of CsA at the tissue level in the nanomolar range, which was confirmed *in vitro* in chapter 3 to be effective.

CypA was reported to act like pro-inflammatory cytokines in pancreatitis, as shown *in vitro* that CypA released from damaged acinar cells by CCK induction and human recombinant CypA aggravated CCK-induced acinar cell necrosis with increased cytokine production; *in vivo* CypA was markedly upregulated during AP and widely expressed in disrupted PACs with infiltrated inflammatory cells[458].
Regarding of the pro-inflammatory role of extracellular CypA and the high affinity with CsA at nM, the beneficial of CsA reducing cytokine levels but not necrosis with low dose is possibly due to directly anti-inflammation effect on extracellular

CypA inhibition. It would assume that 5mg/kg is sufficient to bind with CypD and reduce necrosis to reach a maximal beneficial effect.

However, as in a liver fibrosis model shown that low dose NIM811 reduced CypD expression while high dose adversely upregulated its expression[423], suggesting the ineffective of high dose CsA is possibly due to the compensational overexpressed CypD, which deprived the beneficial that observed with medium dose on CypD inhibition. Also, as previously mentioned in chapter 3, high dose CsA could deplete CypB/C due to stimulated secretion to extracellular to aggregate the oxidation status in ER and lead to more ROS production and ER stress. Thirdly, similar with CypA, extracellular CypB was also reported to act as pro-inflammatory cytokines[459]. Both of the last two pathways with high dose CsA could lead to a vicious cycle that further promote inflammation, increase the MPTP opening and transcriptionally upregulate the CypD level to exacerbate the further pore opening and cell death.

Chapter 5

Evaluation of novel cyclophilin inhibitors on acute biliary pancreatitis

5.1 Summary

Administration of SEL1233 at low to high doses markedly reduced all local and systemic injury, with more profound reduction seen with high dose. The early twice daily dosing of 20mg/kg SEL1233 showed the most consistent reduction in a broad range of parameters, including both local and remote organ damage, systemic immunologic responses and pancreatic histopathologic score while the delayed administration of SEL1233 resulted in less efficacy in TLCS-AP, showing limited local severity alleviation but had no significant reduction on distant organ damage level, intraperitoneally administration with SEL1233 at later time point was significantly less protective across all majority parameters, suggesting the timing of intervention that targeted pancreatic injury especially early treatment delivery is an important issue in future endeavour to gain optimal benefits in drug discovery.

The 4 doses of 1233 showed less protection compare to the early BID dosing, suggesting that there may have some accumulative off-target effect on higher dose. The data described in this chapter demonstrate that SEL1233 is highly effective in protecting against acute biliary pancreatitis induced with TLCS.

A possible pulmonary toxicity induced by the high volume of PEG400 contained solvent indicates that appropriate formulation should be developed in future experiment.

5.2 Introduction

Prior experience has indicated the potential benefit for the treatment of AP with the approach that inhibit cyclophilins to prevent or delay induction of MPTP opening. As the enormous side effects have been observed with CsA, several chemical modifications of the naturally occurring cyclosporins have been tried in attempts to modulate the immunosuppressive activity and the affinities across different cyclophilins. Peptolide is a naturally occurring cyclodepsipeptide, which is a new cyclosporin- like ligand. Peptolide 214-103 from peptolide family is described in the free crystalline state and bound to cyclophilin, despite showing a very different conformation from CsA in the free crystal, similar conformation when bound to cyclophilin and similar biology activity has been observed with $CsA^{460-462}$. The peptolides 214-103 differs from CsA in the amino acids position 2, 5, 8 and 10 (Abu-2, Val-5, D-Ala-8 and MeLeu-10), which are replaced by threonine-2, leucine-5, D-2-hydroxyisovaleric acid-8 and leucine-10, respectively (**Figure 5.1**).

In this chapter, novel compounds with PPIase inhibition but better solubility, more selectively targeting on CypD and less immunosuppressive activity including SEL3714, SEL3639 that derived from CsA and SEL1233 which originates from peptolides 214-103, were applied to investigate the possibility of applying cyclophilin inhibitors synthesized by Cypralis on clinical relevant experimental biliary pancreatitis. Minor chemical modification was made to the original CsA and peptolide 214-103 main structure to synthesize these three compounds, the structure of which were not shown due to confidential agreement.

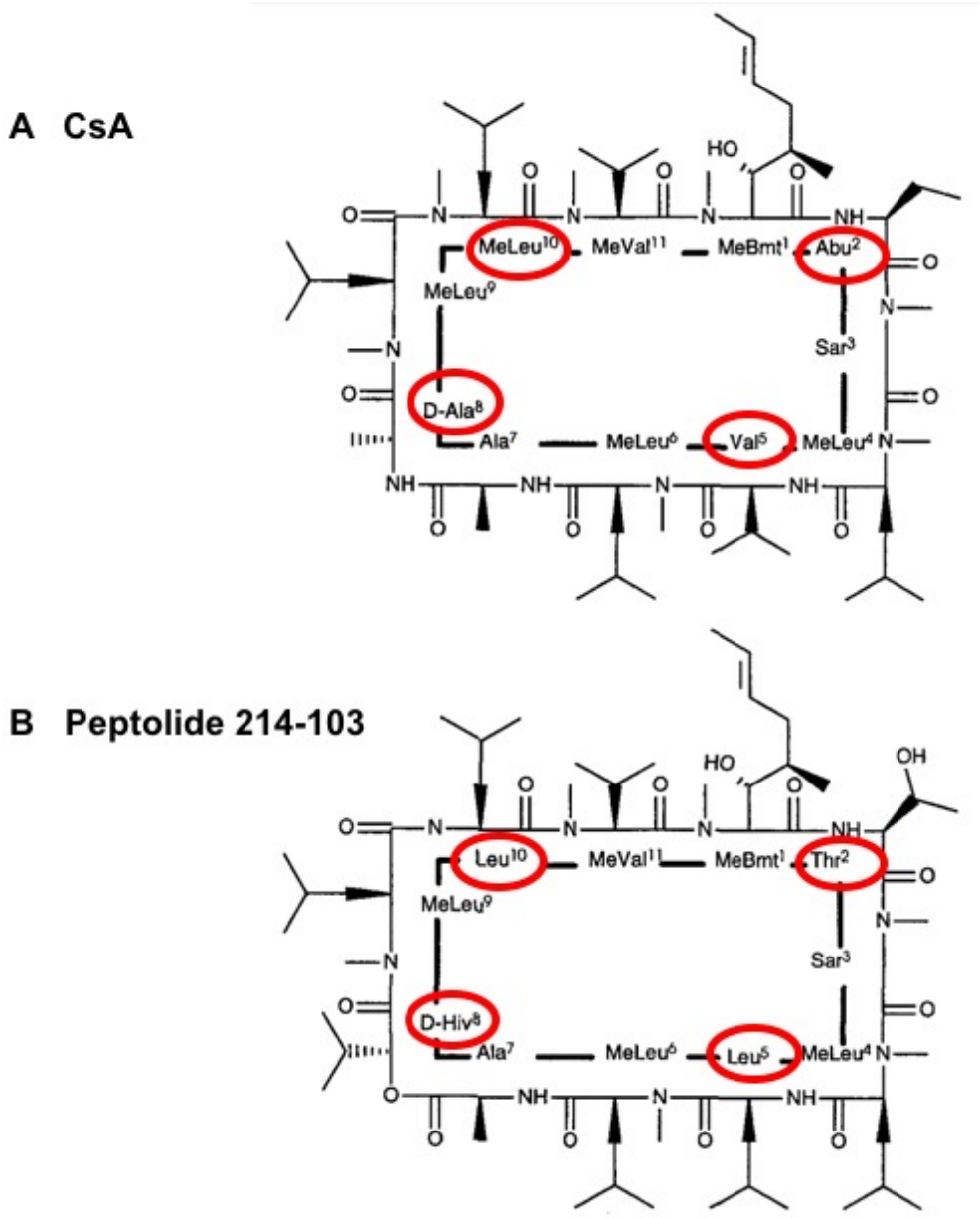

Figure 5.1 Amino acid residues comparison between CsA and Peptolide-214

(A) Formula of CsA, the prefix Me indicates N-methylation, **(B)** Formula for the cyclic peptolide 214-103, D-Hiv is D-2-hydroxyisovalericacid, which forms an ester linkage. Differences between Peptiolide-214 and CsA were shown in the amino acids position 2, 5, 8 and 10 (Modified from Taylor P et al., 1996[460]).

Despite the fact that bile acids, fatty acid ethyl ester and secretagogus has long been studied in eliciting local pancreatic acinar cell injury and distant organ injury, the detailed time course scale and pattern for major cellular events are still not fully characterized. With more consensus in toxin induced pancreatitis manifested a large range of intracellular events, the aberrant intracellular Ca^{2+} signalling and the following MPTP opening were widely assumed to occur early in a series intra-pancreatic cellular events to trigger acute pancreatitis and necrosis[172, 237]. Thus, early intervention was thought to be an important therapeutic strategy for AP. However, most studies that investigated the intervention time point in AP showed beneficial effects when treatment was given prophylactically, which does not fit into the clinical practice that patients only admitted after the symptom onset or diagnosed, which varies from hours to days, even weeks. Whether all patients would benefit from such treatment as tested here is uncertain, as the treatment was administered just 1 h after disease induction. Whether there would be any protective effects if the treatments were given later after disease induction remains to be further determined.

Therefore, upon first examining effects of all these novel compounds to select out a promising product which could possibly apply on further investigation, the study was also designed to fully evaluate the effects of the selected candidate compound and to determine possibility of using any practical preferable dosing regimen like twice daily, based on pharmacodynamics to define dose response, efficacy and intervention time of candidate compound in experimental acute biliary pancreatitis on a clinical acceptable basis.

5.3 Methods

5.3.1 Determine the candidate compound

3 different cyclophilin inhibitors, including CsA analogue SEL3714 and SEL3639, and the other one SEL1233 derived from peptiolides-214 were initially dissolved in DMSO and further freshly diluted with 10% cremophor in saline before dosing. TLCS-AP was induced as previously described in chapter 2. Based on results from preliminary study of CsA, compounds were administered intraperitoneally at 5mg/kg, 1h after TLCS perfusion with either single, 3 (every 8 hours) or 4 (every 6 hours) doses according to their half-life. The 12-week-old male C57BL/6J mice were randomly divided into 7 groups (6 mice/ per group) as listed below: (1) control group with sham laparotomy only, (2) positive AP group with TLCS common duct perfusion, (3) solvent control group with AP induction plus solvent injection (10% cremophor dissolved in saline with 1% DMSO), (4-5) 2 treatment groups with SEL3639 and SEL1233 at 5mg/kg administration by 4 i.p injections every 6 hours for 24h, (6) treatment group with SEL3714 at 5mg/kg administration by 3 i.p injection every 8 hours for 24h and (7) treatment group with SEL3714 at 5mg/kg administration by single i.p injection.

5.3.2 Dose response study of candidate compound

Ready to use formulation (dissolved in PG 10%, PEG400 30%, ethanol 10% and water 30%) was supplied by Cypralis at low (L, 0.5 mg/mL), medium (M, 2mg/mL) and high (H, 5mg/mL) concentration for intraperitoneal dosing. Formulation was stored in 4 ℃ and kept on ice during dosing period.

Pharmacokinetics study was firstly conducted on male adult C57BL/6J mice. Sampling was conducted at 1, 2, 4, and 8 h time point after single intraperitoneal injection of 4mL/kg dosing volume with each formulation, *i.e*, low (L, 2 mg/kg), medium (M, 8 mg/kg) and high (H, 20 mg/kg) dosage of candidate compound. Immediately following asphyxia in CO_2 and death confirmation, blood was collected from ventricular camera through cardiac puncture into ethylenediaminetetraacetic acid (EDTA) pre-coated tube. The pancreas was quickly removed, washed in cold PBS, dried on sterilized swap and weighed before snapping frozen. The blood and pancreas samples were then sent to Cypralis on dry ice to determine blood and tissue drug levels.

Candidate compound dose response in TLCS-AP was conducted on male 12-week old C57BL/6J mice, which were randomly divided in to 6 groups listed as below: (1) negative control group with sham laparotomy surgery only, (2) positive AP group with TLCS common duct perfusion, (3) solvent control group with AP induction plus solvent injection, and (4-6) compound treatment groups with different dosages at 2, 8, and 20 mg/kg. Compound ready to use formulation at different concentrations supplied with Cypralis were given on a *bis in die* (BID, twice daily) basis. 1st dosing was given at 1h after TLCS perfusion, followed by the 2nd dosing at 12h after the first dosing. Mice were sacrificed at 24 h after TLCS infusion, samples were collected for routinely severity assessing as described in chapter 2.

5.3.3 Efficacy study of candidate compound

Candidate compound ready to use formulation with ethanol free solvent (dissolved in 5% succinic acid, 30% PEG400 and ddH_2O) was supplied by Cypralis. Formulation was stored in 4 ℃ and kept on ice during dosing period. TLCS-AP was induced as previously described in chapter 2. Candidate compound was employed by intraperitoneally injection at optimum dosage, starting at 1 h after induction with either *bis in die* (BID, 2 times a day) or *quarter in die* (QID, 4 times a day, Q6H) dosing. Alternatively, dosing started 7h after model induction with BID dosing. Samples were harvested at 24 h. Standard AP severity assessment was conducted as previously described in chapter 2. The experimental 12 –week-old male C57BL/6J mice were randomly divided into 6 groups listed as below: (1) negative control group with saline perfusion following laparotomy, (2) positive AP group with TLCS common duct perfusion, (3) solvent control group with AP induction plus solvent injection (0.05M succinic acid and 5% PEG400), (4-6) treatment with candidate compound at optimum dosage, BID, starting 1h or 7h after AP induction, and QID starting 1h after induction. The study dosing regimen design was illustrated in **Figure 5.2**.

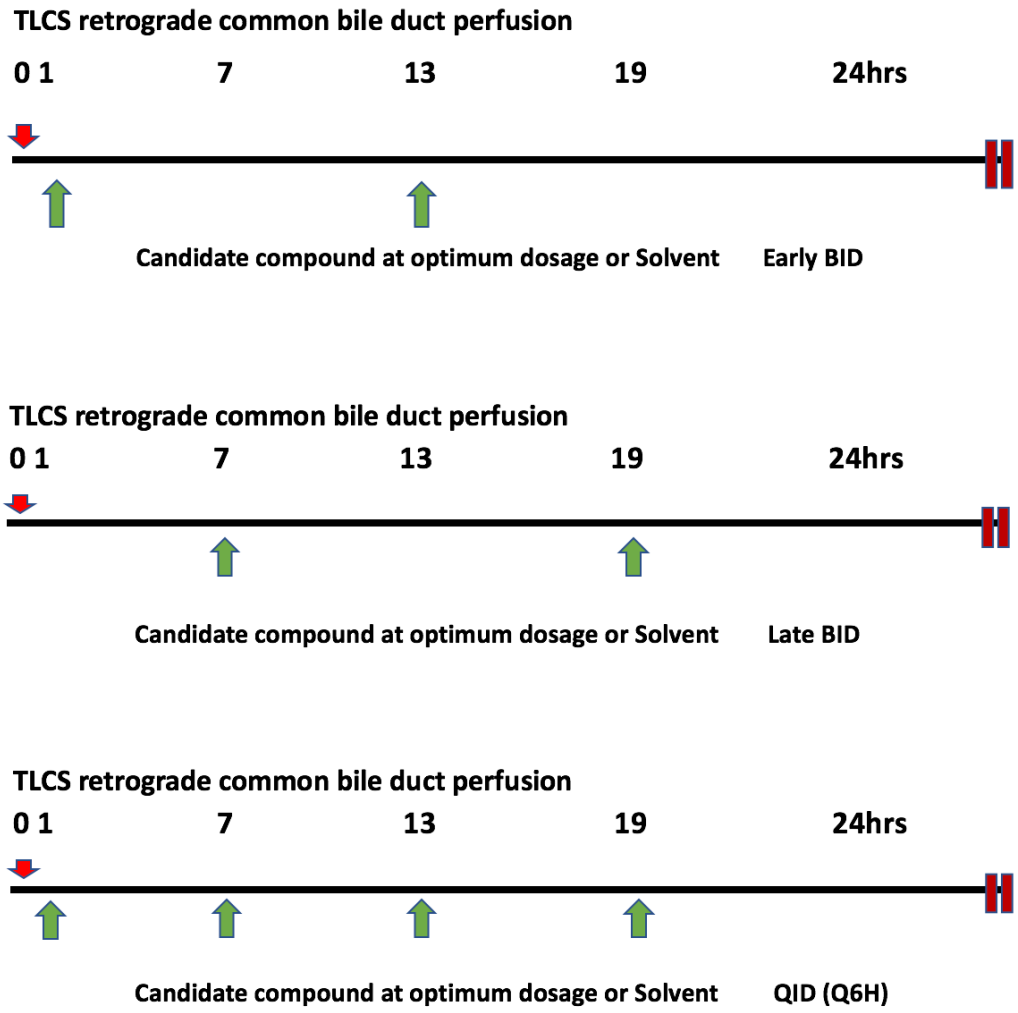

Figure 5.2 Candidate compound dosing regimen in TLCS-AP

Candidate compound or solvent (0.05M succinic acid and 5% PEG400) was employed by intraperitoneal injection at the optimum dosage, starting at 1 h after induction with either *bis in die* (BID, 2 times a day) or *quarter in die* (QID, 4 times a day, Q6H) dosing. Alternatively, dosing started 7h after model induction with BID dosing. Samples were harvested at 24 h.

5.4 Results

5.4.1 Results: determine the candidate compound

Biliary AP perfused with bile acid TLCS resulted in substantial elevation of all biochemical, immunological and histological parameters (**Figure 5.3**). Solvent with 10% cremophor used for cyclophilin inhibitors showed no difference with TLCS – AP groups. Although various doses were applied, three compounds at 5 mg/kg given every 6h consistently showed reduction across all parameters.

Among 3 compounds, SEL1233 significantly reduced pro-inflammatory cytokine IL-6, $p<0.01$ (**Figure 5.3B**), pancreatic MPO, $p<0.05$ (**Figure 5.3C**), pancreatic necrosis score (**Figure 5.3E**), with a trend to reduce serum amylase, $p=0.055$ (**Figure 5.3A**) and lung MPO, $p=0.054$ (**Figure 5.3D**).

Although all compounds with different dosages showed significant alleviation of overall pancreatic histopathological scoring, SEL-1233 administered at 5mg/kg, 4 doses within 24h, revealing the most effective reduction, $p<0.01$(**Figure 5.3F**) compare to the TLCS-AP group.

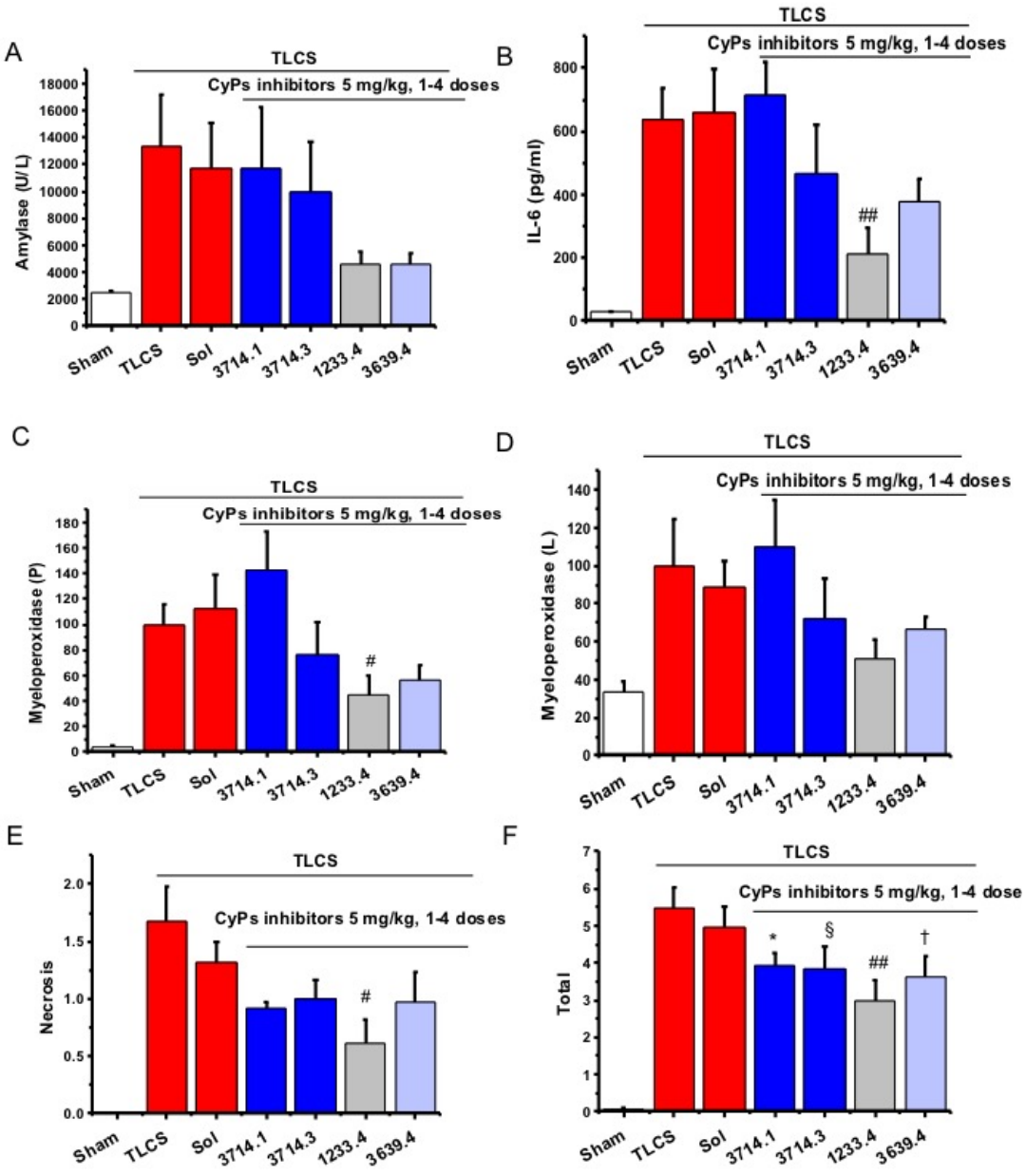

Figure 5.3 Effects of SEL compounds on the severity of TLCS-AP

Cyclophilin inhibitors or solvent (10% cremophor dissolved in saline with 1%DMSO) were administered 5mg/kg by i.p injections, 3714 was given by single or 3 doses, 1233 and 3639 were administered for 4 doses. 1233 significantly reduced **(B)** Serum IL-6, **(C)** Pancreatic MPO, **(E)** Pancreatic necrosis score, **(F)** Overall pancreatic histopathological score and 1233 also consistently showing trend in decreasing **(A)** Serum amylase and **(D)** Pulmonary MPO. $^{\#\#}P<0.01$, $^{*,\S,\#,\dagger}P<0.05$ compared to TLCS-AP group. Values are mean ± SEM of 6 mice per group.

5.4.2 Results: dose response of candidate compound

After determined SEL1233 is the best compound among all tested compounds, levels of SEL1233 in plasma and pancreas were measured at various time points following single IP dose (measurement and results plot was conducted by Cypralis). Plasma and pancreatic levels of SEL1233 remain steady within 2 h at all three dosages, however, there is no detectable compound levels in plasma while it is still detectable but showed a dramatic falling period in pancreas after 2 hours at 2 mg/kg dosage. For medium dosage at 8 mg/kg, the plasma level of SEL1233 started to fall after 2 h, but stays above 800 ng/mL for another 4 hours after initial fall, whereas the pancreatic level of SEL1233 keeps smooth (above 16000 ng/g tissue) throughout the whole period within 8 h. Similar with the steady state present in pancreas at medium dosage, the drug levels following high dosage (20 mg/kg) of SEL1233 administration were also observed steady along 8 h in both plasma and pancreas above 1400 ng/mL in plasma and 100000 ng/g tissue (**Figure 5.4**)

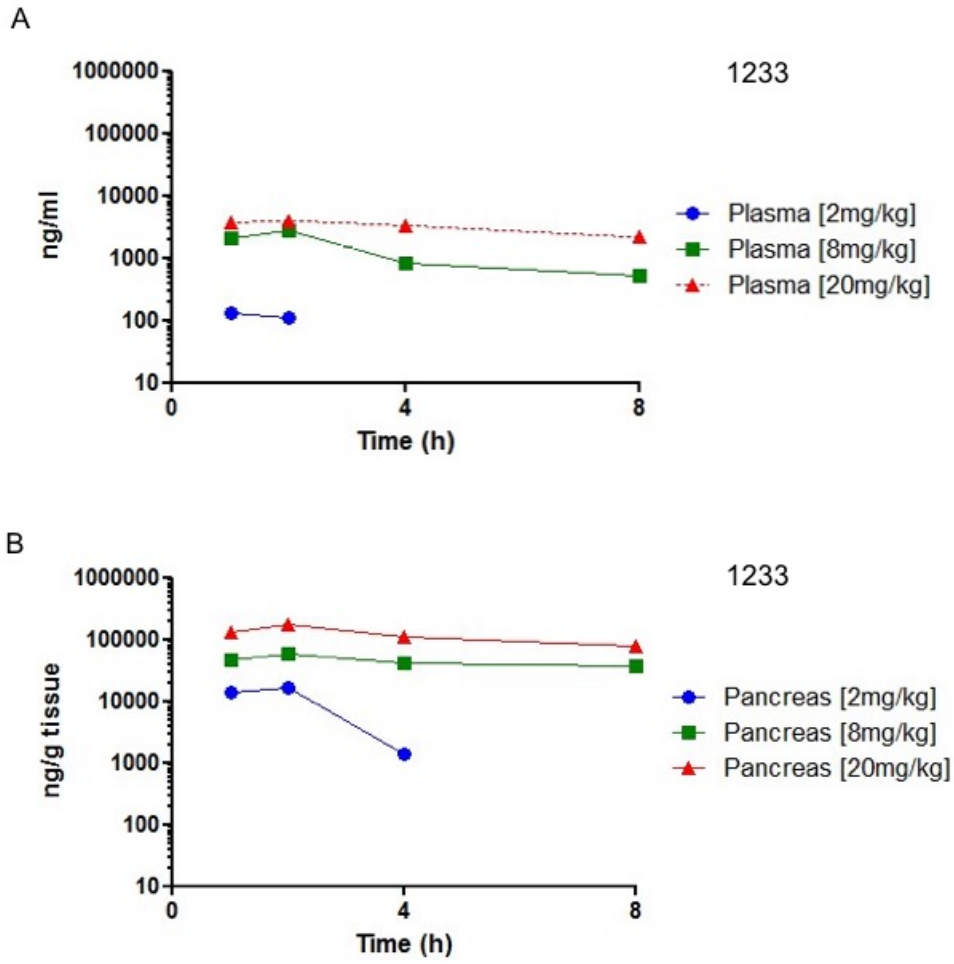

Figure 5.4 Plasma and pancreatic levels of SEL1233 following single i.p injection

SEL1233 concentration in **(A)** plasma and **(B)** pancreas at 1, 2, 4 and 8 hours following single i.p injection of 2 mg/kg, 8 mg/kg and 20 mg/kg dosages.

TLCS infused AP model produced markedly increased serum amylase, inflammatory IL-6 level, local and distant organ neutrophil infiltration marker, as well as typical histopathological damage features with necrosis, following SEL1233 at 2mg/kg, 8mg/kg and 20mg/kg dosing every 12h intraperitoneally, all dosages showing significantly reduction of anti-inflammatory effect on serum IL-6 (**Figure 5.5B)**. SEL1233 at 8 and 20 mg/kg consistently reduced serum amylase (**Figure 5.5A**), serum IL-6 (**Figure 5.5B**), pancreatic MPO (**Figure 5.5C**), pancreatic histopathology overall score (**Figure 5.5F**) significantly and showing close to border significance trend to reduce pancreatic necrosis (**Figure 5.5E**).

With more pronounced reduction observed in local pancreatic injury at 20mg/kg dosing group, this effective dosage, however, barely had any beneficial on pulmonary MPO, but appear to exacerbate the lung injury with PG/PEG /ethanol contained solvent (**Figure 5.5D**).

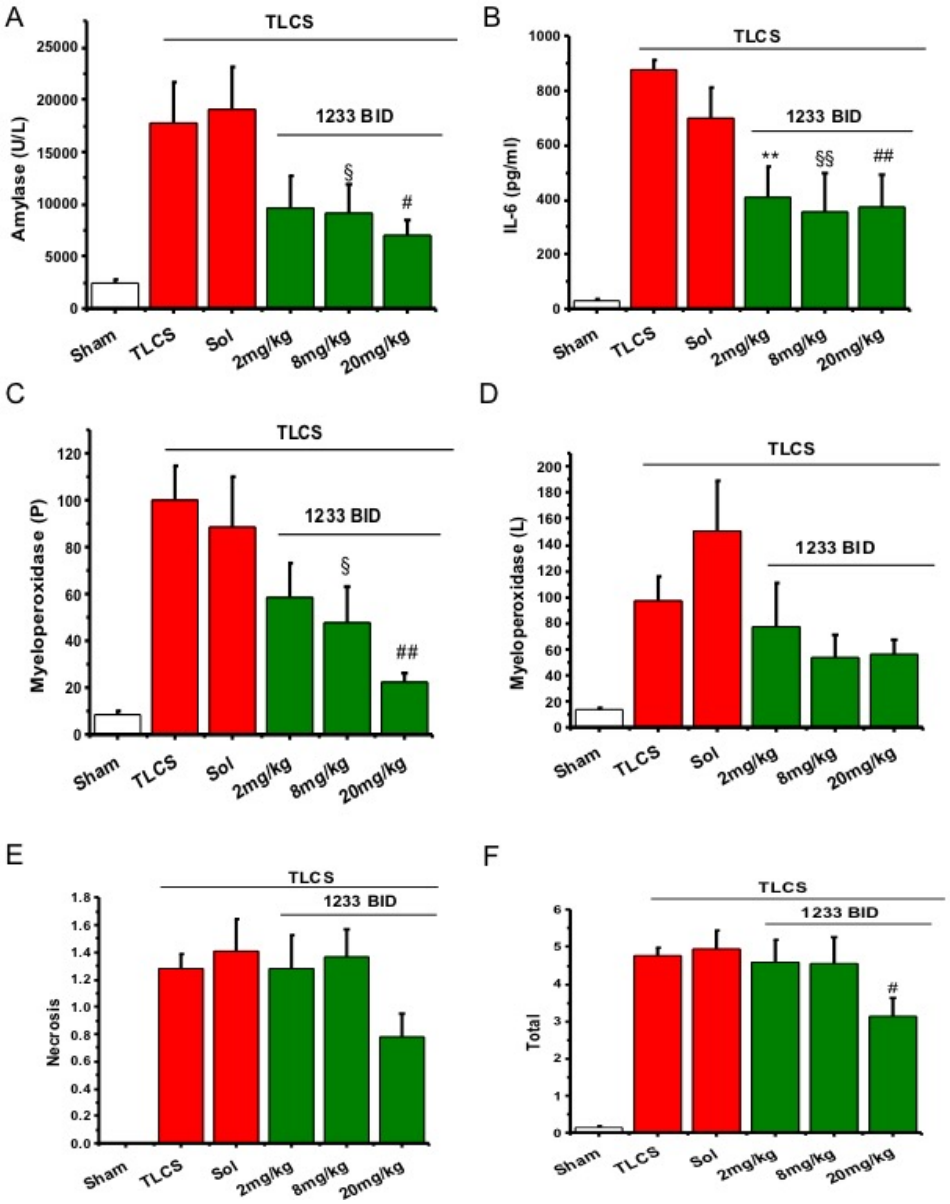

Figure 5.5 SEL 1233 dose response on the severity of TLCS-AP

SEL1233 were given at 2, 8, and 20 mg/kg twice daily following retrograde common bile duct perfusion of TLCS. Solvent with 10% ethanol and 30% PEG 400 was used. SEL1233 at 20mg/kg significantly alleviating **(A)** Serum amylase, **(B)** Serum IL-6 **(C)** Pancreatic MPO and **(F)** Overall pancreatic histopathological score, also showing reduction trend in **(D)**Pulmonary MPO and **(E)** Pancreatic necrosis. $^{**, §§, ##}P<0.01$, $^{§, #}P < 0.05$ compared to TLCS-AP group.

Values are mean ± SEM of 6 mice per group.

5.4.3 Results: efficacy of candidate compound

Having selected out the candidate compound SEL1233 with optimum dosage at 20mg/kg, further evaluation with new solvent based formulation was conducted in TLCS-AP with initial administration started either 1h (early) or 6h (late) after TLCS perfusion.

20mg/kg SEL1233 administered with all regimens dramatically minimized the serum amylase level (**Figure 5.6A**, $P<0.01$) and to some extent reduced local inflammation shown as pancreatic MPO (**Figure 5.6C**), unlike the effect observed in serum amylase, however, the late BID SEL1233 dosing only has limited effect in reducing pancreatic MPO and does not protect against systemic inflammation shown in IL-6 (**Figure 5.6B**) or pulmonary MPO (**Figure 5.6D**) with TLCS-AP. Surprisingly, the newly developed ethanol free solvent (0.05M succinic acid + 5% PEG 400) administration in TLCS-AP, still tends to increase the pulmonary MPO level, however, with same dosing regimen used in last section, early BID dosing of SEL1233 at 20mg/kg with ethanol free formulation significantly reduced lung MPO shown in **Figure 5.6D** while same dosing regimen with solvent containing ethanol before in **Figure 5.5D** did not. It has also been noticed that frequent administration of SEL1233 at 20mg/kg for 4 doses within 24h greatly reduced biochemical parameters such as serum amylase and neutrophil sequestration shown in MPO activity especially pulmonary MPO, but started to show less efficacy in IL-6 reduction (**Figure 5.6**).

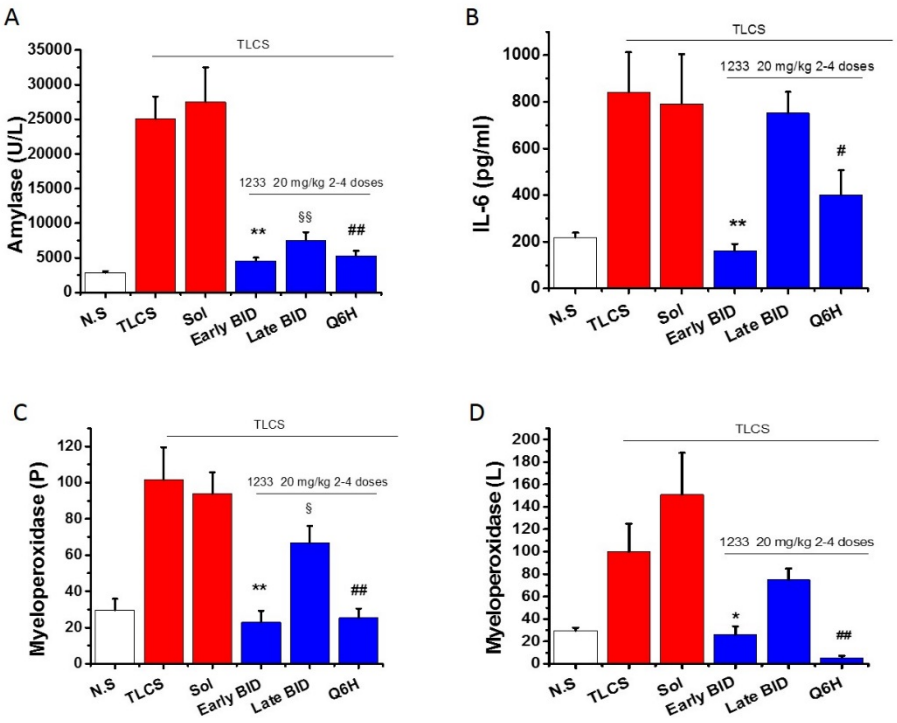

Figure 5.6 Effects of late SEL 1233 on the severity of TLCS-AP

20 mg/kg SEL1233 were given following retrograde common bile duct perfusion of TLCS, Alcohol free solvent (5% succinic acid + 30% PEG 400) was used. SEL1233 at 20mg/kg early BID dosing remarkably decreased all the biochemical parameters shown in **(A)** Serum amylase, **(B)** Serum IL-6**, (C)** Pancreatic MPO and **(D)** Pulmonary MPO. $^{**, §§, ##}P<0.01$, $^{*, §, #}P < 0.05$ compared to TLCS-AP group. Values are mean ± SEM of 6 mice per group.

While duct saline perfusion only showed minor oedema and occasional infiltration (**Figure 5.7a A**), the bile acid TLCS infusion/TLCS infusion with solvent injection produced typical histopathological features of AP with oedema, neutrophil infiltration and necrosis (**Figure 5.7a B** and **C**), which were greatly improved in pancreatic morphology appearances with early SEL1233 treatment (**Figure 5.7a D**), whereas late treatment only has limited protection (**Figure 5.7a E**). Interestingly, 4 doses of SEL1233 at 20 mg/kg (**Figure 5.7a F**) is less protective with more necrosis and neutrophil infiltration observed compare to BID dosing. The pancreatic histopathology score (**Figure 5.7b**) revealed that with early BID dosing, SEL1233 at 20 mg/kg greatly reduced the overall pancreatic histopathologic score ($P< 0.05$) and tend to reduce the necrosis as well. Although all three dosing regimens alleviated the local neutrophil infiltration shown in pancreatic morphology, early BID dosing showed the most effective reduction achieving the similar level with saline perfusion group (**Figure 5.7 D**).

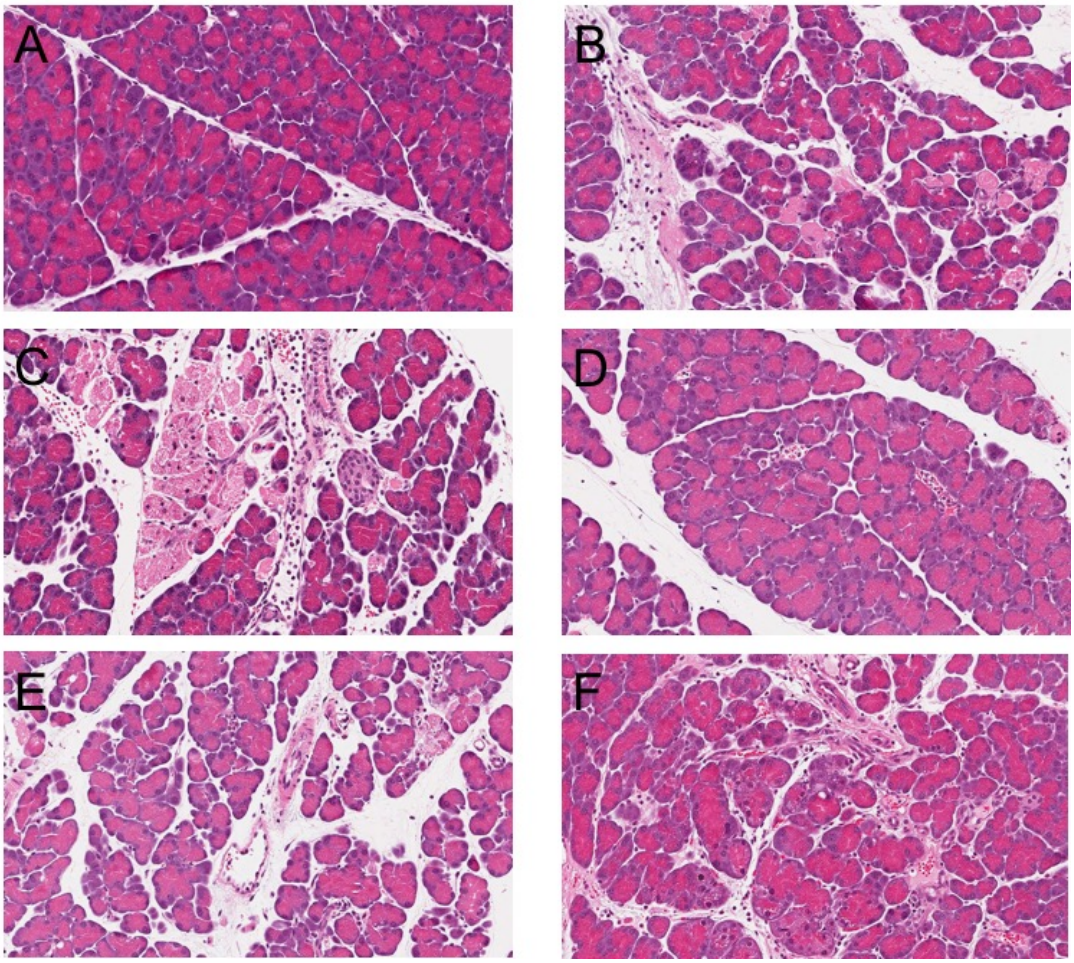

Figure 5.7 (a) Representative images on pancreatic morphology in TLCS -AP

Mice received retrograde common bile duct perfusion of 50μL TLCS or saline. SEL 1233 was initially given at 1h (early) or 6h (late) with various doses after perfusion and mice were sacrificed at 24 h. Histopathological images were shown in **(A)** Saline perfusion, **(B)** TLCS perfusion. **(C)** TLCS + solvent, **(D)** TLCS + SEL1233 20 mg/kg *2 early, **(E)** TLCS + SEL1233 20 mg/kg *2 late and **(F)** TLCS + SEL1233 20 mg/kg *4 early. Haematoxylin and Eosin stained with magnification × 200. Early BID dosing of SEL1233 greatly improved the pancreatic morphology.

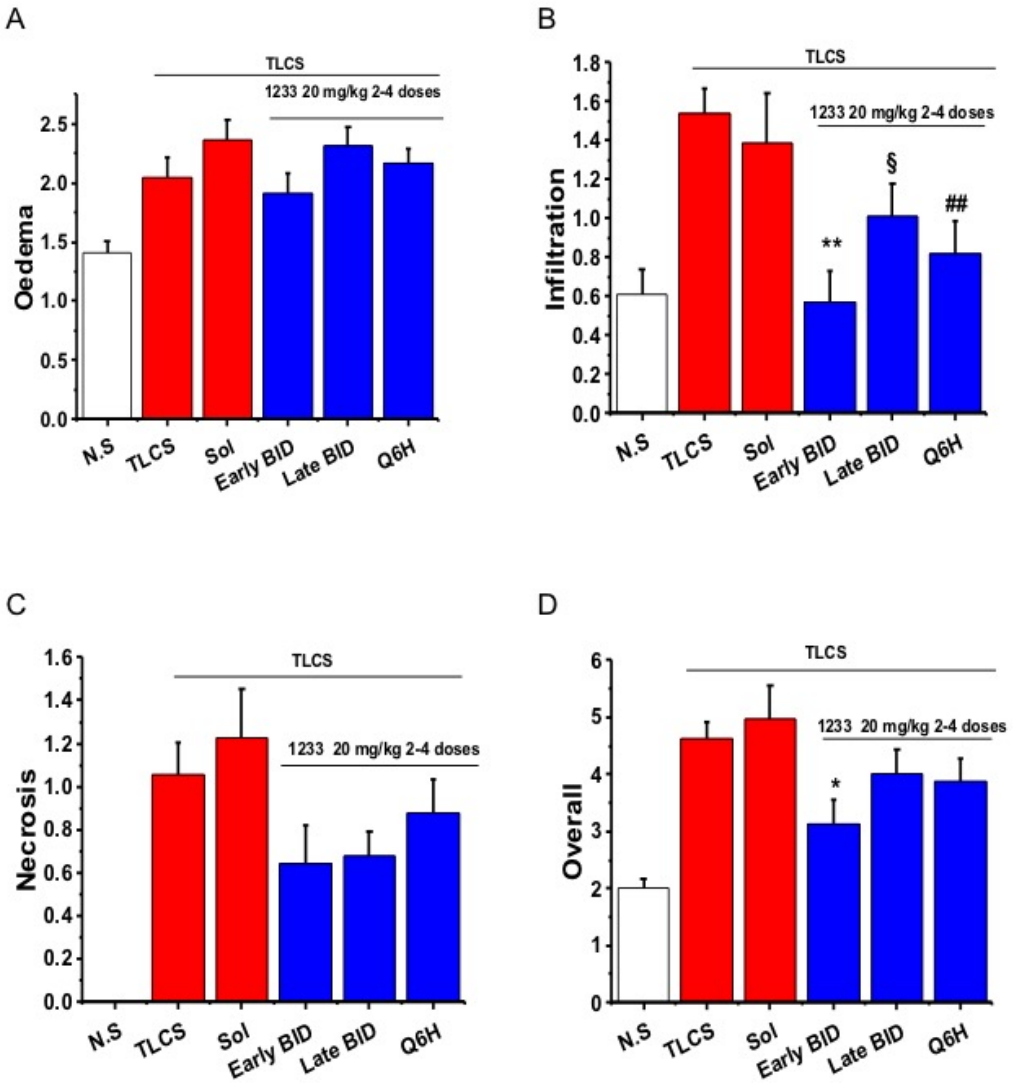

Figure 5.7 (b) SEL1233 efficacy on pancreatic histopathology score in TLCS-AP

Mice received retrograde common bile duct perfusion of 50 μL TLCS or saline. SEL 1233 was initially given at 1h (early) or 6h (late) with various doses after perfusion and mice were sacrificed at 24 h. Histopathological changes were shown in **(A)** Oedema score, **(B)** Infiltration score, **(C)** Necrosis score, and **(D)** Overall score. SEL1233 early BID dosing greatly reduced the pancreatic overall and infiltration score. $^{*,\S}P < 0.05$, $^{**,\#\#}P<0.01$ compared to TLCS-AP group. Values are mean ± SEM of 6 mice per group.

5.5 Discussion

Notably, among all these compounds, SEL1233, which is designed and structured with 2-3 folds higher affinity to CypD and greater solubility compare to CsA showed the best effects among tested compounds. Although there is slightly discrepancy in the structure across the 3 compounds used in this study, being derived from CsA or peptolides, all of them share the common basic structure and similarity to inhibit cyclophilins, except 1233 showed more potent affinity to CypD over other cyclophilins.

Results obtained from compounds other than 1233 also demonstrated some beneficial effects but were smaller in magnitude, which were such as to exclude these from further study. Compound 1233 showed distinctive and consistent reduction across all the parameters to alleviate TLCS-AP further validating the importance of MPTP inhibition. These findings also support the potential validity of using the CypD inhibitor SEL1233 as a treatment for AP and provides proof-of-principle evidence for SEL1233 application for this purpose, which should be assessed in other models of experimental AP.

Having approximately 3 or 4 hours' half-life, which is much shorter than CsA, compounds administered with repeated 4 doses within 24h seem to show a higher possibility in producing the beneficial effects. Thus, characterization of pharmacokinetics (PK) and optimisation of dosing regimen protocol are required for any further experiments apply SEL1233 in experimental acute pancreatitis.

Indeed, in line with PK results, this study also indicates that based on a BID

approach, the 20mg/kg dose of SEL1233 showed the most marked protection in TLCS-AP, more than 8mg/kg and 2mg/kg, presumably because the highest dose tested here provided the most favourable pharmacodynamics with BID dosing. Compared to previous in vivo studies in which genetic or pharmacological CypD inhibition appeared to dramatically reduce the impact of experimental acute biliary pancreatitis, the results obtained here are not as marked before. There are two reasons likely to account for this. Firstly, the negative control group used here was different from that used in previous studies with only sham laparotomy but not saline perfusion. Previously a ductal injection of saline was applied in the control group, inducing modest change in the head of the pancreas (e.g. oedema). Secondly, the solvent used here contained ethanol, a known precipitant of acute pancreatitis, which may have exacerbated the systemic damage and compromised the beneficial effects of SEL1233. The solvent should be changed to exclude ethanol in further in vivo studies testing the efficacy of SEL1233.

Notably, the PK data showed that there is still SEL1233 in the pancreas at 4h while the plasma level is already undetectable following lower dose administration, which suggested that there might be compound accumulation in pancreas in some extent, suggesting avoiding possible side effects in in the pancreas, a long- term dosing for high dose of SEL 1233 should be avoided.

In terms of the intervention time, administration of SEL1233 early at 1h after disease induction was markedly effective across a representative range of both local and systemic biochemical, immunologic and histopathologic response in biliary pancreatitis. Intraperitoneally administration of SEL1233 from a later time point after disease induction was significantly less protective across a broad range of

pancreatic and systemic parameters compared to early intervention in the biliary model. Contradictory to mice, human pancreatitis normally have a longer biological time course with typically pancreatic necrosis detected days even weeks, which emphasized the importance of the initial treatments.

These data provide robust confirmation of the hypothesis that CypD has a role in acute pancreatitis and further corroborate of applying inhibition of CypD with cyclophilin inhibitors is a potential therapeutic target for acute pancreatitis.

There are several issues need to be further clarified, however. Firstly, regarding to the appropriate solvent, sharing PEG 400 composition, both solvents formulation induced increased lung MPO level compared to TLCS alone group. Although the newly developed ethanol free solvent seems to exacerbate the lung MPO to a comparable level that induced by the ethanol included solvent formulation, SEL1233 has greatly improved its capabilities to reduce lung MPO level. This suggests that not only ethanol but PEG 400 content might be a second issue to exacerbate the lung injury, and ethanol may interfere with compounds to compromise the effect. One study on the effects of individual solvent in pulmonary toxicity and inflammation found that MPO measured in the bronchoalveolar lavage fluid (BALF) showed significant increase in 10% ethanol, 0.1% and 2% PEG-400. The same study also showed that in 28-day exposure to 10% ethanol, lung tissue showing mild pulmonary congestion, while with 2% PEG400, there was moderate pulmonary congestion and both solvents exposure lead to inflammatory cells concentrated as shown in pulmonary histopathology[463]. Another lung injury study depicts that treatment with surfactant and 5% PEG400 combination worsen the mean PaO_2, $PaCO_2$ and peak inspiratory pressure values 3h after treatment[464].

Secondly, substantial application of SEL1233 (20mg/kg at 4 doses) with enormously depletion of the pulmonary neutrophil sequestration even lower than the saline perfusion group, suggested the powerful neutrophil inhibition action with high dose SEL1233, which also confirms previous studies on RA that CsA act as anti-inflammatory role to inhibit neutrophil function and chemotaxis in a dose response manner reaching 80% inhibition at highest concentration[465]. The phenomenon that CsA and its analogue greatly reduced the inflammation shown in markedly reduced MPO level suggest the role of such compounds in AP acts not only in MPTP inhibition but possibly through other pathways that may including neutrophil chemotaxis inhibition involved with extracellular cyclophilins.

On the other hand, there is a mode for TLCS-induced injury via Ca^{2+} - dependent activation of serine/threonine phosphatase calcineurin, involved intra-acinar protease activation through NF-κB nuclear translocation[466, 467]. SEL1233, across all dosages. are generally effective in reducing inflammation, suggesting possible role on calcineurin inhibition as CsA did.

CHAPTER 6

Evaluating effects of SEL1233 in FAEE-AP and CER-AP

6.1 Summary

The findings obtained in this chapter demonstrated that intraperitoneal administration of SEL1233, a novel cyclophilin inhibitor with higher affinity to CypD, at 20mg/kg 2 h after disease induction, barely alleviated disease severity except for reduced pancreatic trypsin level in FAEE- and CER-AP. Treatment with both CsA and SEL1233 in *Ppif*$^{-/-}$ at 20mg/kg counteract the beneficial effects of MPTP inhibition in caerulein induced AP, confirmed the possible off-target effects on other cyclophilins, also suggested that the dose of CsA or analogues when perform a treatment, should be monitored with attention.

6.2 Introduction

Previous study with cyclophilin inhibitor SEL1233, showed great improvement in all parameters with early BID dosing at 20mg/kg in TLCS induced acute biliary pancreatitis. To fully investigate the potential significance of SEL1233 in a wider range of AP models rather than biliary alone, this chapter was designed to further evaluate the effects of SEL1233 in alcoholic AP and secretagogue induced AP.

Heavy alcohol consumption is one of the predominant aetiologies of AP in western countries[468] with the proportion ranges from 19% to 32%[469, 470]. The non-oxidative alcohol metabolism pathway forms the fatty acid ethyl ester, based on which our group has previously developed novel alcoholic model[196]. However, due to the acute toxicity that pure ethanol brought, there is 10-20% mortality with this model, for mice below 25g, the mortality can exceed 30% within 6-8 h. Driven by the demanding needs for such a clinical relevant model, to develop a much safer approach, a further modification based on this model with a series pilot studies have

been conducted and finally optimized the protocol through raising the concentration of POA and lowering the ethanol density with saline and PEG400 involved formulation.

Previous study describes in chapter 5 suggested that SEL1233 at 20 mg/kg markedly reduced pancreatic histology scoring and local injury as well as distant lung injury and systemic inflammation in experimental biliary acute pancreatitis induced by retrograde common duct perfusion of bile acid TLCS, however, it protected neither alcoholic or hyperstimulation AP with no improvement across biochemical and immunological parameters. Studies with CsA in chapter 4 depicted that high dosage administration of CsA may exacerbate the systemic inflammation in experimental acute pancreatitis, which was believed to be off-target effects that attributed to ER stress via CypB inhibition.

The SEL1233, which originated from CsA related peptolides-214103, was modified with both cyclophilins binding sites and calcineurin binding sites, which enabled SEL1233 to possess the higher selectivity across different cyclophilins especially with 2-3 folds higher affinity to CypD but much less potent immune-suppression activity compared to CsA. With such inhibitors, it would be interesting to know what effects would be when all other main cyclophilins were inhibited and partially discriminate from calcineurin inhibition. Such data will be essential to clarify the off-target effects.

To get further support for the hypothesis that high dose cyclophilin inhibitors are responsible for off-target inhibition and to further define the possible cyclophilin

subtype involvement and to differentiate the correlation between CypD with off-target effects, this set of experiment was designed to demonstrate the effects of high dose CsA and SEL1233 on the CypD knock out mice.

This chapter has described the study to examine the effects of SEL1233 on modified alcoholic FAEE-AP model and CER-AP model, and further experiments designed to discriminate the high dose induced off-target effect of cyclophilin inhibitors.

6.3 Methods

Modified FAEE-AP model and CER-AP were employed to examine the effects of SEL1233. For the modified FAEE-AP model, POA was originally dissolved in pure ethanol, to make a 640mM stock. A further 2.5 times dilution was freshly made with equal part of PEG400 and saline each time before injection. The final formulation consists of 30% PEG400, 30% saline and 40% ethanol and POA (300 mg/kg). SEL-1233 (0.05M succinic acid + 5% PEG400 as solvent) formulation was supplied by Cypralis. Both models received 20 mg/kg SEL1233 or its solvent firstly administered by i.p injection 2h after the first FAEE/CER induction, a second dose was given 12hs later for modified FAEE model. Mice were sacrificed at 24h or 12h after the initial FAEE/CER injection (**Figure 6.1**). For each model, adult male C57BL/6J mice were randomly divided into 6 groups: (1) negative control group with saline injection, (2) positive AP group with toxin injection, (3) solvent control group with AP induction plus solvent injection, (4) treatment with 20mg/kg SEL1233 by single i.p injection in CER-AP or starting 2h after AP induction by 2 doses every 12h in modified FAEE-AP. The humanly killing and sample collection were conducted according to the description in chapter 2.

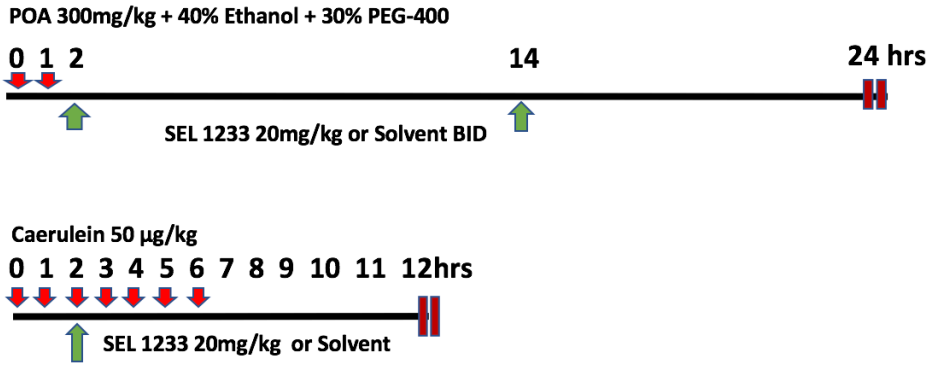

Figure 6.1 SEL 1233 dosing protocol in modified FAEE-and CER-AP

20mg/kg SEL1233 or its solvent (0.05M succinic acid + 5% PEG400) was administered intraperitoneally 2h after the first FAEE/caerulein injection, twice in FAEE-AP and single dose in CER-AP.

To further study the possible off-target effects, male adult wild type or CypD knock out mice (*Ppif*$^{-/-}$) were employed to receive 7 hourly intraperitoneal injections of caerulein (50µg/kg), 20 mg/kg SEL1233 or CsA was administered 2 hours after the first caerulein injection and mice were sacrificed at 12 hours after the induction. Wild type and CypD knockout (PPIF) male adult C57BL/6J mice were randomly divided into 5 groups: (1) negative control group with saline injection, (2) positive AP group with caerulein injection, (3) solvent control group with AP induction plus solvent injection (10% cremophor dissolved in saline with 1% DMSO), (4) positive AP group in *Ppif*$^{-/-}$ mice with caerulein injection plus single 20mg/kg CsA injection, (5) positive AP group in *Ppif*$^{-/-}$ mice with caerulein injection plus single 20mg/kg SEL1233 injection. Sample collection and severity assessment was conducted as previously described in chapter 2.

6.4 Results

6.4.1 Results: define the pathological pattern for modified FAEE-AP.

FAEE produced massive necrosis characterized as focal marginal lobule pattern along with pancreatic oedema and neutrophil infiltration in previous studies. With modified protocol, successful diseases induction was confirmed by histopathologic change and increased serum amylase level at 24h, similar focal necrosis pattern but mild injury with oedematous acini, inflammatory cell infiltration and scattered necrosis has been observed (**Figure 6.2A**) and serum amylase dramatically increased to the peak at 6h followed by gradually decline (**Figure 6.2B**). Interestingly, both significant local injury shown as pancreatic trypsin and MPO activity were reached to the peak at 24h, the pancreatic trypsin activity, however, only had a small rise at 6h, followed by gradually increase till 12h and finally further increase till 24h (**Figure 6.3A**), whereas pancreatic MPO has a sharp rise from the initial all through till 12h and then gradually reached to the highest level at 24h (**Figure 6.3B**), suggesting aggressive inflammation during first 12h. Unlike the local injury pattern, the systemic injury shown in serum IL-6 (**Figure 6.3C**) and pulmonary MPO (**Figure 6.3D**) present a peak injury effect at 6h and then gradually recovered to control level at 24h.

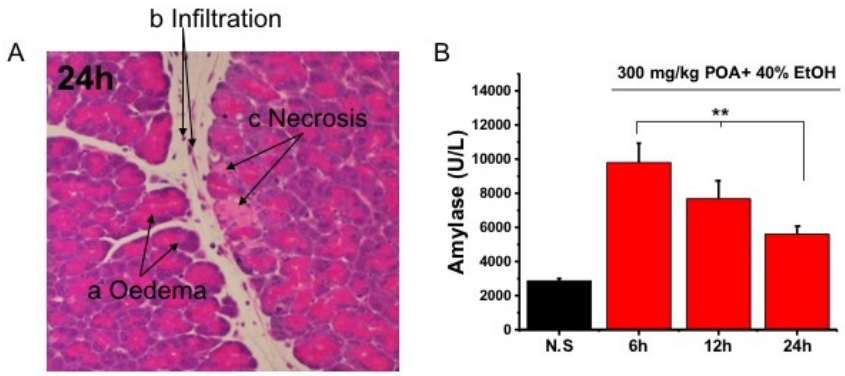

Figure 6.2 Confirmation of AP induction in modified FAEE- AP

(A) Pancreatic histopathology at 24h, **(B)** Amylase time course. **P<0.01 compared to 6h time point. Values are mean ± SEM of 6 mice per group.

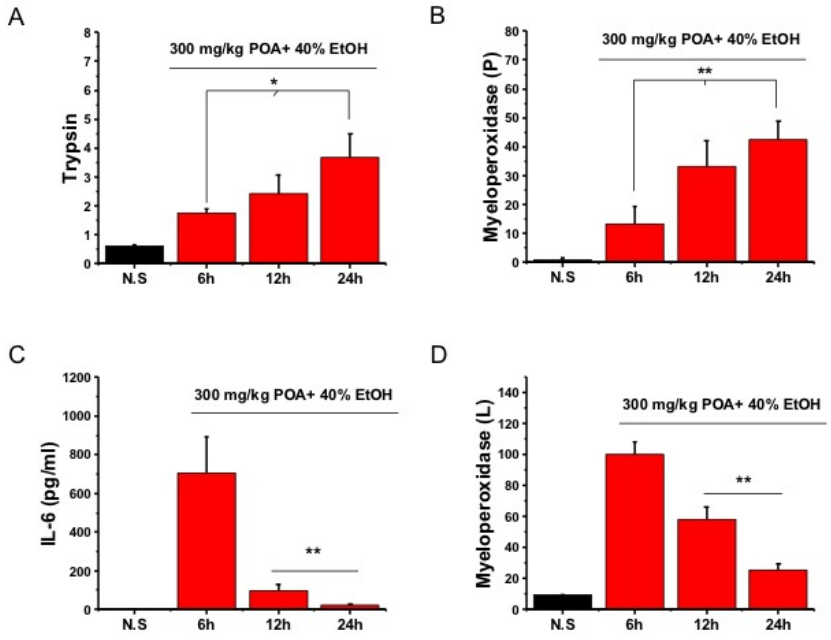

Figure 6.3 Time course characterization of modified FAEE -AP

Local injury shown in pancreatic **(A)** Trypsin activity and **(B)** Pan MPO significantly increased to the peak at 24h. Systemic injury presented in **(C)** serum IL-6 and **(D)** Lung MPO significantly increased to the peak at 6h and recovered to control level at 24h. *P<0.05, **P<0.01 compare to 6h time point.

Values are mean ± SEM of 6 mice per group.

6.4.2 Result: effects of SEL1233 on modified FAEE-AP and CER-AP

20mg/kg SEL1233 had no significant impact on any biochemical (**Figure 6.4 A1**), immunological (**Figure 6.4 A2**), neutrophil sequestration (**Figure 6.5 A2 and A3**) or histopathology scoring (**Figure 6.6 A**) in FAEE-AP, but showing reduction trend on pancreatic trypsin activity (**Figure 6.5 A1**). The solvent (0.05M succinic and 5% PEG400) adversely promoted amylase level (**Figure 6.4 A1**) and local neutrophil shown as pancreatic MPO (**Figure 6.5 A2**) in modified FAEE-AP.

Similarly, or even worse in CER-AP, 20mg/kg SEL1233 significantly increased serum amylase (**Figure 6.4 B1)**, IL-6 (**Figure 6.4 B2**), pancreatic MPO (**Figure 6.5 B2**) and showing ascending trend in Lung MPO (**Figure 6.5 B3**) and histopathology scoring (**Figure 6.6 B**), however, statistically decreased pancreatic trypsin activity, $P<0.05$ (**Figure 6.5 B1**) no significant increase has seen with solvent in CER-AP.

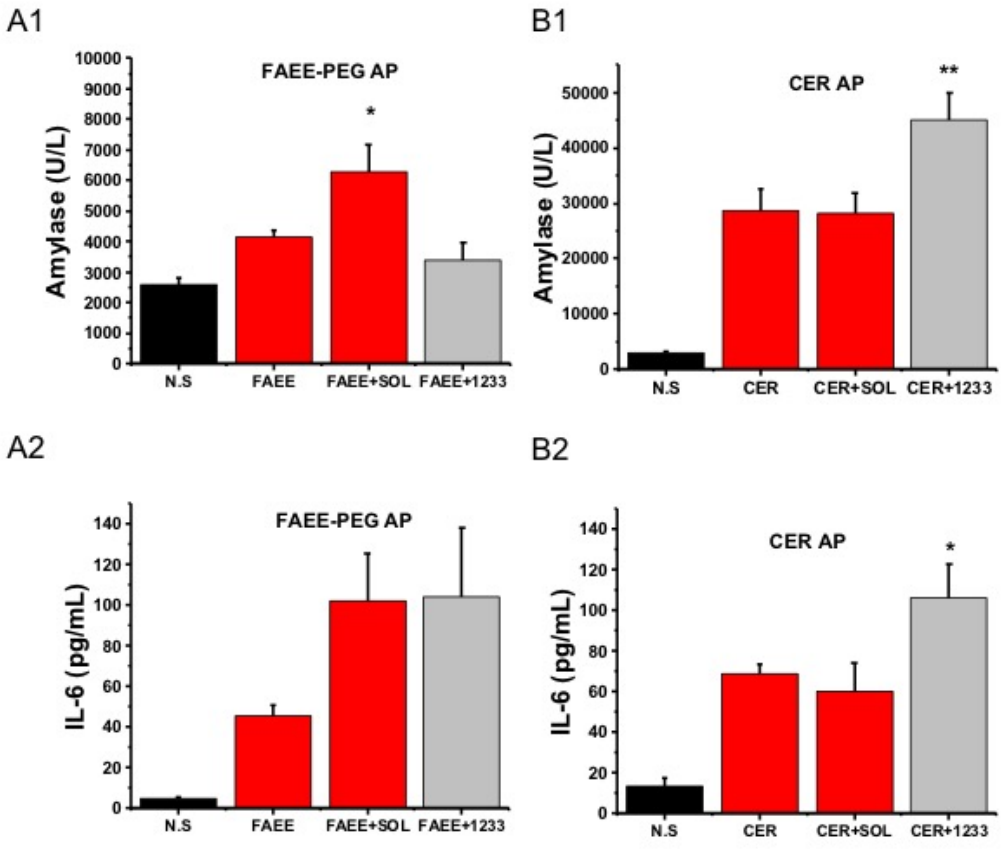

Figure 6.4 Effects of 1233 on serum Amylase and IL-6 in modified FAEE- and CER-AP

1233 at 20mg/kg or solvent (0.05M succinic and 5% PEG400) was administered in modified FAEE-AP or CER-AP 2h after the first toxin injection with BID or single dosing. Mice were sacrificed at 24h or 12h in two models, respectively.

Modified FAEE-AP: **(A1)** serum amylase and **(A2)** IL-6

CER-AP: **(B1)** serum amylase and **(B2)** IL-6

***P*<0.01, **P*<0.05, compared to FAEE- or CER-AP group.

Values are mean ± SEM of 6 mice per group.

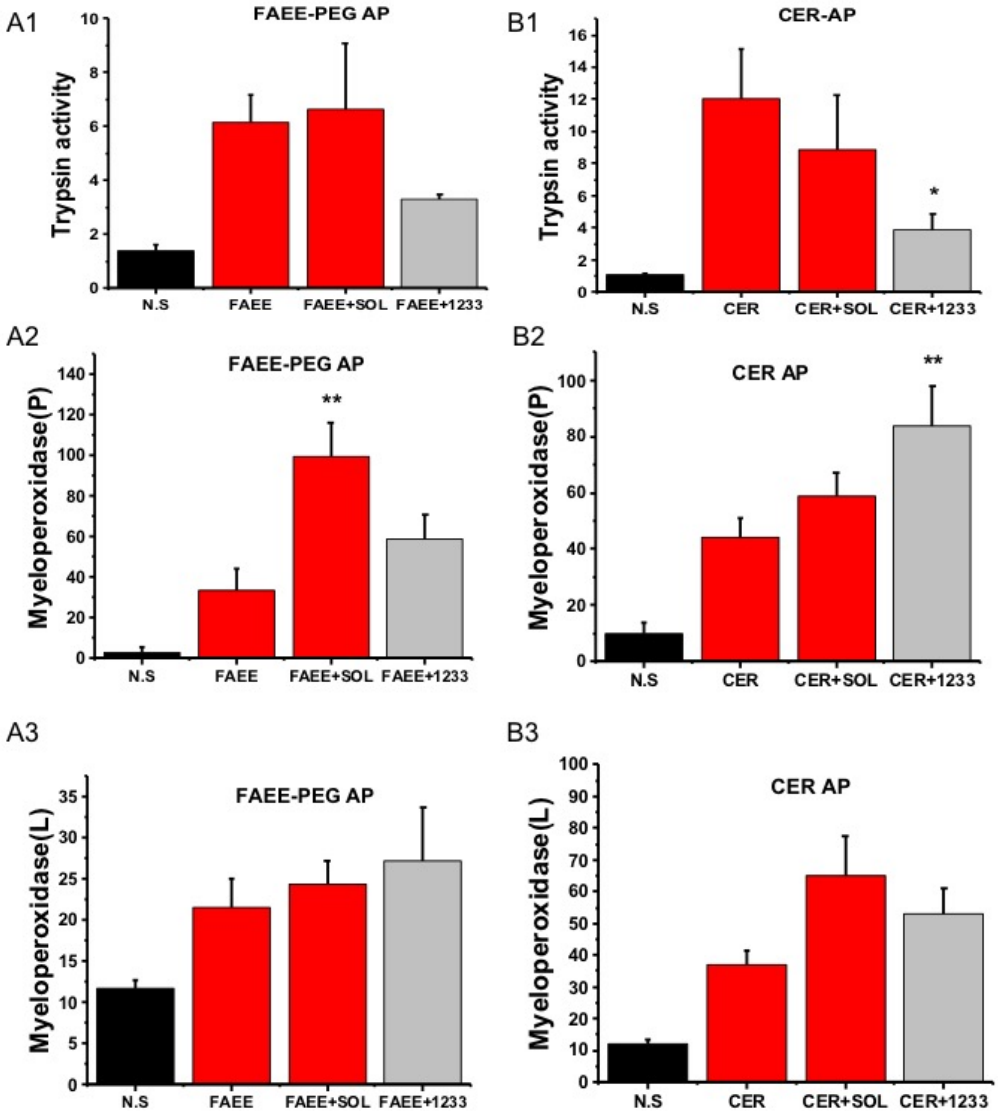

Figure 6.5 Effects of 1233 on trypsin activity and myeloperoxidase in modified FAEE- and CER-AP

1233 20mg/kg treated mice shown reduced **(1)** trypsin activity level in **(A)** modified FAEE-AP and **(B)** CER-AP. Solvent greatly increased **(A2)** pancreatic MPO in FAEE-AP while 1233 not solvent increased **(B2)** pancreatic MPO in CER-AP with statistical significance (All $P<0.05$). No difference seen with **(3)** lung MPO in both models. *$P<0.05$ compare to FAEE- or CER-AP group.

Values are mean ± SEM of 6 mice per group.

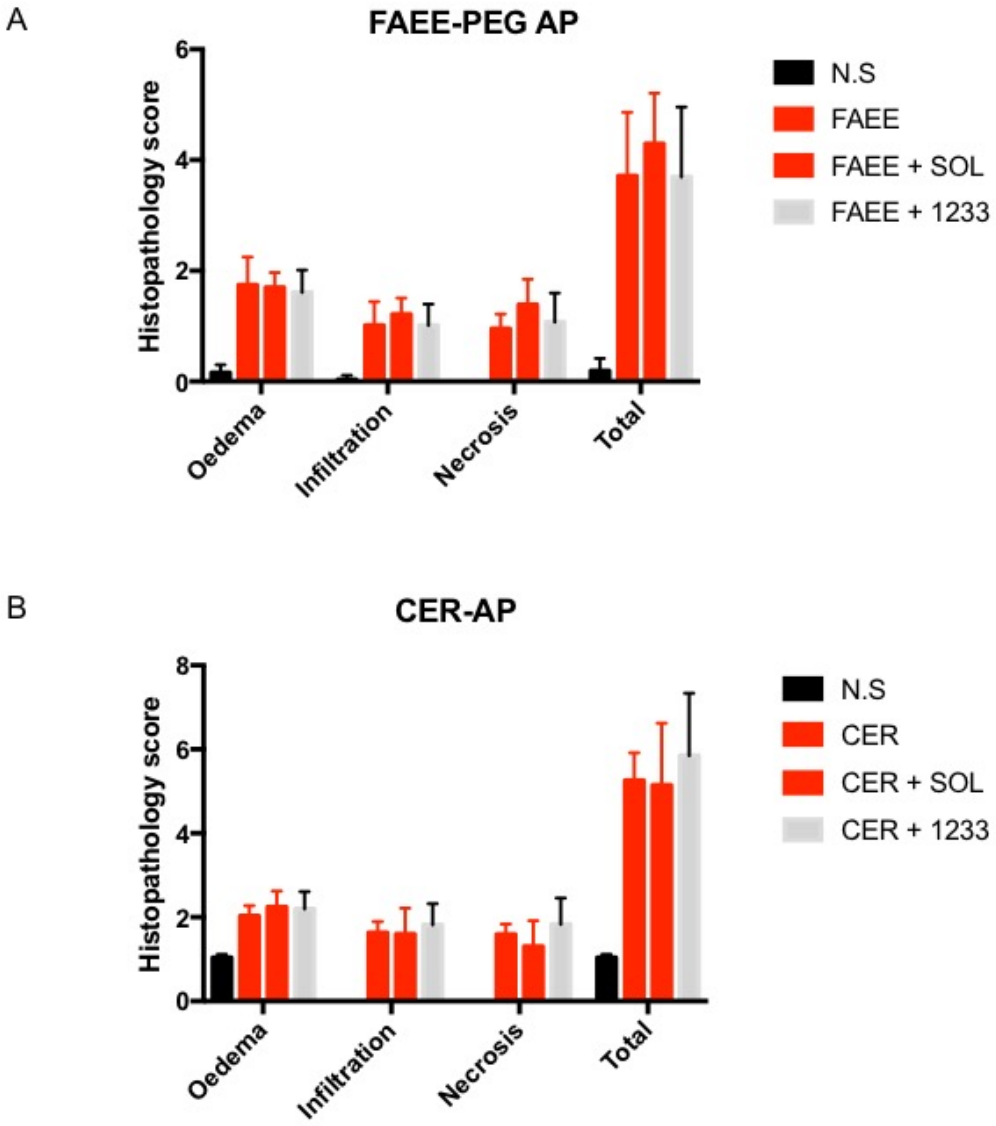

Figure 6.6 Effects of SEL1233 on histopathology score in FAEE- and CER-AP

No significant improvement in SEL1233 20mg/kg treated mice shown as pancreatic oedema, infiltration, necrosis or overall histopathologic score in **(A)** modified FAEE-AP and **(B)** CER-AP. Values are mean ± SEM of 6 mice per group.

6.4.3 Results: define off-target effects

Both WT and CypD ablation (*Ppif*$^{-/-}$, PPIF) mice were subjected to 7 hourly 50μg/kg caerulein injections to induce AP. 20mg/kg SEL1233 and CsA were administered 2h after first toxin injection by single i.p injection. Serum amylase (**Figure 6.7)** showed significantly reduction in CypD knockout mice following caerulein injection, however, neither 1233 nor CsA at 20 mg/kg protected from the increased amylase. On the contrary, both cyclophilin inhibitors showed statistically further elevation compare to CER-AP group in WT mice. In *Ppif*$^{-/-}$ received two inhibitors, the beneficial from CypD knockout has been counter balanced. While CsA showing great anti-inflammation effects on IL-6 on both WT and *Ppif*$^{-/-}$ mice, 1233 however, only reduced IL-6 level on *Ppif*$^{-/-}$ mice, but adversely further increased IL-6 level in WT mice (**Figure 6.8A**). Interestingly, but vice versa, while 1233 showing significant trypsin reduction in both type of mice, CsA however, only significantly decreased trypsin level in wild type but not *Ppif*$^{-/-}$ mice at 20mg/kg (**Figure 6.8B**). As for MPO, both 1233 and CsA had no reduction in pancreatic MPO, with 1233 had a statistically increase (**Figure 6.8C)**, whereas 1233 does not affect lung MPO, but CsA at 20mg/kg exacerbated the pulmonary neutrophil sequestration status in both type of mice (**Figure 6.8D**).

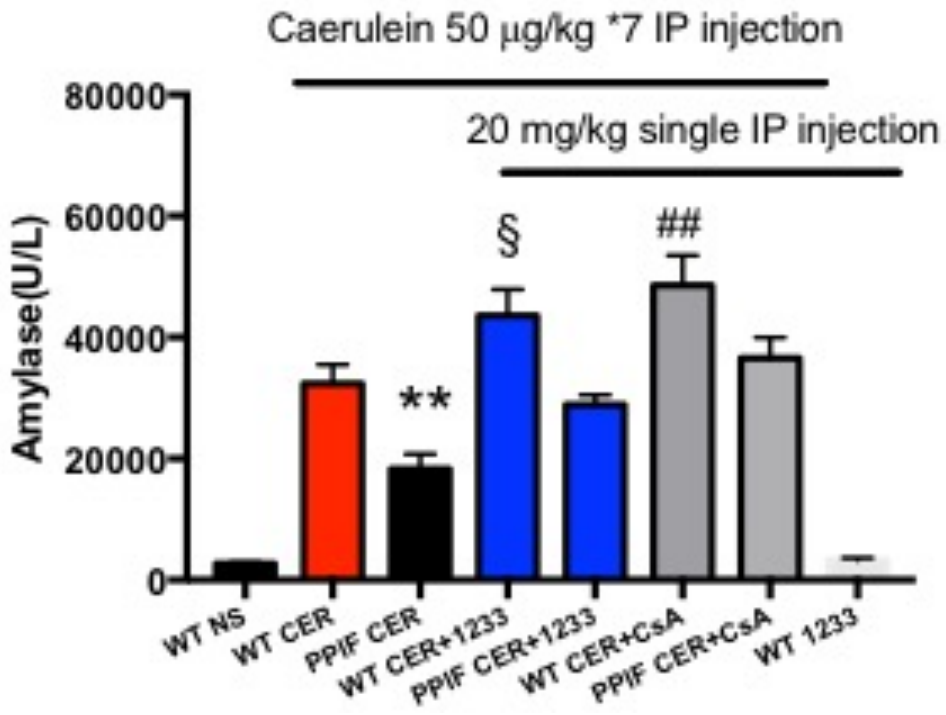

Figure 6.7 Effects of 1233 and CsA on amylase with WT and Ppif$^{-/-}$ mice

1233 and CsA at 20mg/kg were administered in 7 hourly caerulein injection induced AP on both WT and *Ppif*$^{-/-}$ mice, *Ppif*$^{-/-}$ significantly reduced caerulein induced serum amylase, both 1233 and CsA adversely increased amylase in WT-AP mice, and counterbalanced amylase level in *Ppif*$^{-/-}$ mice. 1233 alone showed no effects on amylase level. $^{**}P<0.01$, $^{*}P<0.05$ compared to WT CER-AP group**.** Values are mean ± SEM of 6 mice per group.

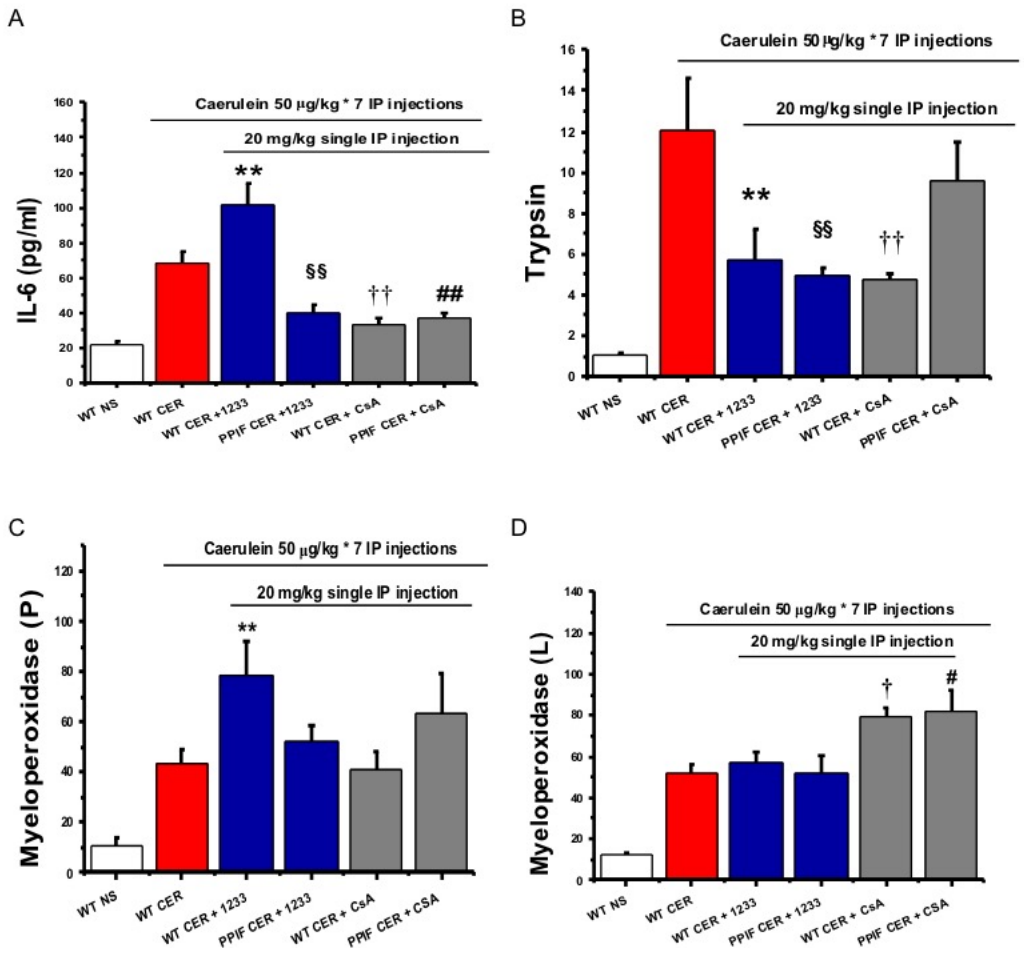

Figure 6.8 Effects of 1233 and CsA local and systemic inflammation with WT and Ppif$^{-/-}$ mice

1233 and CsA at 20mg/kg were administered in 7 hourly caerulein injection induced AP on both WT and *Ppif*$^{-/-}$ mice. Graphs illustrated **(A)** IL-6, **(B)** Trypsin activity, **(C)** Pancreatic MPO and **(D)** lung MPO. **, §§, ††, ## $P<0.01$, †, # $P<0.05$ compared to WT CER -AP group**.** Values are mean ± SEM of 6 mice per group.

Typical pancreatic histopathological changes shown in caerulein treated wild type mice (**Figure 6.9a B1**) with oedema, infiltration and homogeneous distributed necrosis, while *ppif*$^{-/-}$ greatly abolish diffused necrosis, inflammatory infiltration and alleviate the acinar oedema (**Figure 6.9a C1**).

In WT mic, both 1233 (**Figure 6.9a B2**) and CsA (**Figure 6.9a B3**) at 20mg/kg seldom reduce the pathologic pancreatic injury induced necrosis by caerulein, but 1233 appear to increase the inflammatory infiltration. While in *ppif*$^{-/-}$ mice, both 1233 (**Figure 6.9a C2**) and CsA counteract the beneficial that shown with *ppif*$^{-/-}$ alone in caerulein induced injury with slightly better effect under CsA treatment (**Figure 6.9a C3**).

The blinded histopathology scoring (**Figure 6.9b)** showing that *ppif*$^{-/-}$ significantly reduced pancreatic overall, necrosis and inflammatory infiltration scoring, however, both 1233 and CsA exhibit neutralized effect in *ppif*$^{-/-}$ mice received caerulein treatment with CsA showing less offset increase.

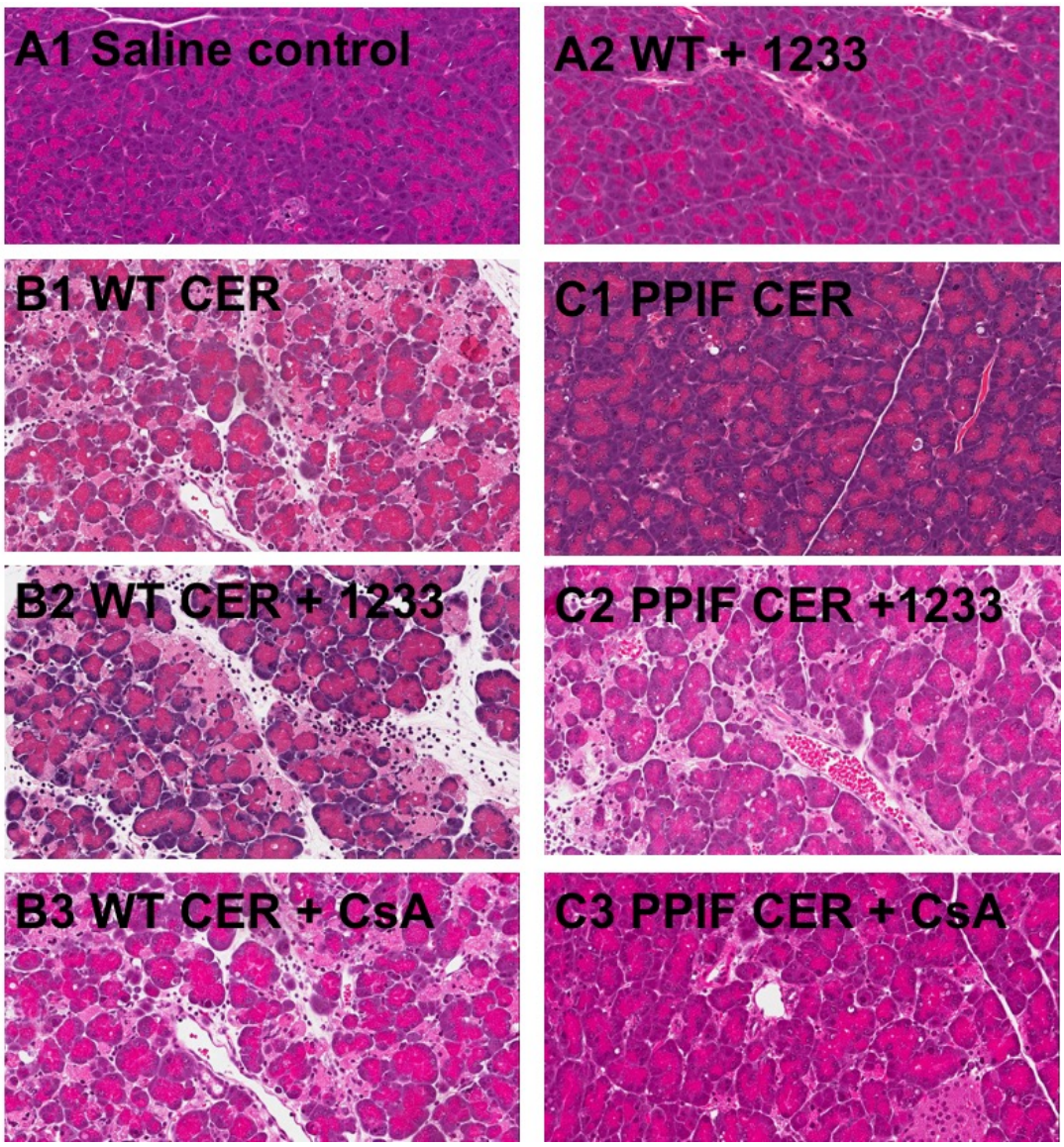

Figure 6.9 (a) Representative images on pancreatic morphology in CER -AP with high dose cyclophilin inhibitors in WT (B) and ppif $^{-/-}$ mice (C)

Mice received 7 hourly i.p injections of caerulein (50 µg/kg), 20 mg/kg SEL1233 or CsA was administered 2 hours after induction and mice were sacrificed at 12 hours after the first injection. Histopathological images were shown in **(A1)** Saline injection, **(A2)** single 1233 injection alone, **(B1)** Caerulein injection in WT mice, **(B2)** Caerulein injection + 1233 20 mg/kg in WT mice, **(B3)** Caerulein injection + CsA 20 mg/kg in WT mice, **(C1)** Caerulein injection in *Ppif*$^{-/-}$ mice, **(C2)** Caerulein injection + 1233 20 mg/kg in *Ppif*$^{-/-}$mice, **(C3)** Caerulein injection + CsA 20 mg/kg in *Ppif*$^{-/-}$ mice. Magnification × 200.

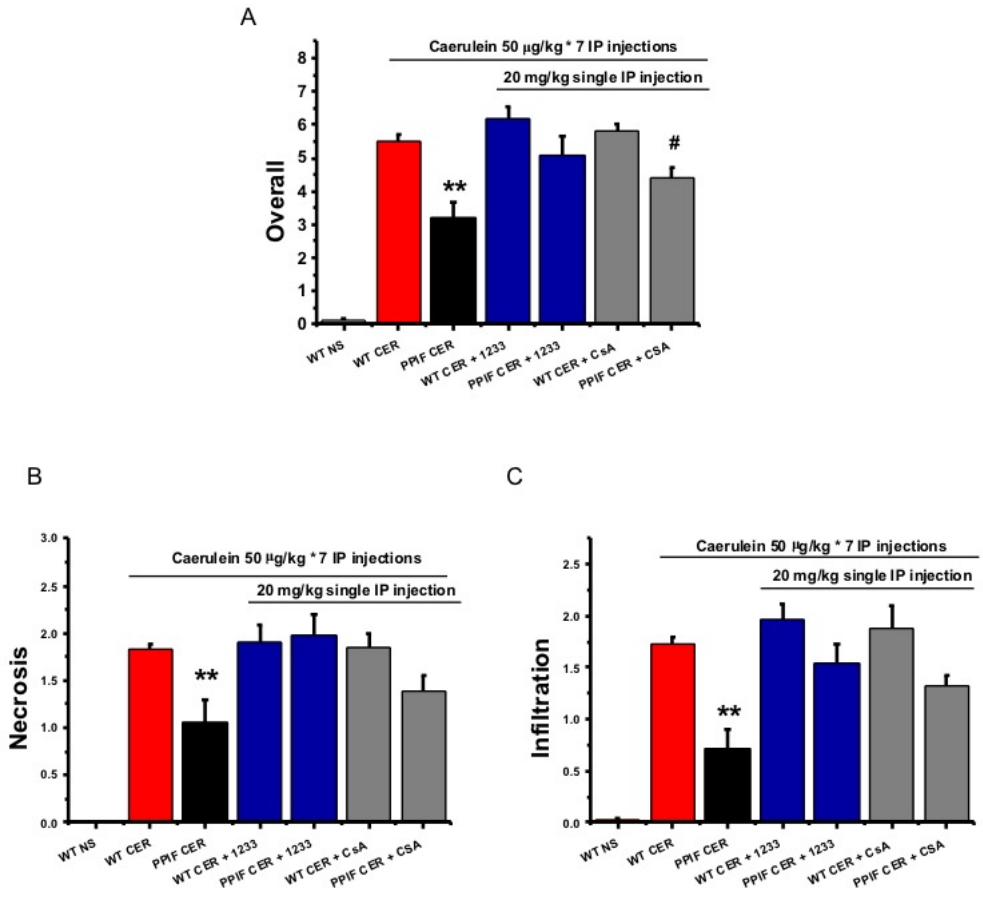

Figure 6.9 (b) Histopathology scoring in CER-AP with high dose cyclophilin inhibitors in WT and ppif$^{-/-}$ mice

Mice received 7 hourly i.p injections of caerulein (50 µg/kg), 20 mg/kg SEL1233 or CsA was administered at 2 hours and mice were sacrificed at 12 hours after the first injection. Histopathological scoring was shown in **(A)** Overall score, **(B)** Necrosis score and **(C)** Infiltration score.

Ppif$^{-/-}$ significantly reduced caerulein induced pancreatic overall, necrosis and infiltration score, both 1233 and CsA at 20mg/kg had no effect on caerulein induced pancreatic injury in WT mice, but counteract the beneficial effects in *Ppif*$^{-/-}$ mice with CsA showing less offset impact. $^{**}P < 0.01$, $^{\#}P < 0.05$, compared to WT CER group, values are mean ± SEM of 6 mice per group.

6.5 Discussion

TLCS-, FAEE- and CER-induced AP models are mechanistically dissimilar but can share a number of biological properties of AP such as prominent serum amylase surge, inflammation and typical histopathologic features such as oedema, necrosis and infiltration, however, due to different pathways that each toxin involves as described in chapter 1, the exact morphology pattern and response to treatment vary.

The pilot experiment described in chapter 4 has shown that unlike in TLCS- induced AP, CsA has a very narrow therapeutic range in FAEE-and CER-AP, with only 2mg/kg or 5mg/kg dosage showed most efficient beneficial improvement, respectively. In the light of these findings that low dosage with CsA which achieved the best effects, the reason that SEL1233 at 20mg/kg does not have any effect on both models firstly may simply attributes to the high dosage that applied in this setting which beyond the therapeutic range. And possibly inhibit other cyclophilins which induced off-target effects such as ER stress. Indeed, both high dose of 1233 and CsA counterbalanced the beneficial effects of CypD knockout in *Ppif*$^{-/-}$ mice. While 1233 has greater affinity on CypD but less immunosuppression compares to CsA, and 1233 showing exacerbation on IL-6 in WT mice but CsA showing exacerbation on trypsin in *Ppif*$^{-/-}$ mice, suggesting a possible role for calcineurin inhibition in anti-inflammation effects. While 1233 effectively reduced trypsin activity through CypD inhibition, lack of immunosuppression lead to effectiveness on IL-6, CsA, however, too powerful to over inhibit other cyclophilins in *Ppif*$^{-/-}$, which could possibly induce further ER stress and ROS production to adversely promote the trypsin activation.

The narrow therapeutic index in both models with CsA, may also suggest that the beneficial acts on extracellular cyclophilins which were massively released upon injury. Compare to the mitochondrial CypD, these extracellular pro-inflammatory like cyclophilins are presumably easy to bind and interact with, in which case, the beneficial effect of CsA in these two models may greatly rely on the anti-inflammation response due to extracellular cyclophilin inhibition, which directly inhibit neutrophil recruitment.

The third explanation for the ineffective 1233 in other 2 models may relate to the vicious solvent PEG400 as shown in Chapter 5 (figure 5.5D and figure 5.6D) that solvents sharing PEG400 induced comparable extra lung myeloperoxidase injury, which on one hand, PEG has been reported to induce pulmonary injury and myeloperoxidase accumulation as mentioned in chapter 5; on the other hand, the solvent may greatly change the structure conformation of compound (information provided by Cypralis), in turn limit the effectively binding with target cyclophilin. The solvent showing more toxic with FAEE-AP is very likely due to the model itself was induced with PEG-based formulation, which doubled the risk to induce more injury. Notably, as the modified FAEE-model showing a transit pulmonary injury reached the highest level at 6h, but gradually recovered after 12h; the present study with 1233 were conducted on 24h scale, the lung injury has already relieved at which time point, while the pancreatic injury reached to the peak at 24h. Thus, the solvent showing a more profound impact on pancreatic MPO but modest effect on lung MPO.

Apart from CypD involved MPTP inhibition, another target of CsA, the NFAT inhibition is also a possible accountable explanation. In a double-deficient for NFATp (c2) and NFAT4 (c3) mice, enlargement of peripheral lymphoid organs, with massive splenomegaly has been observed, revealing disruption of the normal architecture by numerous granulomas and a marked increase in mast cells and eosinophils[471]. In a separate explorative experiment, mice with high dose SEL1233 at 20mg/kg, BID i.p administration regimen for one week also developed the similar splenomegaly phenomenon (data not shown), suggesting that the high dose of SEL1233 can greatly inhibit the NFAT family. Other studies also indicate that CsA at 30mg/kg i.p injection is expected to totally inhibit calcineurin activity in skeletal muscle[392]. Here in pancreas, with SEL1233 at 20mg/kg dosage through intraperitoneal injection is possibly in a large extent blocked the NFAT. It is likely that the transcription factor NFAT regulates a self-defending genetic program to prevent further higher degree damage of PACs, however, a fundamental blockage may in turn lead to detrimental effects that could induce compensatory anti-inflammatory response.

Finally, previously study suggests that in different forms of AP there are significant differences in the epigenetic control of gene transcription contributing to the severity of disease responses, treatment with I-BET-762, an inhibitor of the bromodomain and extra-terminal (BET) protein family significantly reduced biochemical, cytokine and histopathological responses in TLCS- and FAEE-AP, but not CER-AP[472]. The variety and complexity of different pancreatitis forms are huge challenge which requires not only mechanistic but also well designed transcriptional study to facilitate further drug development in pancreatitis.

Despite the effectiveness of CypD preferable SEL1233 in alleviating inflammation in caerulein-mediated pancreatitis, both high dose of SEL1233 and CsA favourably influenced the trypsinogen activation, which in parallel with the view that trypsinogen activation does not appear necessary for either local or systemic inflammation[473].

The partially improved pancreatic histopathological morphology in caerulein treated *Ppif*$^{-/-}$ mice, suggesting that MPTP opening or CypD involved MPTP opening is not the only mechanism that induced the pancreatic injury by caerulein. Most studies suggest that during pancreatitis, intra-pancreatic trypsinogen activation and NF-κB activation, were thought to be two major early independent cellular events, the Intra-acinar trypsinogen activation leads to acinar death which accounts for 50% of the pancreatic damage in AP. However, progression of local and systemic inflammation in AP does not require trypsinogen activation[474]. Studies suggested that early NF-κB activation in acinar cells is a direct response induced by caerulein [475], and might be responsible for progression of AP.

The results obtained with high dose MPTP inhibitors in both models showing a greatly reduction in pancreatic trypsin activity but not local or systemic inflammation, which is not necessarily in disagreement with the view that MPTP inhibition prevents acute pancreatitis, this discrepancy is most likely attributable to a higher dose of pharmacological MPTP inhibition with either CsA or SEL1233 that may affect other early events of pancreatitis due to non-specific inhibition of other cyclophilins other than CypD, especially a number of rapid signalling cascades including NF-*κ*B/Rel activation, which triggers disease-specific inflammatory

processes. This is presumably through inhibition of CypB/C which increase the burden for protein folding, aggregating ER stress, and finally lead to cell death and consequently further inflammation through already activated NF- κB in early stages of pancreatitis.

The better effect observed with CsA compare to SEL1233 in *Ppif*$^{-/-}$ mice may link to the anti-inflammatory effects of CsA which inhibits the calcineurin activation and extracellular CypA actions on neutrophils to prevent inflammation. As a powerful immunosuppressant, of 25 natural cyclosporins and some 750 analogues prepared in the laboratory none have shown, *in vitro*, indications of greater pharmacological activity than that of CsA[476]. This powerful immunosuppressant, however, due to its non-specificity, when apply at high dose, possibly further increases ER stress, and the anti- inflammatory effects of calcineurin inhibition are largely compromised.

CHAPTER 7

Genetic and Pharmacological CypD inhibition in chronic pancreatitis (CP)

7.1 Summary

The well characterized repetitive caerulein model of CP was used to examine the therapeutic efficacy of genetic and pharmacological MPTP inhibition *in vivo*. Both genetic MPTP inhibition with CypD ablation or pharmacological cyclophilin inhibition with SCY-635/CC-4635 proved to be protective in the development of repetitive caerulein induced chronic pancreatitis shown better reserved pancreatic function with acinar cell and enzymatic content protection, less collagen deposition.

CypD inhibition also accelerates the recovery of acinar cell, possible due to its role in cell proliferation. However, deletion of CypD had less consistent effects on PSC activation, suggesting a rather indirect effect based on cell protection of reducing the extent of cell death and collagen production or degradation.

Despite the non-immunosuppressive analogue SCY-635/CC-4635 avoid the possible profibrotic signalling cascades activated by calcineurin, the nonspecific inhibition of cyclophilin A may remain a potential interferer which could possibly limit the beneficial effects of CypD inhibition.

7.2 Introduction

Previous studies demonstrate targeting MPTP inhibition reduce necrotic cell death activation in pancreatic acinar cell, showing potent beneficial as therapeutic treatment for AP. With increasing evidence suggesting a continuum of acute, recurrent and chronic in pancreatitis, based on the necrosis-fibrosis theory that inflammation and necrosis from repeated episodes of AP lead to scarring and tissue fibrosis with ductal obstruction[477], it is hypothesized (chapter 1) that CypD

inhibition also plays a role in the development of CP through alleviating necrosis, inflammation from AP episodes to reduce following acinar cell atrophy, tissue remodelling and fibrosis.

CsA as the famous cyclophilin inhibitors has been shown great beneficial in reducing necrosis in MPTP involved diseases, and with adequate dosing regimen effectively improved acute pancreatitis as demonstrated in chapter 4, which could be a choice for the possible treatment. However, CsA has long been reported to exert a profibrotic action correlated with TGF-β1 upregulation[478, 479] and shown to greatly distort pancreatic repair, transforming caerulein induced pancreatitis into a fibrotic chronic-like disease[480], which has paradoxically been used to induce models of CP. These studies, however, were mostly employed CsA administration at 15-20 mg/kg by daily subcutaneous or intraperitoneal injection for at least 2 weeks using olive oil or ethanol as vehicle. Emerging data suggests that the profibrotic action of CsA is due to calcineurin inhibition or high dose CsA administration induced ER stress, which facilitate the development and application of a large quantities of non-immunosuppressive CsA analogue products such as NIM811, DEB025 and SCY-635. Indeed, on the contrary, far from proposing that CsA may promote fibrosis, studies with CsA at low does or non-immunosuppressive analogue NIM811 /DEB025 treatment significantly reduced fibrosis or TGF- β1 expression and collagen synthesis either *in vitro* HPCs[421, 422] or *in vivo* multiple liver fibrosis model [419, 423] and muscular dystrophic model [315, 392, 426] as mentioned in chapter 1. Under such condition, it was worthwhile to test both genetic and pharmacological cyclophilin inhibition in chronic pancreatitis to further validate this strategy.

Within CsA structure, residues 4 through 7, on the opposing face of the molecule, constitute the calcineurin binding domain. Chemical modification in these residues can produce dramatic effect on the biological activity of immunosuppression with CsA[412]. Similar to DEB025, SCY-635 differs from CsA at residues position 3 and 4 (**Figure 7.1**), containing a dimethylamino-ethylthio substituent at the 3-sarcosine alpha carbon atom and a hydroxyl substituent at the gamma carbon of the 4 N-methyl leucine residues, which makes SCY-635 a novel non-immunosuppressive cyclosporin-based analogue. It has been clinically tested for hepatitis C and progressed to phase II clinical trial with no evidence of dose-limiting clinical or laboratory toxicity was identified at any dose level. Without any modification on cyclophilin binding residues, SCY-635 retains the ability to efficiently inhibit the peptidyl prolyl isomerase activity at nanomolar concentrations and showed no detectable inhibition of calcineurin phosphatase activity at concentrations up to 2 μM[414, 481, 482].

SCY-635/CC-4635 has never been tested before in fibrotic diseases, however, in respect to its similar biological activity and good oral bioavailability (**Figure 7.2**) compare to CsA and DEB025, which warrants SCY-635 further investigation as a novel therapeutic agent for the treatment of CP.

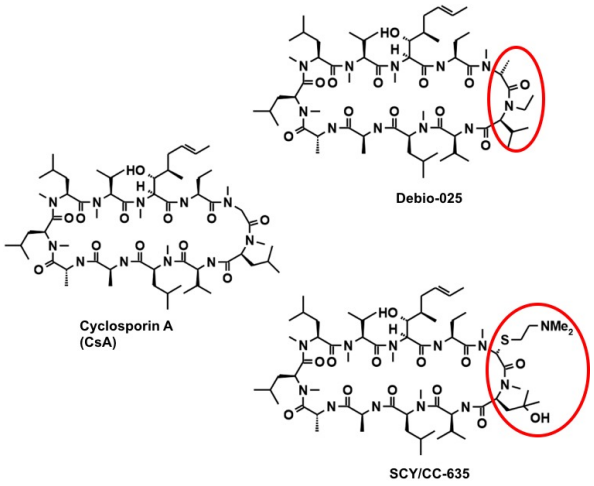

Figure 7.1 Structure comparison of CsA, DEB025 and SCY- 635

Chemical structures of CsA, DEB025 and SCY-635. SCY-635 differs from CsA at two positions. The alpha carbon atom of sarcosine at position 3 contains the dimethylamino-ethylthio substituent. The gamma carbon atom of the N-methyl leucine at position 4 contains a hydroxyl group.

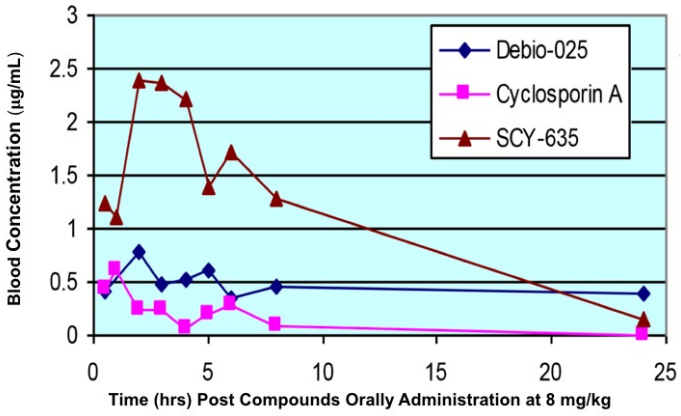

Figure 7.2 Bioavailability comparison of CsA, DEB025 and SCY-635

SCY-635 concentrations in blood showing a better bioavailability compare to CsA and DEB025 following oral delivery at 8 mg/kg in mice (provided by Cypralis). Following oral administration, SCY-635 was well absorbed into the systemic circulation. Maximum blood concentrations were observed around 4hrs in rodents.

To prove the hypotheses, this study was designed to test the effects of both genetic and pharmacologic CypD inhibition with recurrent AP episodes developed chronic pancreatic injury by using repetitive caerulein injections, which mimics the natural progression from acute to recurrent and finally developed chronic pancreatitis. In addition, to examine the effects of CypD inhibition on pancreatic regeneration after recurrent pancreatitis, mice were allowed to recover for another two weeks following the last caerulein injection.

7.3 Methods

7.3.1 Genetic CypD inhibition in CP

Repetitive intraperitoneal caerulein injections (50 μg/kg) was employed thrice weekly for 2 to 4 consecutive weeks as previously described in chapter 2 (**Figure 7.3**). Adult CypD knockout and age/sex matched wild type C57BL/6J mice were randomly divided into 8 groups: (1-2) control group with saline injections for 2 or 4 weeks in WT mice, (3-4) CP group with caerulein injection in WT mice for 2 or 4 weeks, (5-6) CP group with caerulein injection in *Ppif*$^{-/-}$ mice for 2 or 4 weeks, (7-8) CP group in WT or *Ppif*$^{-/-}$ mice with caerulein injection for 4 weeks plus 2-week recovery. Mice were sacrificed 3 days after the last caerulein injection by CO_2 asphyxia. Blood and tissue sample were collected for further assay and staining as described in chapter 2.

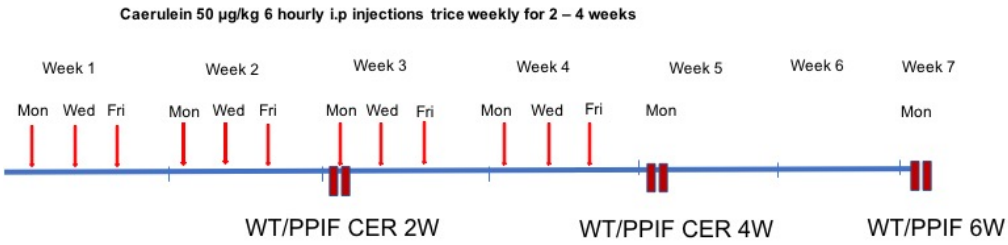

Figure 7.3 Time scale for effects of CypD ablation in CP

7.3.2 Pharmacological cyclophilin inhibition in CP

Repetitive intraperitoneal caerulein injections (50 µg/kg) was employed thrice weekly for 2 weeks as previous described in chapter 2. Male adult C57BL/6J mice were randomly divided into 4 groups: (1) control group with saline injections for 2 weeks, (2) CP group with caerulein injection for 2 weeks, (3) CP group with caerulein injection plus solvent injection (10% cremophor dissolved in saline with 1% DMSO) for 2 weeks, (4) CP group with caerulein injection plus twice daily 2mg/kg SCY-635 (CC-4635) i.p injections for 2 weeks. Mice were sacrificed 3 days after last caerulein injections, blood and tissue were collected for further assay and staining as described in chapter 2.

7.4 Results

7.4.1 Effects of *Ppif*$^{-/-}$ in chronic pancreatic morphology

In the normal pancreas of WT (**Figure 7.4 A0**) and *Ppif*$^{-/-}$ mice (**Figure 7.4 B0**) with saline injections, the acinar units were tightly packed (**Figure 7.4 A0**), whereas when subjected to repetitive AP episodes for 2weeks, WT mice developed abnormal architecture including prominent dilated intra-acinar luminal (DL) and acinar duct metaplasia (ADM), tubular complexes, accompanied with more fibrosis accumulation (**Figure 7.4 A1**) compared to *Ppif*$^{-/-}$ mice (**Figure 7.4 B1**). With

sustained caerulein challenge for another 2 weeks, a marked morphologic change in the pancreas evident at 4 weeks showing typical histopathological feature of CP with massive atrophied acinar area and acinar cell loss, closely proximate islets, ducts and vascular structures, increased cellularity of the peri-acinar stroma at the edges of lager lobules, inflammatory infiltration and acinar cell vacuolization also developed in WT mice (**Figure 7.4 A2**), whereas deletion of CypD still maintain most of the acinar cell areas in the ensuing 2 weeks with less fibrosis content (**Figure 7.4 B2**). Following another 2-week caerulein withdraw period, pancreata in both WT (**Figure 7.4 A3**) and *Ppif*$^{-/-}$ mice (**Figure 7.4 B3**) had almost complete recovery with reformed acinar cell architecture, while localised replacement with fat tissue and fibrotic foci could observed only in WT mice.

Trichrome staining (**Figure 7.5**) with blue colour shown intensive peri-acinar fibrosis at 2weeks and large amount of fibrosis at intra- and inter-lobular and interstitial space in WT mice compare to *Ppif*$^{-/-}$ mice.

Pancreata/body weight ratio is used to quantify pancreatic gland atrophy, as shown in **Figure 7.6**, the ratio decreased after 4-week caerulein treatment in both WT and *Ppif*$^{-/-}$ mice, but recovered thereafter when caerulein treatment disseised with more regain on *Ppif*$^{-/-}$ mice.

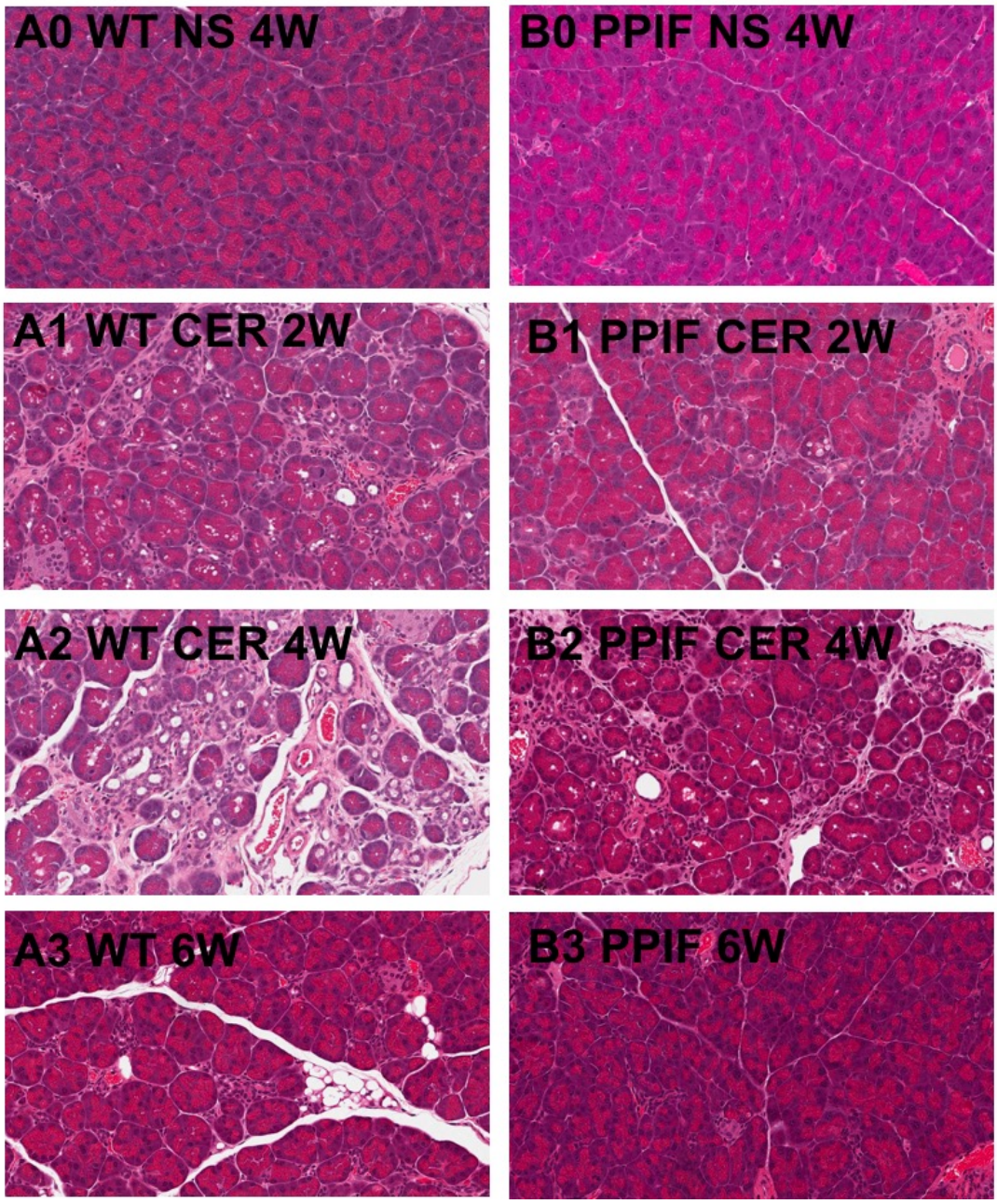

Figure 7.4 Representative pancreatic morphology in WT and Ppif$^{-/-}$ mice with repetitive caerulein injection

WT**(A)** and *Ppif*$^{-/-}$ **(B)** mice received 6 hourly caerulein or saline injection every Mon, Wed and Fri up to 4 weeks. Sample were collected at 2 **(1)**, 4 **(2)**, and 6 **(3)** weeks after the first caerulein or saline injection. Typical histopathological features of CP shown in WT mice at 4weeks with acinar cell loss, acinar duct metaplasia (ADM), fibrosis accumulation, etc **(A2)**. Magnification: x 200

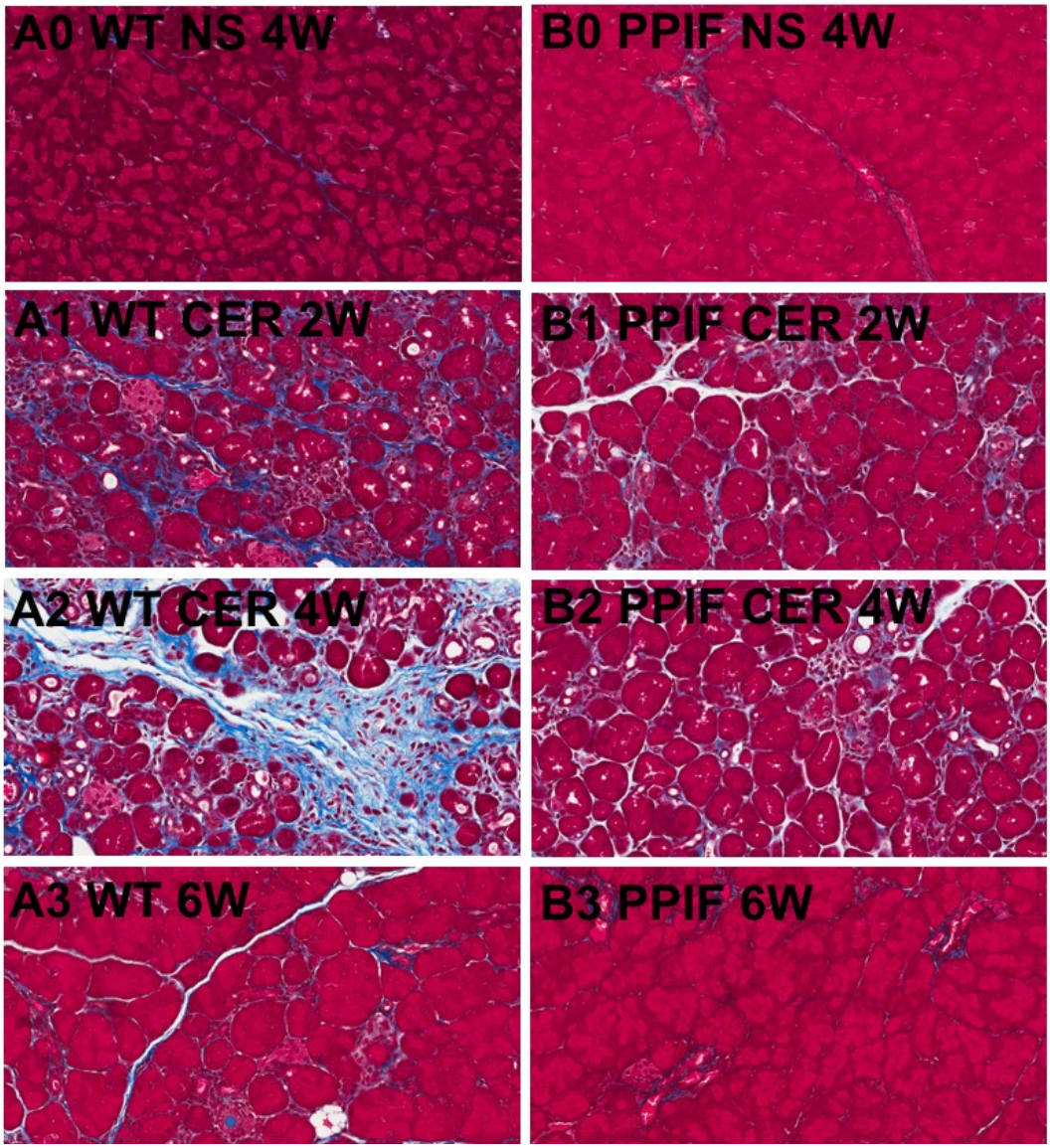

Figure 7.5 Visualisation of fibrosis in pancreatic morphology (Trichrome)

WT**(A)** and Ppif$^{-/-}$ **(B)** mice received 6 hourly caerulein or saline injection thrice weekly for 4 weeks. Sample were collected at 2**(1)**, 4 **(2)**, and 6 **(3)** weeks after the first injection. Fibrosis deposition shown in blue colour extensively accumulated in peri-acinar, interlobular and interstitial parts throughout whole exocrine pancreas in 4-week WT mice compare to *Ppif*$^{-/-}$. Both wild and *Ppif*$^{-/-}$ type had partially recovered deposition after 2 week caerulein withdraw period. Magnification: x 20**.**

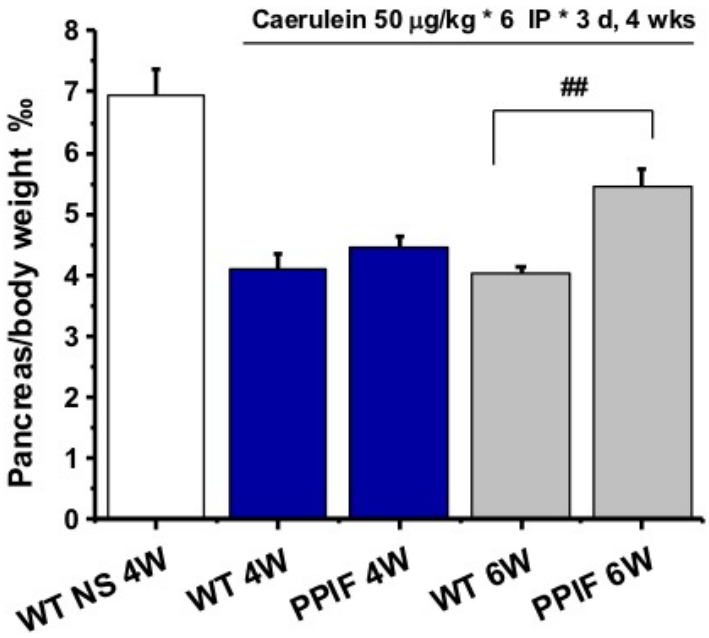

Figure 7.6 Effects of genetic MPTP inhibition on pancreatic/body weight

Mice received six i.p injections of either saline or 50 µg/kg caerulein every Mon, Wed and Friday for 4 weeks, sample were collected at 4 or 6 weeks after first injection. **(A)** pan/body weight ratio **(B)** trypsin activity at 4 or 6wk after first injection.

$^{\#\#}P < 0.01$, WT compared to *Ppif*$^{-/-}$ mice at 6 weeks.

Values are mean ± SEM of 6 mice per group.

7.4.2 Effects of *Ppif*$^{-/-}$ in pancreatic fibrosis

Sirius red stained normal pancreas, connective tissue was localized primarily around ducts and small blood vessels with thin strands extending between larger lobules (**Figure 7.7 A0**), while sustained caerulein challenge induced massive collagen deposition observed in peri-acinar and intra-/inter-lobular areas throughout the exocrine gland in WT mice (**Figure 7.7**). Further quantification with image J suggested that in mice treated with repetitive caerulein, the relative collagen deposition was sharply increased by week 2 in both mice type with much higher proportion in WT mice, and the deposition continued to elevate for the remainder of the treatment, whereas only subtle increase observed for collagen deposition in *Ppif*$^{-/-}$ mice after first 2 weeks (**Figure 7.7**).

The collagen induced cytokine TGF-β1 level was quantified by ELISA, showing markedly increase follow recurrent caerulein treatment in both wild and CypD knock out group. *Ppif*$^{-/-}$ mice however, significantly reduced TGF-β1 secretion level compare to wild type at 2 weeks and 4 weeks point. After a further 2-week recovery period without caerulein stimulation, the TGF-β1 level dropped back with no difference between each other group (**Figure 7.8**).

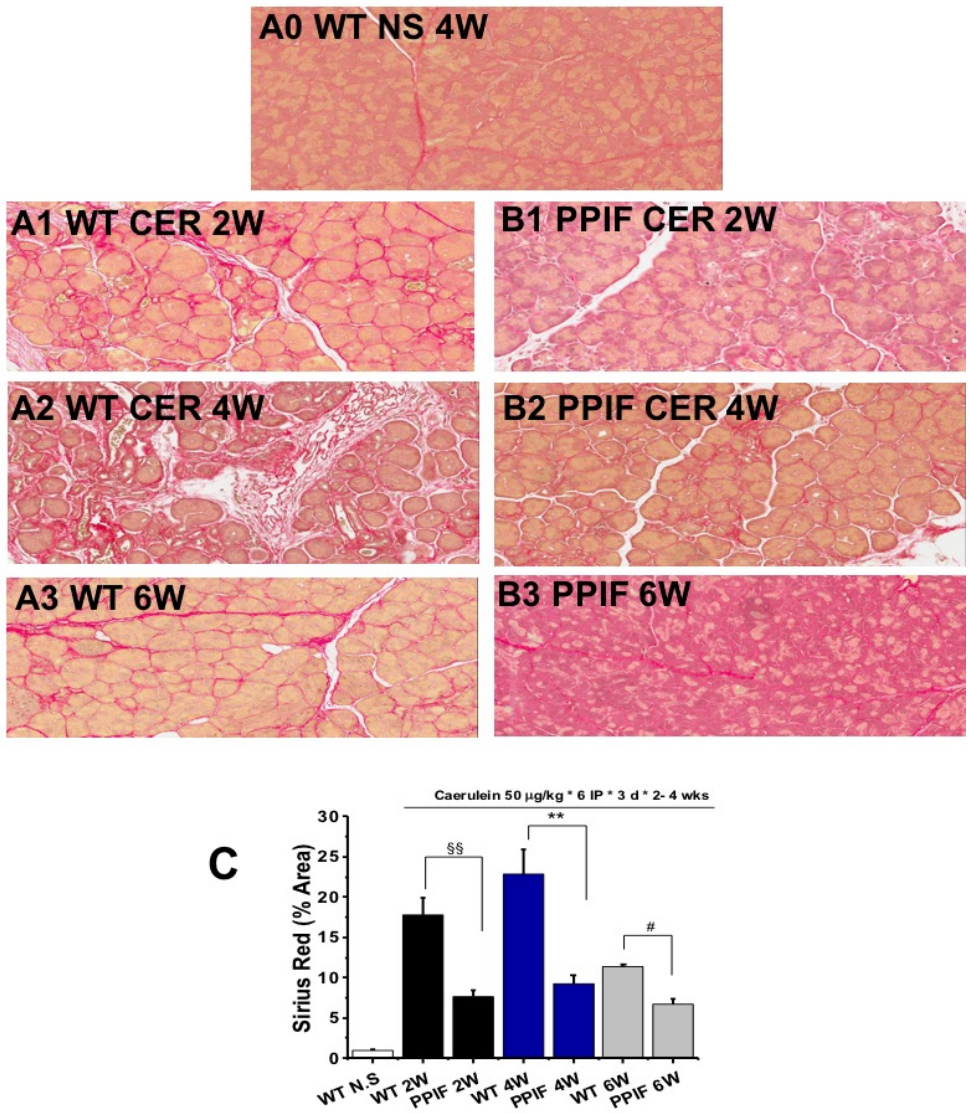

Figure 7.7 Visualisation of fibrosis in pancreatic morphology (Picro Sirius Red)

WT**(A)** and *Ppif*$^{-/-}$ **(B)** mice received 6 hourly caerulein or saline injection thrice weekly up to 4 weeks. Sample were collected at 2 **(1)**, 4 **(2)**, and 6 **(3)** weeks after the first injection. **(C)** Fibrosis deposition quantification shown significant higher accumulation in 2- and 4-week WT mice compare to *Ppif*$^{-/-}$. Both wild and *Ppif*$^{-/-}$ type had partially recovered deposition after 2 week caerulein withdraw period. Magnification: x 200**.** $^{\#}P<0.05$, §§, $^{**}P<0.01$ compare to *Ppif*$^{-/-}$ mice at same time point, Values are mean ± SEM of 6 mice per group.

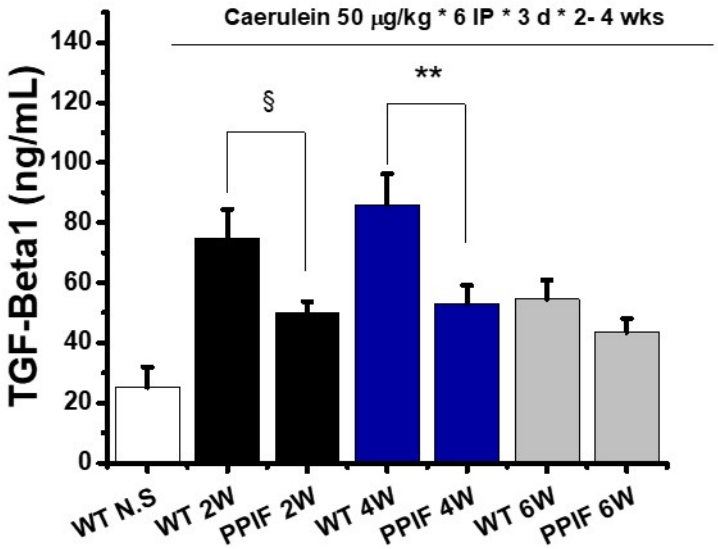

Figure 7.8 Serum TGF-β1 quantified by ELISA

WT and *Ppif*$^{-/-}$ mice received 6 hourly caerulein or saline injection thrice weekly up to 4 weeks. Sample were collected at 2, 4 and 6 weeks after the first injection. Serum TGF- β1 quantification shown marked increase in wild type mice, *Ppif*$^{-/-}$ mice significant reduced serum TGF- β1 level compared to wild type in 2- and 4-week WT mice. $^{\S}P<0.05$, $^{**}P<0.01$ compare to *Ppif*$^{-/-}$ mice at same time point. Values are mean ± SEM of 6 mice per group.

7.4.3 Effects of *Ppif*$^{-/-}$ on reserved pancreatic enzymatic function

After challenge with repetitive AP episode for 4 weeks, WT mice showing significantly reduced secretion of serum amylase in response to pancreatic injury compare to *Ppif*$^{-/-}$ mice. Even with further 2 weeks' recovery, amylase secretion level remains statistically lower compare to *Ppif*$^{-/-}$ mice **(Figure 7.9 A)**.

Similarly, both WT and *Ppif*$^{-/-}$ mice showing markedly reduced pancreatic reserved amylase following 4-week AP episodes, however, CypD depletion significantly protected reserved amylase with 50% higher level than WT mice. Both groups regain reserved enzymatic level after discontinued AP episodes **(Figure 7.9 B)**.

Deletion of CypD showing amplified trypsinogen activation response following repetitive AP challenge, while WT mice barely have any reserved trypsinogen capacity for activation in response to caerulein acinar (**Figure 7.10 A**). Similar with trypsin activity, deletion of CypD rather than reduce pancreatic lipase, but promote upregulation of lipase accumulated in pancreas at 2 and 4 weeks (**Figure 7.10 B**). Pancreatic/body weight ratio was significantly reduced after repetitive AP episodes in both WT and *Ppif*$^{-/-}$, showing no difference at 4-week period.

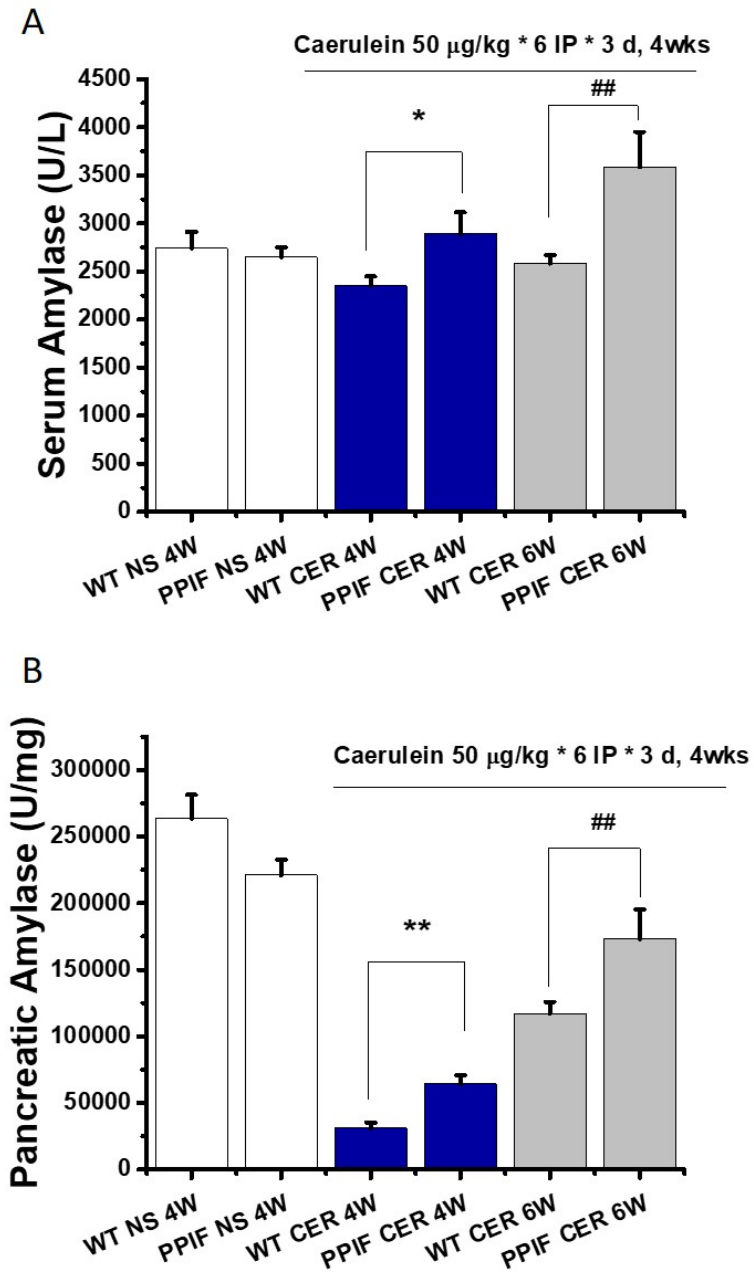

Figure 7.9 Effect of genetic MPTP inhibition on amylase

Mice received six i.p injections of either saline or 50 µg/kg caerulein every Mon, Wed and Friday for 4 weeks, sample were collected at 4 or 6 weeks after first caerulein injection. **(A)** Serum amylase and **(B)** pancreatic amylase at 4 or 6wk after first injection. *$P < 0.05$, **, $^{\#\#}P < 0.01$, 4-or 6-week wild type compared to *Ppif*$^{-/-}$ group. Values are mean ± SEM of 6 mice per group.

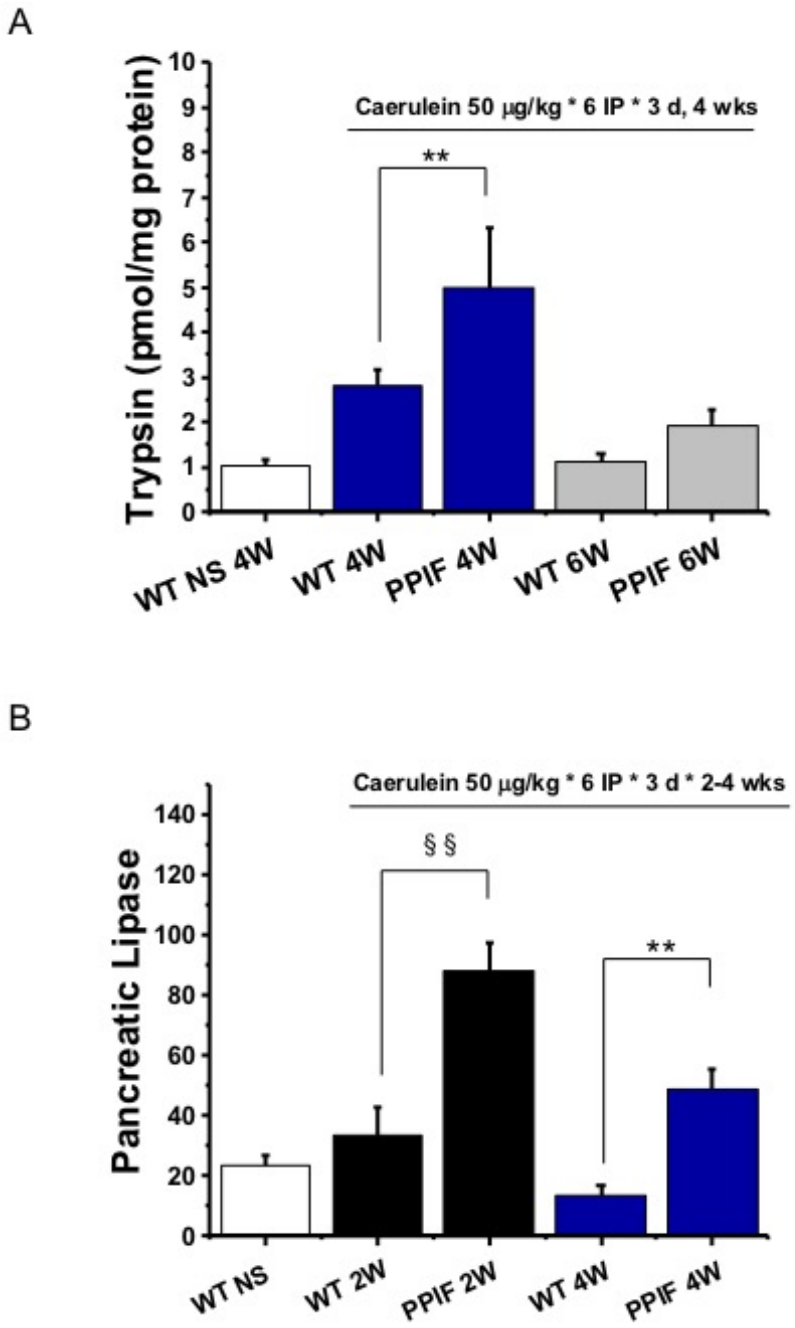

Figure 7.10 Effect of genetic MPTP inhibition on trypsin and lipase function

Mice received six i.p injections of either saline or 50 µg/kg caerulein every Mon, Wed and Friday for 2-4 weeks, samples were collected at 2, 4 or 6 weeks after first caerulein injection. §§, $^{**}P < 0.01$, 2 or 4 weeks wild type compared to *Ppif*$^{-/-}$ group. Values are mean ± SEM of 6 mice per group.

7.4.4 Effects of *Ppif*$^{-/-}$ in PSCs activation

Immunohistochemistry staining for α-SMA, the activation marker of PSC, both WT mice and *Ppif*$^{-/-}$ mice showing compatible PSCs activation status following 2- or 4-week caerulein treatment (**Figure 7.8**), with no significant difference (data not shown) as quantified with image J, using a method previously described[483].

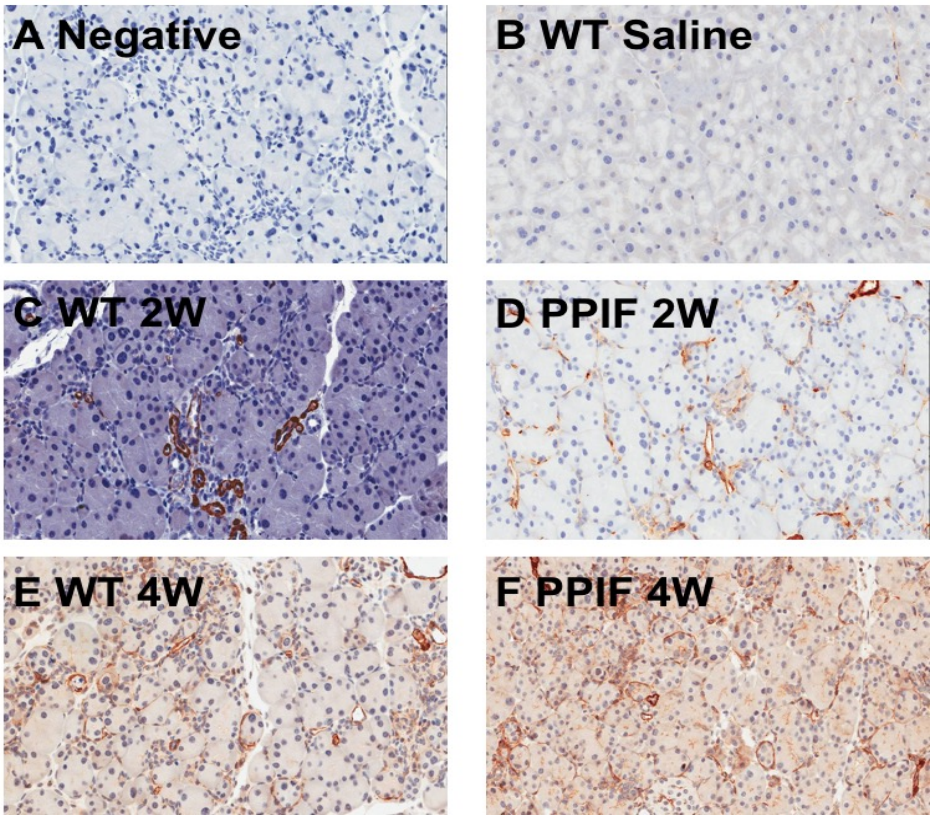

Figure 7.11 Effect of genetic MPTP inhibition on α-SMA

Mice received 6 i.p injections of either saline or 50 μg/kg caerulein every Mon, Wed and Friday for 4 weeks, sample were collected at 2 or 4 weeks after first injection. α-SMA expression at 2 or 4 weeks after first caerulein injection.

7.4.5 Effects of SCY-635/CC-4635 inhibition in CP

Following 2-week repetitive AP episodes induced by caerulein, all groups with recurrent caerulein injection developed acinar cell loss (**Figure 7.12**), structure alteration accompanied with peri-acinar, and substantial interstitial collagen deposition (**Figure 7.13 B, D**). Though without statistical significance, the quantification with image J showed that SCY-635/CC-4635/CC635 group exhibited around 18% reduction on collagen deposition compare to compound untreated group (**Figure 7.13 E**).

Despite unimpressive results on morphology and fibrosis, the enzymatic level with CC-4635 treatment, however, showed significant improvement on both circulating (**Figure 7.14 A**) and reserved amylase (**Figure 7.14 B**) compared to untreated group after 2-week caerulein episodes. Unlike Amylase, enzymatic assay for secreted lipase showed an increase with caerulein injection, but presenting less increase with SCY-635/CC-4635 administration (**Figure 7.15 A**), No significant difference between CP and CC-4635 treated group for pancreatic lipase level (**Figure 7.15 B**). The activation of PSCs shown as α-SMA expression, however, exhibited a trend with less expression implicates less activated PSCs in CC-4635 treated group suggested by preliminary results following positive cell grading scoring (**Figure 7.16**), further image analysis is currently ongoing by independent investigators.

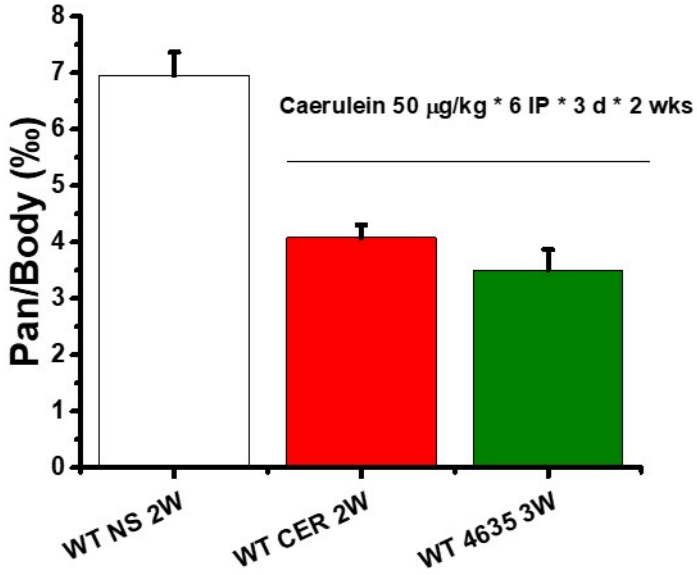

Figure 7.12 Effect of CC-4635 on pan/body weight

Mice received 6 i.p injections of either saline or 50 μg/kg caerulein every Mon, Wed and Friday for 2 weeks, sample were collected at 2 weeks after first injection.

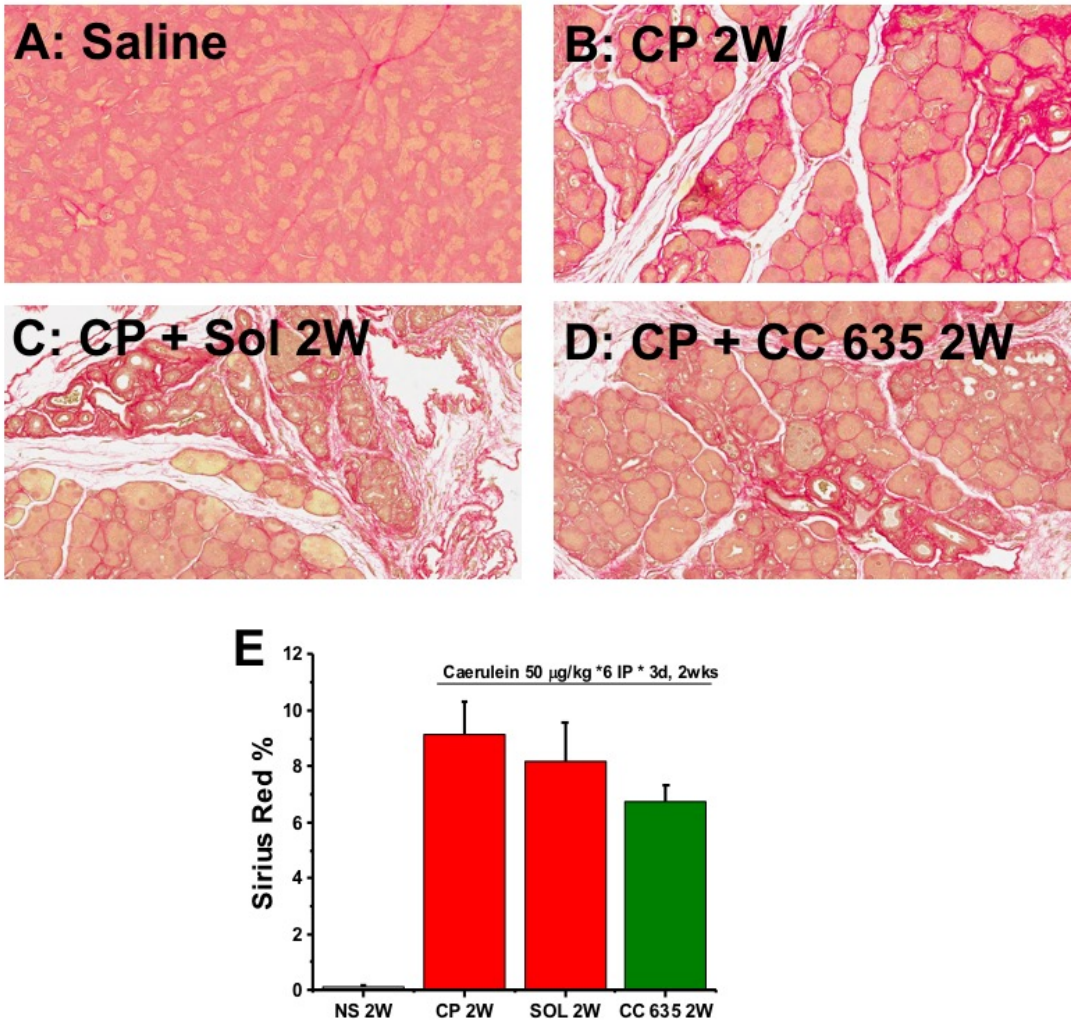

Figure 7.13 Effect of CC-4635 on collagen deposition

Mice received six i.p injections of either saline or 50 µg/kg caerulein every Mon, Wed and Friday for 2 weeks, sample were collected at 2 weeks after first injection. CC-4635 showing capacity (18% reduction) to reduce collagen deposition compare to untreated group following 2-week repetitive caerulein injections, shown in fibrosis visualization of 4 groups with **(A)** saline control, **(B)** caerulein injection, **(C)** caerulein plus solvent and **(D)** caerulein plus CC-4635 treatment and **(E)** collagen deposition quantification with image J expressed as percentage of the total area. Values are mean ± SEM of 6 mice per group.

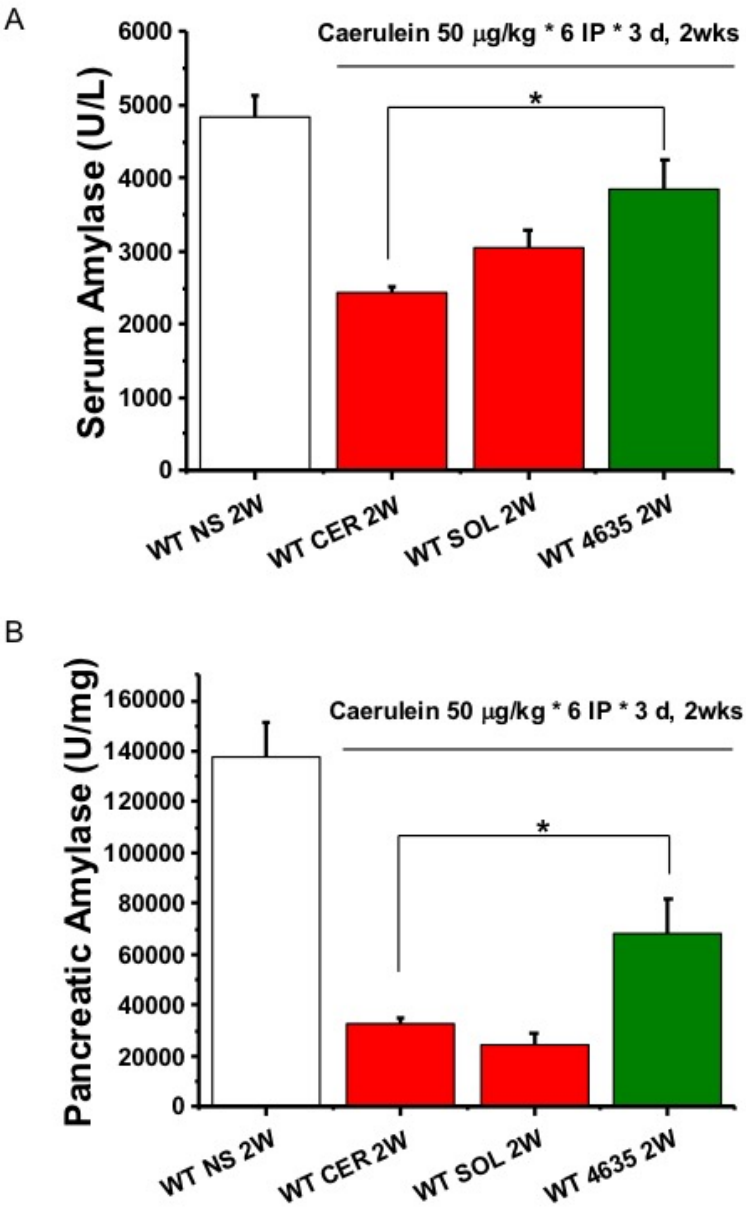

Figure 7.14 Effect of CC-4635 on amylase

Mice received six i.p injections of either saline or 50 μg/kg caerulein every Mon, Wed and Friday for 2 weeks, sample were collected at 2 weeks after first injection. **(A)** saline control, **(B)** caerulein injection, **(C)** caerulein plus solvent and **(D)** caerulein plus CC-4635 treatment**.** CC-4635 treated group showing statistically improvement of either circulated or reserved amylase content compare to untreated group. *$P < 0.05$, 2 weeks wild type with CC-4635 treatment compared to untreated group. Values are mean ± SEM of 6 mice per group.

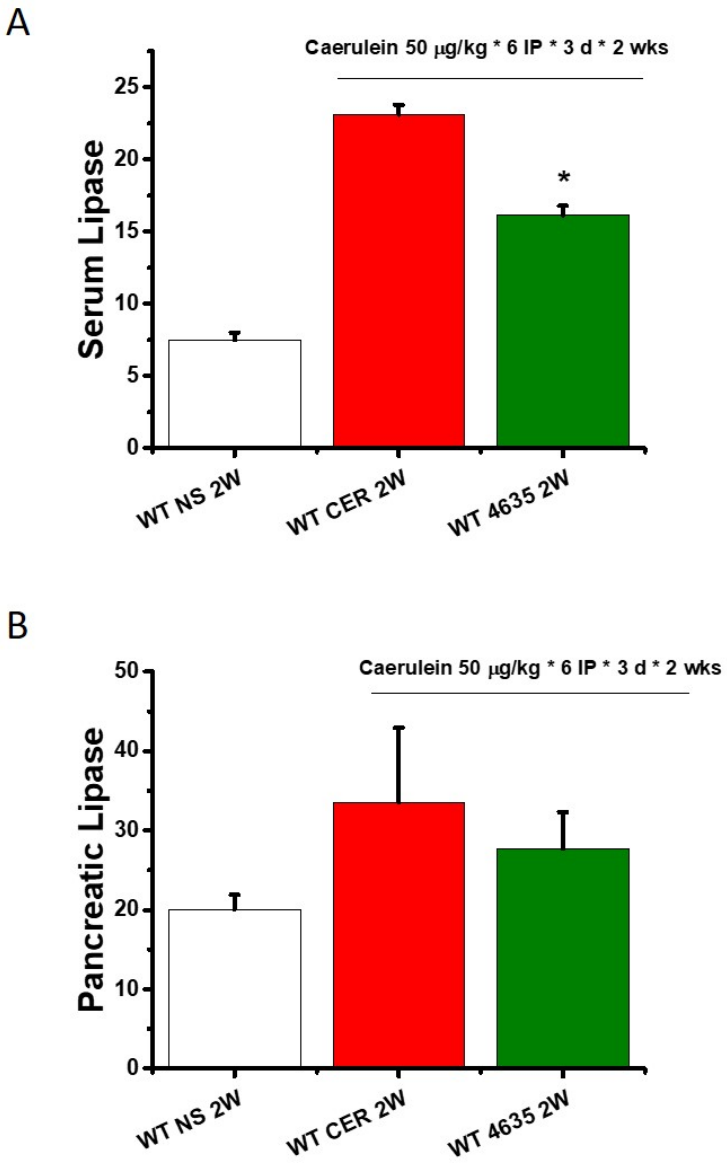

Figure 7.15 Effect of CC-4635 on lipase

Mice received six i.p injections of either saline or 50 μg/kg caerulein every Mon, Wed and Friday for 2 weeks, sample were collected at 2 weeks after first injection. **(A)** saline control, **(B)** caerulein injection, **(C)** caerulein plus CC-4635 treatment**.** CC-4635 treated group showing statistically improvement of secreted lipase, but no difference with reserved lipase content compared to untreated group. *$P < 0.05$, 2-week wild type with CC-4635 treatment compared to untreated group. Values are mean ± SEM of 6 mice per group.

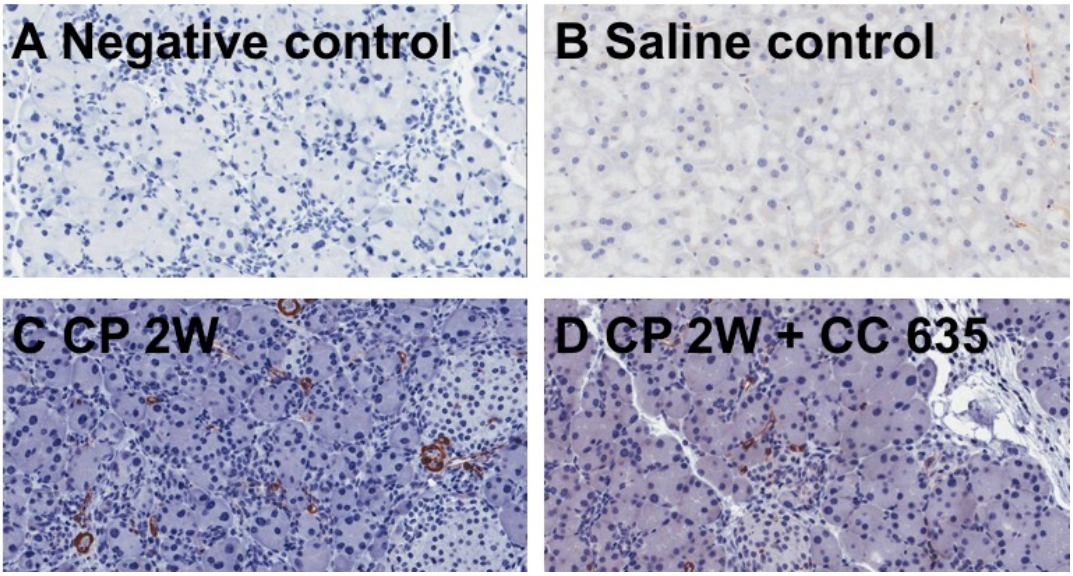

Figure 7.16 Effect of CC-4635 on α-SMA expression

Mice received 6 i.p injections of either saline or 50 μg/kg caerulein every Mon, Wed and Friday for 2 weeks, sample were collected at 2 weeks after first injection. CC-4635 treated group showing less α-SMA expression trend (+) compared to CP group (++) suggested by preliminary grading quantification scored by investigator, further fully image analysis will be conducted by 2 independent investigators.

7.5 Discussion

Mitochondria dysfunction resulting in necrotic cell death and profound inflammation in AP, which sensitize pancreas to repeated episodes of AP, RAP further lead to sustained PACs injury, followed by release of pro-inflammatory mediators that promote both immune cell infiltration and activation of PSCs. Upon activation, PSCs promote inflammation and fibrosis through secretion of cytokines and chemokines[427].

Although pancreatic acinar cell atrophy, inflammatory cell infiltration, and fibrosis after repetitive episodes of AP were observed in both WT and *Ppif*$^{-/-}$ mice, these pancreatic damages manifested a more severe degree in WT mice, suggesting MPTP partially improved pancreatic morphology and function impairment in chronic pancreatitis.

PSCs is the central cell that responsible for fibrosis, which in normal pancreas, locates in periacinar or periductal spaces with minimal proliferation. Upon pancreatic injury, in response to cytokines, PSCs activated and transformed to myofibroblast-like cells with proliferation and upregulation of α-SMA, and produce abundant ECM such as collagen[484]. The current study, however, present results with unaffected PSC activation in *Ppif*$^{-/-}$ mice, but reduced TGF-β1 expression and significantly reduced collagen deposition level. Study showed that MPTP is involved in collagen IV related muscular disease[485], suggesting common signalling pathway linking cell ECM interactions and mitochondria function. It is possible that MPTP inhibition doesn't directly acts on the activation of PSC, but may indirectly impact the synthesis and production of ECM or MMPs showing less produced or far

more degraded ECM to maintain the balance and homeostasis between ECM production and degradation state, this is also likely to connected with the reduced cell death relevant cytoprotection and less inflammation that decrease the expression of TGF- β1, which, at some point, explained the partially but not fully abolished improvement in chronic pancreatitis.

The decreased circulating enzyme level in CP due to chronic inflammation and fibrosis can reflect the atrophy extent of PACs, which is responsible for synthesis and secretion of enzymes[484]. In *Ppif*$^{-/-}$ mice the relatively well reserved pancreatic morphology and enzymatic level indicates that MPTP inhibition could protect architecture and function of acinar cell against repetitive caerulein induced sustainable acinar cell damage.

Pancreatitis in humans and animal models appear to recover via regeneration of acinar cells. This regenerative process involves transient phases of inflammation, metaplasia and redifferentiation, driven by cell-cell interactions between PACs, leukocytes and PSCs. Imbalances between these pro-inflammatory and pro-differentiation pathways contribute to chronic pancreatitis[484]. Better capacity for pancreatic mass regain during recovery period shown in *Ppif*$^{-/-}$ mice also implicates that instead of fibre remodelling, with highly plasticity degree of acinar cell, during prolonged caerulein treatment, WT pancreatic acinar cell loses the polarity and typical function to synthesize and secret enzyme such as amylase, but gain markers of ductal and progenitor cells, while MPTP inhibition maintains the morphology and function of acinar cell with highly preserved amylase against acinar cell loss through

resistant to cell death, accelerate and facilitate the proliferation and regeneration of acinar cell during recovery period.

Unlike the pattern with amylase, on the other hand, both pancreatic trypsin and lipase activity showing an amplified increase in *Ppif*$^{-/-}$ mice compare to WT type. It is possible that 1) in response to recurrent caerulein injections, the *Ppif*$^{-/-}$ mice over-reacted to the toxins to initiate moderate inflammation, as sustained anti-inflammatory reaction drives pancreatic promote healing process and the subsequent fibrosis, the over-reactive response may maintain *Ppif*$^{-/-}$ to retain in self-limited acute pancreatitis, damper the following tissue remodelling, acinar cell differentiation, and ECM deposition. 2) Or simply due to constantly regeneration of PACs in response to caerulein treatment, through synthesis or cell proliferation, as reported by Tavecchio[486] that CypD regulates cell cycle progression, knock down of CypD resulted in faster and more stained transition into S-phase. results in increased cell proliferation. Studies also pointed out that mitochondria calcium played a role in liver regeneration after partial hepatectomy[487], and CsA non-immunosuppressive analogue NIM811 stimulated liver regeneration by inhibiting CypD[424].

Despite the paradox that CsA showing irreversible profibrotic action synergistically with caerulein in most studies with higher concentration or dosages, the non-immunosuppressive CsA analogue SCY-635/CC-4635 with a low does at 2mg/kg twice daily i.p injection in present study was shown to protect against pancreatic exocrine function and modest reduction on fibrosis, which is in parallel with previous studies apply CsA or its analogue in HSC suggesting collagen suppression effects. CsA has been shown to modulate collagen degradation and induce collagen

accumulation through disruption of the actin-serving properties of gelsolin, inhibiting the binding step of collagen phagocytsis[488], however, this study administered CsA with 40mg/kg daily i.p injection *in vivo* and 10 μM *in vitro*. Whereas studies in HSCs reporting CsA or its non-immunosuppressive analogue reduce collagen expression and tissue inhibitor of metalloproteinase (TIMP), increase the expression of MMP-1 at 1 μM concentration through suppression on phosphorylation of JNK and p38 MAPK and weakly suppression of ERK1/2 signalling [421]

Ikeda reported that both CsA and tacrolimus inhibited DNA synthesis in HSCs, but only CsA suppressed collagen synthesis[420], suggesting the suppression is calcineurin independent, and most likely act through cyclophilins. Further study treated HSCs with NIM811, also showed collagen production suppression and cell proliferation effect, enhances collagenase activity and enhanced the expression of Smad7, to reduce the expression of TGF-b-RI[422]. Unlike the profibrotic results on CsA with most studies, all these positive results with CsA were conducted with rather low concentration or with the calcineurin-independent analogue.

Fibrosis is a complex process resulting from an overall imbalance between ECM synthesis and ECM degradation. Compare to the CypD deletion results, CC-4635 achieved less potent effects on collagen deposition. With respect to the lack of calcineurin inhibition, CC-4635 still retains compatible biological activity with CsA in terms of the binding capacity on cyclophilins other than CypD. As mentioned before in chapter 1, extracellular CypA acts an extracellular pro-inflammatory cytokine, but also has an anti-fibronectin role to upregulate MMP-9[291] . It is possible

that CsA analogue CC-4635 could effectively inhibit extracellular CypA with high affinity to limit inflammation, however, at the same time, interfere with the healing and remodelling to supress collagen degradation by downregulating MMP-9, like CsA does on MMP-9 suppression[489], may render the beneficial from CypD inhibition with reduced collagen deposition is partially overcome and renders by CypA/CD147 suppression, which is also consistent with the report that NIM 811 treatment profoundly reduced the expression of inflammatory cytokines and adhesion molecules such as TNF-α, IL-1β and ICAM-1[490]. This anti-inflammation effect of CsA analogue due to CypA inhibition also explains the suppression of α-SMA by CC-4635, while CypD single knock out does not affect the activation of α-SMA due to a possible pro-inflammation status, as Tavecchio[486] reported that deletion or reduction of CypD directs mitochondria-to-nuclei inflammatory gene expression. Notably, as CypB is component of a complex which assist procollagen biosynthesis[491, 492], inhibition of CypB also inhibit collagen synthesis, which has previously confirmed in a rat liver fibrosis model to clarify that both CypB and CypD are responsible for rat liver fibrosis[423], which also explains that CypD single knock out partially protected collagen deposition.

As CypB and CypC are both ER-based cyclophilins with compensational regulatory mechanism to each other, while double knockout or with their co- inhibitor CsA cause detrimental side effects, single knock out of either would not lead to cellular perturbations[384]. Thus, a more specific non-immunosuppressive cyclophilin inhibitor with higher affinity on both CypB and D inhibition might be an idea target for chronic pancreatitis.

CHAPTER 8

Overview

8.1 CypD as a drug target in pancreatitis

Ever since 1980s, the permeabilization of inner mitochondria membrane due to opening of a ATP- synthase dimmer formed, mitochondrial matrix protein CypD facilitated pore has progressed from single cardiac ischemia/reperfusion injury[493] related detrimental mechanism to a universal cell death differentiation process involved in unprecedented multiple diseases, including muscular dystrophy[315], Parkinson's disease[316], multiple sclerosis[317, 318], Alzheimer's disease and aging[319-321] that resulted from sustained disseminated bioenergetics catastrophe condition, leading to disputation of mitochondrial transmembrane electrochemical proton gradient, followed by ATP depletion, and finally cell death, which become an ideal target that educing great interest.

Following the findings that genetic CypD protects both cellular and experimental APs from PAC damage and cell death[237], pharmacologic inhibition with DEB025, the non-immunosuppressive analogue of CsA, however, seem to lose its efficacy at high does. To address and fully characterize the phenomenon and develop efficient but safe therapy that could further facilitate clinical setting, current study was firstly designed to validate the possibility of using novel cyclophilin inhibitors in AP. Further driven by the notion that acute, recurrent and chronic pancreatitis are disease continuum, and based on the theories of necro-fibrosis as well as sequential AP events in the development of CP pathogenesis from recurrent AP episodes, it has been hypothesized that a strategy like CypD inhibition to reduce necrosis from AP episodes may possibly adapted to CP treatment. Thus, the present study also extended to explore the effects of CypD inhibition in the development and recovery of CP.

In Chapter 3, the protective capabilities of CsA against pancreatic toxins (TLCS, POA and caerulein) induced cell injury, including necrotic and apoptotic cell death as well as ROS production and ER based chaperone expression have been described. The findings of this chapter demonstrate that CsA significantly inhibited TLCS-, POA- and CER- induced necrotic cell death of mouse PACs in a biphasic concentration and time dependent manner with less efficacy at high concentrations. The protection of CsA over TLCS induced necrotic cell death accompanying with reduced ROS production and CypB overexpression in TLCS treated PACs, while modest effect on caspase 3/7 dependent apoptosis has been observed. On the contrary, the adverse effects of high concentration CsA on PACs exacerbate the ROS production and promoted apoptosis, as seen in CER treated PACs that CsA upregulated ER chaperone GRP-78 and ROS production, to promote toxin-induced caspase 3/7 related apoptosis. Whereas CsA had no impact in ROS production on POA treated PACs due to POA induced maximal necrosis among 3 toxins which diminished mitochondria ROS production capacity. The beneficial of cyclophilin inhibitor CsA, consistently observed at low micromolar concentration, highlights the dual role of ROS in regulating and shifting cell death pattern as well as the possible interlink with ER-based chaperone.

Data in chapter 4, demonstrate that CsA is highly effective in protecting against EAP with optimal dosing regimen and proper formulation. Single i.p administration of CsA at low to medium dosage markedly reduced both local and systemic injury across all three AP models, however, CsA at high dosage tend to exacerbate the inflammation defined by pro-inflammatory cytokine IL-6 in FAEE- and CER-AP, suggesting the higher dose of CsA may off-target and induce cell death related

inflammation. These results are in line with adverse impact of CsA which encountered in alternative animal models such as ischemic injury, *etc*. The results obtained in EAP models do not support the use of high dose CsA in AP.

Upon potential treatment value with cyclophilin inhibitors was observed, in chapter 5, a series of novel synthesized cyclophilin inhibitors have been evaluated for AP. Among all tested compounds, SEL 1233 originated from peptolides with higher affinity to CypD but less immunosuppression has stand out for its remarkable beneficial in acute biliary pancreatitis with a PK based dosing regimen and early intervention. A possible pulmonary toxicity induced by the solvent also raised the issue that safe and appropriate formulation should be developed in future experiment.

Inspired by the promising data of SEL1233 on biliary pancreatitis, it was further examined in another two types of pancreatitis models. Surprisingly, in chapter 6, this compounds with optimum dosing regimen defined on biliary pancreatitis turned out to be ineffective in FAEE- and CER-AP apart from the parameter of trypsin activity, which has modest reduction. Notably, the PEG-contained formulation has been proved to be toxic, especially for inflammation. Further studies conducted with treatment of both CsA and SEL1233 in *Ppif*$^{-/-}$ mice with 20mg/kg showed counterbalanced effects over CypD knockout beneficial in CER-AP, confirmed the off-target effects on other cyclophilins which exacerbate the inflammation.

Finally, in chapter 7, the well characterized repetitive caerulein induced CP model were employed, for which reflects human CP progression from recurrent AP episodes to examine the role of CypD in development and recovery of CP. The therapeutic efficacy of pharmacological CypD inhibition with non-immunosuppressive CsA analogue SCY-635/CC-4635 has also been evaluated. Both genetic and pharmacological MPTP inhibition have proved to be protective in the development of CP from recurrent AP episodes, shown better reserved acinar cell with functional enzyme content, and less collagen deposition. Following either 2- or 4- week repetitive caerulein induction, *Ppif*$^{-/-}$ mice developed modest pancreatic morphological changes. with relatively intact acini and well preserved enzymatic content. Remarkable reduction on collagen deposition with less circulating TGF-β1level has also been observed in *Ppif*$^{-/-}$ mice. On the contrary, WT C57bL/6J mice exhibit impressive acinar structure distortion with both peri-acinar and intra-/inter lobular collagen deposition as shown with Sirius red and trichrome, massive acinar cell loss with sharply decreased amylase reservation and secretion. After caerulein withdraw, another 2-week recovery period was followed to examine the regeneration in both type of mice, while *Ppif*$^{-/-}$ mice showing greatly improved pan/body ratio and tightly packed acinar cell, the WT mice, however, with no regain on pan/body weight ratio but more fat tissue replaced parenchyma, suggests that CypD inhibition accelerate the recovery of acinar cell. Interestingly, data obtained in chapter 7, however, also suggests that deletion of CypD had less consistent effects on PSCs activation as seen with comparable α-SMA expression level in both type of mice, further suggesting a rather indirect effect based on acinar cell protection of reducing the extent of cell death and collagen production or degradation.

Evident by both genetic and pharmacological MPTP inhibition via CypD in acute and chronic pancreatitis provided further possibility for the treatment direction in pancreatitis.

8.2 Alternative treatment targets for AP

Whilst most clinical trials targeting on protease inhibition, anti-inflammation, antioxidants, *etc*. barely achieve any consistent beneficial, evidence has revealed the potential for AP therapy via the prevention of Ca^{2+}-dependent mitochondrial damage. Multiple approaches are indicated from preclinical findings, including Ca^{2+} entry inhibition through Orai1 blockage[494], MPTP inhibition targeting cyclophilin D[237], and inhibition of inositol 1, 4, 5-trisphosphate receptor- mediated Ca^{2+} release by caffeine[495]. Since disruption of Ca^{2+} homeostasis has long been regarded as the central initial role in the development of AP, strategies targeting on reducing Ca^{2+} overload of pancreatic acinar cells induced mitochondrial dysfunction provided possibility of specific treatment for AP. Indeed, with Orai1 inhibitor CM 4620 has recently (1/8/2018) entered Phase-II clinical trials for pancreatitis in USA, highlighting the major progress in pancreatic translational work, the strategies focused on Ca^{2+}-dependent mitochondrial damage exhibit tremendous potentiality in shifting to clinical setting. As the effective high dose of caffeine extending into toxicity, studies focused on safe and efficient products targeting on MPTP inhibition become imminent and valuable to guide further clinical trials.

8.3 Potential translational targets for CP treatment

Results from recurrent inflammatory episodes, the replacement of pancreatic parenchyma by fibrous connective tissue leads to progressive exocrine and

endocrine pancreatic insufficiency in CP. Due to poor understanding on the biology of physiopathology, no therapeutic products available to reverse the inflammatory and fibrotic process, current medical treatment of CP is unsatisfactory with primarily aim to control symptoms like abdominal pain and manage complications such as steatorrhea and diabetes. Therefore, developing novel interventions for CP represents a high priority and could possibly fill the unmet medical gap to improve quality of life. The major clinic-pathological event in CP is recurrent or persistent inflammation. Although the precise progression mechanism is unknown, the major driver of the process seems to be multiple immune cells involved including monocyte, type 2 macrophages[496], mast cells[497], T lymphocytes[498-500] and pancreatic stellate cell[501]. Thus, many immunomodulatory agents have been tried in chronic pancreatitis mainly in experimental models showed therapeutic benefit inhibiting pancreatic stellate cell proliferation and collagen synthesis with IFN-β and IFN-γ inhibition[502], reducing fibrosis level with either loss or receptor antagonist of complement component 5[503], decreasing pancreatic M2 macrophages and reducing fibrosis with blocking IL-4/IL-3 by a blocking peptide[504].

8.4 Challenge in developing and application cyclophilin inhibitors

8.4.1 Efficacy

CsA and its analogues are highly hydrophobic with poor solubility, tolerance and variable absorption. The protection afforded by CsA is likely limited by its availability, which could possibly counterbalance the efficacy of MPTP inhibition.

Due to its low water solubility, CsA is administered in viscous formulations that may also have high ethanol content. The results from chapter 5, however, suggests

that the ethanol or high concentration PEG based formulation may possibly produce synergistic effects on lung injury with combinatorial pancreatic stimuli. Furthermore, the viscous formulations with ethanol or PEG result in a wide variability in bioavailability. CsA and analogues are poorly absorbed after oral administration, primarily in the small intestine, and has a bioavailability of about 30% (range 5 to 70%) in healthy volunteers. With a clinical therapeutic range at 150-250 ng/ml in blood for CsA, maximum blood concentrations of cyclosporin are usually observed 1 to 8 hours after oral administration, and a second peak may be noted due to enhanced absorption following a meal, as bile increases cyclosporin absorption, or may represent excretion of CsA as a sulphate conjugate in the bile, which is then degraded to the parent compound and reabsorbed. Great efforts in improving the bioavailability of CsA have been made to enable the drug more water-soluble by attach a conjugating group through a modification in the MeBmt side chain. The other strategy for improving the therapeutic index is to generate analogues to improve the PK profiles on metabolism and clearance of CsA to improve the bioavailability.

With appropriate formulation to improve both solubility and bioavailability of the compound, it may possibly increase the beneficial power of MPTP inhibition. As the current formulation is still unsatisfied and possibly induce lung toxicity, the next step firstly requires the collaboration between both chemists and researchers to design and validate a PEG/alcohol free solvent, which is safe, soluble but stable formulation with good tolerance and high efficacy before better translating the therapy to clinical research. With appropriate formulation and optimal dosing regimen, further CP experiments using 5mg/kg either SEL1233 or CC-4635 will be conducted to validate

the efficacy. Finally, with agreement and endeavour from academia, industry and clinician's collaboration, the promising candidate compound will be finally applied on human trials with scientifically designed protocol and ethic approval.

It is also crucial to ensure that the treatment is effective to MPTP inhibition with optimized therapeutic dose range. The effects of CsA have been shown to be related to its concentration in various organs and settings. The time- and does –dependent toxicity has been reported in a large variety of disease including cardiovascular and hepatic diseases, showing better effects on lower concentration or dosages. Studies even suggested that a rather lower dose of DEB025 for instance 1-3 mg/kg deserved to be investigated[418].

It appears to have some heterogeneity in different modes of CsA delivery as seen the discriminate bioavailability in intravenous, subcutaneous, intraperitoneal, and oral administration. Although intraperitoneal delivery is considered a parenteral route of administration, the pharmacokinetics of substances administered intraperitoneally are more similar to those seen after oral administration[505], because the primary route of absorption is into the mesenteric vessels, which drain into the pass through the liver. Therefore, substances administered intraperitoneally may undergo hepatic metabolism before reaching the systemic circulation. In addition, a small amount of intraperitoneal injection may pass directly across the diaphragm through small lacunae and into the thoracic lymph, which also partially explained the early transit lung injury with ethanol and PEG formulation observed in chapter 6.

8.4.2 Safety

The natural CypD inhibitor CsA, compasses the ability to inhibit majority of cyclophilins, despite its beneficial role in immunosuppression and MPTP inhibition, the application is strongly limited by substantial considerable incidence of adverse events, the most common of which are hypertrichosis, gingival hyperplasia, and neurological and gastrointestinal effects. These are usually with mild to moderate severity and resolve on dosage reduction.

As mentioned in Chapter 7, the natural CypD inhibitor CsA was generally regarded as pro-fibrogenic and correlated with TGF-β1. It has even been used paradox to induced CP.

In terms of its pro-fibrogenity, all studies have applied CsA as long-term treatment with a higher dose, as for its use on CP induction, studies applied CsA together with other precipitants including either alcohol or caerulein synergistically, while CsA alone does not show any fibrosis induction.

The most studied nephrotoxicity of CsA is thought to be rely on the dose-dependent calcineurin inhibition[506, 507] and CypB/C mediated, possibly CypA involved ER stress[295, 379, 382, 384], which can be abolished by ER stress inhibitor salubrinal. While CypA and B are ubiquitously expressed, the bone marrow originated CypC expression is tissue specific, mostly in kidney, early detailed examination on mouse kidney reveals that kidney cells expressing ER resident CypC correspond to the proximal tubule S3 segment of the nephron where has been shown to sustained

histopathological damage from high dosages of CsA, raising the possibility that CypC may be mediator of the toxic effects of CsA[304].

The comprehensive knowledge of profibrotic signalling events specifically accompanying the immunomodulatory activity, which need a reliable benefit-risk assessment under therapeutic regimens. Therefore, new approaches with non-immunosuppressive products such as DEB025, NIM811, SCY-635/CC-4635 are highly demanding, within the maximal optimized range for MPTP inhibition, or apply CsA with concomitant drugs such as ER stress inhibitor salubrinal may ultimately minimize or eliminate the risk of drug toxicity, allowing CsA or its analogue for the capability to improve MPTP inhibition with higher affinity to CypD but lowering the risk of nephrotoxicity.

As a member of PPIase family, cyclophilins involved in a large range of both physiological and pathophysiological biology activities, with extensive crosslinking and overlapping between each other due to similar structure. Therefore, developing and discovering compounds that can selectively inhibit any single member of cyclophilins such as CypD will be the challenge to medicinal chemistry. With new inhibitory templates which may deliver improved selectivity, SEL1233 has distinguished from the CsA analogues, with improved selectivity on CypD, however, the application of 1233 exerted limited effects in FAEE-and CER-AP, suggesting a rather sophisticated mechanism network that any subtle structure modification may possibly change the activity of efficacy.

8.5 Importance of intervention time in pancreatitis

8.5.1 Early treatment in AP

Patients with MAP (80%) recover within few days without experiencing any further problems. But those with SAP (20%) require prolonged hospital stay, critical care support, and resulted in 15-20% risk of death[508]. The clinical course of SAP classically occurs in two phases. The first lasts 1–2 weeks and presents with features of systemic inflammatory response and organ dysfunction. Necrosis of the inflamed pancreas often occurs during this period. This phase may resolve or may progress to a second phase, consisting of sepsis and multiple organ failure 2–3 weeks later. Pancreatic necrosis is a major determinant of disease progression, the presence of necrosis dramatically raises the mortality rate in AP[509, 510]. This is usually associated with infection of necrotic pancreatic or peri-pancreatic tissue; without surgical intervention, it has a very high mortality[511]. While sterile necrosis is associated with 5% to 10% mortality rate, the mortality rate increase to 20% to 30% when necrosis becomes infected. Patients with necrotizing pancreatitis are more than twice as likely to die if the necrosis become infected[512]. Thus, early recognition and treat is necessary.

With respect to the MPTP opening is reversible on both a short (ms) and a long (seconds) time scale, as shown directly by electrophysiological observation[513] and as well as indirect by monitoring mitochondria polarization tracer fluxes[369, 514, 515]. Sustained opening leads to an irreversible pathological change with massive cell death, which clearly requires early intervention. The importance of intervening in the first few minutes to prevent MPTP opening is most crucial.

The current study with 1233 also suggested the importance of early intervention, with administration 1h after disease induction showing greater reduction across all of the severity markers compare to a late administration at 6h after. Similar results were shown in other studies targeting on MPTP inhibition. One study on renal ischemia/ reperfusion injury has reported that both 3mg/kg and 10 mg/kg CsA administered as a single bolus reduces the risk of vascular toxicity, improved renal mitochondria calcium retention capacity and renal function, delaying MPTP opening in a renal I/R injury model. However, with same low dose at 3mg/kg, late administration didn't show any beneficial while high dose at 10mg/kg still showed the best effect when administered late[516].

SFA, inhibit mitochondria CypD without affecting calcineurin activity, was also reported to be cardioprotective when administered at the onset of myocardial reperfusion, but the protective effects of MPTP inhibition were completely lost if SFA was administered after first 15 min of myocardial reperfusion had elapsed[517].

8.5.2 Early diagnosis and treatment in CP

The prognosis of CP is poor with the mortality rate approximately two-fold higher than the general population, pancreatic cancer also develops relatively frequently in CP[35]. While early state CP still with preserved pancreatic function and potentially reversible features[518], the early diagnosis and proper intervention are extremely important, which could possibly prevent the late irreversible features and complications of CP. Being difficult and challenging for the early diagnosis of CP, however, the propagated concept of early-stage CP[519, 520] encourage the medical

treatment for the earlier stages of CP by picking up the patients suspicious for early CP who fits in the clinical signs and providing medical treatment.

The mechanism of CP progression is regarded with five disease stages: from at risk, AP-RAP to Early CP, Established and finally end-Stage CP, which further links to critical systems and various cell types that respond differently to injury and inflammation, including nervous and DNA repair system, and PACs, duct cell, PSCs and islet cells[521]. With wealth of data support that AP, RAP, and CP represent a disease continuum[42, 43], early intervention with a strategy like MPTP inhibition which benefit both AP and CP could possibly protect against the progression into advanced stages.

8.6 Evaluation of experimental pancreatitis models

TLCS-AP, FAEE-AP and CER-AP are 3 main experimental acute pancreatitis models used in the current thesis with distinctive mechanism described in chapter 1.6. Each model has their own advantages or limitations. The main features of the 3 AP models were shown in **Table 8.1**. Investigator should be aware the characteristics of each model and carefully choose suitable animal model to get reliable evidence.

The bile acid TLCS-induced AP was widely accepted as a representative model of severe acute pancreatitis that shows pancreatic necrosis and reflected the pathogenesis of clinical biliary AP. With respect to its surgical common bile duct cannulation required procedure, the successful induction of this model requires

delicate techniques under dissection microscope, which may cause extra surgical procedure related injury due to poor surgery performance and affect research results.

The non-oxidative alcohol metabolite FAEE induced AP was a novel alcoholic model developed previously in our group with highly clinical relevance, however, due to a 10% mortality caused by acute fatty acid/ethanol toxicity, this model is suggested to be conducted on mice weighing 25-30g with better tolerance and with special care using heat pat to keep warm and 2 doses of analgesia agent to relieve pain.

EAP induced by caerulein hyper-stimulation is the most extensively used model of AP in research settings due to its highly reproducible, economical character and easy to conduct.

Mimicking the human recurrent AP may progress to CP pathogenesis, repeated bouts of caerulein-induced acute pancreatitis in the course of several weeks was used to induce chronic pancreatitis. Similar to the caerulein induced AP, this CP model is easy to conduct and reproducible, however with less clinical relevant cause in terms of most RAP progressed CP cases were originated from gallstone and alcohol in clinical studies.

Table 8.1 Comparison of TLCS-AP, FAEE-AP and CER-AP

EAP models	Toxins	Procedure	Severity	Advantage	Limitation
TLCS-AP (Biliary)	Bile acid (TLCS)	Common bile duct cannulation	Severe	Clinical relevance	Surgical procedure related complication
FAEE-AP (Alcoholic)	Fatty acid /Ethanol	Intraperitoneal injection	Severe	Clinical relevance	Mortality
CER-AP	caerulein	Intraperitoneal injection	Moderate	Simplicity and highly reproducible	Less clinical relevance

8.7 Future prospect and approach in pancreatitis treatment

The discovery and development of novel medical products that benefit patients with pancreatitis remains a remarkably challenging endeavour. The use and outcome of animal models are pivotal to bridge the translational gap to the clinic[522].

With the encouraging preclinical results that novel cyclophilin inhibitor 1233 targeting MPTP inhibition has shown its effective potential in treating biliary AP model, raising the possibility of further translating the therapy to clinical research.

Pancreatic injury inhomogeneity across different experimental models is paralleled with a number of various signalling pathways involved in different toxins initiated

response. Accordingly, the phenotypical subsets of pancreatitis represent a major challenge for clinical trial conduction. Over the past decade, therapeutic strategies have evolved toward a personalized approach, which has the potential to tailor therapy with the best response and highest safety margin to ensure better patient care[523]. Despite compound 1233 has shown its effective potential in treating biliary AP model, failure to alleviate both local and systemic injury in alcoholic- and caerulein hyper-stimulation-AP models suggesting a need for personalized treatment strategy. With application compound 1233 to biliary or gallstone aetiology classified AP subset, might be a new approach based on personal disease cause oriented treatment strategy in further drug development for AP. Similarly, with implementation novel MPTP inhibitor on patients with more than once AP recurrence to prevent the progression to CP might be an early intervention which could possibly benefit the later life quality.

8.8 Conclusion

The beneficial role of CypD inhibition has been validated in this study on both acute and chronic pancreatitis, despite the elucidation of molecular mechanisms during progression into CP still require further input, it is confident that the current approach for MPTP inhibition via CypD is logical and promising.

Over the last decades, cyclophilin inhibition started to unfold, from binary interaction for immunosuppression via calcineurin inhibition, into a viable approach towards treating a wide variety of disease entities, including MPTP inhibition, virus replication inhibition, an-inflammation through extracellular receptor binding process inhibition, supporting chaperone role inhibition, etc. which provides a promising novel strategy in such disease like pancreatitis that involves combined actions under multivariate including cell death, inflammation, ROS generation, ER

stress and fibrosis. However, constant research endeavours in this field requires much more interlink between multidiscipline involvement to better balance each factor's effect.

However, CsA and its analogues may exert variable effects owing to its interaction with calcineurin, NK-1 receptor, and all the non-mitochondrial cyclophilins such as CypB/C. The discovery of non-immunosuppressive cyclophilin inhibitors such as DEB025, NIM811 and SCY-635/CC-4635 allow cyclophilin inhibition to be considered in a broader disease spectrum and provide more directions on modify chemical structure to discriminate affinity with different subtype. Simultaneously, the advent of a new form cyclophilin inhibitor that targeting CsA to mitochondria in neuron and cardiovascular disease[524, 525], to minimize extra-mitochondrial interactions and improve cytoprotection provided novel approach on the application of cyclophilin inhibitors. Thus, synthesis of modified mitochondrial-targeted non-immunosuppressive CsA with specific much-improved CypD binding affinity but absent or modest binding potential on the prototype, may improve the safety and efficiency of compounds for the treatment of pancreatitis to ease the off-target effects and cross the delivery hinders.

References

1. Yadav D, Lowenfels AB. Trends in the epidemiology of the first attack of acute pancreatitis: a systematic review. Pancreas 2006;33:323-30.
2. Fagenholz PJ, Castillo CF, Harris NS, et al. Increasing United States hospital admissions for acute pancreatitis, 1988-2003. Ann Epidemiol 2007;17:491-7.
3. Frey CF, Zhou H, Harvey DJ, et al. The incidence and case-fatality rates of acute biliary, alcoholic, and idiopathic pancreatitis in California, 1994-2001. Pancreas 2006;33:336-44.
4. Sandzén B, Haapamäki MM, Nilsson E, et al. Cholecystectomy and sphincterotomy in patients with mild acute biliary pancreatitis in Sweden 1988 - 2003: a nationwide register study. BMC Gastroenterol 2009;9:80.
5. Omdal T, Dale J, Lie SA, et al. Time trends in incidence, etiology, and case fatality rate of the first attack of acute pancreatitis. Scand J Gastroenterol 2011;46:1389-98.
6. Satoh K, Shimosegawa T, Masamune A, et al. Nationwide epidemiological survey of acute pancreatitis in Japan. Pancreas 2011;40:503-7.
7. Shen HN, Chang YH, Chen HF, et al. Increased risk of severe acute pancreatitis in patients with diabetes. Diabet Med 2012;29:1419-24.
8. Yadav D, Lowenfels AB. The epidemiology of pancreatitis and pancreatic cancer. Gastroenterology 2013;144:1252-61.
9. Quinlan JD. Acute pancreatitis. Am Fam Physician 2014;90:632-9.
10. Gullo L, Migliori M, Olah A, et al. Acute pancreatitis in five European countries: etiology and mortality. Pancreas 2002;24:223-7.
11. Pendharkar SA, Salt K, Plank LD, et al. Quality of life after acute pancreatitis: a systematic review and meta-analysis. Pancreas 2014;43:1194-200.
12. Peery AF, Crockett SD, Barritt AS, et al. Burden of Gastrointestinal, Liver, and Pancreatic Diseases in the United States. Gastroenterology 2015;149:1731-1741.e3.
13. Koutroumpakis E, Slivka A, Furlan A, et al. Management and outcomes of acute pancreatitis patients over the last decade: A US tertiary-center experience. Pancreatology 2017;17:32-40.
14. Vege SS, DiMagno MJ, Forsmark CE, et al. Initial Medical Treatment of Acute Pancreatitis: American Gastroenterological Association Institute Technical Review. Gastroenterology 2018;154:1103-1139.
15. Spanier BW, Dijkgraaf MG, Bruno MJ. Epidemiology, aetiology and outcome of acute and chronic pancreatitis: An update. Best Pract Res Clin Gastroenterol 2008;22:45-63.
16. Peery AF, Dellon ES, Lund J, et al. Burden of gastrointestinal disease in the United States: 2012 update. Gastroenterology 2012;143:1179-1187.e3.
17. Kedia S, Dhingra R, Garg PK. Recurrent acute pancreatitis: an approach to diagnosis and management. Trop Gastroenterol 2013;34:123-35.
18. Testoni PA. Acute recurrent pancreatitis: Etiopathogenesis, diagnosis and treatment. World J Gastroenterol 2014;20:16891-901.
19. Kolodecik T, Shugrue C, Ashat M, et al. Risk factors for pancreatic cancer: underlying mechanisms and potential targets. Front Physiol 2013;4:415.

20. Sakorafas GH, Tsiotou AG. Etiology and pathogenesis of acute pancreatitis: current concepts. J Clin Gastroenterol 2000;30:343-56.
21. Somogyi L, Martin SP, Venkatesan T, et al. Recurrent acute pancreatitis: an algorithmic approach to identification and elimination of inciting factors. Gastroenterology 2001;120:708-17.
22. Gullo L, Migliori M, Pezzilli R, et al. An update on recurrent acute pancreatitis: data from five European countries. Am J Gastroenterol 2002;97:1959-62.
23. Khurana V, Ganguly I. Recurrent acute pancreatitis. Jop 2014;15:413-26.
24. Pant C, Sferra TJ, Lee BR, et al. Acute Recurrent Pancreatitis in Children: A Study From the Pediatric Health Information System. J Pediatr Gastroenterol Nutr 2016;62:450-2.
25. Majumder S, Chari ST. Chronic pancreatitis. The Lancet 2016;387:1957-1966.
26. Andren-Sandberg A. Chronic pancreatitis. N Am J Med Sci 2011;3:355-7.
27. Beglinger C. Diagnosis of chronic pancreatitis. Dig Dis 2010;28:359-63.
28. Braganza JM, Lee SH, McCloy RF, et al. Chronic pancreatitis. Lancet 2011;377:1184-97.
29. Whitcomb DC, Frulloni L, Garg P, et al. Chronic pancreatitis: An international draft consensus proposal for a new mechanistic definition. Pancreatology 2016;16:218-24.
30. Lin YK, Johnston PC, Arce K, et al. Chronic Pancreatitis and Diabetes Mellitus. Curr Treat Options Gastroenterol 2015;13:319-31.
31. Lohr JM, Dominguez-Munoz E, Rosendahl J, et al. United European Gastroenterology evidence-based guidelines for the diagnosis and therapy of chronic pancreatitis (HaPanEU). United European Gastroenterol J 2017;5:153-199.
32. Levy P, Barthet M, Mollard BR, et al. Estimation of the prevalence and incidence of chronic pancreatitis and its complications. Gastroenterol Clin Biol 2006;30:838-44.
33. DiMagno MJ, DiMagno EP. Chronic pancreatitis. Curr Opin Gastroenterol 2010;26:490-8.
34. DiMagno MJ, DiMagno EP. Chronic pancreatitis. Curr Opin Gastroenterol 2012;28:523-31.
35. Yamabe A, Irisawa A, Shibukawa G, et al. Early diagnosis of chronic pancreatitis: understanding the factors associated with the development of chronic pancreatitis. Fukushima J Med Sci 2017;63:1-7.
36. Lévy P, Domínguez-Muñoz E, Imrie C, et al. Epidemiology of chronic pancreatitis: burden of the disease and consequences. United European Gastroenterol J 2014;2:345-54.
37. Wang LW, Li ZS, Li SD, et al. Prevalence and clinical features of chronic pancreatitis in China: a retrospective multicenter analysis over 10 years. Pancreas 2009;38:248-54.
38. Comfort MW, Gambill EE, Baggenstoss AH. Chronic relapsing pancreatitis; a study of 29 cases without associated disease of the biliary or gastrointestinal tract. Gastroenterology 1946;6:376-408.
39. Kloppel G, Maillet B. The morphological basis for the evolution of acute pancreatitis into chronic pancreatitis. Virchows Arch A Pathol Anat Histopathol 1992;420:1-4.

40. Ammann RW, Muellhaupt B. Progression of alcoholic acute to chronic pancreatitis. Gut 1994;35:552-6.
41. Whitcomb DC. Hereditary pancreatitis: new insights into acute and chronic pancreatitis. Gut 1999;45:317-22.
42. Sankaran SJ, Xiao AY, Wu LM, et al. Frequency of progression from acute to chronic pancreatitis and risk factors: a meta-analysis. Gastroenterology 2015;149:1490-1500.e1.
43. Ahmed Ali U, Issa Y, Hagenaars JC, et al. Risk of Recurrent Pancreatitis and Progression to Chronic Pancreatitis After a First Episode of Acute Pancreatitis. Clin Gastroenterol Hepatol 2016;14:738-46.
44. Lankisch PG, Breuer N, Bruns A, et al. Natural history of acute pancreatitis: a long-term population-based study. Am J Gastroenterol 2009;104:2797-805; quiz 2806.
45. Yasuda T, Ueda T, Takeyama Y, et al. Long-term outcome of severe acute pancreatitis. J Hepatobiliary Pancreat Surg 2008;15:397-402.
46. Hirota M, Shimosegawa T, Masamune A, et al. The sixth nationwide epidemiological survey of chronic pancreatitis in Japan. Pancreatology 2012;12:79-84.
47. Ueda T, Kuroda Y, Takeyama Y, et al. Long-term outcome of acute pancreatitis. Suizo 2005;20:455-464.
48. Whitcomb DC. What is personalized medicine and what should it replace? Nat Rev Gastroenterol Hepatol 2012;9:418-24.
49. Whitcomb DC. Genetics and alcohol: a lethal combination in pancreatic disease? Alcohol Clin Exp Res 2011;35:838-42.
50. Pham A, Forsmark C. Chronic pancreatitis: review and update of etiology, risk factors, and management. F1000Res 2018;7.
51. Crockett SD, Wani S, Gardner TB, et al. American Gastroenterological Association Institute Guideline on Initial Management of Acute Pancreatitis. Gastroenterology 2018;154:1096-1101.
52. IAP/APA evidence-based guidelines for the management of acute pancreatitis. Pancreatology 2013;13:e1-15.
53. Moggia E, Koti R, Belgaumkar AP, et al. Pharmacological interventions for acute pancreatitis. Cochrane Database Syst Rev 2017;4:Cd011384.
54. Bang UC, Semb S, Nojgaard C, et al. Pharmacological approach to acute pancreatitis. World J Gastroenterol 2008;14:2968-76.
55. Neumann I, Grassi B, Bdair F, et al. Antiproteases for acute pancreatitis. Cochrane Database of Systematic Reviews 2011.
56. D'Amico D, Favia G, Biasiato R, et al. The use of somatostatin in acute pancreatitis--results of a multicenter trial. Hepatogastroenterology 1990;37:92-8.
57. Gøtzsche PC, Gjørup I, Bonnén H, et al. Somatostatin v placebo in bleeding oesophageal varices: randomised trial and meta-analysis. Bmj 1995;310:1495-8.
58. Luengo L, Vicente V, Gris F, et al. Influence of somatostatin in the evolution of acute pancreatitis. A prospective randomized study. Int J Pancreatol 1994;15:139-44.
59. Wang G, Liu Y, Zhou SF, et al. Effect of Somatostatin, Ulinastatin and Gabexate on the Treatment of Severe Acute Pancreatitis. Am J Med Sci 2016;351:506-12.

60. Andriulli A, Leandro G, Clemente R, et al. Meta-analysis of somatostatin, octreotide and gabexate mesilate in the therapy of acute pancreatitis. Aliment Pharmacol Ther 1998;12:237-45.
61. Uhl W, Buchler MW, Malfertheiner P, et al. A randomised, double blind, multicentre trial of octreotide in moderate to severe acute pancreatitis. Gut 1999;45:97-104.
62. Heinrich S, Schafer M, Rousson V, et al. Evidence-based treatment of acute pancreatitis: a look at established paradigms. Ann Surg 2006;243:154-68.
63. McKay C, Baxter J, Imrie C. A randomized, controlled trial of octreotide in the management of patients with acute pancreatitis. Int J Pancreatol 1997;21:13-9.
64. Wang R, Yang F, Wu H, et al. High-dose versus low-dose octreotide in the treatment of acute pancreatitis: a randomized controlled trial. Peptides 2013;40:57-64.
65. Li J, Wang R, Tang C. Somatostatin and octreotide on the treatment of acute pancreatitis - basic and clinical studies for three decades. Curr Pharm Des 2011;17:1594-601.
66. Kitagawa M, Hayakawa T. Antiproteases in the treatment of acute pancreatitis. Jop 2007;8:518-25.
67. Valderrama R, Perez-Mateo M, Navarro S, et al. Multicenter double-blind trial of gabexate mesylate (FOY) in unselected patients with acute pancreatitis. Digestion 1992;51:65-70.
68. Buchler M, Malfertheiner P, Uhl W, et al. Gabexate mesilate in human acute pancreatitis. German Pancreatitis Study Group. Gastroenterology 1993;104:1165-70.
69. Chen HM, Chen JC, Hwang TL, et al. Prospective and randomized study of gabexate mesilate for the treatment of severe acute pancreatitis with organ dysfunction. Hepatogastroenterology 2000;47:1147-50.
70. Imaizumi H, Kida M, Nishimaki H, et al. Efficacy of continuous regional arterial infusion of a protease inhibitor and antibiotic for severe acute pancreatitis in patients admitted to an intensive care unit. Pancreas 2004;28:369-73.
71. Piascik M, Rydzewska G, Milewski J, et al. The results of severe acute pancreatitis treatment with continuous regional arterial infusion of protease inhibitor and antibiotic: a randomized controlled study. Pancreas 2010;39:863-7.
72. Kingsnorth AN, Galloway SW, Formela LJ. Randomized, double-blind phase II trial of Lexipafant, a platelet-activating factor antagonist, in human acute pancreatitis. Br J Surg 1995;82:1414-20.
73. McKay CJ, Curran F, Sharples C, et al. Prospective placebo-controlled randomized trial of lexipafant in predicted severe acute pancreatitis. Br J Surg 1997;84:1239-43.
74. Johnson CD, Kingsnorth AN, Imrie CW, et al. Double blind, randomised, placebo controlled study of a platelet activating factor antagonist, lexipafant, in the treatment and prevention of organ failure in predicted severe acute pancreatitis. Gut 2001;48:62-9.
75. Dellinger EP, Tellado JM, Soto NE, et al. Early antibiotic treatment for severe acute necrotizing pancreatitis: a randomized, double-blind, placebo-controlled study. Ann Surg 2007;245:674-83.

76. Bai Y, Gao J, Zou DW, et al. Prophylactic antibiotics cannot reduce infected pancreatic necrosis and mortality in acute necrotizing pancreatitis: evidence from a meta-analysis of randomized controlled trials. Am J Gastroenterol 2008;103:104-10.
77. Garcia-Barrasa A, Borobia FG, Pallares R, et al. A double-blind, placebo-controlled trial of ciprofloxacin prophylaxis in patients with acute necrotizing pancreatitis. J Gastrointest Surg 2009;13:768-74.
78. Hackert T, Werner J. Antioxidant therapy in acute pancreatitis: experimental and clinical evidence. Antioxid Redox Signal 2011;15:2767-77.
79. Leung PS, Chan YC. Role of oxidative stress in pancreatic inflammation. Antioxid Redox Signal 2009;11:135-65.
80. Sateesh J, Bhardwaj P, Singh N, et al. Effect of antioxidant therapy on hospital stay and complications in patients with early acute pancreatitis: a randomised controlled trial. Trop Gastroenterol 2009;30:201-6.
81. Ockenga J, Borchert K, Rifai K, et al. Effect of glutamine-enriched total parenteral nutrition in patients with acute pancreatitis. Clin Nutr 2002;21:409-16.
82. Sahin H, Mercanligil SM, Inanc N, et al. Effects of glutamine-enriched total parenteral nutrition on acute pancreatitis. Eur J Clin Nutr 2007;61:1429-34.
83. Monfared S, Vahidi H, Abdolghaffari AH, et al. Antioxidant therapy in the management of acute, chronic and post-ERCP pancreatitis: A systematic review. World J Gastroenterol 2009;15:4481-90.
84. Bansal D, Bhalla A, Bhasin DK, et al. Safety and efficacy of vitamin-based antioxidant therapy in patients with severe acute pancreatitis: a randomized controlled trial. Saudi J Gastroenterol 2011;17:174-9.
85. Siriwardena AK, Mason JM, Balachandra S, et al. Randomised, double blind, placebo controlled trial of intravenous antioxidant (n-acetylcysteine, selenium, vitamin C) therapy in severe acute pancreatitis. Gut 2007;56:1439-44.
86. Besselink MG, van Santvoort HC, Buskens E, et al. Probiotic prophylaxis in predicted severe acute pancreatitis: a randomised, double-blind, placebo-controlled trial. Lancet 2008;371:651-659.
87. Besselink MG, van Santvoort HC, Renooij W, et al. Intestinal barrier dysfunction in a randomized trial of a specific probiotic composition in acute pancreatitis. Ann Surg 2009;250:712-9.
88. Tenner S, Baillie J, DeWitt J, et al. American College of Gastroenterology guideline: management of acute pancreatitis. Am J Gastroenterol 2013;108:1400-15; 1416.
89. Abraham P, Rodriques J, Moulick N, et al. Efficacy and safety of intravenous ulinastatin versus placebo along with standard supportive care in subjects with mild or severe acute pancreatitis. J Assoc Physicians India 2013;61:535-8.
90. Balldin G, Borgstrom A, Genell S, et al. The effect of peritoneal lavage and aprotinin in the treatment of severe acute pancreatitis. Res Exp Med (Berl) 1983;183:203-13.
91. Barreda L, Targarona J, Milian W, et al. [Is the prophylactic antibiotic therapy with Imipenem effective for patients with pancreatic necrosis?]. Acta Gastroenterol Latinoam 2009;39:24-9.

92. Berling R, Genell S, Ohlsson K. High-dose intraperitoneal aprotinin treatment of acute severe pancreatitis: a double-blind randomized multi-center trial. J Gastroenterol 1994;29:479-85.
93. Bredkjaer HE, Bulow S, Ebbehoj N, et al. [Treatment of acute pancreatitis with indomethacin. A controlled study of the formation of pseudocysts and their subsequent course]. Ugeskr Laeger 1988;150:2902-3.
94. Chen SY, Wang JY, Shanghai Collaboration Group on Ulinastatin Clinical Trials FT. Ulinastatin in the treatment of acute pancreatitis: A multicenter clinical trial. Chinese Journal of Digestive Diseases 2009;3:70-74.
95. Choi TK, Mok F, Zhan WH, et al. Somatostatin in the treatment of acute pancreatitis: a prospective randomised controlled trial. Gut 1989;30:223-7.
96. Debas HT, Hancock RJ, Soon-Shiong P, et al. Glucagon therapy in acute pancreatitis: prospective randomized double-blind study. Canadian journal of surgery. Journal canadien de chirurgie 1980;23:578-580.
97. Delcenserie R, Yzet T, Ducroix JP. Prophylactic antibiotics in treatment of severe acute alcoholic pancreatitis. Pancreas 1996;13:198-201.
98. Delcenserie R, Pagenault M, Hastier P, et al. Prophylactic ciprofloxacin treatment in acute necrotizing pancreatitis: A prospective randomized multicenter clinical trial. Gastroenterology 2001;120:A25.
99. Dürr HK, Maroske D, Zelder O, et al. Glucagon therapy in acute pancreatitis. Report of a double-blind trial. Gut 1978;19:175-9.
100. Finch WT, Sawyers JL, Schenker S. A prospective study to determine the efficacy of antibiotics in acute pancreatitis. Ann Surg 1976;183:667-71.
101. Imrie CW, Benjamin IS, Ferguson JC, et al. A single-centre double-blind trial of Trasylol therapy in primary acute pancreatitis. Br J Surg 1978;65:337-41.
102. Isenmann R, Runzi M, Kron M, et al. Prophylactic antibiotic treatment in patients with predicted severe acute pancreatitis: a placebo-controlled, double-blind trial. Gastroenterology 2004;126:997-1004.
103. Kronborg O, Bulow S, Joergensen PM, et al. A randomized double-blind trial of glucagon in treatment of first attack of severe acute pancreatitis without associated biliary disease. Am J Gastroenterol 1980;73:423-5.
104. Luiten EJ, Hop WC, Lange JF, et al. Controlled clinical trial of selective decontamination for the treatment of severe acute pancreatitis. Ann Surg 1995;222:57-65.
105. Martinez E, Navarrete F. A controlled trial of synthetic salmon calcitonin in the treatment of severe acute pancreatitis. World J Surg 1984;8:354-9.
106. Death from acute pancreatitis. M.R.C. multicentre trial of glucagon and aprotinin. Lancet 1977;2:632-5.
107. Nordback I, Sand J, Saaristo R, et al. Early treatment with antibiotics reduces the need for surgery in acute necrotizing pancreatitis--a single-center randomized study. J Gastrointest Surg 2001;5:113-8; discussion 118-20.
108. Olah A, Belagyi T, Poto L, et al. Synbiotic control of inflammation and infection in severe acute pancreatitis: a prospective, randomized, double blind study. Hepatogastroenterology 2007;54:590-4.
109. Paran H, Neufeld D, Mayo A, et al. Preliminary report of a prospective randomized study of octreotide in the treatment of severe acute pancreatitis. J Am Coll Surg 1995;181:121-4.

110. Pederzoli P, Bassi C, Vesentini S, et al. A randomized multicenter clinical trial of antibiotic prophylaxis of septic complications in acute necrotizing pancreatitis with imipenem. Surg Gynecol Obstet 1993;176:480-3.
111. Pederzoli P, Cavallini G, Falconi M, et al. Gabexate mesilate vs aprotinin in human acute pancreatitis (GA.ME.P.A.). A prospective, randomized, double-blind multicenter study. Int J Pancreatol 1993;14:117-24.
112. Pettilä V, Kyhälä L, Kylänpää ML, et al. APCAP - activated protein C in acute pancreatitis: a double-blind randomized human pilot trial. Crit Care 2010;14:R139.
113. Rokke O, Harbitz TB, Liljedal J, et al. Early treatment of severe pancreatitis with imipenem: a prospective randomized clinical trial. Scand J Gastroenterol 2007;42:771-6.
114. Sainio V, Kemppainen E, Puolakkainen P, et al. Early antibiotic treatment in acute necrotising pancreatitis. Lancet 1995;346:663-7.
115. Sharma B, Srivastava S, Singh N, et al. Role of probiotics on gut permeability and endotoxemia in patients with acute pancreatitis: a double-blind randomized controlled trial. J Clin Gastroenterol 2011;45:442-8.
116. Sillero C, Perez-Mateo M, Vazquez N, et al. Controlled trial of cimetidine in acute pancreatitis. European Journal of Clinical Pharmacology 1981;21:17-21.
117. Trapnell JE, Rigby CC, Talbot CH, et al. A controlled trial of Trasylol in the treatment of acute pancreatitis. BJS 1974;61:177-182.
118. Vege SS, Atwal T, Bi Y, et al. Pentoxifylline Treatment in Severe Acute Pancreatitis: A Pilot, Double-Blind, Placebo-Controlled, Randomized Trial. Gastroenterology 2015;149:318-320.e3.
119. Wang X, Li W, Niu C, et al. Thymosin alpha 1 is associated with improved cellular immunity and reduced infection rate in severe acute pancreatitis patients in a double-blind randomized control study. Inflammation 2011;34:198-202.
120. Wang G, Wen J, Wilbur RR, et al. The effect of somatostatin, ulinastatin and Salvia miltiorrhiza on severe acute pancreatitis treatment. Am J Med Sci 2013;346:371-6.
121. Xue P, Deng LH, Zhang ZD, et al. Effect of antibiotic prophylaxis on acute necrotizing pancreatitis: results of a randomized controlled trial. J Gastroenterol Hepatol 2009;24:736-42.
122. Yang F, Wu H, Li Y, et al. Prevention of severe acute pancreatitis with octreotide in obese patients: a prospective multi-center randomized controlled trial. Pancreas 2012;41:1206-12.
123. Morris-Stiff GJ, Bowrey DJ, Oleesky D, et al. The antioxidant profiles of patients with recurrent acute and chronic pancreatitis. Am J Gastroenterol 1999;94:2135-40.
124. Shah NS, Makin AJ, Sheen AJ, et al. Quality of life assessment in patients with chronic pancreatitis receiving antioxidant therapy. World J Gastroenterol 2010;16:4066-71.
125. Bhardwaj P, Garg PK, Maulik SK, et al. A randomized controlled trial of antioxidant supplementation for pain relief in patients with chronic pancreatitis. Gastroenterology 2009;136:149-159.e2.
126. Kirk GR, White JS, McKie L, et al. Combined antioxidant therapy reduces pain and improves quality of life in chronic pancreatitis. J Gastrointest Surg 2006;10:499-503.

127. Dhingra R, Singh N, Sachdev V, et al. Effect of Antioxidant Supplementation on Surrogate Markers of Fibrosis in Chronic Pancreatitis: A Randomized, Placebo-Controlled Trial. Pancreas 2013;42:589-595.
128. Siriwardena AK, Mason JM, Sheen AJ, et al. Antioxidant therapy does not reduce pain in patients with chronic pancreatitis: the ANTICIPATE study. Gastroenterology 2012;143:655-663.e1.
129. Banks PA, Hughes M, Ferrante M, et al. Does allopurinol reduce pain of chronic pancreatitis? Int J Pancreatol 1997;22:171-6.
130. Bilton D, Schofield D, Mei G, et al. Placebo-Controlled Trials of Antioxidant Therapy Including S-Adenosylmethionine in Patients with Recurrent Nongallstone Pancreatitis. Drug Investigation 1994;8:10-20.
131. De las Heras Castano G, Garcia de la Paz A, Fernandez MD, et al. Use of antioxidants to treat pain in chronic pancreatitis. Rev Esp Enferm Dig 2000;92:375-85.
132. Dite P, Ruzicka M, Zboril V, et al. A prospective, randomized trial comparing endoscopic and surgical therapy for chronic pancreatitis. Endoscopy 2003;35:553-8.
133. Durgaprasad S, Pai CG, Vasanthkumar, et al. A pilot study of the antioxidant effect of curcumin in tropical pancreatitis. Indian J Med Res 2005;122:315-8.
134. Jarosz M, Orzeszko M, Rychlik E, et al. Antioxidants in the treatment of chronic pancreatis, 2010.
135. Salim AS. Role of oxygen-derived free radical scavengers in the treatment of recurrent pain produced by chronic pancreatitis. A new approach. Arch Surg 1991;126:1109-14.
136. Uomo G, Talamini G, Rabitti PG. Antioxidant treatment in hereditary pancreatitis. A pilot study on three young patients. Dig Liver Dis 2001;33:58-62.
137. Windsor JA, Escott A, Brown L, et al. Novel strategies for the treatment of acute pancreatitis based on the determinants of severity. J Gastroenterol Hepatol 2017;32:1796-1803.
138. Jagannath S, Garg PK. Novel and Experimental Therapies in Chronic Pancreatitis. Dig Dis Sci 2017;62:1751-1761.
139. Chang EB, Leung PS. Pancreatic Physiology. In: Leung PS, ed. The Gastrointestinal System: Gastrointestinal, Nutritional and Hepatobiliary Physiology. Dordrecht: Springer Netherlands, 2014:87-105.
140. Gorelick FS, Jamieson JD. Chapter 49 - Structure–function Relationships in the Pancreatic Acinar Cell. In: Johnson LR, Ghishan FK, Kaunitz JD, Merchant JL, Said HM, Wood JD, eds. Physiology of the Gastrointestinal Tract (Fifth Edition). Boston: Academic Press, 2012:1341-1360.
141. Alderton GK. The importance of polarity. Nature Reviews Cancer 2008;8:162.
142. Dolman NJ, Gerasimenko JV, Gerasimenko OV, et al. Stable Golgi-mitochondria complexes and formation of Golgi Ca(2+) gradients in pancreatic acinar cells. J Biol Chem 2005;280:15794-9.
143. Apte MV, Pirola RC, Wilson JS. Pancreatic stellate cells: a starring role in normal and diseased pancreas. Front Physiol 2012;3.
144. Ferdek PE, Jakubowska MA. Biology of pancreatic stellate cells—more than just pancreatic cancer. Pflugers Arch 2017;469:1039-50.
145. Clapham DE. Calcium signaling. Cell 2007;131:1047-58.

146. Carafoli E, Krebs J. Why Calcium? How Calcium Became the Best Communicator. J Biol Chem 2016;291:20849-20857.
147. Petersen OH. Ca2+ signalling and Ca2+-activated ion channels in exocrine acinar cells. Cell Calcium 2005;38:171-200.
148. Kar P, Parekh AB. Distinct spatial Ca2+ signatures selectively activate different NFAT transcription factor isoforms. Mol Cell 2015;58:232-43.
149. Kim MC, Chung WS, Yun DJ, et al. Calcium and Calmodulin-Mediated Regulation of Gene Expression in Plants. Mol Plant 2009;2:13-21.
150. Petersen OH. Electrophysiology of mammalian gland cells. Physiol Rev 1976;56:535-77.
151. Heilbrunn LV, Wiercinski FJ. The action of various cations on muscle protoplasm. Journal of Cellular and Comparative Physiology 1947;29:15-32.
152. Means AR, Rasmussen CD. Calcium, calmodulin and cell proliferation. Cell Calcium 1988;9:313-9.
153. Whitaker M. Calcium at fertilization and in early development. Physiol Rev 2006;86:25-88.
154. Criddle DN, Gerasimenko JV, Baumgartner HK, et al. Calcium signalling and pancreatic cell death: apoptosis or necrosis? Cell Death Differ 2007;14:1285-94.
155. Chandra R, Liddle RA. Neural and Hormonal Regulation of Pancreatic Secretion. Curr Opin Gastroenterol 2009;25:441-6.
156. Afroze S, Meng F, Jensen K, et al. The physiological roles of secretin and its receptor. Ann Transl Med 2013;1.
157. Lam AKM, Galione A. The endoplasmic reticulum and junctional membrane communication during calcium signaling. Biochimica et Biophysica Acta (BBA) - Molecular Cell Research 2013;1833:2542-2559.
158. Lee HC. Mechanisms of calcium signaling by cyclic ADP-ribose and NAADP. Physiol Rev 1997;77:1133-64.
159. Petersen OH. Ca2+ signaling in pancreatic acinar cells: physiology and pathophysiology. Braz J Med Biol Res 2009;42:9-16.
160. Chvanov M, Walsh CM, Haynes LP, et al. ATP depletion induces translocation of STIM1 to puncta and formation of STIM1-ORAI1 clusters: translocation and re-translocation of STIM1 does not require ATP. Pflugers Arch 2008;457:505-17.
161. Li J, Zhou R, Zhang J, et al. Calcium signaling of pancreatic acinar cells in the pathogenesis of pancreatitis. World J Gastroenterol 2014;20:16146-52.
162. Petersen OH, Gerasimenko OV, Tepikin AV, et al. Aberrant Ca(2+) signalling through acidic calcium stores in pancreatic acinar cells. Cell Calcium 2011;50:193-9.
163. Tinel H, Cancela JM, Mogami H, et al. Active mitochondria surrounding the pancreatic acinar granule region prevent spreading of inositol trisphosphate-evoked local cytosolic Ca(2+) signals. Embo j 1999;18:4999-5008.
164. Park MK, Ashby MC, Erdemli G, et al. Perinuclear, perigranular and sub-plasmalemmal mitochondria have distinct functions in the regulation of cellular calcium transport. Embo j 2001;20:1863-74.
165. Petersen OH. Specific mitochondrial functions in separate sub-cellular domains of pancreatic acinar cells. Pflugers Arch 2012;464:77-87.
166. Ashby MC, Craske M, Park MK, et al. Localized Ca(2+) uncaging reveals polarized distribution of Ca(2+)-sensitive Ca(2+) release sites: mechanism of unidirectional Ca(2+) waves. J Cell Biol 2002;158:283-92.

167. Berna MJ, Jensen RT. Role of CCK/gastrin receptors in gastrointestinal/metabolic diseases and results of human studies using gastrin/CCK receptor agonists/antagonists in these diseases. Curr Top Med Chem 2007;7:1211-31.
168. Berna MJ, Seiz O, Nast JF, et al. CCK1 and CCK2 receptors are expressed on pancreatic stellate cells and induce collagen production. J Biol Chem 2010;285:38905-14.
169. Gryshchenko O, Gerasimenko JV, Gerasimenko OV, et al. Calcium signalling in pancreatic stellate cells: Mechanisms and potential roles. Cell Calcium 2016;59:140-4.
170. Gryshchenko O, Gerasimenko JV, Gerasimenko OV, et al. Ca(2+) signals mediated by bradykinin type 2 receptors in normal pancreatic stellate cells can be inhibited by specific Ca(2+) channel blockade. J Physiol 2016;594:281-93.
171. Won JH, Zhang Y, Ji B, et al. Phenotypic changes in mouse pancreatic stellate cell Ca2+ signaling events following activation in culture and in a disease model of pancreatitis. Mol Biol Cell 2011;22:421-36.
172. Ward JB, Petersen OH, Jenkins SA, et al. Is an elevated concentration of acinar cytosolic free ionised calcium the trigger for acute pancreatitis? Lancet 1995;346:1016-9.
173. Voronina S, Longbottom R, Sutton R, et al. Bile acids induce calcium signals in mouse pancreatic acinar cells: implications for bile-induced pancreatic pathology. J Physiol 2002;540:49-55.
174. Criddle DN, Murphy J, Fistetto G, et al. Fatty acid ethyl esters cause pancreatic calcium toxicity via inositol trisphosphate receptors and loss of ATP synthesis. Gastroenterology 2006;130:781-93.
175. Gerasimenko JV, Flowerdew SE, Voronina SG, et al. Bile acids induce Ca2+ release from both the endoplasmic reticulum and acidic intracellular calcium stores through activation of inositol trisphosphate receptors and ryanodine receptors. J Biol Chem 2006;281:40154-63.
176. Raraty M, Ward J, Erdemli G, et al. Calcium-dependent enzyme activation and vacuole formation in the apical granular region of pancreatic acinar cells. Proc Natl Acad Sci U S A 2000;97:13126-31.
177. Petersen OH, Sutton R. Ca2+ signalling and pancreatitis: effects of alcohol, bile and coffee. Trends Pharmacol Sci 2006;27:113-20.
178. Gryshchenko O, Gerasimenko JV, Peng S, et al. Calcium signalling in the acinar environment of the exocrine pancreas: physiology and pathophysiology. The Journal of Physiology 2018;596:2663-2678.
179. Criddle DN, Raraty MG, Neoptolemos JP, et al. Ethanol toxicity in pancreatic acinar cells: mediation by nonoxidative fatty acid metabolites. Proc Natl Acad Sci U S A 2004;101:10738-43.
180. Chiang JYL. Bile Acid Metabolism and Signaling. Compr Physiol 2013;3:1191-212.
181. Bernard C. Leçons de physiologie expérimentale appliquée à la médecine Editor Bailliere, J.-B. Paris. Paris: J.B. Baillière et fils, 1856.
182. Perides G, Laukkarinen JM, Vassileva G, et al. Biliary acute pancreatitis in mice is mediated by the G-protein-coupled cell surface bile acid receptor Gpbar1. Gastroenterology 2010;138:715-25.
183. Dawson PA, Lan T, Rao A. Bile acid transporters. J Lipid Res 2009;50:2340-57.

184. Geyer N, Diszhazi G, Csernoch L, et al. Bile acids activate ryanodine receptors in pancreatic acinar cells via a direct allosteric mechanism. Cell Calcium 2015;58:160-70.
185. DiMagno MJ. Oktoberfest binge drinking and acute pancreatitis: is there really no relationship? Clin Gastroenterol Hepatol 2011;9:920-2.
186. Lange LG. Nonoxidative ethanol metabolism: formation of fatty acid ethyl esters by cholesterol esterase. Proc Natl Acad Sci U S A 1982;79:3954-7.
187. Laposata EA, Lange LG. Presence of nonoxidative ethanol metabolism in human organs commonly damaged by ethanol abuse. Science 1986;231:497-9.
188. Gukovskaya AS, Mouria M, Gukovsky I, et al. Ethanol metabolism and transcription factor activation in pancreatic acinar cells in rats. Gastroenterology 2002;122:106-18.
189. Haber PS, Apte MV, Applegate TL, et al. Metabolism of ethanol by rat pancreatic acinar cells. J Lab Clin Med 1998;132:294-302.
190. Haber PS, Apte MV, Moran C, et al. Non-oxidative metabolism of ethanol by rat pancreatic acini. Pancreatology 2004;4:82-9.
191. Lankisch PG, Lowenfels AB, Maisonneuve P. What is the risk of alcoholic pancreatitis in heavy drinkers? Pancreas 2002;25:411-2.
192. Yadav D, Papachristou GI, Whitcomb DC. Alcohol-associated pancreatitis. Gastroenterol Clin North Am 2007;36:219-38, vii.
193. Gukovsky I, Lugea A, Shahsahebi M, et al. A rat model reproducing key pathological responses of alcoholic chronic pancreatitis. Am J Physiol Gastrointest Liver Physiol 2008;294:G68-79.
194. Werner J, Laposata M, Fernandez-del Castillo C, et al. Pancreatic injury in rats induced by fatty acid ethyl ester, a nonoxidative metabolite of alcohol. Gastroenterology 1997;113:286-94.
195. Werner J, Saghir M, Warshaw AL, et al. Alcoholic pancreatitis in rats: injury from nonoxidative metabolites of ethanol. Am J Physiol Gastrointest Liver Physiol 2002;283:G65-73.
196. Huang W, Booth DM, Cane MC, et al. Fatty acid ethyl ester synthase inhibition ameliorates ethanol-induced Ca2+-dependent mitochondrial dysfunction and acute pancreatitis. Gut 2014;63:1313-24.
197. Lampel M, Kern HF. Acute interstitial pancreatitis in the rat induced by excessive doses of a pancreatic secretagogue. Virchows Arch A Pathol Anat Histol 1977;373:97-117.
198. Niederau C, Ferrell LD, Grendell JH. Caerulein-induced acute necrotizing pancreatitis in mice: protective effects of proglumide, benzotript, and secretin. Gastroenterology 1985;88:1192-204.
199. Ethridge RT, Chung DH, Slogoff M, et al. Cyclooxygenase-2 gene disruption attenuates the severity of acute pancreatitis and pancreatitis-associated lung injury. Gastroenterology 2002;123:1311-22.
200. McEntee G, Leahy A, Cottell D, et al. Three-dimensional morphological study of the pancreatic microvasculature in caerulein-induced experimental pancreatitis. BJS 1989;76:853-855.
201. Klar E, Schratt W, Foitzik T, et al. Impact of microcirculatory flow pattern changes on the development of acute edematous and necrotizing pancreatitis in rabbit pancreas. Dig Dis Sci 1994;39:2639-44.

202. Gorelick FS, Lerch MM. Do Animal Models of Acute Pancreatitis Reproduce Human Disease? Cellular and Molecular Gastroenterology and Hepatology 2017;4:251-262.
203. Murphy JA, Criddle DN, Sherwood M, et al. Direct activation of cytosolic Ca2+ signaling and enzyme secretion by cholecystokinin in human pancreatic acinar cells. Gastroenterology 2008;135:632-41.
204. Saluja AK, Lerch MM, Phillips PA, et al. Why does pancreatic overstimulation cause pancreatitis? Annu Rev Physiol 2007;69:249-69.
205. Saillan-Barreau C, Clerc P, Adato M, et al. Transgenic CCK-B/gastrin receptor mediates murine exocrine pancreatic secretion. Gastroenterology 1998;115:988-96.
206. Mossner J, Sprenger C, Secknus R, et al. Comparison between the synthetic cholecystokinin analogues caerulein and Thr28NlE31CCK25-33(CCK9) with regards to plasma bioactivity, degradation rate and stimulation of pancreatic exocrine function. Z Gastroenterol 1991;29:59-64.
207. Apte MV, Phillips PA, Fahmy RG, et al. Does alcohol directly stimulate pancreatic fibrogenesis? Studies with rat pancreatic stellate cells. Gastroenterology 2000;118:780-94.
208. Masamune A, Kikuta K, Satoh M, et al. Alcohol activates activator protein-1 and mitogen-activated protein kinases in rat pancreatic stellate cells. J Pharmacol Exp Ther 2002;302:36-42.
209. Masamune A, Satoh A, Watanabe T, et al. Effects of ethanol and its metabolites on human pancreatic stellate cells. Dig Dis Sci 2010;55:204-11.
210. Sah RP, Saluja AK. Trypsinogen activation in acute and chronic pancreatitis: is it a prerequisite? Gut 2011;60:1305-7.
211. Biczo G, Vegh ET, Shalbueva N, et al. Mitochondrial dysfunction, through impaired autophagy, leads to endoplasmic reticulum stress, deregulated lipid metabolism, and pancreatitis in animal models. Gastroenterology 2017.
212. Mukherjee R, Criddle DN, Gukvoskaya A, et al. Mitochondrial injury in pancreatitis. Cell Calcium 2008;44:14-23.
213. Booth DM, Murphy JA, Mukherjee R, et al. Reactive oxygen species induced by bile acid induce apoptosis and protect against necrosis in pancreatic acinar cells. Gastroenterology 2011;140:2116-25.
214. Gerasimenko OV, Gerasimenko JV. Mitochondrial function and malfunction in the pathophysiology of pancreatitis. Pflugers Arch 2012;464:89-99.
215. Maleth J, Rakonczay Z, Jr., Venglovecz V, et al. Central role of mitochondrial injury in the pathogenesis of acute pancreatitis. Acta Physiol (Oxf) 2013;207:226-35.
216. Galluzzi L, Vitale I, Aaronson SA, et al. Molecular mechanisms of cell death: recommendations of the Nomenclature Committee on Cell Death 2018. Cell Death & Differentiation 2018;25:486-541.
217. Elliott MR, Ravichandran KS. The dynamics of apoptotic cell clearance. Dev Cell 2016;38:147-60.
218. Bhatia M. Apoptosis versus necrosis in acute pancreatitis. Am J Physiol Gastrointest Liver Physiol 2004;286:G189-96.
219. Mareninova OA, Sung KF, Hong P, et al. Cell death in pancreatitis: caspases protect from necrotizing pancreatitis. J Biol Chem 2006;281:3370-81.
220. Singh L, Bakshi DK, Majumdar S, et al. Mitochondrial dysfunction and apoptosis of acinar cells in chronic pancreatitis. J Gastroenterol 2008;43:473-83.

221. Maacke H, Kessler A, Schmiegel W, et al. Overexpression of p53 protein during pancreatitis. British Journal Of Cancer 1997;75:1501.
222. Kroemer G, Galluzzi L, Brenner C. Mitochondrial membrane permeabilization in cell death. Physiol Rev 2007;87:99-163.
223. Bernardi P. Mitochondrial Permeability Transition Pore. In: Lane WJLD, ed. Encyclopedia of Biological Chemistry. Waltham: Academic Press, 2013:162-167.
224. Bernardi P, Di Lisa F. The mitochondrial permeability transition pore: Molecular nature and role as a target in cardioprotection. Journal of Molecular and Cellular Cardiology 2015;78:100-106.
225. Kokoszka JE, Waymire KG, Levy SE, et al. The ADP/ATP translocator is not essential for the mitochondrial permeability transition pore. Nature 2004;427:461-5.
226. Baines CP, Kaiser RA, Sheiko T, et al. Voltage-dependent anion channels are dispensable for mitochondrial-dependent cell death. Nat Cell Biol 2007;9:550-5.
227. Kwong JQ, Davis J, Baines CP, et al. Genetic deletion of the mitochondrial phosphate carrier desensitizes the mitochondrial permeability transition pore and causes cardiomyopathy. Cell Death Differ 2014;21:1209-17.
228. Baines CP, Kaiser RA, Purcell NH, et al. Loss of cyclophilin D reveals a critical role for mitochondrial permeability transition in cell death. Nature 2005;434:658-62.
229. Nakagawa T, Shimizu S, Watanabe T, et al. Cyclophilin D-dependent mitochondrial permeability transition regulates some necrotic but not apoptotic cell death. Nature 2005;434:652-8.
230. Giorgio V, Bisetto E, Soriano ME, et al. Cyclophilin D modulates mitochondrial F0F1-ATP synthase by interacting with the lateral stalk of the complex. J Biol Chem 2009;284:33982-8.
231. Giorgio V, von Stockum S, Antoniel M, et al. Dimers of mitochondrial ATP synthase form the permeability transition pore. Proc Natl Acad Sci U S A 2013;110:5887-92.
232. Voronina S, Barrow S, Simpson A, et al. Dynamic changes in the ATP levels in the cytosol and mitochondria of pancreatic acinar cells: effects of calcium-releasing secretagogues and inducers of acute pancreatitis. Gastroenterology 2010;138:1976-87.
233. Voronina SG, Barrow SL, Simpson AW, et al. Dynamic changes in cytosolic and mitochondrial ATP levels in pancreatic acinar cells. Gastroenterology 2010;138:1976-87.
234. Voronina S, Tepikin A. Mitochondrial calcium in the life and death of exocrine secretory cells. Cell Calcium 2012;52:86-92.
235. Voronina S, Okeke E, Parker T, et al. How to win ATP and influence Ca2+ signaling. Cell Calcium 2014;55:131-138.
236. Shalbueva N, Mareninova OA, Gerloff A, et al. Effects of Oxidative Alcohol Metabolism on the Mitochondrial Permeability Transition Pore and Necrosis in a Mouse Model of Alcoholic Pancreatitis. Gastroenterology 2013;144:437-446.e6.
237. Mukherjee R, Mareninova OA, Odinokova IV, et al. Mechanism of mitochondrial permeability transition pore induction and damage in the pancreas: inhibition prevents acute pancreatitis by protecting production of ATP. Gut 2016;65:1333-46.

238. van der Bliek AM, Shen Q, Kawajiri S. Mechanisms of mitochondrial fission and fusion. Cold Spring Harb Perspect Biol 2013;5.
239. Schrepfer E, Scorrano L. Mitofusins, from Mitochondria to Metabolism. Mol Cell 2016;61:683-694.
240. Daumke O, Roux A. Mitochondrial Homeostasis: How Do Dimers of Mitofusins Mediate Mitochondrial Fusion? Curr Biol 2017;27:R353-r356.
241. Gukovskaya AS, Pandol SJ, Gukovsky I. New insights into the pathways initiating and driving pancreatitis. Curr Opin Gastroenterol 2016.
242. Almanza A, Carlesso A, Chintha C, et al. Endoplasmic reticulum stress signalling - from basic mechanisms to clinical applications. Febs j 2018.
243. Gorlach A, Klappa P, Kietzmann T. The endoplasmic reticulum: folding, calcium homeostasis, signaling, and redox control. Antioxid Redox Signal 2006;8:1391-418.
244. Meldolesi J, Pozzan T. The endoplasmic reticulum Ca2+ store: a view from the lumen. Trends Biochem Sci 1998;23:10-4.
245. Braakman I, Hebert DN. Protein Folding in the Endoplasmic Reticulum. Cold Spring Harb Perspect Biol 2013;5.
246. Hwang J, Qi L. Quality Control in the Endoplasmic Reticulum: Crosstalk between ERAD and UPR pathways. Trends Biochem Sci 2018;43:593-605.
247. Benham AM. Endoplasmic Reticulum redox pathways: in sickness and in health. Febs j 2018.
248. Kubisch CH, Logsdon CD. Endoplasmic reticulum stress and the pancreatic acinar cell. Expert Rev Gastroenterol Hepatol 2008;2:249-60.
249. Ruggiano A, Foresti O, Carvalho P. ER-associated degradation: Protein quality control and beyond. The Journal of Cell Biology 2014;204:869.
250. Malhotra JD, Kaufman RJ. ER Stress and Its Functional Link to Mitochondria: Role in Cell Survival and Death. Cold Spring Harb Perspect Biol 2011;3.
251. Harding HP, Zhang Y, Ron D. Protein translation and folding are coupled by an endoplasmic-reticulum-resident kinase. Nature 1999;397:271-4.
252. Lee AH, Chu GC, Iwakoshi NN, et al. XBP-1 is required for biogenesis of cellular secretory machinery of exocrine glands. Embo j 2005;24:4368-80.
253. Calfon M, Zeng H, Urano F, et al. IRE1 couples endoplasmic reticulum load to secretory capacity by processing the XBP-1 mRNA. Nature 2002;415:92-6.
254. Marciniak SJ, Yun CY, Oyadomari S, et al. CHOP induces death by promoting protein synthesis and oxidation in the stressed endoplasmic reticulum. Genes Dev 2004;18:3066-77.
255. Hiramatsu N, Chiang WC, Kurt TD, et al. Multiple Mechanisms of Unfolded Protein Response-Induced Cell Death. Am J Pathol 2015;185:1800-8.
256. Morishima N, Nakanishi K, Takenouchi H, et al. An endoplasmic reticulum stress-specific caspase cascade in apoptosis. Cytochrome c-independent activation of caspase-9 by caspase-12. J Biol Chem 2002;277:34287-94.
257. Kubisch CH, Sans MD, Arumugam T, et al. Early activation of endoplasmic reticulum stress is associated with arginine-induced acute pancreatitis. Am J Physiol Gastrointest Liver Physiol 2006;291:G238-45.
258. Kubisch CH, Logsdon CD. Secretagogues differentially activate endoplasmic reticulum stress responses in pancreatic acinar cells. Am J Physiol Gastrointest Liver Physiol 2007;292:G1804-12.

259. Danino H, Ben-Dror K, Birk R. Exocrine pancreas ER stress is differentially induced by different fatty acids. Exp Cell Res 2015;339:397-406.
260. Kowalik AS, Johnson CL, Chadi SA, et al. Mice lacking the transcription factor Mist1 exhibit an altered stress response and increased sensitivity to caerulein-induced pancreatitis. Am J Physiol Gastrointest Liver Physiol 2007;292:G1123-32.
261. Liu Y, Yang L, Chen KL, et al. Knockdown of GRP78 promotes apoptosis in pancreatic acinar cells and attenuates the severity of cerulein and LPS induced pancreatic inflammation. PLoS One 2014;9:e92389.
262. Suyama K, Ohmuraya M, Hirota M, et al. C/EBP homologous protein is crucial for the acceleration of experimental pancreatitis. Biochem Biophys Res Commun 2008;367:176-82.
263. Wu JS, Li WM, Chen YN, et al. Endoplasmic reticulum stress is activated in acute pancreatitis. J Dig Dis 2016;17:295-303.
264. Sah RP, Garg SK, Dixit AK, et al. Endoplasmic reticulum stress is chronically activated in chronic pancreatitis. J Biol Chem 2014;289:27551-61.
265. Lugea A, Tischler D, Nguyen J, et al. Adaptive unfolded protein response attenuates alcohol-induced pancreatic damage. Gastroenterology 2011;140:987-97.
266. Harding HP, Zeng H, Zhang Y, et al. Diabetes mellitus and exocrine pancreatic dysfunction in perk-/- mice reveals a role for translational control in secretory cell survival. Mol Cell 2001;7:1153-63.
267. Murphy M P. How mitochondria produce reactive oxygen species. Biochem J 2009;417:1-13.
268. Liemburg-Apers DC, Willems P, Koopman WJH, et al. Interactions between mitochondrial reactive oxygen species and cellular glucose metabolism. Arch Toxicol 2015;89:1209-26.
269. Reverendo M, Mendes A, Arguello RJ, et al. At the crossway of ER-stress and proinflammatory responses. Febs j 2018.
270. Sah RP, Saluja A. Molecular mechanisms of pancreatic injury. Curr Opin Gastroenterol 2011;27:444-51.
271. Haynes CM, Titus EA, Cooper AA. Degradation of misfolded proteins prevents ER-derived oxidative stress and cell death. Mol Cell 2004;15:767-76.
272. Xue X, Piao JH, Nakajima A, et al. Tumor necrosis factor alpha (TNFalpha) induces the unfolded protein response (UPR) in a reactive oxygen species (ROS)-dependent fashion, and the UPR counteracts ROS accumulation by TNFalpha. J Biol Chem 2005;280:33917-25.
273. Armstrong JA, Cash NJ, Ouyang Y, et al. Oxidative stress alters mitochondrial bioenergetics and modifies pancreatic cell death independently of cyclophilin D, resulting in an apoptosis-to-necrosis shift. J Biol Chem 2018;293:8032-8047.
274. Ryu GR, Lee E, Chun HJ, et al. Oxidative stress plays a role in high glucose-induced activation of pancreatic stellate cells. Biochem Biophys Res Commun 2013;439:258-63.
275. Masamune A, Kikuta K, Watanabe T, et al. Fibrinogen induces cytokine and collagen production in pancreatic stellate cells. Gut 2009;58:550-9.
276. Lang K, Schmid FX, Fischer G. Catalysis of protein folding by prolyl isomerase. Nature 1987;329:268-70.

277. Siekierka JJ, Hung SH, Poe M, et al. A cytosolic binding protein for the immunosuppressant FK506 has peptidyl-prolyl isomerase activity but is distinct from cyclophilin. Nature 1989;341:755-7.
278. Rahfeld JU, Rucknagel KP, Schelbert B, et al. Confirmation of the existence of a third family among peptidyl-prolyl cis/trans isomerases. Amino acid sequence and recombinant production of parvulin. FEBS Lett 1994;352:180-4.
279. Fischer G, Bang H, Mech C. [Determination of enzymatic catalysis for the cis-trans-isomerization of peptide binding in proline-containing peptides]. Biomed Biochim Acta 1984;43:1101-11.
280. Saibil H. Chaperone machines for protein folding, unfolding and disaggregation. Nat Rev Mol Cell Biol 2013;14:630-42.
281. Daum S, Schumann M, Mathea S, et al. Isoform-Specific Inhibition of Cyclophilins. Biochemistry 2009;48:6268-6277.
282. Davis TL, Walker JR, Campagna-Slater V, et al. Structural and biochemical characterization of the human cyclophilin family of peptidyl-prolyl isomerases. PLoS Biol 2010;8:e1000439.
283. Ryffel B, Woerly G, Greiner B, et al. Distribution of the cyclosporine binding protein cyclophilin in human tissues. Immunology 1991;72:399-404.
284. Mesa A, Somarelli JA, Herrera RJ. Spliceosomal Immunophilins. FEBS Lett 2008;582:2345-51.
285. Galat A, Bua J. Molecular aspects of cyclophilins mediating therapeutic actions of their ligands. Cell Mol Life Sci 2010;67:3467-88.
286. Baugh J, Gallay P. Cyclophilin involvement in the replication of hepatitis C virus and other viruses. Biol Chem 2012;393:579-87.
287. Chen J, Chen S, Wang J, et al. Cyclophilin J Is a Novel Peptidyl-Prolyl Isomerase and Target for Repressing the Growth of Hepatocellular Carcinoma. PLoS One 2015;10.
288. Pushkarsky T, Yurchenko V, Vanpouille C, et al. Cell surface expression of CD147/EMMPRIN is regulated by cyclophilin 60. J Biol Chem 2005;280:27866-71.
289. Koletsky AJ, Harding MW, Handschumacher RE. Cyclophilin: distribution and variant properties in normal and neoplastic tissues. J Immunol 1986;137:1054-9.
290. Damsker JM, Bukrinsky MI, Constant SL. Preferential chemotaxis of activated human CD4+ T cells by extracellular cyclophilin A. J Leukoc Biol 2007;82:613-8.
291. Yang Y, Lu N, Zhou J, et al. Cyclophilin A up-regulates MMP-9 expression and adhesion of monocytes/macrophages via CD147 signalling pathway in rheumatoid arthritis. Rheumatology (Oxford) 2008;47:1299-310.
292. Hampton RY. ER-associated degradation in protein quality control and cellular regulation. Curr Opin Cell Biol 2002;14:476-82.
293. Meunier L, Usherwood YK, Chung KT, et al. A subset of chaperones and folding enzymes form multiprotein complexes in endoplasmic reticulum to bind nascent proteins. Mol Biol Cell 2002;13:4456-69.
294. Lilley BN, Ploegh HL. Multiprotein complexes that link dislocation, ubiquitination, and extraction of misfolded proteins from the endoplasmic reticulum membrane. Proc Natl Acad Sci U S A 2005;102:14296-301.

295. Kim J, Choi TG, Ding Y, et al. Overexpressed cyclophilin B suppresses apoptosis associated with ROS and Ca2+ homeostasis after ER stress. J Cell Sci 2008;121:3636-48.
296. Watashi K, Ishii N, Hijikata M, et al. Cyclophilin B is a functional regulator of hepatitis C virus RNA polymerase. Mol Cell 2005;19:111-22.
297. Swanson SK, Born T, Zydowsky LD, et al. Cyclosporin-mediated inhibition of bovine calcineurin by cyclophilins A and B. Proc Natl Acad Sci U S A 1992;89:3741-5.
298. Bukrinsky MI. Cyclophilins: unexpected messengers in intercellular communications. Trends Immunol 2002;23:323-5.
299. Lee J, Kim SS. An overview of cyclophilins in human cancers. J Int Med Res 2010;38:1561-74.
300. Choi JW, Schroeder MA, Sarkaria JN, et al. Cyclophilin B supports Myc and mutant p53-dependent survival of glioblastoma multiforme cells. Cancer Res 2014;74:484-96.
301. Rycyzyn MA, Reilly SC, O'Malley K, et al. Role of cyclophilin B in prolactin signal transduction and nuclear retrotranslocation. Mol Endocrinol 2000;14:1175-86.
302. Lee J, Choi TG, Ha J, et al. Cyclosporine A suppresses immunoglobulin G biosynthesis via inhibition of cyclophilin B in murine hybridomas and B cells. Int Immunopharmacol 2012;12:42-9.
303. Choi JW, Sutor SL, Lindquist L, et al. Severe osteogenesis imperfecta in cyclophilin B-deficient mice. PLoS Genet 2009;5:e1000750.
304. Friedman J, Weissman I, Friedman J, et al. An analysis of the expression of cyclophilin C reveals tissue restriction and an intriguing pattern in the mouse kidney. Am J Pathol 1994;144:1247-56.
305. Chapman DC, Stocki P, Williams DB. Cyclophilin C Participates in the US2-Mediated Degradation of Major Histocompatibility Complex Class I Molecules. PLoS One 2015;10:e0145458.
306. Friedman J, Trahey M, Weissman I. Cloning and characterization of cyclophilin C-associated protein: a candidate natural cellular ligand for cyclophilin C. Proc Natl Acad Sci U S A 1993;90:6815-9.
307. Kong W, Lin BW, Li S, et al. Cyclophilin C-associated protein/Mac-2 binding protein colocalizes with calnexin and regulates the expression of tissue transglutaminase. J Cell Physiol 2010;223:151-7.
308. Trahey M, Weissman IL. Cyclophilin C-associated protein: a normal secreted glycoprotein that down-modulates endotoxin and proinflammatory responses in vivo. Proc Natl Acad Sci U S A 1999;96:3006-11.
309. Kong W, Longaker MT, Lorenz HP. Cyclophilin C-associated protein is a mediator for fibronectin fragment-induced matrix metalloproteinase-13 expression. J Biol Chem 2004;279:55334-40.
310. Yamaguchi R, Hosaka M, Torii S, et al. Cyclophilin C-associated protein regulation of phagocytic functions via NFAT activation in macrophages. Brain Research 2011;1397:55-65.
311. Giorgio V, Soriano ME, Basso E, et al. Cyclophilin D in mitochondrial pathophysiology. Biochimica et Biophysica Acta (BBA) - Bioenergetics 2010;1797:1113-1118.
312. Elrod JW, Molkentin JD. Physiologic functions of cyclophilin D and the mitochondrial permeability transition pore. Circ J 2013;77:1111-22.

313. Menazza S, Wong R, Nguyen T, et al. CypD−/− hearts have altered levels of proteins involved in Krebs cycle, branch chain amino acid degradation and pyruvate metabolism. Journal of Molecular and Cellular Cardiology 2013;56:81-90.
314. Alam MR, Baetz D, Ovize M. Cyclophilin D and myocardial ischemia–reperfusion injury: A fresh perspective. Journal of Molecular and Cellular Cardiology 2015;78:80-89.
315. Millay DP, Sargent MA, Osinska H, et al. Genetic and pharmacologic inhibition of mitochondrial-dependent necrosis attenuates muscular dystrophy. Nat Med 2008;14:442-7.
316. Thomas B, Banerjee R, Starkova NN, et al. Mitochondrial permeability transition pore component cyclophilin D distinguishes nigrostriatal dopaminergic death paradigms in the MPTP mouse model of Parkinson's disease. Antioxid Redox Signal 2012;16:855-68.
317. Forte M, Gold BG, Marracci G, et al. Cyclophilin D inactivation protects axons in experimental autoimmune encephalomyelitis, an animal model of multiple sclerosis. Proc Natl Acad Sci U S A 2007;104:7558-63.
318. Warne J, Pryce G, Hill JM, et al. Selective Inhibition of the Mitochondrial Permeability Transition Pore Protects against Neurodegeneration in Experimental Multiple Sclerosis. J Biol Chem 2016;291:4356-73.
319. Du H, Guo L, Zhang W, et al. Cyclophilin D deficiency improves mitochondrial function and learning/memory in aging Alzheimer disease mouse model. Neurobiology of Aging 2011;32:398-406.
320. Du H, Guo L, Zhang W, et al. Cyclophilin D deficiency improves mitochondrial function and learning/memory in aging Alzheimer disease mouse model. Neurobiol Aging 2011;32:398-406.
321. Guo L, Du H, Yan S, et al. Cyclophilin D deficiency rescues axonal mitochondrial transport in Alzheimer's neurons. PLoS One 2013;8:e54914.
322. Klawitter J, Pennington A, Klawitter J, et al. Mitochondrial cyclophilin D ablation is associated with the activation of Akt/p70S6K pathway in the mouse kidney. Scientific Reports 2017;7:10540.
323. Schumann M, Ihling CH, Prell E, et al. Identification of low abundance cyclophilins in human plasma. Proteomics 2016;16:2815-2826.
324. Arora K, Gwinn WM, Bower MA, et al. Extracellular cyclophilins contribute to the regulation of inflammatory responses. J Immunol 2005;175:517-22.
325. Satoh K, Nigro P, Berk BC. Oxidative Stress and Vascular Smooth Muscle Cell Growth: A Mechanistic Linkage by Cyclophilin A. Antioxid Redox Signal 2010;12:675-82.
326. Schlegel J, Redzic JS, Porter CC, et al. Solution characterization of the extracellular region of CD147 and its interaction with its enzyme ligand cyclophilin A. J Mol Biol 2009;391:518-35.
327. Hasaneen NA, Cao J, Pulkoski-Gross A, et al. Extracellular Matrix Metalloproteinase Inducer (EMMPRIN) promotes lung fibroblast proliferation, survival and differentiation to myofibroblasts. Respiratory Research 2016;17:17.
328. Barnes AM, Carter EM, Cabral WA, et al. Lack of cyclophilin B in osteogenesis imperfecta with normal collagen folding. N Engl J Med 2010;362:521-8.
329. Yurchenko V, Constant S, Bukrinsky M. Dealing with the family: CD147 interactions with cyclophilins. Immunology 2006;117:301-9.

330. Jin ZG, Melaragno MG, Liao DF, et al. Cyclophilin A is a secreted growth factor induced by oxidative stress. Circ Res 2000;87:789-96.
331. Kim H, Kim WJ, Jeon ST, et al. Cyclophilin A may contribute to the inflammatory processes in rheumatoid arthritis through induction of matrix degrading enzymes and inflammatory cytokines from macrophages. Clin Immunol 2005;116:217-24.
332. Gwinn WM, Damsker JM, Falahati R, et al. Novel approach to inhibit asthma-mediated lung inflammation using anti-CD147 intervention. J Immunol 2006;177:4870-9.
333. Allain F, Vanpouille C, Carpentier M, et al. Interaction with glycosaminoglycans is required for cyclophilin B to trigger integrin-mediated adhesion of peripheral blood T lymphocytes to extracellular matrix. Proc Natl Acad Sci U S A 2002;99:2714-9.
334. Yurchenko V, Constant S, Eisenmesser E, et al. Cyclophilin-CD147 interactions: a new target for anti-inflammatory therapeutics. Clin Exp Immunol 2010;160:305-17.
335. Naoumov NV. Cyclophilin inhibition as potential therapy for liver diseases. J Hepatol 2014;61:1166-74.
336. Borel JF, Kis ZL, Beveridge T. The History of the Discovery and Development of Cyclosporine (Sandimmune®). In: Merluzzi VJ, Adams J, eds. The Search for Anti-Inflammatory Drugs: Case Histories from Concept to Clinic. Boston, MA: Birkhäuser Boston, 1995:27-63.
337. Wenger RM. Synthesis of Cyclosporine and Analogues: Structural Requirements for Immunosuppressive Activity. Angewandte Chemie International Edition in English 1985;24:77-85.
338. Tribe HT. The discovery and development of cyclosporin. Mycologist 1998;12:20-22.
339. Jeffery JR. Cyclosporine analogues. Clin Biochem 1991;24:15-21.
340. Bertault-Peres P, Bonfils C, Fabre G, et al. Metabolism of cyclosporin A. II. Implication of the macrolide antibiotic inducible cytochrome P-450 3c from rabbit liver microsomes. Drug Metab Dispos 1987;15:391-8.
341. Combalbert J, Fabre I, Fabre G, et al. Metabolism of cyclosporin A. IV. Purification and identification of the rifampicin-inducible human liver cytochrome P-450 (cyclosporin A oxidase) as a product of P450IIIA gene subfamily. Drug Metab Dispos 1989;17:197-207.
342. Shaw PM, Barnes TS, Cameron D, et al. Purification and characterization of an anticonvulsant-induced human cytochrome P-450 catalysing cyclosporin metabolism. Biochem J 1989;263:653-63.
343. Kronbach T, Fischer V, Meyer UA. Cyclosporine metabolism in human liver: identification of a cytochrome P-450III gene family as the major cyclosporine-metabolizing enzyme explains interactions of cyclosporine with other drugs. Clin Pharmacol Ther 1988;43:630-5.
344. Maurer G, Loosli HR, Schreier E, et al. Disposition of cyclosporine in several animal species and man. I. Structural elucidation of its metabolites. Drug Metab Dispos 1984;12:120-6.
345. Maurer G. Metabolism of cyclosporine. Transplant Proc 1985;17:19-26.
346. Freeman DJ. Pharmacology and pharmacokinetics of cyclosporine. Clin Biochem 1991;24:9-14.
347. Henricsson S. A Sulfate Conjugate of Cyclosporin. Pharmacology & Toxicology 1990;66:53-55.

348. Christians U, Schlitt HJ, Bleck JS, et al. Measurement of cyclosporine and 18 metabolites in blood, bile, and urine by high-performance liquid chromatography. Transplant Proc 1988;20:609-13.
349. Christians U, Strohmeyer S, Kownatzki R, et al. Investigations on the metabolic pathways of cyclosporine: II. Elucidation of the metabolic pathways in vitro by human liver microsomes. Xenobiotica 1991;21:1199-210.
350. Christians U, Strohmeyer S, Kownatzki R, et al. Investigations on the metabolic pathways of cyclosporine: I. Excretion of cyclosporine and its metabolites in human bile--isolation of 12 new cyclosporine metabolites. Xenobiotica 1991;21:1185-98.
351. Rosano TG, Freed BM, Pell MA, et al. Cyclosporine metabolites in human blood and renal tissue. Transplant Proc 1986;18:35-40.
352. Thomson AWE. Cyclosporin: mode of Action and Clinical Applications (Book). Annals of Internal Medicine 1990;113:1004.
353. Wagner O, Schreier E, Heitz F, et al. Tissue distribution, disposition, and metabolism of cyclosporine in rats. Drug Metab Dispos 1987;15:377-83.
354. Burckart GJ, Venkataramanan R, Ptachcinski RJ, et al. Cyclosporine Absorption Following Orthotopic Liver Transplantation. The Journal of Clinical Pharmacology 1986;26:647-651.
355. Lemaire M, Maurer G, Wood AJ. Cyclosporin. Pharmacokinetics and metabolism. Prog Allergy 1986;38:93-107.
356. Lemaire M, Fahr A, Maurer G. Pharmacokinetics of cyclosporine: inter- and intra-individual variations and metabolic pathways. Transplant Proc 1990;22:1110-2.
357. Potter B, Palmer RA, Withnall R, et al. Two new cyclosporin folds observed in the structures of the immunosuppressant cyclosporin G and the formyl peptide receptor antagonist cyclosporin H at ultra-high resolution. Org Biomol Chem 2003;1:1466-74.
358. Fric J, Zelante T, Wong AY, et al. NFAT control of innate immunity. Blood 2012;120:1380-9.
359. Crabtree GR. Calcium, calcineurin, and the control of transcription. J Biol Chem 2001;276:2313-6.
360. Baines CP, Molkentin JD. STRESS signaling pathways that modulate cardiac myocyte apoptosis. J Mol Cell Cardiol 2005;38:47-62.
361. Kaminska B, Tyburczy M, Gabrusiewicz K, et al. Glioblastoma: Anti-tumor Action of Cyclosporin A and Functionally Related Drugs. In: Hayat MA, ed. Tumors of the Central Nervous System, Volume 2: Gliomas: Glioblastoma (Part 2). Dordrecht: Springer Netherlands, 2011:241-253.
362. Pyrzynska B, Mosieniak G, Kaminska B. Changes of the trans-activating potential of AP-1 transcription factor during cyclosporin A-induced apoptosis of glioma cells are mediated by phosphorylation and alterations of AP-1 composition. J Neurochem 2000;74:42-51.
363. Ciechomska I, Pyrzynska B, Kazmierczak P, et al. Inhibition of Akt kinase signalling and activation of Forkhead are indispensable for upregulation of FasL expression in apoptosis of glioma cells. Oncogene 2003;22:7617-27.
364. Pyrzynska B, Serrano M, Martinez AC, et al. Tumor suppressor p53 mediates apoptotic cell death triggered by cyclosporin A. J Biol Chem 2002;277:14102-8.

365. Gitter BD, Waters DC, Threlkeld PG, et al. Cyclosporin A is a substance P (tachykinin NK1) receptor antagonist. Eur J Pharmacol 1995;289:439-46.
366. Lang K, Drell TLt, Lindecke A, et al. Induction of a metastatogenic tumor cell type by neurotransmitters and its pharmacological inhibition by established drugs. Int J Cancer 2004;112:231-8.
367. Munoz M, Rosso M, Gonzalez A, et al. The broad-spectrum antitumor action of cyclosporin A is due to its tachykinin receptor antagonist pharmacological profile. Peptides 2010;31:1643-8.
368. Sliwa M, Markovic D, Gabrusiewicz K, et al. The invasion promoting effect of microglia on glioblastoma cells is inhibited by cyclosporin A. Brain 2007;130:476-89.
369. Al-Nasser I, Crompton M. The entrapment of the Ca2+ indicator arsenazo III in the matrix space of rat liver mitochondria by permeabilization and resealing. Na+-dependent and -independent effluxes of Ca2+ in arsenazo III-loaded mitochondria. Biochem J 1986;239:31-40.
370. Crompton M, Costi A, Hayat L. Evidence for the presence of a reversible Ca2+-dependent pore activated by oxidative stress in heart mitochondria. Biochem J 1987;245:915-8.
371. Crompton M, Ellinger H, Costi A. Inhibition by cyclosporin A of a Ca2+-dependent pore in heart mitochondria activated by inorganic phosphate and oxidative stress. Biochem J 1988;255:357-60.
372. Broekemeier KM, Dempsey ME, Pfeiffer DR. Cyclosporin A is a potent inhibitor of the inner membrane permeability transition in liver mitochondria. J Biol Chem 1989;264:7826-30.
373. Halestrap AP, Davidson AM. Inhibition of Ca2(+)-induced large-amplitude swelling of liver and heart mitochondria by cyclosporin is probably caused by the inhibitor binding to mitochondrial-matrix peptidyl-prolyl cis-trans isomerase and preventing it interacting with the adenine nucleotide translocase. Biochem J 1990;268:153-60.
374. Tanveer A, Virji S, Andreeva L, et al. Involvement of Cyclophilin D in the Activation of A mitochondrial Pore by Ca2+ and Oxidant Stress. European Journal of Biochemistry 1996;238:166-172.
375. Basso E, Fante L, Fowlkes J, et al. Properties of the permeability transition pore in mitochondria devoid of Cyclophilin D. J Biol Chem 2005;280:18558-61.
376. Mihatsch MJ, Olivieri W, Marbet U, et al. Giant mitochondria in renal tubular cells and cyclosporin A. Lancet 1981;1:1162-3.
377. Kahan BD. Cyclosporine. N Engl J Med 1989;321:1725-38.
378. Bechstein WO. Neurotoxicity of calcineurin inhibitors: impact and clinical management. Transpl Int 2000;13:313-26.
379. Pallet N, Bouvier N, Bendjallabah A, et al. Cyclosporine-induced endoplasmic reticulum stress triggers tubular phenotypic changes and death. Am J Transplant 2008;8:2283-96.
380. Pallet N, Thervet E, Anglicheau D. c-Jun-N-Terminal Kinase Signaling Is Involved in Cyclosporine-Induced Epithelial Phenotypic Changes. J Transplant 2012;2012:348604.
381. Wilmes A, Limonciel A, Aschauer L, et al. Application of integrated transcriptomic, proteomic and metabolomic profiling for the delineation of mechanisms of drug induced cell stress. Journal of Proteomics 2013;79:180-194.

382. Ram BM, Ramakrishna G. Endoplasmic reticulum vacuolation and unfolded protein response leading to paraptosis like cell death in cyclosporine A treated cancer cervix cells is mediated by cyclophilin B inhibition. Biochim Biophys Acta 2014;1843:2497-512.
383. Jeong K, Kim H, Kim K, et al. Cyclophilin B is involved in p300-mediated degradation of CHOP in tumor cell adaptation to hypoxia. Cell Death Differ 2014;21:438-50.
384. Stocki P, Chapman DC, Beach LA, et al. Depletion of cyclophilins B and C leads to dysregulation of endoplasmic reticulum redox homeostasis. J Biol Chem 2014;289:23086-96.
385. Echigo Y, Inoue K, Kogire M, et al. Effects of cyclosporine and tacrolimus (FK 506) on acute pancreatitis in mice. Arch Surg 1995;130:64-8.
386. Oie E, Bjornerheim R, Clausen OP, et al. Cyclosporin A inhibits cardiac hypertrophy and enhances cardiac dysfunction during postinfarction failure in rats. Am J Physiol Heart Circ Physiol 2000;278:H2115-23.
387. Qian NS, Xu XP, Chen Y, et al. Protective effect of cyclosporin A on brain injury in rats with acute necrotic pancreatitis. Life Sci 2010;87:64-8.
388. Nazareth W, Yafei N, Crompton M. Inhibition of anoxia-induced injury in heart myocytes by cyclosporin A. J Mol Cell Cardiol 1991;23:1351-4.
389. Griffiths EJ, Halestrap AP. Mitochondrial non-specific pores remain closed during cardiac ischaemia, but open upon reperfusion. Biochem J 1995;307 (Pt 1):93-8.
390. Weller B, Massa R, Karpati G, et al. Glucocorticoids and immunosuppressants do not change the prevalence of necrosis and regeneration in mdx skeletal muscles. Muscle Nerve 1991;14:771-4.
391. Stupka N, Gregorevic P, Plant DR, et al. The calcineurin signal transduction pathway is essential for successful muscle regeneration in mdx dystrophic mice. Acta Neuropathol 2004;107:299-310.
392. De Luca A, Nico B, Liantonio A, et al. A multidisciplinary evaluation of the effectiveness of cyclosporine a in dystrophic mdx mice. Am J Pathol 2005;166:477-89.
393. Sharma KR, Mynhier MA, Miller RG. Cyclosporine increases muscular force generation in Duchenne muscular dystrophy. Neurology 1993;43:527-32.
394. Mueller EA, Kovarik JM, van Bree JB, et al. Improved dose linearity of cyclosporine pharmacokinetics from a microemulsion formulation. Pharm Res 1994;11:301-4.
395. Hausenloy D, Boston-Griffiths E, Yellon D. Cyclosporin A and cardioprotection: from investigative tool to therapeutic agent. Br J Pharmacol 2012;165:1235-45.
396. Trankle C, Thurber CJ, Toldo S, et al. Mitochondrial Membrane Permeability Inhibitors in Acute Myocardial Infarction: Still Awaiting Translation. JACC: Basic to Translational Science 2016;1:524-535.
397. Piot C, Croisille P, Staat P, et al. Effect of cyclosporine on reperfusion injury in acute myocardial infarction. N Engl J Med 2008;359:473-81.
398. Ghaffari S, Kazemi B, Toluey M, et al. The effect of prethrombolytic cyclosporine-A injection on clinical outcome of acute anterior ST-elevation myocardial infarction. Cardiovasc Ther 2013;31:e34-9.
399. Hausenloy D, Kunst G, Boston-Griffiths E, et al. The effect of cyclosporin-A on peri-operative myocardial injury in adult patients undergoing coronary

artery bypass graft surgery: a randomised controlled clinical trial. Heart 2014;100:544-9.
400. Chiari P, Angoulvant D, Mewton N, et al. Cyclosporine protects the heart during aortic valve surgery. Anesthesiology 2014;121:232-8.
401. Ottani F, Latini R, Staszewsky L, et al. Cyclosporine A in Reperfused Myocardial Infarction: The Multicenter, Controlled, Open-Label CYCLE Trial. J Am Coll Cardiol 2016;67:365-374.
402. Cung T-T, Morel O, Cayla G, et al. Cyclosporine before PCI in Patients with Acute Myocardial Infarction. New England Journal of Medicine 2015;373:1021-1031.
403. Di Lisa F, Menabo R, Canton M, et al. Opening of the mitochondrial permeability transition pore causes depletion of mitochondrial and cytosolic NAD+ and is a causative event in the death of myocytes in postischemic reperfusion of the heart. J Biol Chem 2001;276:2571-5.
404. Hausenloy DJ, Maddock HL, Baxter GF, et al. Inhibiting mitochondrial permeability transition pore opening: a new paradigm for myocardial preconditioning? Cardiovasc Res 2002;55:534-43.
405. Lawen A, Traber R. Substrate specificities of cyclosporin synthetase and peptolide SDZ 214-103 synthetase. Comparison of the substrate specificities of the related multifunctional polypeptides. J Biol Chem 1993;268:20452-65.
406. Sanglier JJ, Quesniaux V, Fehr T, et al. Sanglifehrins A, B, C and D, Novel Cyclophilin-binding Compounds Isolated from Streptomyces sp. A92-308110. I. Taxonomy, Fermentation, Isolation and Biological Activity, 1999.
407. Pua KH, Stiles DT, Sowa ME, et al. IMPDH2 Is an Intracellular Target of the Cyclophilin A and Sanglifehrin A Complex. Cell Rep 2017;18:432-442.
408. Lawen A. Biosynthesis of cyclosporins and other natural peptidyl prolyl cis/trans isomerase inhibitors. Biochim Biophys Acta 2015;1850:2111-20.
409. Steadman VA, Pettit SB, Poullennec KG, et al. Discovery of Potent Cyclophilin Inhibitors Based on the Structural Simplification of Sanglifehrin A. J Med Chem 2017;60:1000-1017.
410. Sweeney ZK, Fu J, Wiedmann B. From chemical tools to clinical medicines: nonimmunosuppressive cyclophilin inhibitors derived from the cyclosporin and sanglifehrin scaffolds. J Med Chem 2014;57:7145-59.
411. Paeshuyse J, Kaul A, De Clercq E, et al. The non-immunosuppressive cyclosporin DEB025 is a potent inhibitor of hepatitis C virus replication in vitro. Hepatology 2006;43:761-70.
412. Rosenwirth B, Billich A, Datema R, et al. Inhibition of human immunodeficiency virus type 1 replication by SDZ NIM 811, a nonimmunosuppressive cyclosporine analog. Antimicrob Agents Chemother 1994;38:1763-72.
413. Hopkins S, Scorneaux B, Huang Z, et al. SCY-635, a novel nonimmunosuppressive analog of cyclosporine that exhibits potent inhibition of hepatitis C virus RNA replication in vitro. Antimicrob Agents Chemother 2010;54:660-72.
414. Hopkins S, Gallay P. Cyclophilin Inhibitors: An Emerging Class of Therapeutics for the Treatment of Chronic Hepatitis C Infection. Viruses 2012;4:2558-77.
415. Rasola A, Bernardi P. The mitochondrial permeability transition pore and its adaptive responses in tumor cells. Cell Calcium 2014;56:437-445.

416. Karch J, Kanisicak O, Brody MJ, et al. Necroptosis Interfaces with MOMP and the MPTP in Mediating Cell Death. PLoS One 2015;10:e0130520.
417. Waldmeier PC, Feldtrauer JJ, Qian T, et al. Inhibition of the mitochondrial permeability transition by the nonimmunosuppressive cyclosporin derivative NIM811. Mol Pharmacol 2002;62:22-9.
418. Reutenauer J, Dorchies OM, Patthey-Vuadens O, et al. Investigation of Debio 025, a cyclophilin inhibitor, in the dystrophic mdx mouse, a model for Duchenne muscular dystrophy. Br J Pharmacol 2008;155:574-84.
419. Lie TS, Preissinger H, Bach M, et al. The protective effect of cyclosporine against cirrhotic alteration of the liver. Surgery 1991;110:847-53.
420. Ikeda H, Fujiwara K. Cyclosporin A and FK-506 in inhibition of rat Ito cell activation in vitro. Hepatology 1995;21:1161-6.
421. Nakamuta M, Kohjima M, Fukushima M, et al. Cyclosporine suppresses cell growth and collagen production in hepatic stellate cells. Transplant Proc 2005;37:4598-602.
422. Kohjima M, Enjoji M, Higuchi N, et al. NIM811, a nonimmunosuppressive cyclosporine analogue, suppresses collagen production and enhances collagenase activity in hepatic stellate cells. Liver Int 2007;27:1273-81.
423. Wang H, Zhang Y, Wang T, et al. N-methyl-4-isoleucine cyclosporine attenuates CCl4-induced liver fibrosis in rats by interacting with cyclophilin B and D. Journal of Gastroenterology and Hepatology 2011;26:558-567.
424. Rehman H, Ramshesh VK, Theruvath TP, et al. NIM811 (N-methyl-4-isoleucine cyclosporine), a mitochondrial permeability transition inhibitor, attenuates cholestatic liver injury but not fibrosis in mice. J Pharmacol Exp Ther 2008;327:699-706.
425. Levy G, Villamil FG, Nevens F, et al. REFINE: a randomized trial comparing cyclosporine A and tacrolimus on fibrosis after liver transplantation for hepatitis C. Am J Transplant 2014;14:635-46.
426. Wissing ER, Millay DP, Vuagniaux G, et al. DEB025 is more effective than prednisone in reducing muscular pathology in mdx mice. Neuromuscul Disord 2010;20:753-60.
427. Gu H, Werner J, Bergmann F, et al. Necro-inflammatory response of pancreatic acinar cells in the pathogenesis of acute alcoholic pancreatitis. Cell Death Dis 2013;4:e816-.
428. Lee SB. Mechanistic connection between inflammation and fibrosis. 2010:S22-6.
429. Suthahar N, Meijers WC, Silljé HHW, et al. From Inflammation to Fibrosis—Molecular and Cellular Mechanisms of Myocardial Tissue Remodelling and Perspectives on Differential Treatment Opportunities. Curr Heart Fail Rep 2017;14:235-50.
430. Schinzel AC, Takeuchi O, Huang Z, et al. Cyclophilin D is a component of mitochondrial permeability transition and mediates neuronal cell death after focal cerebral ischemia. Proceedings of the National Academy of Sciences of the United States of America 2005;102:12005.
431. Laukkarinen JM, Van Acker GJ, Weiss ER, et al. A mouse model of acute biliary pancreatitis induced by retrograde pancreatic duct infusion of Na-taurocholate. Gut 2007;56:1590-8.
432. Perides G, van Acker GJ, Laukkarinen JM, et al. Experimental acute biliary pancreatitis induced by retrograde infusion of bile acids into the mouse pancreatic duct. Nat Protoc 2010;5:335-41.

433. Lerch MM, Gorelick FS. Models of acute and chronic pancreatitis. Gastroenterology 2013;144:1180-93.
434. Lorentz K. Approved recommendation on IFCC methods for the measurement of catalytic concentration of enzymes. Part 9. IFCC method for alpha-amylase (1,4-alpha-D-glucan 4-glucanohydrolase, EC 3.2.1.1). International Federation of Clinical Chemistry and Laboratory Medicine (IFCC). Committee on Enzymes. Clin Chem Lab Med 1998;36:185-203.
435. Wildi S, Kleeff J, Mayerle J, et al. Suppression of transforming growth factor β signalling aborts caerulein induced pancreatitis and eliminates restricted stimulation at high caerulein concentrations. Gut 2007;56:685-92.
436. Dawra R, Ku YS, Sharif R, et al. An improved method for extracting myeloperoxidase and determining its activity in the pancreas and lungs during pancreatitis. Pancreas 2008;37:62-8.
437. Weder JK, Haussner K, Bokor MV. Use of fluorogenic substrates to visualize trypsin and chymotrypsin inhibitors after electrophoresis. Electrophoresis 1993;14:220-6.
438. Sato D, Kato T. Novel fluorescent substrates for detection of trypsin activity and inhibitor screening by self-quenching. Bioorg Med Chem Lett 2016;26:5736-5740.
439. Nathan JD, Romac J, Peng RY, et al. Transgenic expression of pancreatic secretory trypsin inhibitor-I ameliorates secretagogue-induced pancreatitis in mice. Gastroenterology 2005;128:717-27.
440. Van Laethem JL, Robberecht P, Resibois A, et al. Transforming growth factor beta promotes development of fibrosis after repeated courses of acute pancreatitis in mice. Gastroenterology 1996;110:576-82.
441. Whittaker P, Kloner RA, Boughner DR, et al. Quantitative assessment of myocardial collagen with picrosirius red staining and circularly polarized light. Basic Res Cardiol 1994;89:397-410.
442. Circu ML, Aw TY. REACTIVE OXYGEN SPECIES, CELLULAR REDOX SYSTEMS AND APOPTOSIS. Free Radic Biol Med 2010;48:749-62.
443. Sano R, Reed JC. ER stress-induced cell death mechanisms. Biochim Biophys Acta 2013;1833.
444. Zeeshan HMA, Lee GH, Kim HR, et al. Endoplasmic Reticulum Stress and Associated ROS. Int J Mol Sci 2016;17.
445. Kruger B, Albrecht E, Lerch MM. The role of intracellular calcium signaling in premature protease activation and the onset of pancreatitis. Am J Pathol 2000;157:43-50.
446. Criddle DN. Reactive oxygen species, Ca(2+) stores and acute pancreatitis; a step closer to therapy? Cell Calcium 2016;60:180-9.
447. Mami I, Tavernier Q, Bouvier N, et al. A Novel Extrinsic Pathway for the Unfolded Protein Response in the Kidney. J Am Soc Nephrol 2016;27:2670-83.
448. Louhimo J, Steer ML, Perides G. Necroptosis Is an Important Severity Determinant and Potential Therapeutic Target in Experimental Severe Pancreatitis. Cell Mol Gastroenterol Hepatol 2016;2:519-535.
449. Wang X, Yousefi S, Simon H-U. Necroptosis and neutrophil-associated disorders. Cell Death & Disease 2018;9:111.
450. Zhu P, Hu S, Jin Q, et al. Ripk3 promotes ER stress-induced necroptosis in cardiac IR injury: A mechanism involving calcium overload/XO/ROS/mPTP pathway. Redox Biology 2018;16:157-168.

451. Saveljeva S, Mc Laughlin SL, Vandenabeele P, et al. Endoplasmic reticulum stress induces ligand-independent TNFR1-mediated necroptosis in L929 cells. Cell Death &Amp; Disease 2015;6:e1587.
452. Schonfeld P, Wojtczak L. Fatty acids decrease mitochondrial generation of reactive oxygen species at the reverse electron transport but increase it at the forward transport. Biochim Biophys Acta 2007;1767:1032-40.
453. Schonfeld P, Wojtczak L. Fatty acids as modulators of the cellular production of reactive oxygen species. Free Radic Biol Med 2008;45:231-41.
454. Krauskopf A, Lhote P, Mutter M, et al. Vasopressin type 1A receptor up-regulation by cyclosporin A in vascular smooth muscle cells is mediated by superoxide. J Biol Chem 2003;278:41685-90.
455. Soriano ME, Nicolosi L, Bernardi P. Desensitization of the permeability transition pore by cyclosporin a prevents activation of the mitochondrial apoptotic pathway and liver damage by tumor necrosis factor-alpha. J Biol Chem 2004;279:36803-8.
456. Banks PA, Bollen TL, Dervenis C, et al. Classification of acute pancreatitis--2012: revision of the Atlanta classification and definitions by international consensus. Gut 2013;62:102-11.
457. Membreno FE, Espinales JC, Lawitz EJ. Cyclophilin inhibitors for hepatitis C therapy. Clin Liver Dis 2013;17:129-39.
458. Yu G, Wan R, Hu Y, et al. Pancreatic acinar cells-derived cyclophilin A promotes pancreatic damage by activating NF-κB pathway in experimental pancreatitis. Biochemical and Biophysical Research Communications 2014;444:75-80.
459. Bukrinsky M. Extracellular cyclophilins in health and disease. Biochim Biophys Acta 2015;1850:2087-95.
460. Taylor P, Mikol V, Kallen J, et al. Conformational polymorphism in peptidic and nonpeptidic drug molecules. Biopolymers 1996;40:585-92.
461. Mikol V, Taylor P, Kallen J, et al. Conformational differences of an immunosuppressant peptolide in a single crystal and in a crystal complex with human cyclophilin A. J Mol Biol 1998;283:451-61.
462. Lazarova T, Weng Z. Cyclosporin A analogues: recent advances. Expert Opinion on Therapeutic Patents 2003;13:1327-1332.
463. Sharma S, Lee J, Gao P, et al. Toxicity profile of solvents by aspiration approach for topical agent delivery to respiratory tract epithelium. Int J Toxicol 2011;30:358-66.
464. Campbell H, Bosma K, Brackenbury A, et al. Polyethylene glycol (PEG) attenuates exogenous surfactant in lung-injured adult rabbits. Am J Respir Crit Care Med 2002;165:475-80.
465. Spisani S, Fabbri E, Muccinelli M, et al. Inhibition of neutrophil responses by cyclosporin A. An insight into molecular mechanisms. Rheumatology (Oxford) 2001;40:794-800.
466. Muili KA, Jin S, Orabi AI, et al. Pancreatic acinar cell nuclear factor kappaB activation because of bile acid exposure is dependent on calcineurin. J Biol Chem 2013;288:21065-73.
467. Muili KA, Wang D, Orabi AI, et al. Bile acids induce pancreatic acinar cell injury and pancreatitis by activating calcineurin. J Biol Chem 2013;288:570-80.
468. Pandol SJ, Gorelick FS, Gerloff A, et al. Alcohol Abuse, Endoplasmic Reticulum Stress and Pancreatitis. Dig Dis 2011;28:776-82.

469. Yadav D. Recent advances in the epidemiology of alcoholic pancreatitis. Curr Gastroenterol Rep 2011;13:157-65.
470. Yadav D, Whitcomb DC. The role of alcohol and smoking in pancreatitis. Nat Rev Gastroenterol Hepatol 2010;7:131-45.
471. Ranger AM, Oukka M, Rengarajan J, et al. Inhibitory function of two NFAT family members in lymphoid homeostasis and Th2 development. Immunity 1998;9:627-35.
472. Huang W, Haynes AC, Mukherjee R, et al. Selective inhibition of BET proteins reduces pancreatic damage and systemic inflammation in bile acid- and fatty acid ethyl ester- but not caerulein-induced acute pancreatitis. Pancreatology 2017;17:689-697.
473. Dawra R, Sah RP, Dudeja V, et al. Intra-acinar trypsinogen activation mediates early stages of pancreatic injury but not inflammation in mice with acute pancreatitis. Gastroenterology 2011;141:2210-2217.e2.
474. Sah RP, Dawra RK, Saluja AK. New insights into the pathogenesis of pancreatitis. Curr Opin Gastroenterol 2013;29:523-30.
475. Steinle AU, Weidenbach H, Wagner M, et al. NF-kappaB/Rel activation in cerulein pancreatitis. Gastroenterology 1999;116:420-30.
476. Lawen A, Traber R, Geyl D. In vitro biosynthesis of [Thr2,Leu5,D-Hiv8,Leu10]-cyclosporin, a cyclosporin-related peptolide, with immunosuppressive activity by a multienzyme polypeptide. J Biol Chem 1991;266:15567-70.
477. Lew D, Afghani E, Pandol S. Chronic Pancreatitis: Current Status and Challenges for Prevention and Treatment. Dig Dis Sci 2017;62:1702-1712.
478. Waiser J, Dell K, Bohler T, et al. Cyclosporine A up-regulates the expression of TGF-beta1 and its receptors type I and type II in rat mesangial cells. Nephrol Dial Transplant 2002;17:1568-77.
479. Sun BK, Li C, Lim SW, et al. Expression of transforming growth factor-beta-inducible gene-h3 in normal and cyclosporine-treated rat kidney. J Lab Clin Med 2004;143:175-83.
480. Vaquero E, Molero X, Tian X, et al. Myofibroblast proliferation, fibrosis, and defective pancreatic repair induced by cyclosporin in rats. Gut 1999;45:269-77.
481. Hopkins S, DiMassimo B, Rusnak P, et al. The cyclophilin inhibitor SCY-635 suppresses viral replication and induces endogenous interferons in patients with chronic HCV genotype 1 infection. Journal of Hepatology 2012;57:47-54.
482. Hopkins S, Bobardt M, Chatterji U, et al. The cyclophilin inhibitor SCY-635 disrupts hepatitis C virus NS5A-cyclophilin A complexes. Antimicrob Agents Chemother 2012;56:3888-97.
483. Varghese F, Bukhari AB, Malhotra R, et al. IHC Profiler: an open source plugin for the quantitative evaluation and automated scoring of immunohistochemistry images of human tissue samples. PLoS One 2014;9:e96801.
484. Murtaugh LC, Keefe M. Regeneration and Repair of the Exocrine Pancreas. Annu Rev Physiol 2015;77:229-49.
485. Biasutto L, Azzolini M, Szabò I, et al. The mitochondrial permeability transition pore in AD 2016: An update. Biochimica et Biophysica Acta (BBA) - Molecular Cell Research 2016;1863:2515-2530.

486. Tavecchio M, Lisanti S, Lam A, et al. Cyclophilin D extramitochondrial signaling controls cell cycle progression and chemokine-directed cell motility. J Biol Chem 2013;288:5553-61.
487. Guerra MT, Fonseca EA, Melo FM, et al. Mitochondrial calcium regulates rat liver regeneration through the modulation of apoptosis. Hepatology 2011;54:296-306.
488. Chan MW, Arora PD, McCulloch CA. Cyclosporin inhibition of collagen remodeling is mediated by gelsolin. Am J Physiol Cell Physiol 2007;293:C1049-58.
489. Doller A, Akool el S, Muller R, et al. Molecular mechanisms of cyclosporin A inhibition of the cytokine-induced matrix metalloproteinase-9 in glomerular mesangial cells. J Am Soc Nephrol 2007;18:581-92.
490. Liu Q, Rehman H, Lemasters JJ, et al. Small-For-Size Liver Transplantation Increases Pulmonary Injury in Rats: Prevention by NIM811: 632. Transplantation 2012;94:654.
491. Cabral WA, Perdivara I, Weis M, et al. Abnormal type I collagen post-translational modification and crosslinking in a cyclophilin B KO mouse model of recessive osteogenesis imperfecta. PLoS Genet 2014;10:e1004465.
492. Terajima M, Taga Y, Chen Y, et al. Cyclophilin-B Modulates Collagen Cross-linking by Differentially Affecting Lysine Hydroxylation in the Helical and Telopeptidyl Domains of Tendon Type I Collagen. J Biol Chem 2016;291:9501-12.
493. Di Lisa F, Carpi A, Giorgio V, et al. The mitochondrial permeability transition pore and cyclophilin D in cardioprotection. Biochimica et Biophysica Acta (BBA) - Molecular Cell Research 2011;1813:1316-1322.
494. Wen L, Voronina S, Javed MA, et al. Inhibitors of ORAI1 Prevent Cytosolic Calcium-Associated Injury of Human Pancreatic Acinar Cells and Acute Pancreatitis in 3 Mouse Models. Gastroenterology 2015;149:481-92.e7.
495. Huang W, Cane MC, Mukherjee R, et al. Caffeine protects against experimental acute pancreatitis by inhibition of inositol 1,4,5-trisphosphate receptor-mediated Ca2+ release. Gut 2017;66:301-313.
496. Xue J, Sharma V, Habtezion A. Immune cells and immune-based therapy in pancreatitis. Immunol Res 2014;58:378-86.
497. Zimnoch L, Szynaka B, Puchalski Z. Mast cells and pancreatic stellate cells in chronic pancreatitis with differently intensified fibrosis. Hepatogastroenterology 2002;49:1135-8.
498. Schmitz-Winnenthal H, Pietsch DH, Schimmack S, et al. Chronic pancreatitis is associated with disease-specific regulatory T-cell responses. Gastroenterology 2010;138:1178-88.
499. Grundsten M, Liu GZ, Permert J, et al. Increased central memory T cells in patients with chronic pancreatitis. Pancreatology 2005;5:177-82.
500. Marrache F, Tu SP, Bhagat G, et al. Overexpression of interleukin-1beta in the murine pancreas results in chronic pancreatitis. Gastroenterology 2008;135:1277-87.
501. Omary MB. The pancreatic stellate cell: a star on the rise in pancreatic diseases. 2007;117:50-9.
502. Baumert JT, Sparmann G, Emmrich J, et al. Inhibitory effects of interferons on pancreatic stellate cell activation. World J Gastroenterol 2006;12:896-901.

503. Sendler M, Beyer G, Mahajan UM, et al. Complement Component 5 Mediates Development of Fibrosis, via Activation of Stellate Cells, in 2 Mouse Models of Chronic Pancreatitis. Gastroenterology 2015;149:765-76.e10.
504. Xue J, Sharma V, Hsieh MH, et al. Alternatively activated macrophages promote pancreatic fibrosis in chronic pancreatitis. Nat Commun 2015;6:7158.
505. Turner PV, Brabb T, Pekow C, et al. Administration of substances to laboratory animals: routes of administration and factors to consider. J Am Assoc Lab Anim Sci 2011;50:600-13.
506. Olyaei AJ, de Mattos AM, Bennett WM. Nephrotoxicity of immunosuppressive drugs: new insight and preventive strategies. Curr Opin Crit Care 2001;7:384-9.
507. Naesens M, Kuypers DR, Sarwal M. Calcineurin inhibitor nephrotoxicity. Clin J Am Soc Nephrol 2009;4:481-508.
508. Johnson CD, Besselink MG, Carter R. Acute pancreatitis. Bmj 2014;349:g4859.
509. Pandol SJ, Raraty M. Pathobiology of alcoholic pancreatitis. Pancreatology 2007;7:105-14.
510. Berzin TM, Mortele KJ, Banks PA. The management of suspected pancreatic sepsis. Gastroenterol Clin North Am 2006;35:393-407.
511. Young SP, Thompson JP. Severe acute pancreatitis. Continuing Education in Anaesthesia Critical Care & Pain 2008;8:125-128.
512. Werge M, Novovic S, Schmidt PN, et al. Infection increases mortality in necrotizing pancreatitis: A systematic review and meta-analysis. Pancreatology 2016;16:698-707.
513. Zoratti M, Szabo I. The mitochondrial permeability transition. Biochim Biophys Acta 1995;1241:139-76.
514. Petronilli V, Pietrobon D, Zoratti M, et al. Free energy coupling between H+-generating and H+-consuming pumps. European Journal of Biochemistry 1986;155:423-431.
515. Blanchet L, Grefte S, Smeitink JA, et al. Photo-induction and automated quantification of reversible mitochondrial permeability transition pore opening in primary mouse myotubes. PLoS One 2014;9:e114090.
516. Lemoine S, Pillot B, Augeul L, et al. Dose and timing of injections for effective cyclosporine A pretreatment before renal ischemia reperfusion in mice. PLoS One 2017;12:e0182358.
517. Hausenloy DJ, Duchen MR, Yellon DM. Inhibiting mitochondrial permeability transition pore opening at reperfusion protects against ischaemia-reperfusion injury. Cardiovasc Res 2003;60:617-25.
518. Whitcomb DC, Shimosegawa T, Chari ST, et al. International consensus statements on early chronic Pancreatitis. Recommendations from the working group for the international consensus guidelines for chronic pancreatitis in collaboration with The International Association of Pancreatology, American Pancreatic Association, Japan Pancreas Society, PancreasFest Working Group and European Pancreatic Club. Pancreatology 2018.
519. Shimosegawa T, Kume K, Satoh K. Chronic pancreatitis and pancreatic cancer: prediction and mechanism. Clin Gastroenterol Hepatol 2009;7:S23-8.

520. Shimosegawa T, Kataoka K, Kamisawa T, et al. The revised Japanese clinical diagnostic criteria for chronic pancreatitis. J Gastroenterol 2010;45:584-91.
521. Uc A, Andersen DK, Bellin MD, et al. Chronic Pancreatitis in the 21st Century - Research Challenges and Opportunities: Summary of a National Institute of Diabetes and Digestive and Kidney Diseases Workshop. Pancreas 2016;45:1365-75.
522. Denayer T, Stöhr T, Van Roy M. Animal models in translational medicine: Validation and prediction. New Horizons in Translational Medicine 2014;2:5-11.
523. Peretti U, Zanon S, Michele R. The personalized medicine for pancreatic ductal adenocarcinoma patients: The oncologist perspective. Endosc Ultrasound 2017;6:S66-s68.
524. Malouitre S, Dube H, Selwood D, et al. Mitochondrial targeting of cyclosporin A enables selective inhibition of cyclophilin-D and enhanced cytoprotection after glucose and oxygen deprivation. Biochem J 2010;425:137-48.
525. Dube H, Selwood D, Malouitre S, et al. A mitochondrial-targeted cyclosporin A with high binding affinity for cyclophilin D yields improved cytoprotection of cardiomyocytes. Biochem J 2012;441:901-7.